Renewable liquid transport fuels from microbes and waste resources

Jenkins, Rhodri

Award date:
2015

Awarding institution:
University of Bath

Renewable liquid transport fuels from microbes and waste resources

Rhodri Wyn Jenkins

A thesis submitted for the degree of Doctor of Philosophy

University of Bath
Department of Chemical Engineering
Centre for Sustainable Chemical Technologies

October 2014

"UNLESS SOMEONE LIKE YOU CARES A WHOLE AWFUL LOT,

NOTHING IS GOING TO GET BETTER. IT'S NOT."

Dr. Seuss, *The Lorax*

ABSTRACT

In order to satisfy the global requirement for transport fuel sustainably, renewable liquid biofuels must be developed. Currently, two biofuels dominate the market; bioethanol for spark ignition and biodiesel for compression ignition engines. However, both fuels exhibit technical issues such as low energy density, poor low temperature performance and poor stability. In addition, bioethanol and biodiesel sourced from first generation feedstocks use arable land in competition with food production, and can only meet a fraction of the current demand.

To address these issues it is vital that biofuels be developed from truly sustainable sources, such as lignocellulosic waste resources, and possess improved physical properties. To improve and control the physical properties of a fuel for specific application, one must be able to tailor the products formed in its production process. All studies within this thesis, therefore, have the aim of assessing the fuels produced for their variability in physical property, or the aim of directing the process considered to specific fuel molecules.

In Chapter 2, spent coffee grounds from a range of geographical locations, bean types and brewing processes were assessed as a potential feedstock for biodiesel production. While the lipid yield was comparable to that of conventional biodiesel sources, the fatty acid profile remained constant irrespective of the coffee source. Despite this lack of variation, the fuel properties varied widely, presumably due to a range of alternative biomolecules present in the lipid. Though coffee biodiesel was produced from a waste product, the fuel properties were found to be akin to palm oil biodiesel, with a high viscosity and pour point. The blend level would therefore be restricted.

In Chapter 3 the coffee lipid, as well as a range of microbial oils potentially derived from renewable sources were transformed into a novel aviation and road transport fuel through cross-metathesis with ethene. Hoveyda-Grubbs 2nd generation catalyst was found to be the most suitable, achieving 41% terminal bond selectivity under optimum conditions. Metathesis yielded three fractions: an alkene hydrocarbon

fraction suitable for aviation, a shorter chain triglyceride fraction that upon transesterification produced a short chain biodiesel fuel, and a multifunctional volatile alkene fraction that could potentially have application in the polymer industry. Though there was variation for the road transport fuel fraction due to the presence of long chain saturates, the compounds fell within the US standard for biodiesel. The aviation fraction lowered the viscosity, increased the energy density, and remained soluble with Jet A-1 down to the required freezing point.

Oleaginous organisms generally only produce a maximum of 40% lipid, leaving a large portion of fermentable biomass. In Chapter 4, a variety of ethyl and butyl esters of organic acids – potentially obtainable from fermentation – were assessed for their suitability as fuels in comparison to bioethanol. One product, butyl butyrate, was deemed suitable as a Jet A-1 replacement while four products, diethyl succinate, dibutyl succinate, dibutyl fumarate and dibutyl malonate, were considered as potential blending agents for diesel. Diethyl succinate, being the most economically viable of the four, was chosen for an on-engine test using a 20 vol% blend of DES (DES 20) on a chassis dynamometer under pseudo-steady state conditions. DES20 was found to cause an increase in fuel demand and NO_x emissions, and a decrease in exhaust temperature, wheel force, and CO emissions.

While fermentation is generally directed to one product, producing unimolecular fuels, they do not convert the entirety of the biomass available. An alternative chemical transformation is pyrolysis. In Chapter 5, zeolite-catalysed fast pyrolysis of a model compound representative of the ketonic portion of biomass pyrolysis vapour – mesityl oxide – was carried out. The aim of this study was to understand the mechanistic changes that occur, which could lead to improved bio-oil yields and more directed fuel properties of the pyrolysis oil. While HZSM-5 and Cu ZSM-5 showed no activity for hydrogenation and little activity for oligomerisation, Pd ZSM-5 led to near-complete selective hydrogenation of mesityl oxide to methyl isobutyl ketone, though this reduced at higher temperatures. At lower temperature (150-250 °C), a small amount of useful oligomerisation was observed, which could potentially lead to a selective pyrolysis oligomerisation reaction pathway.

ACKNOWLEDGMENTS

First and foremost, thanks must go to my supervisor, Dr Chris Chuck. His endless assistance, guidance and encouragement, along with his seemingly infinite optimism, have been invaluable throughout my PhD. I am also grateful to Dr Chris Bannister, whose advice, help and patience specifically in the area of engine testing have been much appreciated.

I would like to thank my industrial collaborators for this PhD, the Airbus Group (formally EADS), for their extra funding for this project. I would like to specifically thank Sarah Nash, John Price, Solange Baena, Odile Pepillion and Isabelle Lombaert-Valot for their important discussion and direction concerning aviation transport and fuel, and well as providing samples of Jet A-1 Kerosene.

I am particularly grateful to my supervisory team during my internship at the National Renewable Energy Laboratory, Dr Mark Nimlos, Dr Calvin Mukarakate, and Dr David Robichaud. Firstly, for letting me come and work in what is undoubtedly one of the most important research facilities in the world, and secondly for providing me with an interesting and challenging project. Thanks must also go to my labmate while at NREL, Tabitha Evans, for showing me to ropes in an unfamiliar research environment.

I must acknowledge the Centre for Sustainable Chemical Technologies, for continuously providing me with incredible opportunities, both academically and professionally. Special thanks must go to Janet Scott, and whose tireless work make the CSCT as good as it can possibly be, to Sheila Apps, whose help with various issues throughout my PhD has been indispensable, and to Jez Cope, for his help and patience with everything computer related.

Thanks must go to the technical teams of Chemistry, Chemical Engineering and Mechanical Engineering for all the assistance with countless aspects of my PhD. I would particularly like to thank Daniel Lou-Hing, Marianne Harkins, Phil Jones and Allan Cox.

For their assistance and discussion in the area of GC-MS analsysis, I must acknowledge Kirsty Barber, Carlo Di Julio, Heather Parker and Rhodri Owen. For their assistance in the lab during their M.Eng projects, thanks to Martin Munro, Chris Fortune and Natasha Stageman.

To the members of the Doctoral Training Centre in Sustainable Chemical Technologies, I thank you all collectively for making these past four years far better than they would otherwise have been, as well as being available for helpful discussion throughout my PhD. Particular thanks to Joe Donnelly, David Miles, Rebecca Bamford, Thomas Forder, Dan Minnett, David McClymont, Ben Firth, Lee Burton, Jess Sharpe and James Tyson. I will certainly, however, have forgotten to mention someone, for which I apologise.

To Lisa Anne Sargeant – A measure of a true friend is one that you have just as much fun competing against as collaborating with. Thank you for your company, your discussion, and your assistance on all things even vaguely biological. You made the last three years a Hell of a lot more bearable.

Particular acknowledgement goes to the Chuck group as a whole – I look forward to seeing you expand and grow beyond what you already have. I consider myself lucky to have been here from the beginning and to have worked in the same lab as you, and apologise for my constant singing and occasional grumpiness.

To Mam and Dad – Sorry I've been a bit of a rubbish son these past four years. Your unending support and understanding throughout what has been a rather arduous period of my life, as well as the rest of it, will never go unappreciated. Thank you.

DISSEMINATION

Journal Articles

As an outcome of this thesis:

Jenkins, R.W., Munro, M., Nash, S., Chuck, C.J. Potential Renewable Oxygenated Biofuels for the Aviation and Road Transport Sectors. *Fuel* **2013** *103*(0), 593-599.

Jenkins, R.W., Stageman, N.E., Fortune, C.F., Chuck, C.J. Effect of the Type of Bean, Processing, and Geographical Location on the Biodiesel Produced from Waste Coffee Grounds. *Energy & Fuels* **2014** *28*(2), 1166-1174.

Jenkins, R.W., Bannister, C.D., Chuck, C.J., Emissions and Performance of a Diethyl Succinate in a Diesel Fuel Blend. *Environmental Science and Technology*, **under review**.

Manuscripts in preparation:

Jenkins, R.W., Sargeant, L.A., Whiffin, F., Donnelly, J., Kaloudis, D., Mozzanega, P., Chuck, C.J. Cross-Metathesis of Renewable Lipid Sources for a Dual Fuel Process.

Further articles co-authored:

Chuck, C.J., Parker H.J., Jenkins, R.W., Donnelly, J. Renewable biofuel additives from the ozonolysis of lignin. *Bioresource Technology* **2013**, *143*, 549-554.

Chuck, C.J., Lou-Hing, D., Dean, R., Sargeant, L.A., Jenkins, R.W. Simultaneous Microwave Extraction and Synthesis of Fatty Acid Methyl Ester from the Oleaginous Yeast *Rhodotorula glutinis*. *Energy* **2014**, *69*, 446-454.

Bendall, S., Birdsall-Wilson, M., Jenkins, R.W., Chew, J., Chuck, C.J., Showcasing Chemical Engineering Principles through the Production of Biodiesel from Spent Coffee Grounds, *The Journal of Chemical Education*, **under review**.

Book chapters

Chuck, C.J., Wagner, J.L., Jenkins, R.W., Biofuels from Microalgae in Chemical Processes for a Sustainable Future. Edited by Letcher, T.M., Scott, J.L., and Patterson, D.A. The Royal Society of Chemistry, **2014**.

Conferences

EADS PhD Showcase, Bristol, UK. May 28-29, 2012. Poster presentation, "Renewable liquid fuels from microbes for aviation and road transport use."

35th Symposium on Biotechnology for Fuels and Chemicals, Portland, Oregon. April 29 - May 2, 2013. Oral Presentation, "The Identification of Potential Renewable Oxygenated Biofuels for the Aviation and Road Transport Sectors."

6th International Conference on Green and Sustainable Chemistry, Nottingham, UK. August 4-7 2013. Poster presentation, "Renewable liquid fuels from microbes for aviation and road transport use."

FISITA World Automotive Congress, Maastricht, The Netherlands. June 2-6, 2014. Oral presentation, "Engine Testing of Potentially Renewable Liquid Biofuels from Microbes for the Aviation and Road Transport."

Prizes

EADS PhD Showcase, Bristol, UK. May 28-29, 2012. Poster prize.

"I'm a Scientist, get me out of here!" Energy zone winner, June 2013.

ABBREVIATIONS

ABE	Acetone-Butanol-Ethanol
ACS	American Chemical Society
AFF	Aviation fuel fraction
AKI	Anti-knock index
API	American Petroleum Institute
ASTM	American Society for Testing and Materials
BL20	Butyl levulinate, 20 % blend with diesel
BtL	Biomass to liquid
C/O	Carbon to oxygen ratio
CFPP	Cold filter plugging point
CFR	Co-operative fuel research
CI	Compression ignition
CN	Cetane number
DCM	Dichloromethane
DES	Diethyl succinate
DES20	Diethyl succinate, 20 % blend with diesel
DMF	2,5-Dimethyl furan
DMIBK	Di(methyl isobutyl ketone)
EADS	European Aeronautic Defence and Space company
ECE	Economic Commission for Europe
ECU	Engine control unit
EL10	Ethyl Levulinate, 10 % blend with diesel
EN	European Standard ("N" from "Norme")
FAAE	Fatty acid alkyl ester
FAME	Fatty acid methyl ester
FFA	Free fatty acid
FSG	Fresh coffee grounds
G1	Grubbs 1st generation catalyst
GC-MS	Gas chromatography - Mass spectrometry
GHG	Greenhouse gas
GT	Glyceryl trioleate
H/C	Hydrogen to carbon ratio
HCCI	Homogeneous charge compression ignition
HFRR	High frequency reciprocating rig

HGII	Hoveyda-Grubbs 2nd generation catalyst
HMF	Hydrooxymethylfurfural
m/z	Mass to charge ratio
MBMS	Molecular beam mass spectrometer
MIBK	Methyl isobutyl ketone
MO	Methyl oleate
MON	Motor research number
MTHF	Methyl-tetrahydrofuran
NMR	Nuclear magnetic resonance
NO_x	Mono-nitrogen oxides
NREL	National Renewable Energy Laboratory
PM	Particulate matter
ppm	Parts per million
RAF	Royal Air Force
RON	Research octane number
rpm	Revolutions per minute
RTF	Road transport fraction
SAR	Silica to alumina ratio
scCO2	Super critical carbon dioxide
SCG	Spent coffee grounds
SI	Spark ignition
SLM	Standard litres per minute
THC	Total hydrocarbons
TIC	Total ion chromatograph
US	United States
vol%	Volume percent
wt%	Weight percent
ZSM-5	Zeolite Socony Mobil 5

TABLE OF CONTENTS

LIST OF FIGURES

LIST OF TABLES

LIST OF SCHEMES

CHAPTER 1

INTRODUCTION

There are significant concerns over the geopolitical, socioeconomic and environmental effects of the continued extraction and use of fossil fuels. Due to the dependence of current global structure on the transport of goods and people, there is a significant need for sustainable liquid fuels. Current replacements – such as biodiesel sourced from vegetable oils and ethanol from sugars and starches – have a number of technical issues which question their sustainability and reduce their applicability. The development of alternatives is therefore a key scientific goal.

In this introductory chapter, the drivers to develop sustainable biofuels are briefly discussed, the characteristics of a drop-in biofuel in terms of its logistical, environmental, economic and technical requirements are outlined, and the current scientific and engineering research in this area is reviewed.

1.1 Opening Remarks

There are growing concerns associated with the use of fossil fuels, which have prompted an intensified search for replacement technologies. Concerns include the increasing scarcity and therefore cost, the security of supply due to the politically unstable regions from which fossil fuels are obtained, as well as the major contribution to anthropogenic climate change.[1] Transport represents a considerable amount of energy and fossil fuel consumption, accounting for 37.5% of UK energy consumption in 2011.[2] The vast majority of transport relies on petroleum oil, accounting for 63.7% of global oil consumption in 2012 (Figure 1.1).[3]

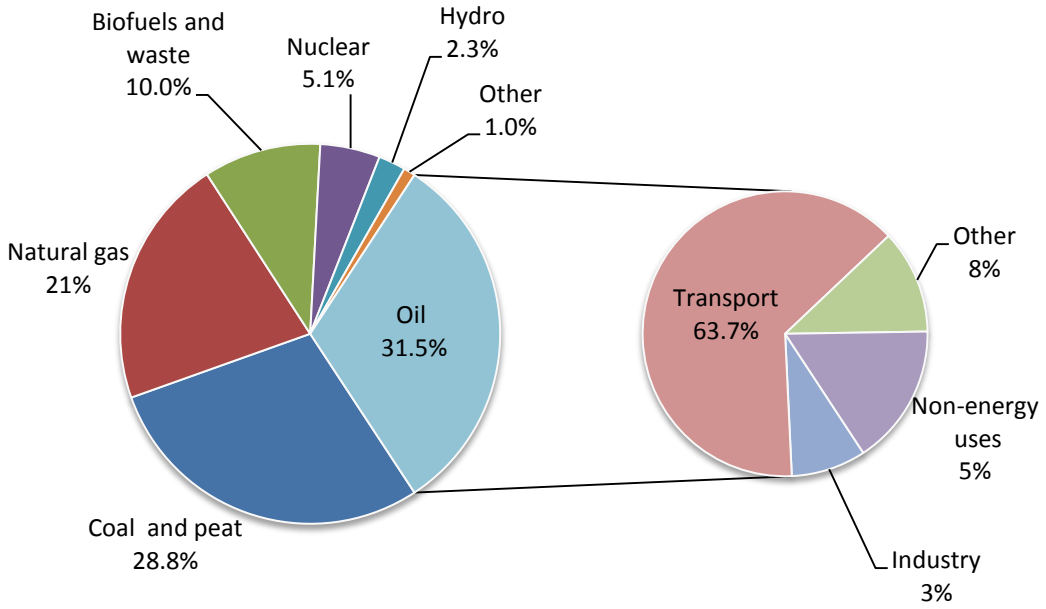

Figure 1.1 Total global energy usage (left), showing the global share of oil usage by sector (right). Data from Key World Energy Statistics, 2014.[3]

A number of novel technologies could replace the internal combustion engine, such as electric vehicles[4] and hydrogen-powered vehicles.[5] These technologies, however, are not without problems. Electric vehicles use batteries, which have a significantly lower energy density when compared to a conventional liquid fuel (0.7 MJ kg^{-1} compared to approximately 45 MJ kg^{-1} [6]), and rare elements such as neodymium and dysprosium are essential to the function of electric vehicles, 97% of which are produced in China.[7] This could ultimately lead to a shift to rare-earth dependency

from oil dependency. Though hydrogen is currently produced by the steam reformation of methane, it does have the potential to be produced without fossil fuel, via the electrolysis of water using renewable electricity. It is, however, expensive. Current estimates for the production of hydrogen via solar-powered water electrolysis are in excess of US $ 8 kg^{-1}.[8] Apart from the high cost of the hydrogen itself, there would be significant investment associated with the replacement of infrastructure. Predictions for a global hydrogen vehicle share of 30-70% by 2050 estimate cumulative infrastructure investments of between US $ 1.2 - 2.7 trillion.[9]

Furthermore, the cars and planes that are currently being produced and are in operation today have a significantly long lifespan. Most commercial aircraft manufactured by Airbus, for example, have a typical lifespan of 60 years.[10] Without legislative mediation, car ownership is likely to rise to over 2 billion units by 2050, therefore drastically increasing the need for liquid fuels in the medium term.[11] Ideally, therefore, replacement fuels must be compatible with the current infrastructure, processes and vehicles, i.e. a 'drop-in' fuel. Alternative liquid fuels, therefore, will be required in the coming decades.

One potential drop-in technology is liquid fuels produced from biomass. Currently, in the road transport sector, two biofuels dominate the market: bioethanol and biodiesel. These are both produced largely from terrestrial plants which need arable land to be grown and therefore can compete with food crops. Further issues include the low energy density of ethanol, poor low temperature properties of biodiesel, and the fluxional cost of the feedstock. A possible alternative to fuels produced from terrestrial plants is the further utilization of waste resources, either directly, or as a feedstock to culture microbes, which can then convert them into useful products via biotransformation.

1.2 CURRENT TRANSPORT FOSSIL FUELS

The vast majority of transport is powered by fossil fuels. In the UK in 2011, 97% of the energy used for transport was fossil-fuel based, of which the vast majority was derived from crude oil.[2] In oil refineries, crude oil undergoes fractional distillation to separate the large, complex molecules from the lighter species with lower boiling-points. Both fractions can then be chemically upgraded to produce broadly three fractions; light distillates (gases, petrol), middle distillates (diesel, kerosene) and heavy distillates (paraffin, lubricating waxes).[12] Two biofuels currently dominate the market – bioethanol from the fermentation of sugars and biodiesel from the transesterification of vegetable oils and animal fats. The general properties of the three most widely used fossil fuels for transport (petrol [US term "gasoline"], diesel, Jet-A1 kerosene) and the two commercial biofuels (bioethanol and biodiesel) are shown in Table 1.1. International standards for all the fuels are presented in Appendix A.

Table 1.1 Composition and general properties of common transport fuels[13-21]

		Petrol	Diesel	Jet A-1 Kerosene	Bioethanol	Biodiesel
Carbon number range		5-13	10-25	9-13	2	16-22
Hydrocarbon composition / %	**Alkanes**	30-50	40-70	50-65	-	-
	Alkenes	2-5	<5	-	-	-
	Cycloalkanes	4-10	10-25	20-30	-	-
	Aromatics	20-50	10-30	10-20	-	-
Boiling range / °C		50-200	200-300	140-280	73	max 360
Melting temperature / °C		-	-	-47	-114	-
Cloud Point / °C		-57	-20 - 10	-	-	-
Pour Point / °C		-35 - -15	-	-	-	-
Flash point / °C		-43	min 55	min 38	9	min 101[a] / 93[b]
Kinematic Viscosity / $mm^2 s^{-1}$		0.37-0.44 (@ 20 °C)	2.00-4.50[a] / 1.9-4.1[b] (@ 40 °C)	Max 8.00 (@ -20 °C)	1.13	3.5-5.0[a] / 1.9-6.0[b] (@ 40°C)
Density @ 15°C / g cm^{-3}		0.720-0.775	0.820-0.845	0.775-0.840	0.794	0.860-0.900
Autoignition temperature / °C		246	210	210	363	374-449

a – from EU standard

b – from US (ASTM) standard

Petrol is volatile and has a low flash point (-43 °C), so can be ignited by a spark at ambient conditions. The first spark ignition (SI) engine was the compressed charge internal combustion engine invented by Nikolaus Otto in 1876.[22] It ran on a four-stroke compression-chamber cycle – intake, compression, power and exhaust – whereby the work was harnessed by the movement of a piston and transmitted to torque and rotation required via a drive shaft.[22] The fuel for this original SI engine was 'illuminating gas', a flammable gaseous fuel produced from coal. The SI engine was perfected for widespread transportation use with liquid fuels by other inventors such as Gottleib Dailmer. The modern properties for petrol are outlined in the standards EN 228 for the EU[13] and ASTM D4813 for the US.[14]

A modified engine with a similar four-stroke cycle was invented at the end of the 19th century by Rudolf Diesel that was more suitable for heavier, less volatile fuels such as vegetable oils or heavier hydrocarbon fractions (later named "diesel" after the inventor).[23] The main modification of the engine was the increased compression ratio, which allowed the fuel to reach its autoignition temperature rather than being ignited by a spark, hence it was termed the compression ignition (CI) engine.[24] Diesel is regulated by the standards EN 590 for the EU,[15] and ASTM D975 for the US.[16] Currently both standards allow for a small percentage of biodiesel to be present: up to 7% and 5% in the EU and US, respectively.

Jet fuel is made from kerosene, a middle distillate fuel of lower carbon number range than diesel, and remains liquid as much lower temperatures while the flash point remains above normal ambient conditions. Current jet engines are gas turbines with a propelling nozzle, whereby air is compressed via a compression turbine before entering the combustion chamber. Upon combustion, fuel is then allowed to expand through the exhaust turbine which drives the compression turbine. This pressurised gas is expelled backwards through a propulsive nozzle generating forward thrust.[25] Jet engines are therefore referred to as "reaction engines". Air Commodore Sir Frank Whittle developed the designs and original patent for a jet engine whilst in the RAF in 1930,[26] and built the first prototype in 1937.[27] The main specifications for the regulations of commercial jet fuel (Jet A-1) are DEF STAN 91-91, issued by the UK's Ministry of Defence,[17] and ASTM D1655.[28]

1.2.1 Fuel Properties

In theory, any hydrocarbon (or oxygenated hydrocarbon), which possesses similar physical properties to those currently used, could be a suitable replacement fuel. There are, of course, other factors that need to be considered before considering any potential fuel as suitable. These include feedstock availability, renewability, economic viability, toxicity, and combustion emissions produced. However, the physical properties of a fuel indicate its quality and are related to the engine emissions and performance, so are tightly regulated in fuel standards. These define the parameters for optimum engine operation, rather than the limits of what the engines can technically run on..

1.2.1.1 Density

The density of a fuel (often expressed in terms of API gravity for a petroleum liquid[29]) is an important property as it is somewhat related to the overall molecular weight of the fuel which in turn is related to many other properties, including viscosity and low temperature performance. It is not, however, a singular indicator of quality. Two fuels of the same density, for example, can have drastically different properties.

For an internal combustion engine, the density of a fuel affects the engine performance directly, as it can affect fuel atomisation efficiency upon injection and therefore combustion. The engine power output will also be affected as most engines control the amount of fuel injected volumetrically. In general a fuel of higher density will cause greater flow resistance, due to the amount of pressure needed to move a higher mass of fuel, leading to poorer injection.[30-31] It is, however, not a hugely significant effect.

1.2.1.2 Distillation Range

The volatility of a fuel is an important property in terms of engine operation and safety, as it can affect starting and normal operation and is closely linked to other fuel properties such as viscosity, flash point and density.[32] This is usually more critical in SI engines, as the fuel is required to be volatile enough to ignite with a spark, though not so volatile that it leads to "vapour lock", i.e. when the fuel is in gas phase in the fuel lines. Furthermore, fuels are a complex mixture of molecules with different boiling temperatures, and therefore the distillation curve can be used to characterise the quality of a fuel. In most standards, it is outlined as a boiling temperature against volume fraction distilled. For gasoline, according to the European standard (EN 228[13]), between 46 and 71 vol% of the fuel must be evaporated at 100 °C, a minimum of 75 vol% must be evaporated at 150 °C, and the final boiling point must be a maximum of 210 °C, leaving a maximum of 2 vol% residue behind. The US standard for gasoline (ASTM D4814[14]) specifies the required distillation in a slightly different way, requiring a 10 vol% recovery at a maximum temperature of between 50-70 °C, 50 vol% recovery at a minimum of 66-77 °C and a maximum of 110-121 °C, 90 vol% recovers at a maximum of 185-190 °C, and a final distillation temperature of 225 °C, leaving a maximum of 2 vol% behind. Standards for diesel and kerosene follow similar trends, with higher temperatures due to the higher carbon number of the fuels.[15-17, 28]

1.2.1.3 Melting Temperature / Pour Point / Cloud Point

The temperatures at which fuels freeze, cloud and pour are all important to the ability of the fuel to flow, and ultimately be pumped to the area of combustion. Though they are linked properties, they are distinct. The melting point is the point at which a substance becomes solid, whereas the pour point is the lowest temperature at which the fuel flows before gelling. A fuel which is below either of these causes major operability problems.[33] Jet fuel is required to remain liquid at extremely low temperatures, and so its melting temperature is regulated to be below -47°C. [17]

The cloud point is the temperature at which dissolved solids in a solution begin to crystallise and cause a transparent mixture to become opaque. In the case of fuels, this is the point at which the species of highest melting point, usually the linear alkenes, precipitate. The presence of these crystals impairs the flow by plugging fuel filters.[34] An alternative measure to the cloud point is the cold filter plugging point (CFPP) which is defined as the temperature whereby the flow is impaired to the point where the engine is rendered inoperable.[35] Diesel fuel, due to the presence of longer chain alkanes, possesses a relatively high cloud point in the range from -20 to +5 °C. However, via treatment with additives, diesel's cloud point and CFPP can be significantly reduced allowing the sale of 'winter diesel', which is separated into two different groups. The first group, for 'temperate' climate zones, is further separated into 6 classes (A-F) which only differ by their CFPP values (5, 0, -5, -10, -15 and -20°C), and the second group, for 'artic' climate zones, is further separated into 5 classes (0-4) also differing on CFPP (-20, -26, -32, -38, and -44°C) as well as cloud point (-10, -16, -22, -28, and -34).[36]

1.2.1.4 Flash Point

The flash point is defined as the temperature at which the vapour of a liquid forms an ignitable mixture with air at atmospheric pressure, and is an important quality of a fuel in terms of safety. Though an important parameter for SI engines, a limit is not specifically outlined in either the US or EU standards for gasoline, though related properties such as maximum vapour pressure, octane number and anti-knock index are. While flash point doesn't affect the combustion of a fuel directly for CI engines it indicates how safe a fuel during its handling, transportation and storage.[37] The flash points for both diesel (52 °C in the US and 55 °C in the EU) and jet fuel (38 °C) are above most ambient temperatures.

1.2.1.5 Viscosity

Viscosity is a measure of flow resistance, and is one of the most important aspects of a fuel as it affects the handling, heating, pumping and atomisation of the fuel. In all fuel standards the viscosity given is the kinematic viscosity, determined by the

time taken for a known volume of fuel to flow under gravity through a capillary tube of a calibrated viscometer.[29]

A fuel of too high viscosity can lead to poor atomisation and delayed / incomplete combustion, increased engine deposits, and could ultimately lead to poor cold temperature performance as viscosity increases as temperature decreases.[32] Conversely if a fuel of too low a viscosity is used, engine seals could fail leading to fuel system leakage which can lead to reduced compression efficiency (and therefore power loss) and increased fuel consumption.

Fuel viscosity is regulated for those fuels obtained from the middle distillates, i.e. diesel and jet fuel. Diesel fuel has to fall between 1.9-4.1 $mm^2 s^{-1}$ in the US, and between 2.0-4.5 $mm^2 s^{-1}$ in the EU (measured at 40 °C). Jet fuel, due to its low temperature requirements, has a maximum allowed viscosity of 8.00 $mm^2 s^{-1}$ at -20 °C, in both the US and EU.

1.2.1.6 Energy Density

The energy density, or calorific value, of a fuel is the energy theoretically obtainable from the fuel via combustion. A higher energy density is desired, as it improves engine performance and vehicle range.[38] As combustion is the exothermic oxidation of a fuel, a fuel with oxygen present in its molecular structure will lead to a lower amount of energy obtainable, and therefore a lower vehicle range. This is a major issue for many biofuels, such as ethanol, as they contain a high proportion of oxygen, whereas the vast majority of fossil fuels only contain trace amounts of oxygenated species. Though not regulated specifically in gasoline or diesel standards, the regulations for Jet A-1 specify that a fuel must have an energy density minimum of 42.80 MJ kg^{-1}.

1.2.1.7 Octane / Cetane Number

One of the most important aspects of a fuel is the delay in ignition on injection in the cylinder. Two scale measurements are used for this in the fuel standards; the octane number and the cetane number. The octane number has a range between

0-100 (compared to heptane and iso-octane, respectively) and is a measurement of the degree to which a fuel can undergo compression before autoignition.[39] There are two different measurements of octane number present in the regulations, research octane number (RON) and motor octane number (MON), determined using a test engine. The fuel's combustion results are then compared with those of *i*-octane and *n*-heptane. Both RON and MON are used in the EU standard for gasoline set at a minimum of 95 and 85, respectively. The US standard for gasoline, however, uses a combined octane rating called "Anti-Knock Index", which is the average of RON and MON and is set at a minimum of 87.

Cetane number is a similar dimensionless measurement, with a range between 0-100 (set at the ignition delay of iso-cetane and cetane, respectively) and is a measurement of how readily a fuel autoignites.[22] High cetane numbers are desired as they reduce engine knock and are reported to reduce undesirable NO_x emissions.[40-41] Therefore fuels with high octane and low cetane numbers are suitable for SI engines, and fuels with low octane numbers and high cetane number are suitable for CI engines. The minimum allowed cetane number for diesel in the EU is 51, while the minimum in the US is 40.

1.2.1.8 Oxidative Stability

Oxidative degradation of fuels is another key issue, as it leads to an increase in viscosity, corrosion, coking, a decrease in energy density, blocked fuel filters and therefore can be detrimental to engine operation.[42,43] One of the major mechanisms by which fuels degrade is termed 'autoxidation', whereby the hydrocarbons react with the dissolved oxygen present in the fuel to form radical species. These then propagate further oxidation leading to the formation of oxygenated species, the precursors for the production of gums and deposits.

The testing methods for a fuel's resistance to degradation are under accelerated oxidation conditions, i.e. high temperature and airflow. These methods generally determine the level of degradation by measuring oxygen content, change in viscosity, or filterable insoluble mass, for which there are maximum levels

allowed.[44] For example, for the ASTM D2274 method, a sample is heated to 95 °C for 16 hours and exposed to air, after which the total insolubles are recorded. The European version for this, EN ISO 12205, only differs slightly in that oxygen is bubbled through the sample. More recently, however, accelerated tests have tended towards the measurement of the volatile carboxylic acids formed in the degradation. Originating from the oleochemical industry, the European standard method EN 14112 or 'Rancimat method' (and more recently the ASTM D525), is carried out by bubbling air at a flow of 10 L h^{-1} through a 3 g sample of the fuel at 110 °C. The airflow, along with the volatile components given off by the oxidising sample, is bubbled through 60 ml of deionized water in which is fitted with an electrode is immersed to measure conductivity. There is a point in the reaction where a sharp increase in conductivity is observed, and the induction point can be determined by the inflection point of this curve (Figure 1.2). Many of the fuel standards quote a minimum induction point, for example 6 hours for EN 228 (gasoline) and 5 hours for ASTM D4814 (gasoline).

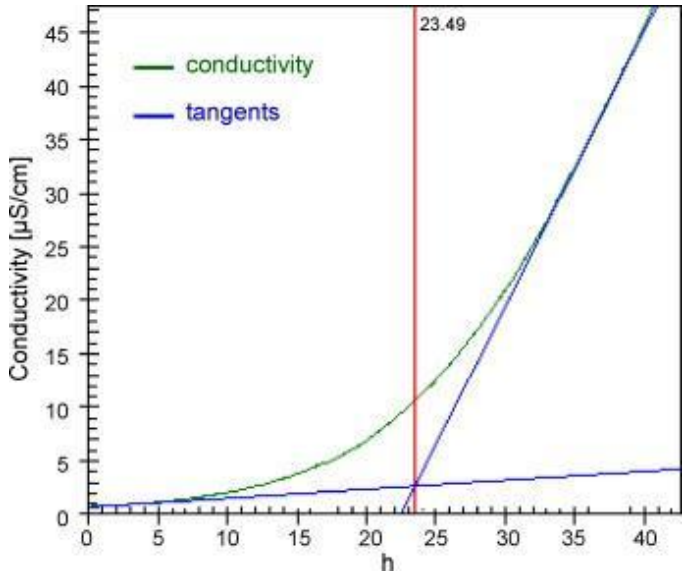

Figure 1.2 Graphical determination of the induction point in standard oxidative stability tests. from Jain and Sharma.[45]

There is disagreement in the applicability of these accelerated tests on a fuel's stability at ambient conditions. Jet fuel, however, is also used as a heat sink on-board aircraft so is exposed to elevated temperatures.[46]

1.2.1.9 LUBRICITY

In the internal combustion engine, a number of moving parts in the combustion chamber, pumps and injectors require lubrication which is typically provided by the fuel. Fuels, therefore, must possess a minimum level of 'lubricity'.[47] Previously sulfurous compounds provided the necessary lubricity. The environmental concerns of fuel sulfur content, which leads to the production of SO_x and subsequently acid rain have led to the production of low-sulfur fuels. This has become a major issue with diesel fuels, increasing the need for fuel reformulation and lubricity-enhancing additives.[48-49]

Lubricity is measured indirectly via a high frequency reciprocating rig (HFRR), whereby a metal plate is submerged in the fuel and a ball-bearing is rubbed across it (1 mm stroke) at a temperature of 60 °C and a frequency of 50 Hz for 75 minutes. After this time, the diameter of the groove worn (the 'wear scar diameter') is measured. For diesel, the allowed wear scar diameter is 460 µm in the EU, and 520 µm in the US. For Jet fuel, the maximum diameter is slightly larger at 850 µm.

1.2.1.10 SOLUBILITY

Though not specifically outlined in regulations for fossil fuels, it is important that a fuel be a singular phase, homogeneous to a molecular level. This is an issue with alternative fuels due to their oxygenated and inherent polar nature. In the case of ethanol, though it itself is soluble with gasoline, it hydroscopic nature solubilises water into ethanol-gasoline blends and lead to phase separation. Any novel fuels, therefore, must remain in one phase with the fuel it will be blending / replacing at the lowest temperature it will be used. Ideally, any novel fuel will be miscible and therefore not limit the blend level.

1.2.1.11 BIOFUEL BLEND ALLOWED

Biofuel blends are included in the majority of road-transport standards for the US and EU. In the EU, a blend of up to 5 vol% ethanol (itself regulated by the standard EN 15376) with gasoline is allowed in the fuel standard EN 228. In the US, ethanol-

gasoline fuels blends have been used since the 1970s. Currently, gasoline which contains up to 10 vol% ethanol (E10, which comprises 90% of vehicle fuel sold in the US[50]) falls within the regulation of ASTM D4814. More recently the EPA approved the use of a 15 vol% ethanol-gasoline blend (E15) to be used in light-duty vehicles produced in 2001 or later. Finally, blends of up to 85 vol% denatured ethanol with gasoline (E85) were approved for use in 'flex-fuel' vehicles. Since then, the standards regulating E85 have changed due to cold-start problems, and so E85 only requires a minimum of 51 vol% ethanol.[51]

Diesel standards, however, allow biodiesel (itself regulated by EN 14214 in the EU and ASTM D975 in the US) blends of up to 7 vol% in the EU and 5 vol% in the US, though a specification for biodiesel blends of between 6-20 vol% with diesel has been created for on- and off- road use in the US.[52] In recent years, two biofuels have gained ASTM approval for use in the aviation industry – Fischer-Tropsh synthetic paraffinic kerosene (FT-SPK) and hydrotreated esters of fatty acids (HEFA) – and can be used in up to a 50 vol% blend with conventional jet fuel.[53]

1.3 RENEWABLE LIQUID FUELS (BIOFUELS)

In contrast to other renewable energy resources biomass is the only source of fixed carbon and as such it is vital for the production of liquid hydrocarbon fuels and chemicals. There is a vast range of different biofuel technologies, which are loosely characterised by three 'generations', though there is little consensus on their exact boundaries. Fuels derived from food crops, such as corn and edible oils, are termed first generation. The second generation includes fuels that are produced from waste oils or non-food crops, such as cellulosic material and inedible oils. Third generation fuels are those derived from photosynthetic microbes.[54]

There are many different technologies that could convert biomass into liquid fuel molecules (Figure 1.3).[55-58] Regardless of the generation, these can be separately broadly into three groups:

i. Fuels derived from the lipids produced by oleaginous plants, animals and microbes.

ii. Fuels derived from the biochemical conversion of biomass (i.e. fermentation).

iii. Fuels derived from the chemical conversion of biomass (i.e. thermochemical conversion and hydrolysate upgrading).

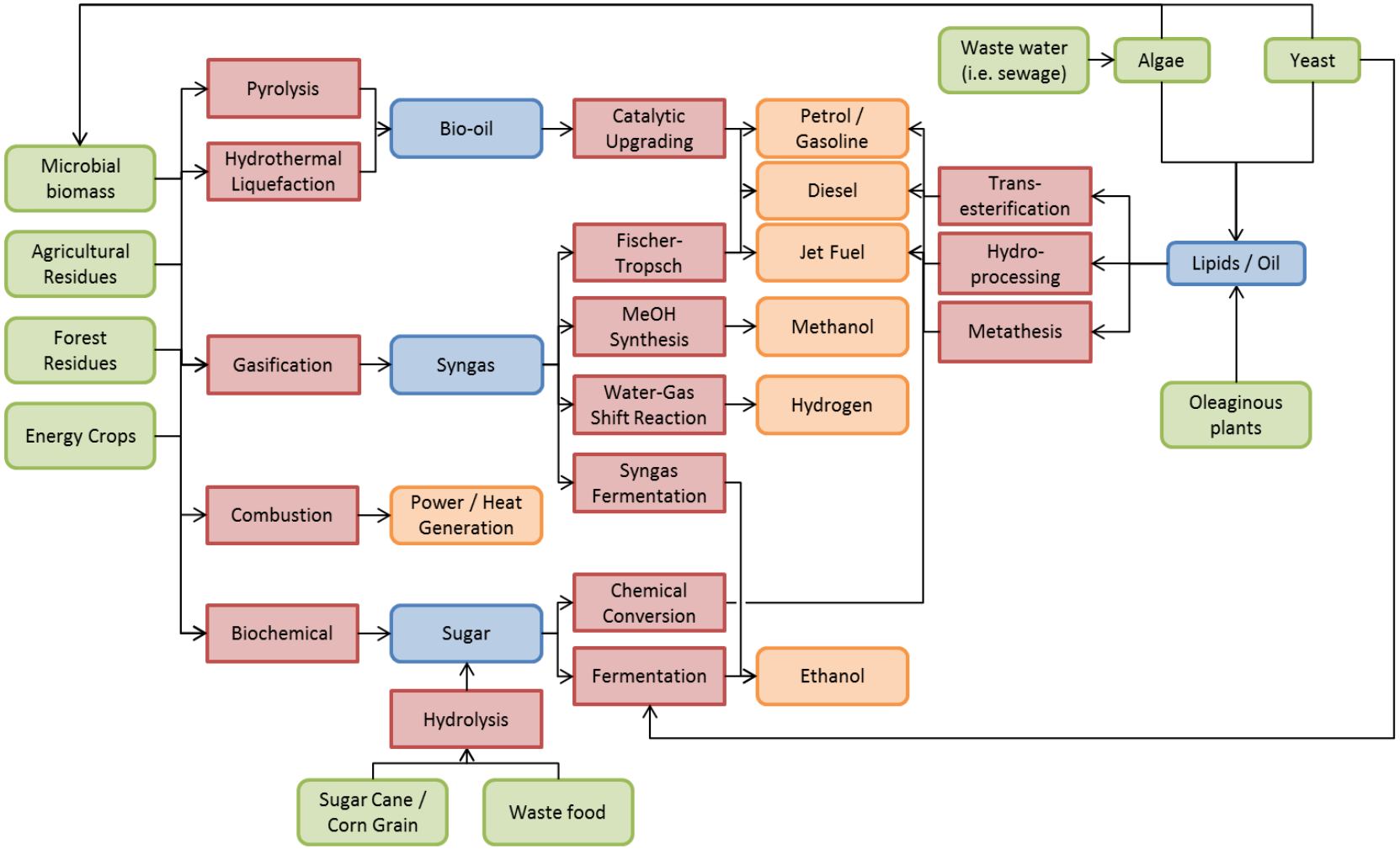

Figure 1.3 Selected pathways from biomass to intermediates and final transport biofuel products. Adapted from Yue, *et al.*[58]

1.4 LIPID DERIVED FUELS

1.4.1 SOURCES AND CHALLENGES

Lipids derived from animal and plant oils are one of the possible feedstocks for a sustainable fuel source. The primary constituent of the lipids are triglycerides which consist of one glycerol 'backbone' and three fatty acid chains of variable carbon length and saturation (Figure 1.4). The triglyceride lipid can be used as a diesel substitute without further chemical upgrading. Interestingly, Rudolf Diesel realized this potential and operated one of his engines purely on peanut oil in the Paris World's Fair in 1900, which "*worked so smoothly very few people were aware of it*".[59] He also realized the need for a renewable fuel in the future, stating in a presentation to the Institution of Mechanical Engineers that "*in any case, [biofuels] make it certain that motor-power can still be produced from the heat of the sun, which is always available for agricultural purposes, even when all our natural stores of solid and liquid fuels are exhausted*".[23]

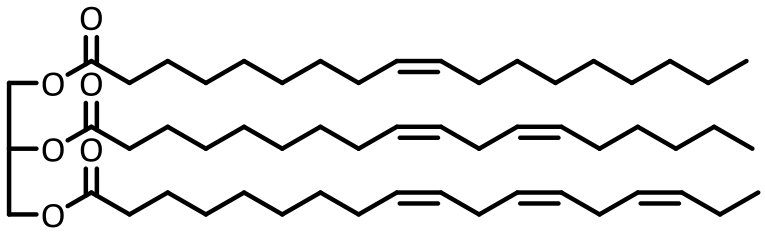

Figure 1.4 Example structure of a triglyceride

However, the triglycerides themselves are not suitable as a diesel replacement due to their high viscosity. This leads to poor atomisation in the combustion chamber[60] which in turn leads to coke deposits, clogged filters and lubricating oil contamination.[61] To address these issues the use of different blend ratios, pre-warming the oil and altering the combustion chamber have been explored and reported.[60] However, the most feasible solution to lower the viscosity of the oil is via chemical transformation. This is most commonly achieved via transesterification of the triglycerides with an alcohol (usually methanol) to produce fatty acid methyl

esters (FAMEs, biodiesel), though other transformation such as metathesis and hydroprocessing are possible alternatives.

First generation lipids are produced from terrestrial oleaginous plants, such as rapeseed, soya, sunflower and palm.[23] Many other edible oils have also shown potential as sources for biodiesel,[62] though are less common. Currently 95% of lipid-based fuel derives from edible oils.[63] There is, however, not enough of these feedstocks to satisfy the global fuel demand. Furthermore, they compete with food production as they require arable land to be produced. Due to the morally questionable practice of producing fuel from land that could otherwise be used to feed an ever-increasing population, much research has gone into the development and production of alternative lipid sources. These include second generation oils such as waste frying oils and animal fats,[64] as well as inedible oil from plants cultivated on marginal land such as jatropha, karanja, and cotton seed.[65-66] However, there are a number of issues with these feedstocks. Waste frying oils and animal fats contain a significant amount of free fatty acids, which are detrimental to catalytic processing and engine performance. The non-edible feedstocks, though capable of producing oil from non-agricultural land, exhibit significantly reduced oil yields when compared to their cultivation on nutrient rich arable land.

More recently, however, there has been increasing research into developing third-generation feedstocks, microbial oils such as algae, yeast and bacteria,[67-68] and other alternative sources such as insects[69] and fungi.[70] These feedstocks have the potential to produce far higher amounts of lipids than terrestrial plants per unit of land area used, are not limited by seasonal growth and need a shorter amount of time to produce the lipids. A number of challenges remain before third generation lipids can be considered commercially viable. Due to the relatively robust nature of algal cell walls, there is a significant amount of process cost in the cultivation and harvesting of the biomass, drying and lipid extraction.[71] For yeasts, the production of the oil is expensive due to the high cost of the nutrient and media to grow them, as well as the significant initial investment required. However, if waste and lignocellulosic resources can be efficiently depolymerised and effectively used to grow the yeasts, the cultivation cost would be drastically reduced.[72]

There is a large variation in triglyceride structure – largely dependent on species and growth conditions – generally in the chain length and saturation of the fatty acids. This variation alters the properties of the fuel produced from them. The common nomenclature used to describe the structure of the fatty acid chains is to follow the number of carbons in the chain by the number of double bonds present, separated by a colon. Frequently included is the position of the double bond from the terminal carbon (i.e. the omega number). Therefore methyl linoleate, which is 18 carbons long and has two carbon-carbon double bonds in its chain, and a double bond on the 6^{th} carbon along the carbon chain, is referred to as "18:2ω6". Table 1.2 shows the different yields and fatty acid profiles of selected lipid feedstocks.[62]

Table 1.2 Oil yield, content and fatty acid profile of various lipid feedstocks.[62, 68-69, 73-80]

Lipid feedstock	Oil yield / l ha^{-} a^{-}	Oil content / %	Fatty acid profile / %														
			14:0	14:1	15:0	16:0	16:1	16:2	16:3	18:0	18:1	18:2	18:3	20:0	20:4	20:5	22:1
Soybean	446	15-20	<0.5	-	-	7.0-11.0	-	-	-	2.0-6.0	19.0-34.0	43.0-56.0	5.0-11.0	<1.0	-	-	-
Rapeseed	1190	38-46	-	-	-	4.9	-	-	-	1.6	33.0	20.4	7.4	-	-	-	23.0
Palm	5950	30-60	0.5-2.0	-	-	32.0-45.0	-	-	-	2.0-7.0	38.0-52.0	5.0-11.0	-	-	-	-	-
Beef tallow	-	-	3.0-6.0	-	-	24.0-32.0	-	-	-	20.0-25.0	37.0-43.0	2.0-3.0	-	-	-	-	-
Jatropha	1892	30-40	0.5-1.4	-	-	12.0-17.0	-	-	-	5.0-9.5	37.0-63.0	19.0-41.0	-	0.3	-	-	-
Karanja	5040[a]	27-39	-	-	-	3.7-7.9	-	-	-	2.4-8.9	44.5-71.3	10.8-18.3	-	6.4-10.0	-	-	-
Cotton	325	45931	0.4	-	-	20.0	-	-	-	2.0	35.0	42.0	0.1-2.1	<0.5	-	-	-
Chlorellla vulgaris **(Algae)**	2310-3850[b]	5.0-58.0	0.1	0.2	-	16.9	0.6	2.0	5.1	6.5	48.2	8.5	11.6	-	-	-	-
Nannochloripsis sp. **(Algae)**	6940-19300[b]	12.0-53.0	6.5	0.1	0.4	36.1	27.6	-	0.1	1.1	19.7	1.2	-	-	2.3	4.5	-
Scenadesmus sp. **(Algae)**	5500-53000[b]	4.0-16.6	2.6	5.5	-	30.8	6.2	-	-	-	2.1	48.1	-	-	-	-	-
Rhodotorula glutinis **(Yeast)**	15000[c]	72.0	-	-	-	18.0	1.0	-	-	6.0	60.0	12.0	2.0	-	-	-	-
Lipomyces starkeyi **(Yeast)**	-	64.0	-	-	-	33.0	4.8	-	-	4.7	55.1	1.6	-	-	-	-	-
Cryptococcus albidus **(Yeast)**	-	65.0	-	-	-	16.0	1.0	-	-	3.0	56.0	-	3.0	-	-	-	-
Pseudomonas aeruginosa **(Bacteria)**	-	38.0	-	-	-	17.6	0.6	-	-	2.8	34.2	-	-	5.3	-	-	-
Galleria mellonella **(Insect)**	-	47.0	0.2	-	-	34.6	2.2	-	-	1.5	53.9	6.6	0.5	-	-	-	-

a – based on assumed yields of the karanja seed (350 trees per hectare, 20,000 seeds per tree, 1.8 g per seed, 40% glyceride species)
b – calculated from yields given in g m^{-2} day^{-1}
c – estimation based on lab results for *R. glutinis* oil yield, and amount of lignocellulosic feedstock (wood, assuming 100 tonnes lignocellulose ha^{-1})

1.4.2 BIODIESEL

Biodiesel is a diesel-replacement biofuel and is generally the term given to fatty acid alkyl esters (FAAEs) which are obtained from biological lipid sources, such as plant oils and animal fats.[23] It commonly represents between 15-25% of annual global biofuel production,[81] with 28.3 billion litres produced worldwide in 2013.[82] The most economical process to produce biodiesel is via the alkali-catalysed (usually sodium or potassium hydroxide) transesterification of triglycerides with three equivalents of alcohol (usually methanol due to its low cost), and so the majority of biodiesel is produced this way (Scheme 1.1).[83] Industrial methods, however, use a slight excess of methanol (usually 4.5-6 equivalents to the triglyceride) to drive the reaction, following Le Chatelier's principle.[84] This process achieves biodiesel in a 98% conversion yield, requiring low processing temperature and pressure, but produces crude glycerol (i.e. containing traces of soap, catalyst and alcohol) as a by-product, for which the purification is energy intensive. Much recent research, therefore, has concentrated on alternative methods for transesterification such as heterogeneously-catalysed[85] and enzyme-catalysed processes[86] which have the advantages of low energy consumption, low soap formation and high glycerol purity obtained.

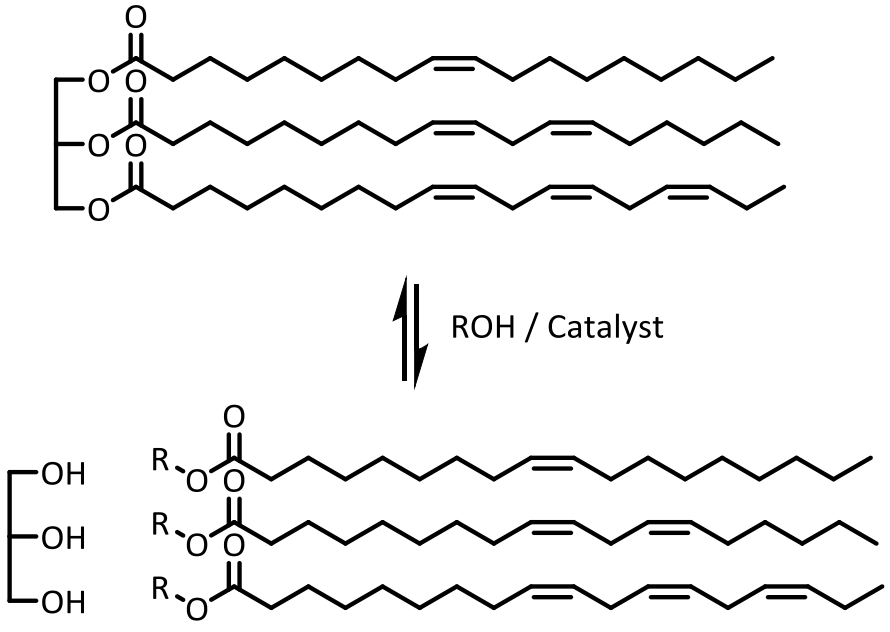

Scheme 1.1 General reaction scheme of the transesterification process for biodiesel production

The properties of biodiesel, and therefore its suitability as a fuel, are determined by the fatty acid methyl ester (FAME) profile. Different FAMEs have vastly different physical properties depending on the saturation and to a lesser extent their chain length. Generally long chain saturates have high viscosities and melting points, together with high cetane numbers. Long chain saturates, therefore, are unsuitable for diesel replacements as they would affect cold temperature operation. Monounsaturates have viscosities more similar to diesel, melting points below 0 °C (though usually above -20 °C), and lower cetane numbers. For the same reason, fuels high in these components are not suitable for aviation as the Jet A-1 standard requires a fuel with a minimum freezing point of -47 °C (Table 1.1).[17] Polyunsaturated esters, however, have extremely low viscosities, melting points significantly lower than conventional diesel (e.g. 18:3 has a melting temperature of below -50 °C) and relatively low cetane numbers.[33] Higher saturation, however, leads to lower oxidative stability.[87] Oxidative degradation of biodiesel leads to a change in fuel properties, such as increased viscosity, with can result in issues with engine performance.[42, 88] Unsaturates can also affect the exhaust emissions, generally increasing the amount of NO_x.[89] This can possibly be attributed to the lower cetane numbers of unsaturated FAMEs, leading to a higher combustion temperature which favours NO_x formation.

While long chains are the most prevalent (C_{16+}), shorter chain esters tend to have lower viscosities, lower melting points and lower cetane numbers than their longer chain counterparts. However, the majority of fatty acids produced by terrestrial crops have carbon numbers ranging from C_{16} to C_{20}, with palmitic acid (16:0), stearic acid (18:0), oleic acid (18:1), linoleic acid (18:2), linolenic acid (18:3) and erucic acid (20:0) being the most common. It should be noted, however, that the FAME profile of biodiesel can depend on the growth conditions of the plant cultivation.[90] As the properties of biodiesel are so dependent on the structure of the FAMEs, standards have been instigated such as EN 14214 in the EU and ASTM D6751 in the US which dictate not only the ranges of each property they must comply to, but also limits the presence of certain species such as methyl linolenate

(to 12 mol%), polyunsaturates of more than 3 double bonds (to 1 mol%) and free glycerides.

Biodiesel is a robust, well-understood fuel technology that has significant potential for further uptake as a drop-in road transport fuel. If the cost of the feedstock could be reduced (it is estimated to account for 70-95% of the overall cost of the fuel[91]), it could become economically competitive with current fossil fuels. However, it is not without issues. A particular disadvantage of biodiesel is its slightly lower energy density compared to its fossil fuel counterpart (by approximately 10%[23]), which reduces the range of the vehicle powered by it. Despite this, biological lipids will become a significant feedstock in the future. Therefore, a number of alternative chemical transformations are being investigated that could lead to improved physical properties. Applying these chemical transformations to lipids from microbes cultivated on sustainable cellulosic resources could produce truly renewable liquid fuels for a range of applications, not just CI engines.

1.4.3 HYDROPROCESSING

One method of creating de-oxygenated biofuels (and therefore improving the physical properties of the fuel obtained) is by hydroprocessing (or 'hydrotreatment'), which in itself contains a number of different mechanisms to produce hydrocarbons from lipid feedstocks. It is a process whereby organic feedstocks which contain double bonds and oxygen-containing functional groups are de-functionalised and converted into saturated hydrocarbons.[92] According to the accepted mechanism, the unsaturated fatty chains are first hydrogenated, forming a saturated triglyceride. This is followed by the scission of the carbon-oxygen single bond to yield propane and three equivalents of long-chain saturated carboxylic acids. These are then de-oxygenated in one of two ways, either by hydrodeoxygenation, which produces water and a long chain alkane of the same carbon number as the carboxylic acid, or by hydrodecarboxylation, producing carbon dioxide and a long chain alkane one carbon shorter than the carboxylic acid (Scheme 1.2).[93]

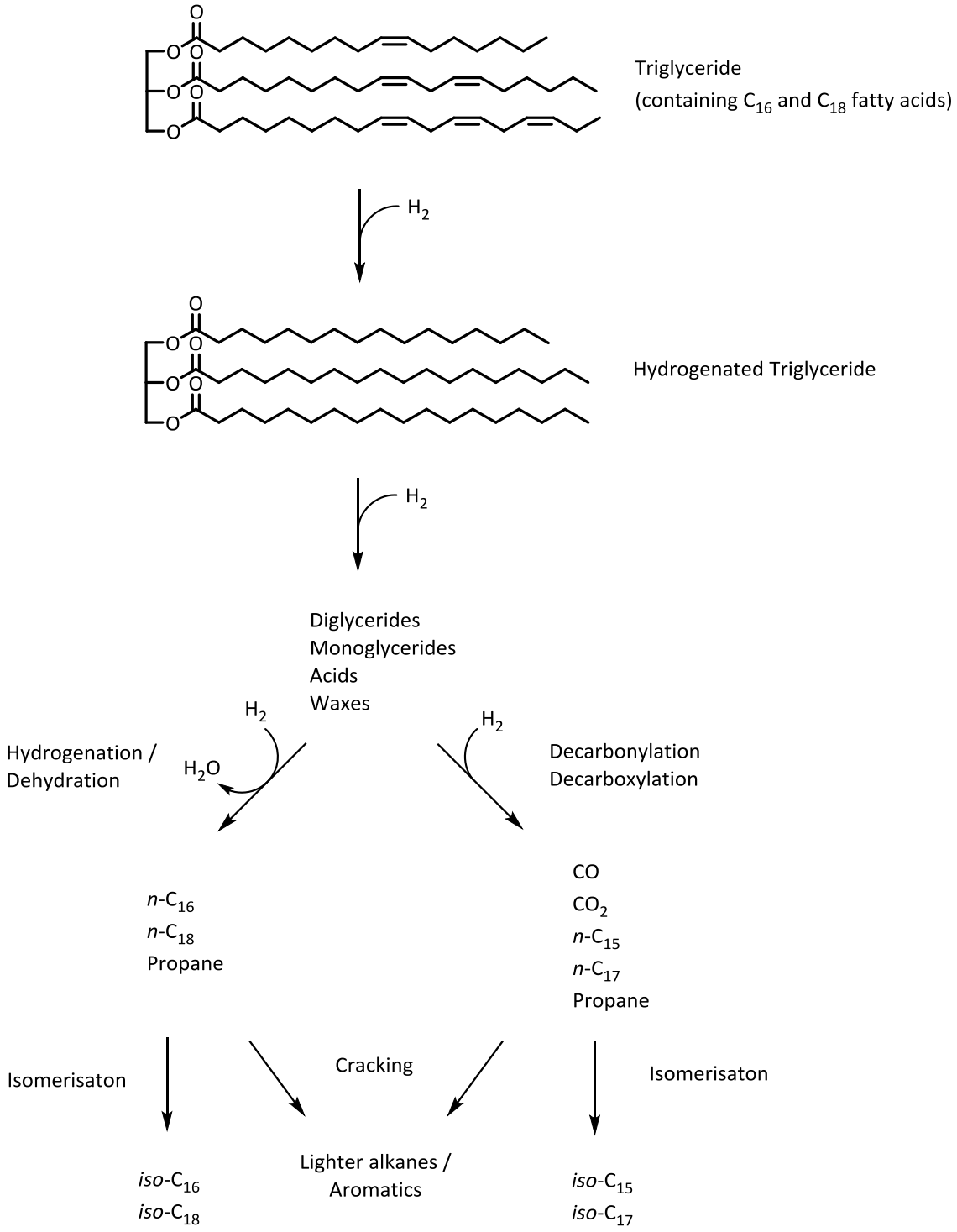

Scheme 1.2 Reaction pathway for the conversion of triglycerides into alkanes via hydrotreatment. Adapted from Corma and Huber.[56]

The hydrotreatment of oils needs relatively high pressures of H_2 (1.5 MPa), moderate temperatures (250 °C), and the presence of heterogeneous catalysts such as sulfur-activated alumina supported NiMo[94] or CoMo.[95] The sulfur used to activate the catalysts however can be an issue if leached into the fuel as the sulfur content of fuels is rigorously regulated. In an investigation of non-sulfur activated metal catalysts, Snåre *et al.* screened a range of carbon and metal oxide supported metal particles (Ni, Mo, Pd, Pt, Ir, Ru, Rh, and Os) for their activity for the decarboxylation of fatty acids, at 300 °C and 600 kPa. It was found that 5% Pd/C was the most active catalyst, converting 100% of the substrate with >98% selectivity to heptadecane.[96]

Hydroprocessing of lipids forms alkanes, which are desirable as these molecules possess higher energy density than biodiesel or bioethanol due to their lack of oxygen. However, their physical properties are still not ideal. The long-chain alkanes formed, between the range of C_{15} and C_{18}, have a melting point above that of the cloud point of diesel. They may, however, have limited applicability as cetane improvers. Therefore to produce a fuel which is more suitable, and that could be used in the aviation sector, further processing must be carried out, such as cracking and isomerisation.[97] Cracking of vegetables oils dates back to the 1920s, where early acidic ($AlCl_3$, Al_2O_3) and basic (MgO, CaO, NaOH) catalysts were used at temperatures between 400-500°C.[98] However, these methods and later ones, employing zeolites, are non-selective. Yields of desirable compounds, therefore, are low due to the production of short chain alkanes. The control of this isomerisation has been a subject of research in recent years.

In a recent report by Wang, *et al.*, a number of Ni-impregnated zeolite catalysts were investigated for their activation as hydrotreatment and subsequent isomerisation catalysts at temperatures of 300-380 °C, 4 MPa hydrogen pressure, in a three-phase, fixed-bed reactor.[99] Using an 8 wt% Ni/SAPO-11 catalyst, soybean oil was 100% converted, with a 74.8% organic liquid yield. This liquid consisted purely of saturated hydrocarbons, 85.6% of which were products of isomerisation and 15.4% of which were products of cracking (reported as C_7-C_{14} alkanes), the rest being long chain linear alkanes. The level of isomerisation reported has produced

fuels more reasonably in line with diesel standards, but a higher level of isomerisation would be needed to produce an aviation-suitable fuel. The issues which inhibit the sustainable large-scale production of hydrotreated fuels from lipids are the current cost of the process and that hydrogen is currently sourced largely from fossil fuels, specifically the steam reformation of natural gas.[100]

1.4.4 METATHESIS

An alternative method for producing hydrocarbons from lipids is by cleaving the double bond moiety via metathesis: the reversible, metal-catalysed exchange of alkene fragments (alkylidene groups) between two alkenes. Olefin metathesis is one of the most important chemical transformations of recent decades, as it is one of the most flexible and facile methods for producing new carbon-carbon bonds. It can be found in industrial processes for specific olefin, polymer and fine chemical synthesis,[101] though applications in medicine, biochemistry, material science and oleochemistry are rapidly growing.[102] Such has been the impact of olefin metathesis that the Nobel Prize for Chemistry in 2005 was awarded to the pioneering researchers in the area: Yves Chauvin (for which the accepted mechanism is named), Robert H. Grubbs (for which the more robust Ru-based catalysts are named) and Richard R. Schrock (for which the more reactive Mo-based catalysts are named). The accepted mechanism involves the direct [2+2] cycloaddition of an alkene to a metal-carbene complex to form a metallocyclobutane intermediate, which can break down to yield a metathesised unsaturated hydrocarbon species and a metal-carbene species. This metal-carbene can then continue the catalytic cycle (Scheme 1.3).[102-103]

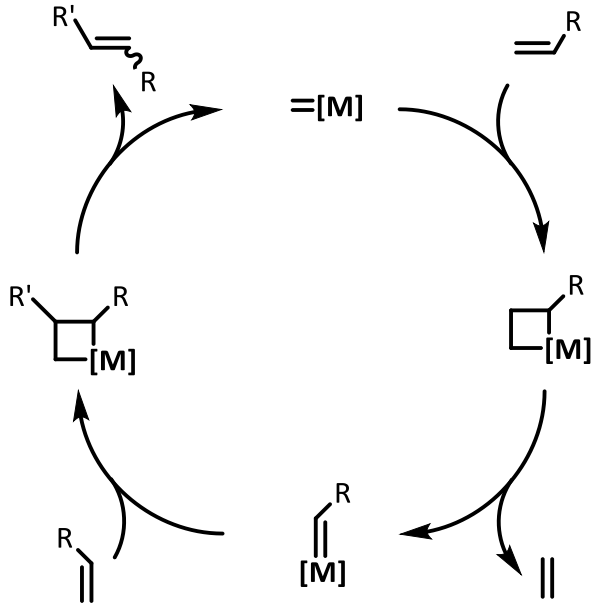

Scheme 1.3 General mechanism of olefin metathesis, adapted from Hérisson and Chauvin.[103] It should be noted that each stage of the mechanism is reversible.

Lipid metathesis is generally used in the polymer[104] and higher value chemical production.[105] Self-metathesis – whereby the double bonds of the fatty acid chains exchange with each other – has been reported in the production of long-chain di-carboxylic acids as a precursor for polymers,[106-107] as well as a potential method to improve the fuel properties of biodiesel.[108] In cross-metathesis, however, an external alkene source is used to cleave the double bond and yield shorter chain compounds.[109-110] Examples of both are shown in Scheme 1.4, using oleic alkyl ester as a substrate.

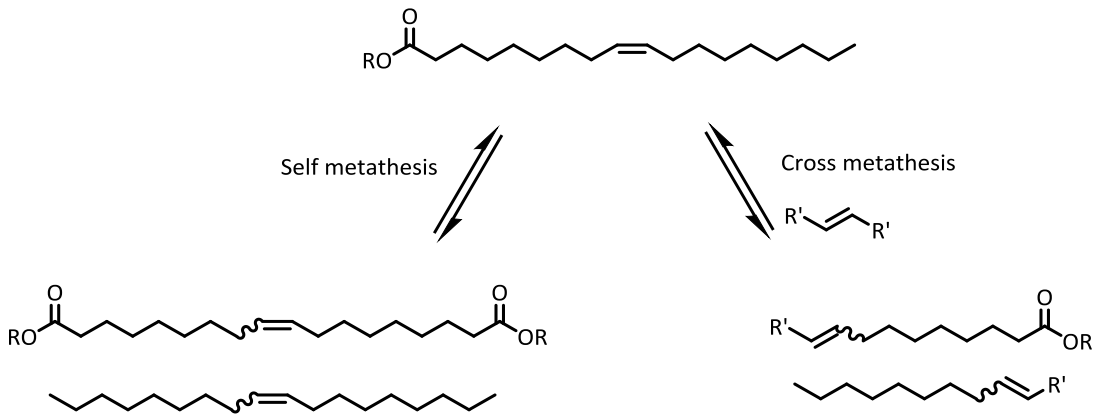

Scheme 1.5 Self- and cross-metathesis of oleic alkyl ester.

The first catalytic system reported to successfully metathesize unsaturated lipids was the homogenous WCl_6/Me_4Sn system, by van Dam *et al.* in 1972.[111] Methyl oleate was self-metathesized using 1-2 mol% of WCl_6/Me_4Sn. Cross-metathesis of methyl oleate and 3-hexene was also investigated, with 20% conversion of the starting materials achieved. The heterogeneous catalyst system 2.5% Re_2O_7/Al_2O_3 has also been used in the metathesis of lipids, using methyl erucate and methyl-10-undecanoate as substrates, which reached 65% and 50% conversion after 20 mins at 70 °C.[112] These catalytic systems, though cheap and easy to prepare, are limited by their low tolerance of the functional groups and moisture in the atmosphere, and therefore only low turnover numbers can be achieved.[113]

Ruthenium alkylidene-based catalysts, such as Grubbs 1st generation catalyst (Figure 1.5, **A**) and subsequent generations were found to have the best functional group tolerance, some of which do not require an inert atmosphere.[114] The majority of metathesis catalyst research currently focuses on these and related catalyst systems. For the self-metathesis of methyl oleate, Grubbs 2nd generation catalyst (Figure 1.5, **B**) has been reported to achieve turnover numbers of up to 4.4×10^5 at very low catalyst loadings (1×10^{-6} mol%).[115] Similar turnover numbers can be reached for the cross-metathesis of internal alkenes, such as 2-butene and 3-hexene with methyl oleate.[116] These internal alkenes, however, are derived from petrochemicals. Ideally, the cross-metathesis of lipids would be achieved with an alkene derived from renewable sources, such as ethene. Cross-metathesis with terminal alkenes such as ethene (ethenolysis) is far less favoured due to the instability of ruthenium methylidenes, the catalytic intermediate formed from the reaction between the alkene and Grubbs catalyst.[117] This leads to turnover numbers of several magnitudes lower than typically reported,[118] and high yields only achievable with far higher catalyst loadings.[110]

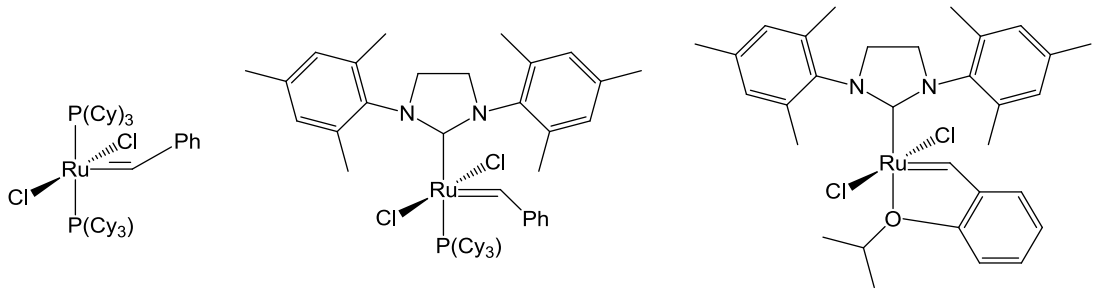

A **B** **C**

Figure 1.5 Molecular structures for a) Grubbs 1st Generation Catalyst; b) Grubbs 2nd Generation Catalyst, and; c) Hoveyda-Grubbs 2nd Generation Catalyst

In the metathesis reactions mentioned, research has been carried out on FAAE lipid model compounds (normally methyl oleate). This allows for easier analysis and conversion calculation. However, for metathesis to be deemed a possible replacement for transesterification, it must be carried out on naturally occurring lipids. Triglycerides have three fatty acid chains of varying length and saturation. Therefore, metathesis of these would result in intramolecular reactions (which are strongly favoured to intermolecular reactions) in both self and cross metathesis. Self-metathesis of olive oil, which consists primarily of glyceryl trioleate, leads to the formation of 9-octadecene, cross-linked fatty acids of the same molecule, and polymeric triglycerides.[119] Metathesis of polyunsaturated fatty acid chains, due to the common distribution of the double bonds present, would lead to the formation of a range of shorter-chain volatile alkenes, such as 1-butene, 1,4-pentadiene and 3-hexene.[120] Though the production of some of these short-chains has been reported in a handful of reports investigating the ethenolysis of polyunsaturated esters,[119-121] the significance of them has been overlooked, though they have the potential to be useful precursors or intermediates for higher value products, and could potentially financially support the production of fuel via metathesis.

For ethenolysis, increasing the concentration of ethene (and therefore the pressure) increases the selectivity for cross-metathesis whilst sacrificing productivity due to increased catalyst deactivation. The ethenolysis of glycerol trioleate yielding three equivalents of 1-decene and one equivalent of tridecenylglycerol (Scheme 1.5), and was investigated using 18 wt% Re_2O_7/Al_2O_3 and 3 wt% $Re_2O_7/SiO_2{\cdot}Al_2O_3$ at 30 bar pressure of ethene and ambient temperature.

The more active catalyst was 18 wt% Re_2O_7/Al_2O_3, reaching 84% conversion after 30 mins.[122] Cross-metathesis with sustainable alkenes could have the potential to produce fuel-like molecules. Currently little work has considered metathesis as a fuel production process, and therefore its viability should be investigated.

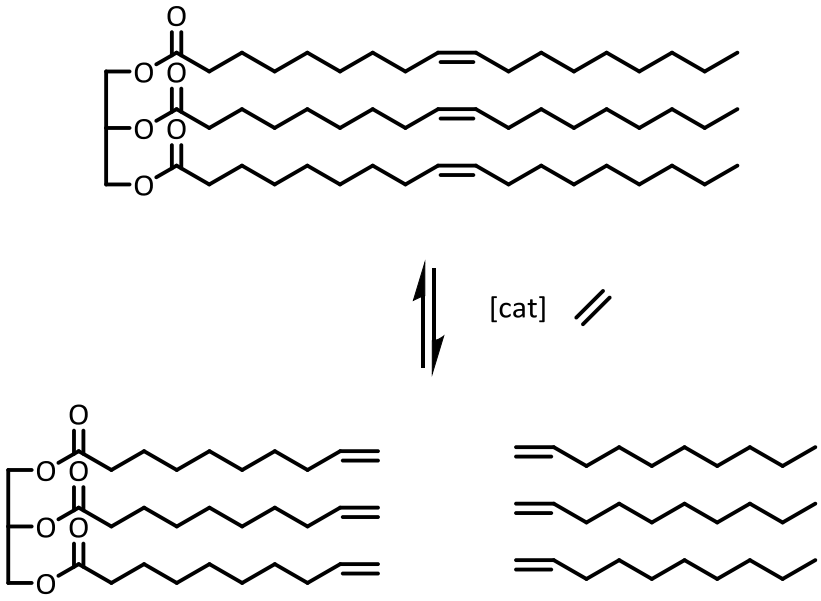

Scheme 1.6 Ethenolysis of glyceryl trioleate

1.5 LIGNOCELLUSOIC BIOMASS DERIVED FUELS

1.5.1 SOURCES AND CHALLENGES

Though lipids provide a good source of relatively pure feedstock for fuel production, they only account for a small fraction of the total biomass produced by an organism. Recent research has focussed on methods that have the potential to convert a much higher proportion of the fixed carbon in a biomass feedstock into liquid fuels.

The first generation of biomass resources are those high in sugars and starches which are converted into fuels through fermentation. These feedstocks include sugar cane and sugar beet from which sucrose can be obtained directly, and those which are high in starch such as corn. The starch must be hydrolysed with an amylase enzyme to produce sugars before the fermentation process can proceed.

The second generation of biomass resources are sourced from lignocellulosic resources that do not compete with food production. These can be in the forms of dedicated energy crops, such as perennial grasses such as switchgrass and miscanthus, or short rotation wood crops such as willow and poplar. Approximately 90% of the dry weight of all plant material consists of cellulose, hemicellulose and lignin (collectively termed 'lignocellulose').[123] One option for the conversion of this biomass is via thermochemical treatment methods, which have the advantage of high yields, though complex mixtures are obtained. A more directed biofuel production is fermentation, however the biomass requires extensive treatment to release the sugars needed.

Other second generation forms of biomass to be used are waste materials; those being agricultural wastes, forestry wastes, municipal and industrial wastes and food waste. All have different potential in terms of social and environmental impact, whether the wastes can be utilised in a biorefinery concept in industries which produce the wastes, or via more local approaches whereby the waste can be collected and taken to a local treatment facility. Waste food is a good example of

this. The majority of non-lipid waste food valorisation techniques involve incineration, composting, and anaerobic digestion to produce methane,[124] though hydrolysed food waste has shown promise as a fermentation feedstock.[125]

As aforementioned, third generation fuels derive from microbes, most generally algae which photosynthesize and incorporate CO_2 from the atmosphere into their biological make-up. The majority of this research has concentrated on algal lipids, though in recent years, the use of algal biomass as a feedstock itself has been considered. This has been reportedly done via fermentation of the algal biomass (with pre-treatment),[126] as well as thermochemical routes (e.g pyrolysis,[127] gasification[128] or hydrothermal liquefaction[129]).

1.5.2 Biological conversion

1.5.2.1 Fermentation

Microbes produce a range of metabolic products (i.e. via fermentation), which have the potential to be used as alternative liquid fuels. The majority of microbes require cultivation on sugar, obtained from sugar and starch rich plants, or lignocellulosic resources, which require pre-treatment. The cellulose and hemicellulose present in lignocellulose, both carbohydrate chains, requires depolymerisation to their sugar units before fermentation can take place. This is done using dilute acidic conditions (for hemicellulose), concentrated acidic conditions (for cellulose), or enzymatic hydrolysis. The lignin portion of lignocellulose, an aromatic polymer, provides structure and a physical barrier that prevents degradation of the cellulosic material. Before hydrolysis and subsequent fermentation can take place, therefore, biomass must be pre-treated to break down the lignin structure and expose the cellulosic portion (Figure 1.6). These include physical pretreatments such as mechanical milling, partial pyrolysis and ultrasound; chemical pretreatments such as ozonolysis, alkaline hydrolysis and organo-solv processes; and biological pretreatments such as enzyme addition and wood-decay fungi.[130-131] This pre-treatment can be the most expensive stage of the biomass-to-fuel process, and therefore much research into increased efficiencies and different methods has taken place.

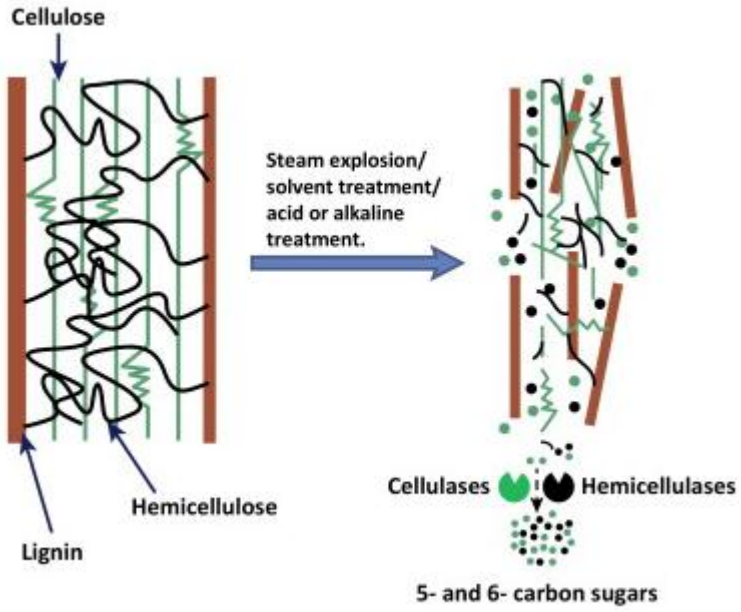

Figure 1.6 Schematic of the role lignocellulosic biomass pre-treatment (adapted from Mir, *et al*.[132])

Bioethanol

Bioethanol is the term given to ethanol produced from biomass through fermentation with the specific purpose to be used as liquid fuel. Industrially it is produced via the fermentation of starches and sugars found in grains and vegetables.[133] The process is well understood and bioethanol is by far the most widely used liquid biofuel, accounting for 75-85% of global biofuel production.[81]

In 1896, Henry Ford's first car – the 'Quadricycle' – ran on pure ethanol. Such was Henry Ford's belief in ethanol that he dubbed it the 'fuel of the future' in an interview with the New York Times in 1925, saying that "*there is fuel in every bit of vegetable that can be fermented*".[134] It was only in the 1920s as oil refining and extraction became significantly cheaper that gasoline became the main fuel source for the automotive industry. However, in the last few decades there has been a resurgence in the production of ethanol fuel, leading to large amounts of agricultural produce such as maize in the US and sugarcane in Brazil.[135]

The use of ethanol as an alternative fuel poses certain advantages, such as reduced greenhouse gas (GHG) and toxic exhaust emissions during combustion,[133] however certain life cycle assessments of ethanol fuel have concluded that it causes a net overall increase in GHGs when compared with gasoline, in particular when

produced from corn stover.[136] Sugarcane-derived ethanol, however, has a very favourable GHG emissions balance due to the high energy output/input ratio of its production (Figure 1.7).

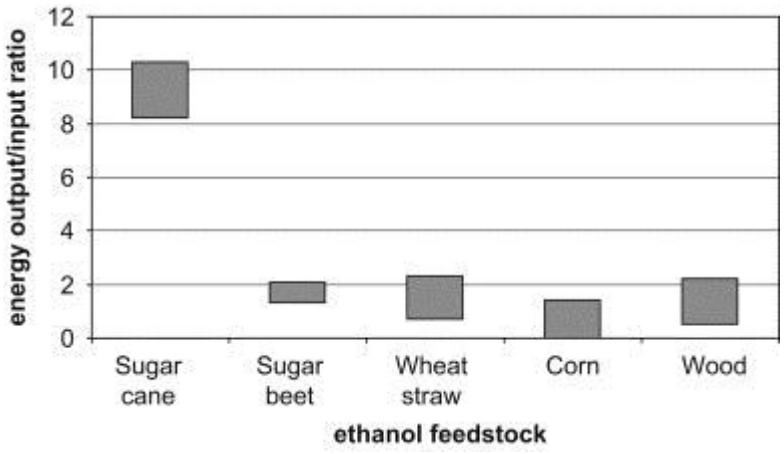

Figure 1.7 Energy balance of ethanol production from different feedstocks, from Goldemburg *et al.*[137]

There are many technical factors which make ethanol undesirable as a complete replacement. Firstly, it has a significantly lower energy density than normal gasoline (approximately two-thirds per unit mass[138]). This is due to its high amount of oxygen, leading to less carbon-hydrogen bonds to be oxidised and therefore a reduced energy density and, in turn, the range of a vehicle using an oxygenated fuel. It can also lead to damage of the engine itself, either by absorbing water from the atmosphere and corroding the metal, or by stiffening and swelling the non-metallic seals.[133] Cars with specifications which allow them to cope with high-alcohol blends have been and are currently in production, though only blends with low quanities of ethanol with gasoline can be deemed 'drop-in' fuels for the all SI vehicles currently on the road. Lastly, if the need for ethanol fuel increases, the production of ethanol could compete with the production of food.

Biobutanol

Though bioethanol is the most efficiently and widely produced alcohol via fermentation for fuel, one promising alternative is biobutanol (generally *n*-butanol) which possesses a number of technical advantages over ethanol. It has a higher energy density and is less corrosive than ethanol, and as such its physical properties

are more closely matched with diesel and blends well with it,[139] and could be used and distributed using current infrastructure. An assessment of net energy gain comparing ethanol and butanol production by Swana, *et al.* found that corn-to-butanol conversion results in a net energy gain of 6.53 MJ L^{-1}, far greater than that for corn-to-ethanol (0.40 MJ L^{-1}). This is attributed to the significant energy needed for separation of the azeotropic mixture formed between water and ethanol.

Despite its technical advantages, however, the major issue associated with butanol fuel is the amount of feedstock and ultimately cost it requires to produce. It was traditionally made by fermentation via the acetone-butanol-ethanol (ABE) process, where the bacteria *Clostridium acetobutylicum* is used to ferment molasses or cereal grains.[140] The process is non-specific, producing acetone and ethanol also in a 6:3:1 ratio with butanol. As such, roughly half the alcohol (by unit volume) is produced than in the equivalent ethanol fermentation. The toxicity of the butanol to the bacteria is also as issue, as they cannot survive at a butanol concentration of above 2%,[54] whereas ethanol-producing yeasts can withstand ethanol concentrations of 15-20%. This reduces the productivity of butanol, increases the water usage, and therefore the cost of production, substantially. An economic assessment for butanol production estimated its production cost at US $ 2.34 kg^{-1}, compared to US $ 0.55 kg^{-1} for ethanol.[141] As such, a significant amount of research is focussing on optimising the ABE process to produce more butanol, into continuous processing and improving butanol recovery so that the concentration does not reach lethal levels. Further efforts are focussed on metabolic and genetic engineering of the bacteria to increase their resistance and selectivity towards butanol.[142]

Butanol has also been considered a potential feedstock for jet fuel, as branched alkanes have been produced via the dehydration of butanol to 1-butene. 1-Butene can then be oligomerised using methylaluminoxane (MAO) activated metallocene catalysts, and the oligomers produced can be hydrogenated to produce branched alkanes suitable for aviation purposes.[143] However, this method requires a large number of chemical steps which, combined with the high cost of butanol, does not make this a cost-effective method to produce alternative liquid fuels.

1.5.3 Chemical Conversion

While fermentation is the major method of producing liquid fuels from biomass, a number of chemical methods are also being researched.

1.5.3.1 Thermochemical

Thermochemical conversion of biomass is an attractive technology, due to its potential to produce liquid fractions directly from biomass at high yields. Different technologies exist which come under the umbrella term of 'thermochemical biomass conversion', differing in their operating conditions, use of catalyst and water presence. They are summarised, along with their product yield ranges, in Table 1.3.

Table 1.3 Summary of different thermochemical treatments of biomass, along with their operating conditions and approximate product yields. Adapted from Nanda, et al.[144]

Conversion technology	**Operating Conditions**	**Product yields**
Slow pyrolysis	Temperature: 300-700°C Vapour residence time: 10-100 min Heating rate: 0.1-1 °C/s	Bio-oil: ~30 wt% Biochar: ~35 wt% Gases: ~35 wt%
Fast pyrolysis	Temperature: 400-800 °C Vapour residence time: 0.5-5 s Heating rate: 10-200 °C/s	Bio-oil: ~50 wt% Biochar: ~20 wt% Gases: ~30 wt%
Flash pyrolysis	Temperature: 800-100 °C/s Vapour residence time: <0.5 s Heating rate: >1000 °C/s	Bio-oil: ~75 wt% Biochar: ~12 wt% Gases: ~13 wt%
Gasification	Temperature: >1000 °C Pressure: 1 bar	CO_2: ~8 vol% CO: ~17 vol% H_2: ~65 vol% CH_4: ~9 vol% C_2H_4: ~0.6 vol% C_2H_6: ~0.3 vol%
Hydrothermal Gasification	Temperature: 300-600 °C (catalytic), 400-900 °C (non-catalytic) Pressure: 230-350 bar	CO_2: 25-52 mol%, CO: 1-13 mol% H_2: 12-68 mol% CH_4: 2-21 mol%
Hydrothermal Liquefaction	Temperature: 250-350 °C Pressure: 50-200 bar	Bio-oil: 3-23 wt% Gases: 1-30 wt% Volatile organics: 1-45 wt% Water solubles 1-17 wt%

Pyrolysis

Pyrolysis is the thermal cracking of biomass in the absence of oxygen. It is similar to a method that has been used for hundreds of years to produce charcoal[145] but also produces gaseous and liquid fractions. Depending on the reaction conditions the ratio of these fractions alters drastically. Slower, low temperature pyrolysis (400°C, >10 minute residence time) promotes a larger solid fraction – termed 'biochar' – whereas faster, high temperature pyrolysis (800°C, <0.5 s) gives liquid fractions of up to 75%.[144] The liquid fraction is called bio-oil and, though not suitable as a fuel itself, can be upgraded and refined to high quality fuels and chemicals. It is the upgrading of the bio-oil to fuel-like molecules which provides significant challenges and should be further investigated.

Gasification

In gasification, biomass is subjected to very high temperatures (as high as 1300 °C if non-catalytic) and reacted with air, oxygen or steam to produce syngas, a gas mixture which contains varying amounts of CO and H_2.[146] Syngas can then be converted into useful fuel compounds by Fischer-Tropsch synthesis.[147]

Hydrothermal techniques

For pyrolysis and gasification, relatively dry conditions and feedstocks are needed for high efficiency conversions to produce high quality gas, liquid and solid fuels. This limits the use of other lignocellulosic sources which are high in water concentration. Therefore, processes which allow for the use of wet biomass have been the subject of research for the last few decades, i.e. hydrothermal conversion. At temperatures between 250-374 °C and pressures between 40-220 bar, hydrothermal liquefaction takes place, whereby the main product is liquid, referred to as bio-oil or bio-crude. Though 'bio-oil' and 'bio-crude' are used interchangeably, some publications define bio-oil as deriving from pyrolysis, while bio-crude derives from hydrothermal liquefaction, due to the differences in their composition.[148] Treating wet biomass with temperatures above 374 °C and pressures above 220 bar (i.e. above the supercritical point of water), gasification reactions dominate and the

process of hydrothermal gasification occurs, resulting in the formation of a syngas of similar composition to that produced by gasification.

1.5.3.4 HYDROLYSATE UPGRADING

As aforementioned, the hydrolysis of cellulose produces sugar monomers and is a vital pre-treatment step in producing fuels from fermentation. The chemical conversion of these sugar monomers is another route to producing liquid fuels (Figure 1.8).[149] By first dehydrating sugar monomers over an acid catalyst, furans such as hydroxymethylfurfural (HMF), furfural and 5-methylfurfural can be produced. Though these can't be used directly as fuels themselves, due to their tendency to polymerise, they are starting materials for a range of liquid fuels. For example, furfural can undergo hydrogenation to produce furfuryl alcohol, tetrahydrofurfuryl alcohol, methylfuran and methyl-tetrahydrofuran (MTHF) though MTHF has been deemed the only suitable fuel substitute, as it is not prone to polymerisation.

HMF can undergo hydrogenolysis using metal catalysts to 2,5-dimethylfuran (DMF), which is a potential gasoline blending agent.[150] HMF can also be upgraded to specific long-chain alkanes (always desirable for their high energy density compared to oxygenates) by aldol-condensation followed by hydrogenation.[151] HMF can also be dehydrated (acid-catalysed) to produce levulinic acid, esters of which have be used as blending agents with both gasoline[150] and diesel.[152] Levulinic acid esters also seem to have potential not just technically but economically, as a recent study by the Dupont chemical companyestimated that on a large scale the production costs could be less than US $ 0.50 per litre.[55]

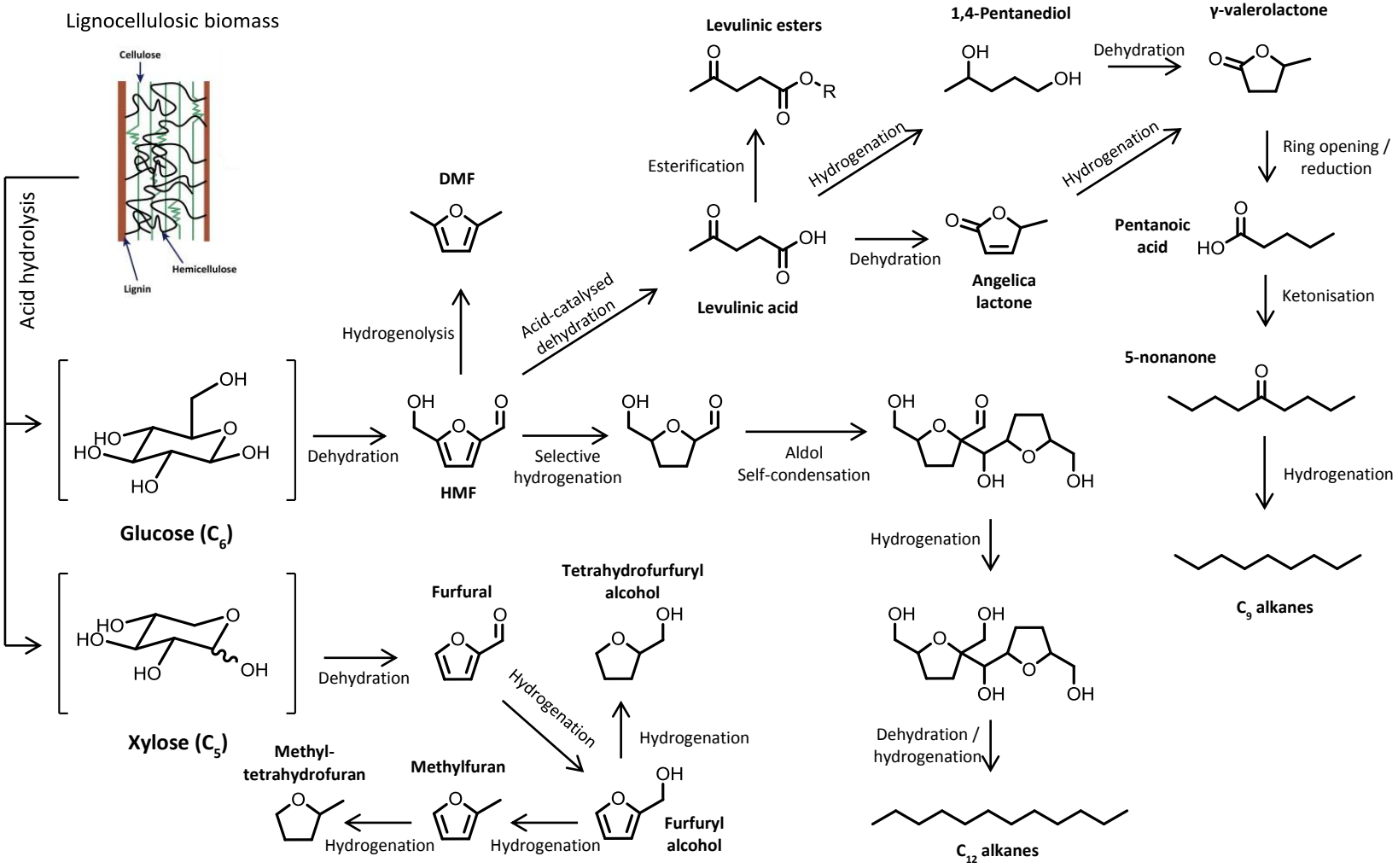

Figure 1.8 Selected pathways for fuel molecules from the lignocellulose hydrolysate upgrading. Adapted from Huber *et al.,*[55] Corma, *et al*.[56] and Alonso, *et al.*[149]

Levulinic acid is also a suitable platform chemical. It can be converted into γ-valerolactone (via dehydration and reduction steps)[153] which can be used as a gasoline additive or further upgraded. Levulinic acid provides another route to produce MTHF, via the hydrogenation of γ-valerolactone and subsequent dehydration of 1,4-pentanediol. It can also be hydrogenated, under alternative conditions, to valeric acid, esters of which show potential as blending agents with gasoline.[150] Valeric acid can also undergo ketonisation to produce 5-nonanone which can be deoxygenated to produce nonene, which can then either undergo hydrogenation to produce nonane, a suitable gasoline fuel, or oligomerisation to longer chains more suitable as a diesel fuel.[154]

1.6 BIOREFINERY CONCEPTS

A large number of biomass technologies have the potential to produce a technically suitable biofuel. However, one of the major issues with current biofuels is the cost of the feedstock and production. This is associated with the high initial capital needed to develop facilities for these processes, the costs of the feedstock when compared to fossil fuels and the cost of the processes, which require extreme conditions or expensive catalysts. One potential solution is to mimic a crude oil refinery and produce more than one product stream from biomass sources, an approach that is commonly termed a biorefinery.

The biorefinery concept produces both fuels and smaller amounts of higher value products in conjunction with one another, thereby off-setting the cost of the fuel production and ultimately reducing the cost of the fuel. The National Renewable Energy Laboratory defines a biorefinery as "*a facility that integrates biomass conversion processes and equipment to produce fuels, power, and chemicals from biomass. The biorefinery concept is analogous to today's petroleum refineries, which produce multiple fuels and products from petroleum. Industrial biorefineries have been identified as the most promising route to the creation of a new domestic biobased industry.*"[155] As these facilities produce a broad range of materials and chemicals, and utilize many different technologies and feedstocks, there is a lot of inherent flexibility associated with their processing capabilities. By allowing for diversification, the risk of investment is significantly reduced.

For lignocellulose, the refinery technologies are based upon the conversion technologies discussed. Most of these methods require high temperatures and pressures, which damage the biomass, and do not allow for separation of different compounds. In biorefineries with microbes, however, mild and inexpensive techniques can be employed to extract the high value products, such as proteins. Many processes have been researched, including mild cell disruption techniques, to allow for the extraction of the different fractions of algae (proteins, lipids, carbohydrates). This leads to isolation and extraction of more higher-value products, further supporting the fuel production from microbes.[156] Microbial

processes can integrate together, supporting one another and allowing for the co-production of two or more products (Figure 1.9).

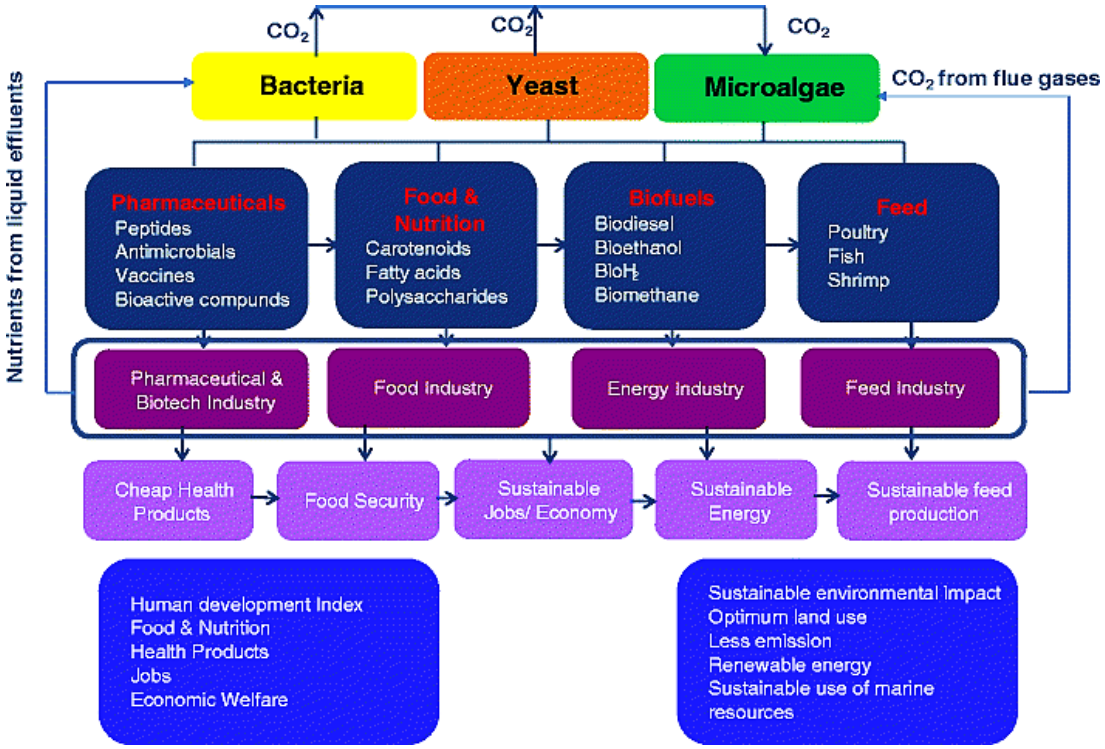

Figure 1.9 Example of integrated microbial processes, and related industries it would potential impact. From da Silva, *et al.*[157]

1.7 CONCLUDING REMARKS

A large number of alternative fuel technologies have been reported, though no one technology will fully address the issues involved in replacement of transport fuels alone. It is likely that to meet the energy and fuel demand of an ever-increasing population, a range of different technologies will have to be implemented. There are, however, three key issues associated with current biofuels which need to be addressed when developing novel liquid fuels:

1. There is insufficient arable land to produce enough sugar and oil feedstock to replace current fossil fuels with bio-derived fuels. Sustainable liquid fuels must therefore be produced from biomass grown on marginal land, renewable lignocellulosic resources, or waste materials.

2. Current liquid biofuels have poor physical properties which inhibit their further utilisation. For bioethanol, increased corrosion and seal swelling limits its use to flex-fuel vehicles, while its lower energy density blocks it use in the aviation sector. For biodiesel, the decreased oxidative stability prevents long term storage, while its high pour and cloud points stops its usage in cold temperature environments and aviation. Sustainable liquid fuels must therefore possess improved physical properties in terms of their technical values and compatibility with current fuels and infrastructure.

3. The chemical structure for current biofuels, specifically for biodiesel, can be variable depending on their feedstock and growth conditions. This leads to variation in the fuel properties, which is undesirable as it can cause the fuel to fall out of specification, causing sub-optimum engine operation. For a fuel to be truly viable as a drop-in replacement, variability in its structure must be significantly reduced to provide predictable fuel properties. This can either be done by the production of a unimolecular fuel, or by production methods which allow for tailoring of the product distribution.

Any novel fuel to be developed, or technology to be investigated, must satisfy one, but ideally all, of these criteria to be deemed a suitable replacement for fossil fuels.

1.8 AIMS & OBJECTIVES

The overall aim of this project is to develop and analyse potential sustainable liquid fuels from microbes and waste resources, with a focus on improved physical properties and product selectivity. Due to the multitude of technologies that possess the potential to produce sustainable liquid fuels, investigations into a number of competing technologies will be carried out. This is to allow for their direct comparison and for an appreciation for how they may be implemented synergistically. The specific objectives of this report are:

1. To assess the use of spent coffee grounds as a sustainable feedstock for biodiesel production, in terms of its physical properties.

2. To investigate the cross-metathesis of triglycerides, a biodiesel feedstock, with ethene as a process to produce two fuels of improved properties and directed structure.

3. To study the potential alternative cellulosic fermentation products, and select the most promising fermentation fuels, in terms of their physical properties, potential cost and availability. Those selected will be engine tested to assess their effect on engine emissions and performance.

4. To examine the transformation of representative ketonic species found in the vapour of lignocellulose pyrolysis bio-oil, over metal-supported zeolite catalysts.

1.9 REFERENCES

1. Kokic, P.; Crimp, S.; Howden, M., A probabilistic analysis of human influence on recent record global mean temperature changes. *Climate Risk Management* **2014,** *3* (0), 1-12.
2. *Digest of United Kingdom Energy Statistics*; Department of Energy and Climate Change: London, 2012
3. *Key World Energy Statistics*; International Energy Agency: Paris, 2014.
4. Tran, M.; Banister, D.; Bishop, J. D. K.; McCulloch, M. D., Realizing the electric-vehicle revolution. *Nature Climate Change* **2012,** *2* (5), 328-333.
5. Mazloomi, K.; Gomes, C., Hydrogen as an energy carrier: Prospects and challenges. *Renewable and Sustainable Energy Reviews* **2012,** *16* (5), 3024-3033.
6. Ngo, C.; Natowitz, J., *Our Energy Future: Resources, Alternatives and the Environment*. Wiley: 2012.
7. POSTnote - Rare Earth Metals. Parliamentary Office of Science and Technology: London, UK, 2011.
8. van de Krol, R.; Grätzel, M., *Photoelectrochemical Hydrogen Production*. Springer: 2011.
9. Ball, M.; Wietschel, M., The future of hydrogen – opportunities and challenges. *International Journal of Hydrogen Energy* **2009,** *34* (2), 615-627.
10. Price, J., Personal Communication. EADS: 2012.
11. *Transport, Energy and CO_2: Moving toward Sustainability*; International Energy Agency: Paris, 2009.
12. Manahan, S. E., *Fundamentals of Environmental Chemistry, Third Edition*. CRC Press: 2008.
13. EN 228:2008, Automotive fuels - Unleaded petrol - Requirements and test methods.
14. ASTM D4814:2013, Standard Specification for Automotive Spark-Ignition Engine Fuel. ASTM International: 2013.
15. EN 590:2009, Automotive fuels - Diesel - Requirements and test methods.
16. ASTM D975:2014, Standard Specification for Diesel Fuel Oils. ASTM International: 2014.
17. British Ministry of Defence, DEF STAN 91-91 Turbine Fuel, Kerosine Type, Jet A-1. MOD: Glasgow, 2011.
18. Speight, J. G.; Kelly, S.; Balat, M.; Demirbas, A.; Ghose, M. K., *The Biofuels Handbook*. Royal Society of Chemistry: 2011.
19. Lapuerta, M. n.; García-Contreras, R.; Campos-Fernández, J.; Dorado, M. P., Stability, Lubricity, Viscosity, and Cold-Flow Properties of Alcohol−Diesel Blends. *Energy & Fuels* **2010,** *24* (8), 4497-4502.
20. EN 14214:2008, Automotive fuels - Fatty acid methyl esters (FAME) for diesel engines - Requirements and test methods.
21. ASTM D6751:2008, Standard Specification for Biodiesel Fuel Blend Stock (B100) for Middle Distillate Fuels. ASTM International: 2008.
22. Stone, R., *Introduction to internal combustion engines*. Macmillan: 1999.
23. Knothe, G.; Gerpen, J. H. V.; Krahl, J., *The biodiesel handbook*. AOCS Press: 2005.
24. Diesel, R. Internal-combustion engine. 1895.
25. Hunecke, K., *Jet Engines: Fundamentals of Theory, Design and Operation*. MBI Publishing Company: 1997.
26. Whittle, F. Improvements relating to the propulsion of aircraft and other vehicles. 1930.
27. Geels, F. W., *Technological Transitions and System Innovations: A Co-evolutionary and Socio-technical Analysis*. Edward Elgar Publishing, Incorporated: 2005.
28. ASTM D1655:2014, Standard Specification for Aviation Turbine Fuels. ASTM International: 2013.

29. Totten, G. E.; Westbrook, S. R.; Shah, R. J., *Fuels and Lubricants Handbook: Technology, Properties, Performance, and Testing*. Astm International: 2003.
30. Ryan, T. W.; Dodge, L. G.; Callahan, T. J., The ffects of vegetable oil properties on injection and combustion in 2 different diesel-engines. *Journal of the American Oil Chemists Society* **1984,** *61* (10), 1610-1619.
31. Bahadur, N. P.; Boocock, D. G. B.; Konar, S. K., Liquid Hydrocarbons from Catalytic Pyrolysis of Sewage Sludge Lipid and Canola Oil: Evaluation of Fuel Properties. *Energy & Fuels* **1995,** *9* (2), 248-256.
32. Alptekin, E.; Canakci, M., Characterization of the key fuel properties of methyl ester–diesel fuel blends. *Fuel* **2009,** *88* (1), 75-80.
33. Knothe, G., Dependence of biodiesel fuel properties on the structure of fatty acid alkyl esters. *Fuel Processing Technology* **2005,** *86* (10), 1059-1070.
34. Mirante, F. I. C.; Coutinho, J. A. P., Cloud point prediction of fuels and fuel blends. *Fluid Phase Equilibria* **2001,** *180* (1–2), 247-255.
35. Echim, C.; Maes, J.; Greyt, W. D., Improvement of cold filter plugging point of biodiesel from alternative feedstocks. *Fuel* **2012,** *93* (0), 642-648.
36. Wauquier, J. P., *Petroleum Refining. Vol 1*. Imprimerie Chirat: 1995.
37. Rao, G. L. N.; Ramadhas, A.; Nallusamy, N.; Sakthivel, P., Relationships among the physical properties of biodiesel and engine fuel system design requirement. *International journal of energy and environment* **2010,** *1* (5), 919-926.
38. Arbab, M. I.; Masjuki, H. H.; Varman, M.; Kalam, M. A.; Imtenan, S.; Sajjad, H., Fuel properties, engine performance and emission characteristic of common biodiesels as a renewable and sustainable source of fuel. *Renewable and Sustainable Energy Reviews* **2013,** *22* (0), 133-147.
39. Mendes, G.; Aleme, H. G.; Barbeira, P. J. S., Determination of octane numbers in gasoline by distillation curves and partial least squares regression. *Fuel* **2012,** *97* (0), 131-136.
40. Knothe, G., A comprehensive evaluation of the cetane numbers of fatty acid methyl esters. *Fuel* **2014,** *119* (0), 6-13.
41. Ladommatos, N.; Parsi, M.; Knowles, A., The effect of fuel cetane improver on diesel pollutant emissions. *Fuel* **1996,** *75* (1), 8-14.
42. Bannister, C. D.; Chuck, C. J.; Bounds, M.; Hawley, J. G., Oxidative stability of biodiesel fuel. *Proceedings of the Institution of Mechanical Engineers, Part D: Journal of Automobile Engineering* **2011,** *225* (1), 99-114.
43. Kabana, C. G.; Botha, S.; Schmucker, C.; Woolard, C.; Beaver, B., Oxidative Stability of Middle Distillate Fuels. Part 1: Exploring the Soluble Macromolecular Oxidatively Reactive Species (SMORS) Mechanism with Jet Fuels. *Energy & Fuels* **2011,** *25* (11), 5145-5157.
44. Lacoste, F.; Lagardere, L., Quality parameters evolution during biodiesel oxidation using Rancimat test. *European Journal of Lipid Science and Technology* **2003,** *105* (3-4), 149-155.
45. Jain, S.; Sharma, M. P., Review of different test methods for the evaluation of stability of biodiesel. *Renewable & Sustainable Energy Reviews* **2010,** *14* (7), 1937-1947.
46. Commodo, M.; Fabris, I.; Groth, C. P. T.; Gulder, O. L., Analysis of Aviation Fuel Thermal Oxidative Stability by Electrospray Ionization Mass Spectrometry (ESI-MS). *Energy & Fuels* **2011,** *25* (5), 2142-2150.
47. Martínez, J. D.; Lapuerta, M.; García-Contreras, R.; Murillo, R.; García, T., Fuel Properties of Tire Pyrolysis Liquid and Its Blends with Diesel Fuel. *Energy & Fuels* **2013,** *27* (6), 3296-3305.
48. Goodrum, J. W.; Geller, D. P., Influence of fatty acid methyl esters from hydroxylated vegetable oils on diesel fuel lubricity. *Bioresource Technology* **2005,** *96* (7), 851-855.
49. Arkoudeas, P.; Karonis, D.; Zannikos, F.; Lois, E., Lubricity assessment of gasoline fuels. *Fuel Processing Technology* **2014,** *122* (0), 107-119.

50. Goldman, S. L.; Kole, C., *Compendium of Bioenergy Plants: Corn*. Taylor & Francis: 2014.
51. ASTM D5798:2014, Standard Specification for Ethanol Fuel Blends for Flexible-Fuel Automotive Spark-Ignition Engines. ASTM International: 2014.
52. ASTM D7467:2013, Standard Specification for Diesel Fuel Oil, Biodiesel Blend (B6 to B20). ASTM International: 2013.
53. ASTM D7566:2014, Standard Specification for Aviation Turbine Fuel Containing Synthesized Hydrocarbons. ASTM International: 2014.
54. Nigam, P. S.; Singh, A., Production of liquid biofuels from renewable resources. *Progress in Energy and Combustion Science* **2011,** *37* (1), 52-68.
55. Huber, G. W.; Iborra, S.; Corma, A., Synthesis of Transportation Fuels from Biomass: Chemistry, Catalysts, and Engineering. *Chemical Reviews* **2006,** *106* (9), 4044-4098.
56. Corma, A.; Iborra, S.; Velty, A., Chemical Routes for the Transformation of Biomass into Chemicals. *Chemical Reviews* **2007,** *107* (6), 2411-2502.
57. Petrus, L.; Noordermeer, M. A., Biomass to biofuels, a chemical perspective. *Green Chemistry* **2006,** *8* (10), 861-867.
58. Yue, D.; You, F.; Snyder, S. W., Biomass-to-bioenergy and biofuel supply chain optimization: Overview, key issues and challenges. *Computers & Chemical Engineering* **2014,** *66*, 36-56.
59. Knothe, G., Historical perspectives on vegetable oil-based diesel fuels. *inform* **2001,** *12* (11), 1103-1107.
60. Sidibe, S. S.; Blin, J.; Vaitilingom, G.; Azoumah, Y., Use of crude filtered vegetable oil as a fuel in diesel engines state of the art: Literature review. *Renewable & Sustainable Energy Reviews* **2010,** *14* (9), 2748-2759.
61. Bhattacharyya, S.; Reddy, C. S., Vegetable-oils as fuels for internal-combustion engines - a review. *Journal of Agricultural Engineering Research* **1994,** *57* (3), 157-166.
62. Karmakar, A.; Karmakar, S.; Mukherjee, S., Properties of various plants and animals feedstocks for biodiesel production. *Bioresource Technology* **2010,** *101* (19), 7201-7210.
63. Atabani, A. E.; Silitonga, A. S.; Badruddin, I. A.; Mahlia, T. M. I.; Masjuki, H. H.; Mekhilef, S., A comprehensive review on biodiesel as an alternative energy resource and its characteristics. *Renewable and Sustainable Energy Reviews* **2012,** *16* (4), 2070-2093.
64. Banković-Ilić, I. B.; Stojković, I. J.; Stamenković, O. S.; Veljkovic, V. B.; Hung, Y.-T., Waste animal fats as feedstocks for biodiesel production. *Renewable and Sustainable Energy Reviews* **2014,** *32* (0), 238-254.
65. Ashraful, A. M.; Masjuki, H. H.; Kalam, M. A.; Rizwanul Fattah, I. M.; Imtenan, S.; Shahir, S. A.; Mobarak, H. M., Production and comparison of fuel properties, engine performance, and emission characteristics of biodiesel from various non-edible vegetable oils: A review. *Energy Conversion and Management* **2014,** *80* (0), 202-228.
66. Banković-Ilić, I. B.; Stamenković, O. S.; Veljković, V. B., Biodiesel production from non-edible plant oils. *Renewable and Sustainable Energy Reviews* **2012,** *16* (6), 3621-3647.
67. Shi, S. B.; Valle-Rodriguez, J. O.; Siewers, V.; Nielsen, J., Prospects for microbial biodiesel production. *Biotechnology Journal* **2011,** *6* (3), 277-285.
68. Ageitos, J. M.; Vallejo, J. A.; Veiga-Crespo, P.; Villa, T. G., Oily yeasts as oleaginous cell factories. *Applied Microbiology and Biotechnology* **2011,** *90* (4), 1219-1227.
69. Manzano-Agugliaro, F.; Sanchez-Muros, M. J.; Barroso, F. G.; Martínez-Sánchez, A.; Rojo, S.; Pérez-Bañón, C., Insects for biodiesel production. *Renewable and Sustainable Energy Reviews* **2012,** *16* (6), 3744-3753.
70. Vicente, G.; Bautista, L. F.; Rodríguez, R.; Gutiérrez, F. J.; Sádaba, I.; Ruiz-Vázquez, R. M.; Torres-Martínez, S.; Garre, V., Biodiesel production from biomass of an oleaginous fungus. *Biochemical Engineering Journal* **2009,** *48* (1), 22-27.

71. Rawat, I.; Ranjith Kumar, R.; Mutanda, T.; Bux, F., Dual role of microalgae: Phycoremediation of domestic wastewater and biomass production for sustainable biofuels production. *Applied Energy* **2011,** *88* (10), 3411-3424.
72. Pinzi, S.; Leiva, D.; López-García, I.; Redel-Macías, M. D.; Dorado, M. P., Latest trends in feedstocks for biodiesel production. *Biofuels, Bioproducts and Biorefining* **2014,** *8* (1), 126-143.
73. Li, Q.; Du, W.; Liu, D., Perspectives of microbial oils for biodiesel production. *Applied Microbiology and Biotechnology.* **2008,** *80* (5), 749-756.
74. Velasquez-Orta, S. B.; Lee, J. G. M.; Harvey, A., Alkaline in situ transesterification of *Chlorella vulgaris*. *Fuel* **2012,** *94* (0), 544-550.
75. Scott, P.; Pregelj, L.; Chen, N.; Hadler, J.; Djordjevic, M.; Gresshoff, P., *Pongamia pinnata*: An Untapped Resource for the Biofuels Industry of the Future. *Bioenergy Research.* **2008,** *1* (1), 2-11.
76. Mata, T. M.; Martins, A. A.; Caetano, N. S., Microalgae for biodiesel production and other applications: A review. *Renewable and Sustainable Energy Reviews* **2010,** *14* (1), 217-232.
77. Griffiths, M.; Hille, R.; Harrison, S. L., Lipid productivity, settling potential and fatty acid profile of 11 microalgal species grown under nitrogen replete and limited conditions. *Journal of Applied Phycology* **2012,** *24* (5), 989-1001.
78. Meng, X.; Yang, J.; Xu, X.; Zhang, L.; Nie, Q.; Xian, M., Biodiesel production from oleaginous microorganisms. *Renewable Energy* **2009,** *34* (1), 1-5.
79. Finke, M. D., Complete nutrient composition of commercially raised invertebrates used as food for insectivores. *Zoo Biology* **2002,** *21* (3), 269-285.
80. de Andrés, C.; Espuny, M. J.; Robert, M.; Mercadé, M. E.; Manresa, A.; Guinea, J., Cellular lipid accumulation by Pseudomonas aeruginosa 44T1. *Applied Microbiology and Biotechnology* **1991,** *35* (6), 813-816.
81. *The State of Food and Agriculture: Biofuels: Prospects, Risks and Oppurtunities*; Food and Agriculture Organization of the United Nations: Rome, 2008.
82. REN21, Renewables 2014: Global status report. 2014.
83. Balat, M.; Balat, H., Progress in biodiesel processing. *Applied Energy* **2010,** *87* (6), 1815-1835.
84. Le Chatelier, H., Sur un enonce general des lois des equilibres chimiques. *Ann. Mines et Carburants* **1888,** *8* (13), 157-382.
85. Semwal, S.; Arora, A. K.; Badoni, R. P.; Tuli, D. K., Biodiesel production using heterogeneous catalysts. *Bioresource Technology* **2011,** *102* (3), 2151-2161.
86. Gog, A.; Roman, M.; Toşa, M.; Paizs, C.; Irimie, F. D., Biodiesel production using enzymatic transesterification – Current state and perspectives. *Renewable Energy* **2012,** *39* (1), 10-16.
87. Chuck, C. J.; Jenkins, R. W.; Bannister, C. D.; Lowe, J. P., Design and preliminary results of an NMR tube reactor to study the oxidative degradation of Fatty Acid Methyl Ester. *Biomass and Bioenergy* **2012,** *47*, 188-194.
88. Chuck, C. J.; Bannister, C. D.; Jenkins, R. W.; Lowe, J. P.; Davidson, M. G., A comparison of analytical techniques and the products formed during the decomposition of biodiesel under accelerated conditions. *Fuel* **2012,** *96* (0), 426-433.
89. Graboski, M. S.; McCormick, R. L.; Alleman, T. L.; Herring, A. M. *The Effect of Biodiesel Composition on Engine Emissions from a DDC Series 60 Diesel Engine*; NREL/SR-510-31461; National Renewable Energy Laboratory: Golden, Colorado, 2003.
90. Trémolières, H.; Trémolières, A.; Mazliak, P., Effects of light and temperature on fatty acid desaturation during the maturation of rapeseed. *Phytochemistry* **1978,** *17* (4), 685-687.
91. Islam, R.; Chhetri, A. B., *Green Petroleum: How Oil and Gas Can Be Environmentally Sustainable*. Wiley: 2012.

92. Choudhary, T. V.; Phillips, C. B., Renewable fuels via catalytic hydrodeoxygenation. *Applied Catalysis A: General* **2011,** *397* (1–2), 1-12.
93. Smith, B.; Greenwell, H. C.; Whiting, A., Catalytic upgrading of tri-glycerides and fatty acids to transport biofuels. *Energy & Environmental Science* **2009,** *2* (3), 262-271.
94. Šimáček, P.; Kubička, D.; Šebor, G.; Pospíšil, M., Hydroprocessed rapeseed oil as a source of hydrocarbon-based biodiesel. *Fuel* **2009,** *88* (3), 456-460.
95. Kubicka, D.; Simacek, P.; Zilkova, N., Transformation of Vegetable Oils into Hydrocarbons over Mesoporous-Alumina-Supported CoMo Catalysts. *Topics in Catalysis* **2009,** *52* (1-2), 161-168.
96. Snåre, M.; Kubičková, I.; Mäki-Arvela, P.; Eränen, K.; Murzin, D. Y., Heterogeneous Catalytic Deoxygenation of Stearic Acid for Production of Biodiesel. *Industrial & Engineering Chemistry Research* **2006,** *45* (16), 5708-5715.
97. Huber, G. W.; Corma, A., Synergies between Bio- and Oil Refineries for the Production of Fuels from Biomass. *Angewandte Chemie International Edition* **2007,** *46* (38), 7184-7201.
98. Zhao, C.; Bruck, T.; Lercher, J. A., Catalytic deoxygenation of microalgae oil to green hydrocarbons. *Green Chemistry* **2013,** *15* (7), 1720-1739.
99. Wang, C.; Liu, Q.; Song, J.; Li, W.; Li, P.; Xu, R.; Ma, H.; Tian, Z., High quality diesel-range alkanes production via a single-step hydrotreatment of vegetable oil over Ni/zeolite catalyst. *Catalysis Today* **2014,** *234* (0), 153-160.
100. Häussinger, P.; Lohmüller, R.; Watson, A. M., Hydrogen, 1. Properties and Occurence. In *Ullmann's Encyclopedia of Industrial Chemistry*, Wiley-VCH Verlag GmbH & Co. KGaA: 2000.
101. Mol, J. C., Industrial applications of olefin metathesis. *Journal of Molecular Catalysis A: Chemical* **2004,** *213* (1), 39-45.
102. Deraedt, C.; d'Halluin, M.; Astruc, D., Metathesis Reactions: Recent Trends and Challenges. *European Journal of Inorganic Chemistry* **2013,** *2013* (28), 4881-4908.
103. Jean-Louis Hérisson, P.; Chauvin, Y., Catalyse de transformation des oléfines par les complexes du tungstène. II. Télomérisation des oléfines cycliques en présence d'oléfines acycliques. *Die Makromolekulare Chemie* **1971,** *141* (1), 161-176.
104. Xia, Y.; Larock, R. C., Vegetable oil-based polymeric materials: synthesis, properties, and applications. *Green Chemistry* **2010,** *12* (11), 1893-1909.
105. Chikkali, S.; Mecking, S., Refining of Plant Oils to Chemicals by Olefin Metathesis. *Angewandte Chemie International Edition* **2012,** *51* (24), 5802-5808.
106. Vilela, C.; Silvestre, A. J. D.; Meier, M. A. R., Plant Oil-Based Long-Chain C_{26} Monomers and Their Polymers. *Macromolecular Chemistry and Physics* **2012,** *213* (21), 2220-2227.
107. Ngo, H.; Jones, K.; Foglia, T., Metathesis of unsaturated fatty acids: Synthesis of long-chain unsaturated-α,ω-dicarboxylic acids. *Journal of the American Oil Chemists' Society* **2006,** *83* (7), 629-634.
108. Montenegro, R. E.; Meier, M. A. R., Lowering the boiling point curve of biodiesel by cross-metathesis. *European Journal of Lipid Science and Technology* **2012,** *114* (1), 55-62.
109. Schrodi, Y.; Ung, T.; Vargas, A.; Mkrtumyan, G.; Lee, C. W.; Champagne, T. M.; Pederson, R. L.; Hong, S. H., Ruthenium Olefin Metathesis Catalysts for the Ethenolysis of Renewable Feedstocks. *CLEAN – Soil, Air, Water* **2008,** *36* (8), 669-673.
110. van der Klis, F.; Le Notre, J.; Blaauw, R.; van Haveren, J.; van Es, D. S., Renewable linear alpha olefins by selective ethenolysis of decarboxylated unsaturated fatty acids. *European Journal of Lipid Science and Technology*. **2012,** *114* (8), 911-918.
111. van Dam, P. B.; Mittelmeijer, M. C.; Boelhouwer, C., Metathesis of unsaturated fatty acid esters by a homogeneous tungsten hexachloride-tetramethyltin catalyst. *Journal of the Chemical Society, Chemical Communications* **1972,** (22), 1221-1222.

112. Ellison, A.; Coverdale, A. K.; Dearing, P. F., Catalytic metathesis of unsaturated esters by alumina supported rhenium oxide. *Applied Catalysis* **1983,** *8* (1), 109-121.
113. Mol, J. C., Metathesis of unsaturated fatty acid esters and fatty oils. *Journal of Molecular Catalysis* **1994,** *90* (1–2), 185-199.
114. Trnka, T. M.; Grubbs, R. H., The Development of L2X2RuCHR Olefin Metathesis Catalysts: An Organometallic Success Story. *Accounts of Chemical Research* **2000,** *34* (1), 18-29.
115. Dinger, M. B.; Mol, J. C., High Turnover Numbers with Ruthenium-Based Metathesis Catalysts. *Advanced Synthesis & Catalysis* **2002,** *344* (6-7), 671-677.
116. Patel, J.; Mujcinovic, S.; Jackson, W. R.; Robinson, A. J.; Serelis, A. K.; Such, C., High conversion and productive catalyst turnovers in cross-metathesis reactions of natural oils with 2-butene. *Green Chemistry* **2006,** *8* (5), 450-454.
117. Hong, S. H.; Wenzel, A. G.; Salguero, T. T.; Day, M. W.; Grubbs, R. H., Decomposition of Ruthenium Olefin Metathesis Catalysts. *Journal of the American Chemical Society* **2007,** *129* (25), 7961-7968.
118. Nickel, A.; Ung, T.; Mkrtumyan, G.; Uy, J.; Lee, C. W.; Stoianova, D.; Papazian, J.; Wei, W. H.; Mallari, A.; Schrodi, Y.; Pederson, R. L., A Highly Efficient Olefin Metathesis Process for the Synthesis of Terminal Alkenes from Fatty Acid Esters. *Topics in Catalysis* **2012,** *55* (7-10), 518-523.
119. Mol, J. C., Application of olefin metathesis in oleochemistry: an example of green chemistry. *Green Chemistry* **2002,** *4* (1), 5-13.
120. Vandam, P. B.; Mittelme.Mc; Boelhouw.C, Homogeneous catalytic metathesis of unsaturated fatty esters - new synthetic method for preparation of unsaturated monocarboxylic and dicarboxylic-acids. *Journal of the American Oil Chemists Society* **1974,** *51* (9), 389-392.
121. Grela, K., *Olefin Metathesis: Theory and Practice*. Wiley: 2014.
122. Sibeijn, M.; Mol, J. C., Ethenolysis of methyl oleate over supported Re-based catalysts. *Journal of Molecular Catalysis* **1992,** *76* (1-3), 345-358.
123. Giovanna, M. A.; Misook, K., Pretreatment Technologies for the Conversion of Lignocellulosic Materials to Bioethanol. In *Sustainability of the Sugar and Sugar-Ethanol Industries*, American Chemical Society: 2010; Vol. 1058, pp 117-145.
124. Lin, C. S. K.; Pfaltzgraff, L. A.; Herrero-Davila, L.; Mubofu, E. B.; Abderrahim, S.; Clark, J. H.; Koutinas, A. A.; Kopsahelis, N.; Stamatelatou, K.; Dickson, F.; Thankappan, S.; Mohamed, Z.; Brocklesby, R.; Luque, R., Food waste as a valuable resource for the production of chemicals, materials and fuels. Current situation and global perspective. *Energy & Environmental Science* **2013,** *6* (2), 426-464.
125. Yan, S.; Wang, P.; Zhai, Z.; Yao, J., Fuel ethanol production from concentrated food waste hydrolysates in immobilized cell reactors by Saccharomyces cerevisiae H058. *Journal of Chemical Technology & Biotechnology* **2011,** *86* (5), 731-738.
126. Harun, R.; Yip, J. W. S.; Thiruvenkadam, S.; Ghani, W. A. W. A. K.; Cherrington, T.; Danquah, M. K., Algal biomass conversion to bioethanol – a step-by-step assessment. *Biotechnology Journal* **2014,** *9* (1), 73-86.
127. Yanik, J.; Stahl, R.; Troeger, N.; Sinag, A., Pyrolysis of algal biomass. *Journal of Analytical and Applied Pyrolysis* **2013,** *103* (0), 134-141.
128. Bagnoud-Velásquez, M.; Brandenberger, M.; Vogel, F.; Ludwig, C., Continuous catalytic hydrothermal gasification of algal biomass and case study on toxicity of aluminum as a step toward effluents recycling. *Catalysis Today* **2014,** *223* (0), 35-43.
129. Elliott, D. C.; Hart, T. R.; Schmidt, A. J.; Neuenschwander, G. G.; Rotness, L. J.; Olarte, M. V.; Zacher, A. H.; Albrecht, K. O.; Hallen, R. T.; Holladay, J. E., Process development for

hydrothermal liquefaction of algae feedstocks in a continuous-flow reactor. *Algal Research* **2013,** *2* (4), 445-454.

130. Kumar, P.; Barrett, D. M.; Delwiche, M. J.; Stroeve, P., Methods for Pretreatment of Lignocellulosic Biomass for Efficient Hydrolysis and Biofuel Production. *Industrial & Engineering Chemistry Research* **2009,** *48* (8), 3713-3729.
131. Sun, Y.; Cheng, J., Hydrolysis of lignocellulosic materials for ethanol production: a review. *Bioresource Technology* **2002,** *83* (1), 1-11.
132. Mir, B. A.; Mewalal, R.; Mizrachi, E.; Myburg, A. A.; Cowan, D. A., Recombinant hyperthermophilic enzyme expression in plants: a novel approach for lignocellulose digestion. *Trends in Biotechnology* **2014,** *32* (5), 281-289.
133. Surisetty, V. R.; Dalai, A. K.; Kozinski, J., Alcohols as alternative fuels: An overview. *Applied Catalysis A: General* **2011,** *404* (1-2), 1-11.
134. Doppenberg, J.; van der Aar, P., *Biofuels: Implications for the Feed Industry*. Wageningen Academic Publishers: 2007.
135. Balat, M.; Balat, H., Recent trends in global production and utilization of bio-ethanol fuel. *Applied Energy* **2009,** *86* (11), 2273-2282.
136. Liska, A. J.; Yang, H.; Milner, M.; Goddard, S.; Blanco-Canqui, H.; Pelton, M. P.; Fang, X. X.; Zhu, H.; Suyker, A. E., Biofuels from crop residue can reduce soil carbon and increase CO_2 emissions. *Nature Climate Change* **2014,** *4* (5), 398-401.
137. Goldemberg, J.; Coelho, S. T.; Guardabassi, P., The sustainability of ethanol production from sugarcane. *Energy Policy* **2008,** *36* (6), 2086-2097.
138. Regalbuto, J. R., Cellulosic Biofuels—Got Gasoline? *Science* **2009,** *325* (5942), 822-824.
139. Jin, C.; Yao, M.; Liu, H.; Lee, C.-f. F.; Ji, J., Progress in the production and application of n-butanol as a biofuel. *Renewable and Sustainable Energy Reviews* **2011,** *15* (8), 4080-4106.
140. Jones, D. T.; Woods, D. R., Acetone-Butanol fermentation revisited. *Microbiological Reviews* **1986,** *50* (4), 484-524.
141. Pfromm, P. H.; Amanor-Boadu, V.; Nelson, R.; Vadlani, P.; Madl, R., Bio-butanol vs. bio-ethanol: A technical and economic assessment for corn and switchgrass fermented by yeast or Clostridium acetobutylicum. *Biomass and Bioenergy* **2010,** *34* (4), 515-524.
142. Kumar, M.; Gayen, K., Developments in biobutanol production: New insights. *Applied Energy* **2011,** *88* (6), 1999-2012.
143. Harvey, B. G.; Meylemans, H. A., The role of butanol in the development of sustainable fuel technologies. *Journal of Chemical Technology & Biotechnology* **2011,** *86* (1), 2-9.
144. Nanda, S.; Mohammad, J.; Reddy, S.; Kozinski, J.; Dalai, A., Pathways of lignocellulosic biomass conversion to renewable fuels. *Biomass Conversion and Biorefinery* **2014,** *4* (2), 157-191.
145. Brown, R. C.; Stevens, C., *Thermochemical Processing of Biomass: Conversion into Fuels, Chemicals and Power*. Wiley: 2011.
146. Metzger, J. O., Production of Liquid Hydrocarbons from Biomass. *Angewandte Chemie International Edition* **2006,** *45* (5), 696-698.
147. Dry, M. E., The Fischer–Tropsch process: 1950–2000. *Catalysis Today* **2002,** *71* (3–4), 227-241.
148. Fatih Demirbas, M., Biorefineries for biofuel upgrading: A critical review. *Applied Energy* **2009,** *86, Supplement 1* (0), S151-S161.
149. Alonso, D. M.; Bond, J. Q.; Dumesic, J. A., Catalytic conversion of biomass to biofuels. *Green Chemistry* **2010,** *12* (9), 1493-1513.
150. Christensen, E.; Yanowitz, J.; Ratcliff, M.; McCormick, R. L., Renewable Oxygenate Blending Effects on Gasoline Properties. *Energy & Fuels* **2011,** *25* (10), 4723-4733.

151. West, R. M.; Liu, Z. Y.; Peter, M.; Dumesic, J. A., Liquid Alkanes with Targeted Molecular Weights from Biomass-Derived Carbohydrates. *ChemSusChem* **2008,** *1* (5), 417-424.
152. Christensen, E.; Williams, A.; Paul, S.; Burton, S.; McCormick, R. L., Properties and Performance of Levulinate Esters as Diesel Blend Components. *Energy & Fuels* **2011**.
153. Bozell, J. J.; Moens, L.; Elliott, D. C.; Wang, Y.; Neuenscwander, G. G.; Fitzpatrick, S. W.; Bilski, R. J.; Jarnefeld, J. L., Production of levulinic acid and use as a platform chemical for derived products. *Resources, Conservation and Recycling* **2000,** *28* (3–4), 227-239.
154. Bond, J. Q.; Martin Alonso, D.; West, R. M.; Dumesic, J. A., γ-Valerolactone Ring-Opening and Decarboxylation over SiO_2/Al_2O_3 in the Presence of Water†. *Langmuir* **2010,** *26* (21), 16291-16298.
155. National Renewable Energy Laboratory NREL: Biofuel Research - What Is A Biorefinery? http://www.nrel.gov/biomass/biorefinery.html.
156. Vanthoor-Koopmans, M.; Wijffels, R. H.; Barbosa, M. J.; Eppink, M. H., Biorefinery of microalgae for food and fuel. *Bioresource Technology* **2013,** *135*, 142-149.
157. da Silva, T.; Gouveia, L.; Reis, A., Integrated microbial processes for biofuels and high value-added products: the way to improve the cost effectiveness of biofuel production. *Applied Microbiology and Biotechnology* **2014,** *98* (3), 1043-1053.

CHAPTER 2

THE POTENTIAL OF WASTE COFFEE GROUNDS AS A BIODIESEL FEEDSTOCK

There is insufficient arable land to produce enough first generation fuels to meet current demands whilst simultaneously feeding a growing population. The use of waste resources as a fuel feedstock, therefore, is one of the key sustainability goals. Many of these resources and their potential are overlooked, though there are many strategies to utilise them. An example of this is spent (i.e. post-brew) coffee grounds which, as processed plant seeds, contain a significant amount of saponifiable lipid. This chapter investigates the viability of waste coffee grounds as a feedstock for biodiesel production. Specifically, an assessment of the variability in oil yield and fuel properties of a range of coffees from different geographical regions, bean types and brewing methods was carried out.

Part of this study was published in the American Chemical Society journal *Energy and Fuels*[1] and garnered interest from national as well as international media, including the BBC and several national newspapers. It also inspired a cartoon by Jonathan Pugh, featured alongside the article about the study in the *Daily Mail*.[2]

2.1 INTRODUCTION

Increasingly waste resources are being investigated as feedstocks for alternative fuel production. While research has focussed on agricultural and forestry residues,[3] food waste[4] and even plastic waste[5] as potential resources, one of the best known examples is the production of biodiesel from waste cooking oil.[6] An alternative source of waste lipids are from spent coffee grounds (SCG).

Coffee is a major worldwide agricultural commodity with over 8.8 million tonnes being produced in 2012,[7] an increase of a million tonnes from 10 years previously. It is also the second most traded commodity globally after petroleum (the third being natural gas).[8] Although it is produced by over 70 countries globally, Brazil dominates the coffee production industry, accounting for 35% of total production, followed by Vietnam at 19% (Figure 2.1).

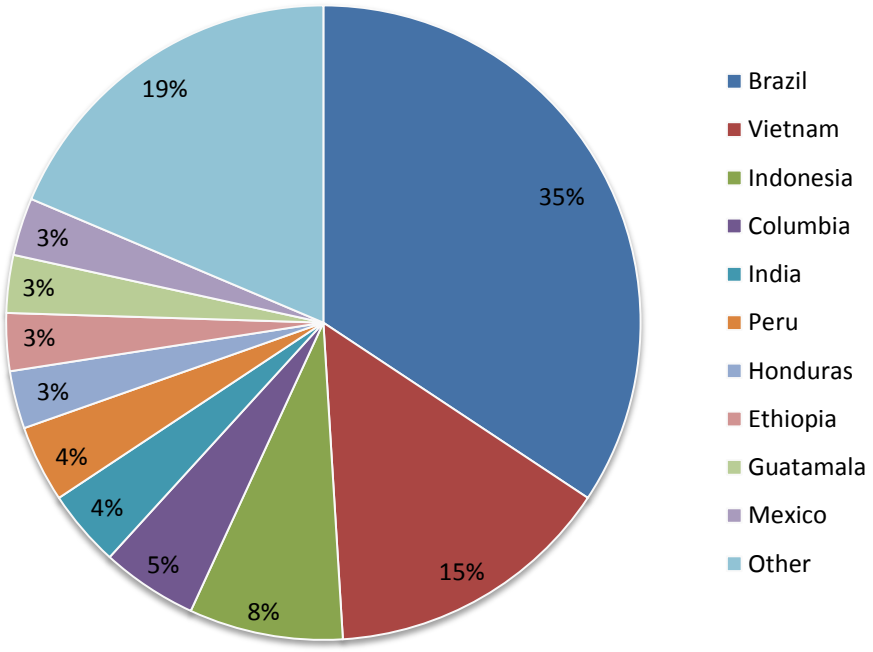

Figure 2.1 Total production of green coffee beans in 2012, adapted from data from the UN Food and Agricultural Organisation.[7]

The *Coffea* genus contains over 90 species,[9] but two species dominate the beverage industry: *Coffea Arabica* and *Coffea canephora*, commonly referred to as Arabica and Robusta.[10] Arabica accounts for 70-75% of total production and is considered to

be of superior quality due to the richer flavour developed during roasting.[11-12] Robusta is commonly used in the freeze dried coffee industry for producing soluble coffee extracts such as 'instant coffee'. Robusta beans are reported to have as much as twice the amount of caffeine as Arabica coffee beans,[13] and so blends of the two beans are commonly sold in order to control the strength of flavour and tailor the amount of caffeine present. The majority of coffee is processed, roasted and then sold, but a small proportion is decaffeinated prior to roasting via solvent treatment. The four solvents most commonly used for the decaffeination process are water, ethyl acetate, supercritical CO_2 ($scCO_2$) and dichloromethane (though recent research has studied the use of bio-renewable agrochemical solvents[14]). For all commercial methods, the unroasted green coffee beans are steamed, the caffeine is extracted using carefully controlled process conditions, the solvent residue is removed from the beans via steam stripping and lastly the beans are dried to restore them to their original moisture content.[15]

Spent coffee grounds (SCG) refer to the solid residue produced after preparation of the coffee beverage or manufacturing of instant coffee.[10] Currently the majority of SCG are discarded as waste, though some are used in composting due to their high nitrogen content. They have little commercial value, although an increased emphasis on waste reduction has increased interest into potential uses. Industry leaders in coffee production are pioneering programmes into waste coffee use, such as Starbucks's higher value product formation from waste coffee via a biorefinery concept[16-17] and Nestlé's use of their spent coffee grounds as a supplement fuel for heat production.[18] The scale and purity of the coffee waste stream has also prompted a variety of research into other potential uses such as a source to produce activated carbon for adsorption processes,[19, 20] non-structural fill material,[21] additives for structural ceramics,[22] and even for novel alcoholic beverage production.[23] As an abundant cellulosic biomass waste resource, fermentation of SCG to produce bioethanol has been investigated[24] and in recent years a significant amount of research on the thermochemical conversion of SCG for bio-oil production[25-28] and coffee SCG-derived bio-oil engine testing[29] has been undertaken.

Coffee beans typically contain between 10-15 wt% lipids stored in the endosperm tissue as an energy reserve for germination and post germination growth, a comparable amount to those found in traditional biodiesel feedstocks such as soybean and rapeseed.[30] Of the lipid 80-95% are triglycerides species,[31-32] which can be transesterified to produce biodiesel.[24] If global coffee production were to remain constant, 1.5 billion litres of biodiesel could be added to the world fuel supply from waste coffee grounds, a figure comparable to waste cooking oil.[32, 33] Oil can be extracted from both fresh and spent coffee beans.

Coffee produces more oil per unit of land area than traditional biodiesel crops, with 386 kg ha^{-1} being reported as opposed to 375 kg ha^{-1} for soybean.[34] As well as the oil potentially extracted from waste coffee grounds, as much as 20% of all coffee beans produced are deemed defective and offer a further source of biofuel.[35-36] However, SCG have an added advantage over these defective beans - due to the heavy processing of the coffee beans prior to commercial use (i.e. grinding into a fine powder), extracting the oil from SCG is relatively facile. This dramatically reduces the impact of the feedstock preparation on the energy and cost of the oil extraction. This will contribute considerably towards the production of biodiesel from waste coffee, as it is report that the cost of feedstock accounts for 70-95% of the overall cost for biodiesel production.[37]

Lipid extraction has an effect on the elemental make-up of the solid residue. For example, Vardon, *et al.* observed a small increase in oxygen (34.0% spent; 38.8% post oil extraction) and nitrogen (2.4% spent; 2.8% post oil extraction). Due to this increase in oxygen, the energy density of the solid residue reduces after lipid extraction (from 23.4 MJ kg^{-1} to 20.1 MJ kg^{-1}). This is comparable to woody biomass (19-21 MJ kg^{-1}) and can be considered a suitable feedstock for thermochemical upgrading or direct energy production through combustion. Spent coffee grounds have the potential for being completely utilized, providing a range of alternative fuels and higher value products (Figure 2.2).

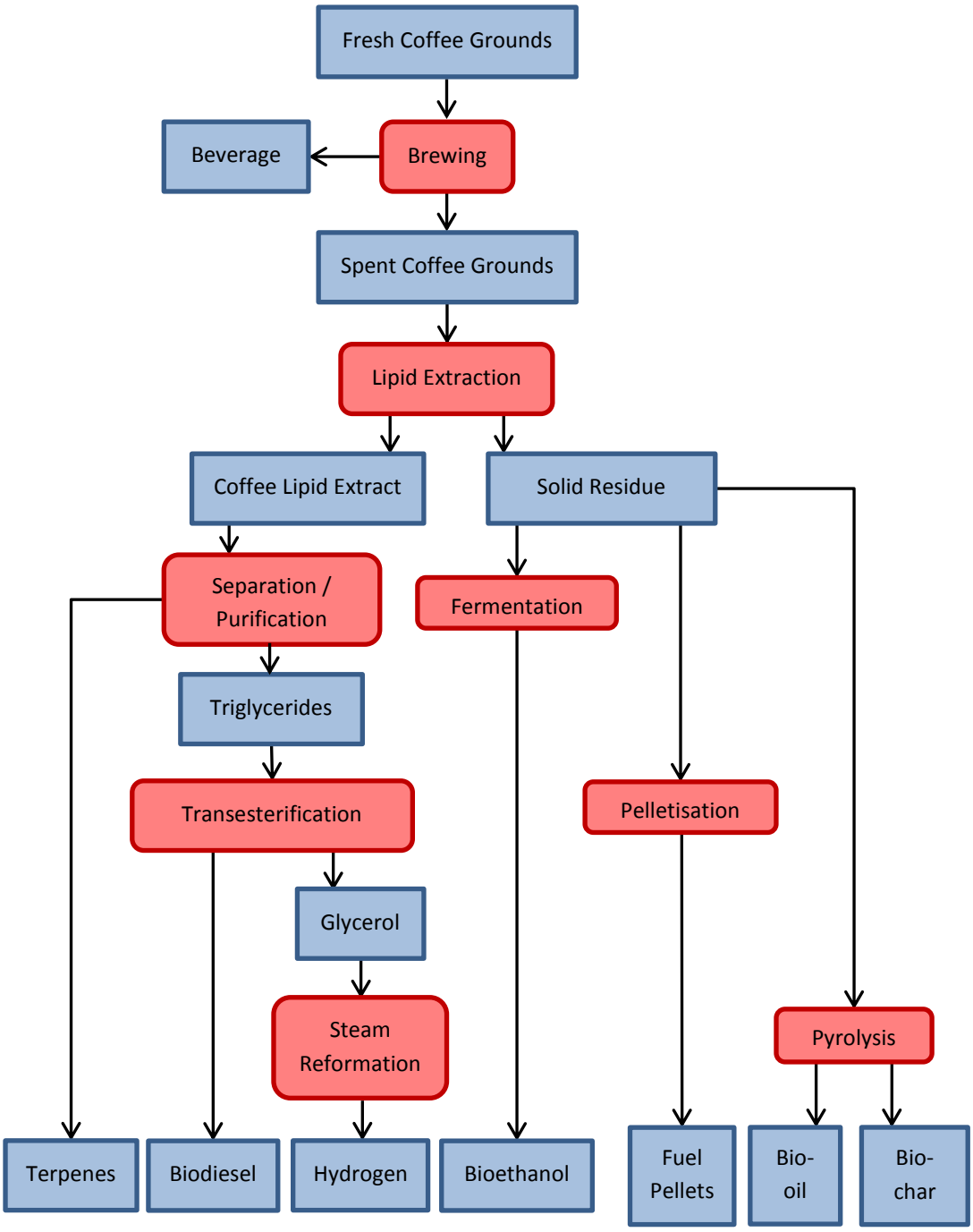

Figure 2.2 Schematic representation of the complete utilisation of spent coffee grounds to produce fuels and higher value products. Adapted from Kondamudi, *et al.* and Vardon *et al.*[25, 32]

Several methods have been successfully investigated for coffee oil extraction such as Soxhlet, microwave and $scCO_2$ extraction.[38-44] In a study of different solvents for oil extraction, Al-Hamamre, *et al*. demonstrated that hexane was the most suitable solvent, yielding >15 wt% oil over 30 minutes using Soxhlet apparatus, as opposed to *n*-pentane, toluene, chloroform, acetone, *i*-propanol, and ethanol.[31] Extraction

using hexane also has an effect on the composition of the oil, as the use of polar solvents leads to a higher extraction of polar lipids, such as sterols and FFAs.

Coffee lipid contains 80-95% triglycerides, with fatty acids, terpenes, sterols and tocopherols accounting for the rest of the mass.[45] These components are generally insoluble in the resulting biodiesel and have to be separated from the fuel prior to use. For example, Oliveira *et al.* produced between 10 to 12 wt% oil from defective coffee beans, though the extracted oil only yielded 74% biodiesel on transesterification.[35] Similarly Al-Hamamre, *et al.* produced a maximum of 86% fatty acid methyl ester (FAME) from a coffee oil produced from SCG.[31]

The FAME produced from coffee oil contains palmitic, stearic, oleic and linoleic acid esters, and as such is a promising source of biodiesel.[31] With alternative oil plants, such as rapeseed or microalgae, the FAME profile varies significantly depending on the growth conditions. However, it is unclear how much the lipid content, the FAME profile and, by extension, the fuel properties of the resulting biodiesel vary for SCGs from different regional locations, different processing and brewing methods.

In this investigation representative coffees from the main growing regions were examined, including decaffeinated coffee and coffee with different ratios of Arabica and Robusta, and were brewed using a range of techniques under controlled conditions. The oils were extracted with heptane and the lipid content, maximum biodiesel yield, FAME profile and key fuel properties assessed.

2.2 EXPERIMENTAL

2.2.1 MATERIALS

The coffee grounds were purchased locally from a number of local supermarkets. Heptane (HPLC grade) was purchased from Fisher Chemicals, whilst sulfuric acid,, methanol (99.5%+), chloroform (99.5%+) and 1,4-dioxane (analytical grade) were obtained from Sigma Aldrich, UK and were not purified further prior to use.

2.2.2 METHODS

2.2.2.1 BREWING METHODS

For this study, four different brewing techniques were used. For the general method, a cafetiere or French press was used. To assess effects of alternative brewing, other methods were also used. These included espresso, filter or “drip-brew”, and AeroPress (Figure 2.3).

Figure 2.3 The brewing methods assessed – cafetiere (top left), espresso (top right), "drip-brew" filter (bottom left) and AeroPress (bottom right).

The general brewing process for the production of the SCG is as follows. Fresh coffee grounds (100 g) were brewed with freshly boiled water (1 l), in a cafetière

(French press) coffee maker. The mixtures were stirred to submerge all the coffee grounds, and then left to settle and brewed over exactly 5 minutes. The cafetière plunger was depressed and the resulting liquid poured off. The solid fraction was separated and the spent coffee grounds were dried in an oven at 67 °C, over 24 hours to reduce the moisture content. This was repeated twice, for a total of three.

To an Aerobie-brand AeroPress, 25 g of ground coffee was added. Approximately 250 ml of freshly boiled water was added to the Aeropress and the coffee slightly agitated. After 1 minute brewing time, the rubber plunger was pushed down, forcing the aqueous fraction through the paper microfilter. The spent coffee grounds was removed, dried for a minimum of 24 hours in an oven at 60°C and weighed before solvent extraction. This was repeated three times, for a total of four. For more information on this type of coffee maker please visit http://www.aeropress.com/.

Using a commercially available filter coffee maker (The Russel-Hobbs Heritage coffee maker), approximately 50 grams was added to the filter inside the filter basket. The reservoir was filled with 500 ml of water. When the machine had reached temperature, the water was turned on and allowed to drip through the ground coffee until the reservoir was empty. The spent coffee grounds were removed dried for a minimum of 24 hours in an oven at 60 °C and weighed before solvent extraction. This was repeated one time, for a total of two.

Using a commercially available espresso machine (The DeLonghi-brand Caffe Treviso), approximately 20 grams of ground was added filter basket inside the portafilter and compacted slightly. Once the portafilter was locked into place and the espresso machine had reached the required temperature, the water was turned on allowed to flow through the coffee. The water was turned off when the flow became clear (approximately 200 ml), under the assumption that most water-soluble compounds in the coffee had been removed. The spent coffee grounds were removed, dried for a minimum of 24 hours in an oven at 60 °C and weighed before solvent extraction. This was repeated four times, for a total of five.

2.2.2.2 Oil Extraction

The coffee grounds were accurately weighed and suspended in fresh heptane (1:10 wt. ratio). The coffee was then stirred for 180 minutes at room temperature. The solvent was replaced with fresh heptane and the extraction undertaken for a further 180 minutes. At this point, less than 0.6 % oil was left in the grounds (determined by preliminary experiments), and no further extractions took place. . The solvent fractions were combined and the heptane removed *in vacuo*.

2.2.2.3 Transesterification

The oil (10g) was added to an excess of methanol (~50 ml) and sulfuric acid (10 wt% in relation to the oil). The reaction mixture was refluxed for 24 hours. On completion of the reaction the mixture was filtered to determine the amount of unsaponifiable material and subsequently washed three times with distilled water to remove the methanol, glycerol and acid catalyst. The glyceride to FAME yield was calculated using ^{1}H NMR spectroscopy to ensure that over 99% of the glyceride species had reacted.

2.2.2.4 Biodiesel Analysis

The biodiesel was analysed by ^{1}H NMR spectroscopy and GC-MS. GC-MS analysis was carried out using the Agilent 7890A Gas Chromatograph equipped with a capillary column (60 m x 0.250 mm internal diameter) coated with DB-23 ([50%-cyanpropyl]-methylpolysiloxane) stationary phase (0.25 µm film thickness) and a He mobile phase (flow rate: 1.2 ml min^{-1}), coupled with an Agilent 5975C inert MSD with Triple Axis Detector. Approximately 50 mg of each sample was dissolved in 10 ml 1,4-dioxane and 1 µl of each solution was loaded onto the column, pre-heated to 150 °C. This temperature was held for 5 minutes and then heated to 250 °C at a rate of 2 °C min^{-1} and then held for 2 minutes. NMR spectroscopic measurements were carried out at 298 K using a Bruker AV300 spectrometer, operating at 300.13 MHz for ^{1}H. Typically samples were made up of 0.05 ml of the oil or biodiesel sample dissolved in 0.5 ml $CDCl_3$. ^{1}H spectra were typically acquired using a 30 degree excitation pulse and a repetition time of 4.2 sec. 0.3 Hz line broadening was

applied before Fourier transform, and spectra were referenced to the residual $CHCl_3$ peak from the solvent (δ 7.26 ppm).

Kinematic viscosities were determined in accordance with ASTM D445. A Canon-Fenske capillary kinematic viscometer was used. Temperature modulation was achieved using a refrigeration/heating unit. Samples within the viscometer were allowed to rest at 40 °C for a minimum of 5 minutes prior to viscosity measurement to allow temperature equilibration. The standard error was found to be ±0.100 mm^2s^{-1} at 40 °C. Pour points of the fuels were determined visually by cooling of 1.5 ml vials of the samples in low temperature freezers and cold rooms of specific temperatures, with periodic checking to see if the pour point had been surpassed. The samples were allowed to rest at each temperature for a minimum of 60 minutes in order to allow equilibration of temperatures. Densities were determined gravimetrically by weight 10 cm^3 ± 0.01cm^{-3} and weighing to an accuracy of ±0.0005 g.

2.3 Results and Discussion

2.3.1 Oil Extraction and Transesterification

While a number of techniques have been reported to extract the oil from coffee effectively, Al-Hamamre, *et al.* demonstrated that hexane was the most suitable, yielding just over 15 wt% oil over only 30 min with a Soxhlet setup.[31] Accordingly, heptane was used in this study, according to an adapted literature method,[46] due to its low toxicity.[47] While coffee grounds have been reported to contain up to 20 wt% lipid, contents of around 10-15 wt% are more commonly reported in the literature.[48] The coffee lipid, however, does not only contain triglyceride species. Other biomolecules present in the lipid portion of coffee beans include terpenes, sterols and tocopherols. These are generally grouped as unsaponifiable compounds, i.e. those species that cannot be transesterified.[49] The unsaponifiable matter can have significantly negative effects on the physical properties of the biodiesel produced, as well as potentially hindering transesterification itself.

In a study of biodiesel made from healthy and defective (i.e. those that are black, or immature) beans originating from Brazil, Oliveira, *et al.* discovered an unsaponifiable content of 19 and 24%, respectively.[35] It was found that the coffee oil used for the study had a high viscosity (170 mPa.s versus refined soybean oil's viscosity of 43 mPa.s), and that the transesterification of both oils lead to lower FAAE yields than was expected, attributed to the unsaponifiable matter present. Two of the main insoluble compounds found in the esterified coffee oil are likely to be the cyclic terpenes commonly found in coffee oil: kahweol and cafestol.[50-52] Both of these products were found to be present in the fresh coffee grounds (FCG) and spent coffee grounds (SCG) oils tested (Figure 2.4).

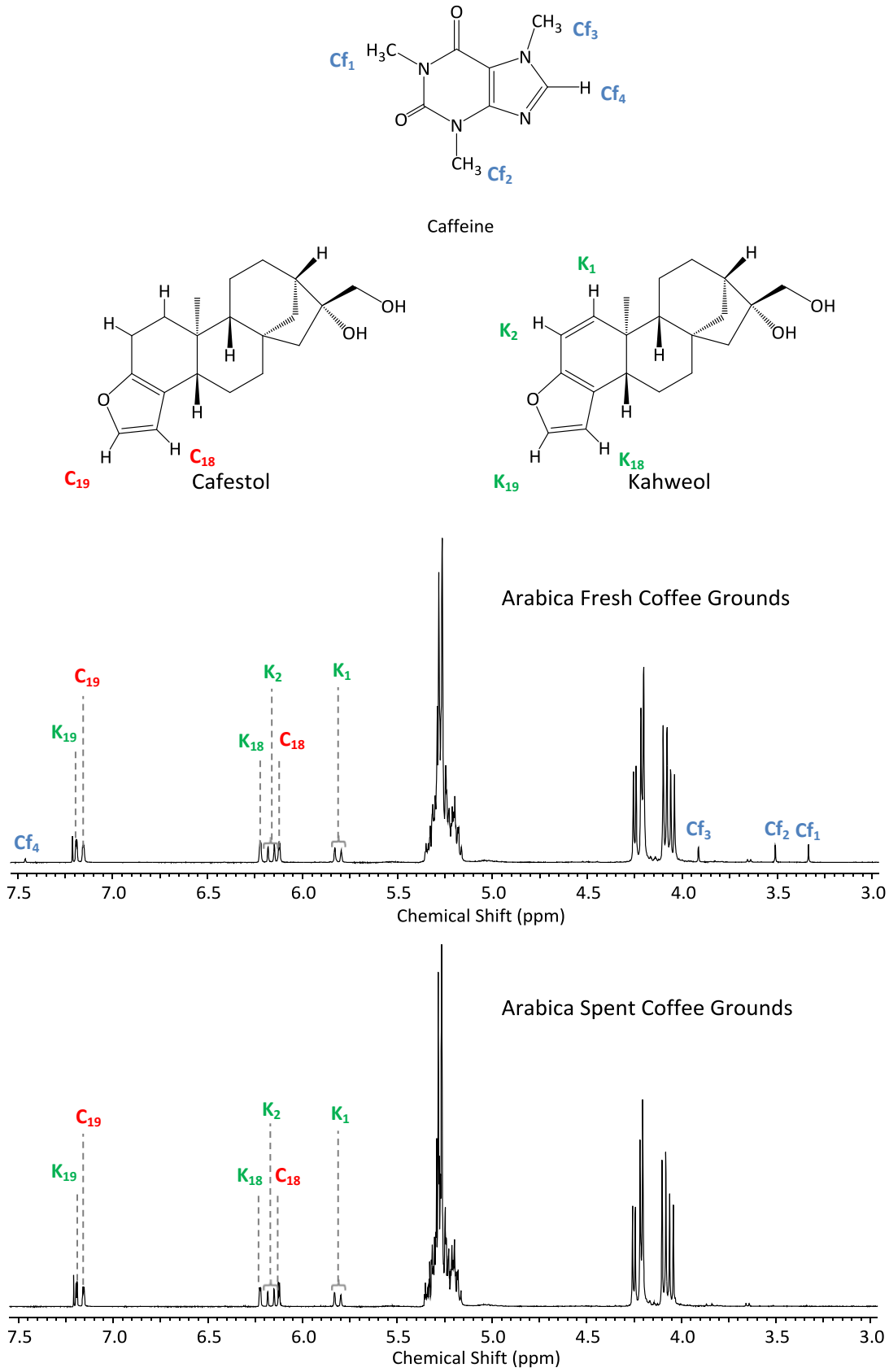

Figure 2.4 Selected signals from ^{1}H NMR spectra of 100% Arabica coffee oil from fresh (top) and spent (bottom) grounds, showing molecular structures of kahweol, cafestol and caffeine. Kahweol and cafestol proton assignments from D'Amelio, *et al.*[52]

It was also found that upon conversion of the lipid (using sulfuric acid as the transesterification catalyst) to biodiesel, the mixture formed a black gelatinous product and sulfuric acid was therefore replaced by sodium methoxide. However, due to the high amount of free fatty acids in coffee oil,[24] the use of such Brønsted base catalysts leads to soap formation and emulsification between the organic fractions and aqueous fractions during work-up. In this study, sulfuric acid was chosen as the transesterification catalyst.

To ensure near-complete transesterification, the oil samples were transesterified with 10 wt% sulfuric acid and an excess of methanol over 24 hours. After this time, the reaction flasks contained a similar dark blue-green, insoluble gelatinous matter as has been reported in previous studies.[35, 48] Prior to washing the reaction mixture with water to remove the methanol, acid catalyst, and glycerol present in the reaction mixture, it was filtered to remove the insolubles, though the oil retained the dark blue-green colour. Upon washing with water, the aqueous layer took on a blue-green hue, suggesting water-soluble species. After further washing with water (200 ml x 3), the organic layer and therefore the product achieved was dark brown, similar to the original colour of the coffee oil. The conversion of this saponifiable material was assessed by ^{1}H NMR spectroscopy to ensure conversions of over 99%.

To assess the effect of geography on the lipid of the coffee bean, coffee grounds from the top 11 coffee producing nations were tested in their fresh state and after using the cafetière brewing method (Figure 2.5). All the coffees examined were 100% *Coffea arabica*. All FCG oils tested contained between 11 – 14 wt% lipid and, upon brewing, around 30% of the weight of the coffee is lost through the brewing process.

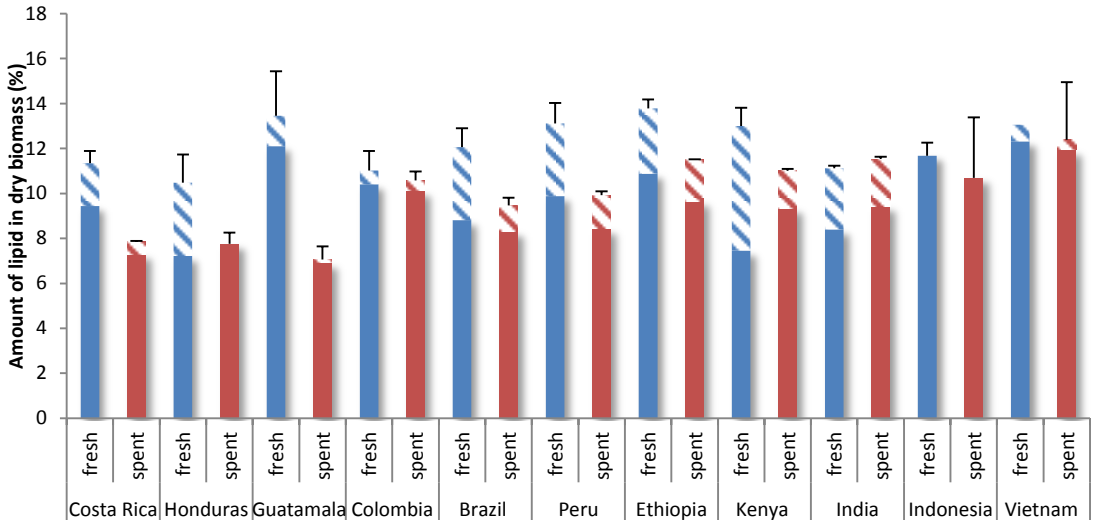

Figure 2.5 Oil content and FAME yield from a range of geographical locations, black bars indicate the amount of lipid extracted from FCG, the blue bars indicate the lipid extracted from SCG (as a percentage of the post-brewed dry coffee biomass). The filled area shows the level of saponifiable matter and the unsaponifiable matter is given as stripes.

Generally SCG yield a lower percentage of oil as a percentage of its dry mass, containing between 7 – 13 wt% lipid. This small overall decrease in lipid content shows that, while the majority of the oil is retained in the coffee ground, some is lost when brewed. Interestingly, the proportion of unsaponifiable material in the lipids is significantly lower in the SCG than the FCG when compared to the total lipid, and so presumably the unsaponifiables are more water soluble than the glyceride species. A larger majority of the oil extracted from SCG is glyceride species, with the brewing removing troublesome biomolecules, potentially leading to an improved fuel compared to FCG biodiesel.

There was seemingly no trend in the lipid content when compared to geographical location. However, it is known that the local climatic conditions, the time of picking and the method of drying all play a large role in the composition of the coffee,[53] which likely vary between regions. For example, green coffee can by produced by either wet or dry processing methods. In wet processing the ripe berries are mechanically processed to remove the pulp and the residues degraded by fermentation. The resulting coffee is dried, conditioned and hulled. In dry processing, entire coffee fruits are dried without removal of the pulp. These different methods are known to change the chemical composition of the beans.[54-55]

Though the amount of overall lipid was seemingly unaffected by geographical origin, the proportions of saponifiable and unsaponifiable were significantly more varied, ranging from below 0.1 total oil mass % for coffee sourced from Indonesia to up to 40 total oil mass % in the lipid sourced from Kenyan FCG.

The decaffeination process, as has been mentioned, is a solvent-pretreatment of the coffee to extract caffeine, and could have an effect on the oil content of the beans. To investigate its effect, the lipid from three different samples of decaffeinated coffee was extracted and analysed (Figure 2.6). Interestingly the process does not seem to affect the lipid content and little difference was observed between the decaffeinated samples and the other coffees used in this study, ranging from 11 – 15 %. The amount of unsaponifiable matter left in the FCG and SCG is also elevated and similar to the other coffees tested, which suggests that the decaffeination process is highly selective for caffeine over alternative biomolecules.

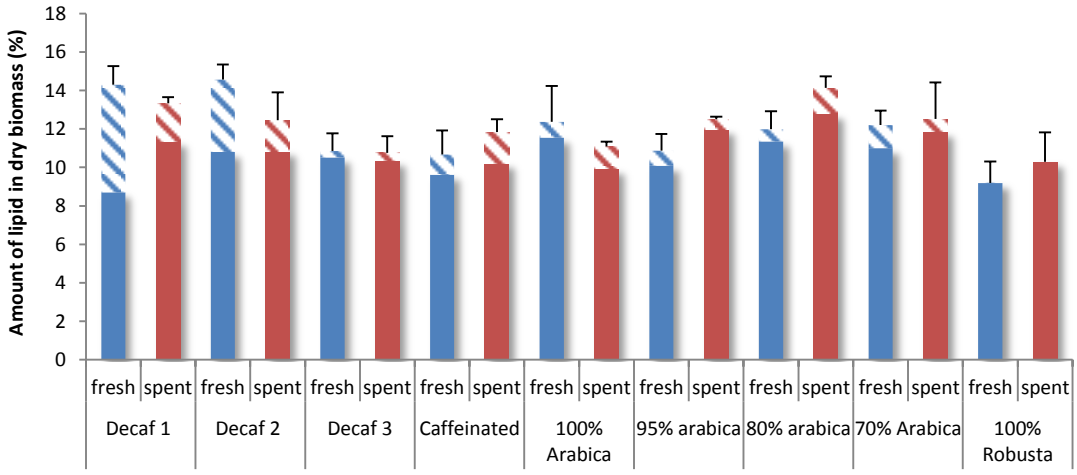

Figure 2.6 Oil content and FAME yield from a range of different strength blends and decaffeinated coffee. Blue bars indicate the amount of lipid extracted from FCG, the red bars indicate the lipid extracted from SCG (as a percentage of the post-brewed dry coffee biomass). The filled area shows the level of saponifiable matter and the unsaponifiable matter is given as stripes.

Another potential effect on the oil content of waste coffee is the presence of Robusta beans. They are typically mixed with Arabica to control the caffeine content and the taste, as Robusta beans are generally bitterer in flavour. It has been reported that Robusta beans have lower lipid content than Arabica.[56-57] Five coffee types; 100% Arabica, 95% Arabica 5% Robusta, 80% Arabica 20% Robusta,

70% Arabica 30% Robusta and 100% Robusta were therefore examined for their lipid content.

The total oil recovered from FCGs and SCGs, composed of varying proportions of Arabica and Robusta, ranging from 9.5% to 13.2% and 11.0% to 14.0%, respectively (Figure 2.6). Though the 100% Robusta coffee has a lower lipid content relative to the 100% Arabica coffee, it cannot be unequivocally stated that all Robusta beans have less lipid than Arabica due to the varying levels for the different blends. The lipid from Robusta, however, contained little unsaponifiable matter. This effect was not as pronounced for the different blends, suggesting that oil yield is not heavily dependent on the coffee composition.

A wide variety of methods are used globally to brew coffee, ranging from the simple, traditional methods to more sophisticated and modern techniques. Generally, they can be separated into three categories: *steeping* methods, *pour-over/drip* methods, and *pressure* methods. Each method can differ in brewing temperature, pressure, coffee/water ratio, contact time and ground size, which ultimately affects the amount and composition of the material extracted. For domestic methods, the amount of water soluble material extracted has been reported to range between 24.2 and 31.4%, depending on the method used.[58] The waste streams for coffee will potentially have different material composition depending on the source, as different brewing methods are used domestically, commercially and industrially, which could affect the composition of the lipid present. In commercial coffee-shops, for example, coffee brewing is generally achieved by espresso and drip-filter techniques. However in the house-hold, a variety of different methods – including cafetière, moka, AeroPress, and "single-serve" pod machines – are used.[59] To assess the effect of these different brewing techniques on the lipid produced, the same coffee (Columbian) was used to brew coffee using a commercially-available espresso machine, an AeroPress coffee maker and a drip-filter coffee maker (Figure 2.7).

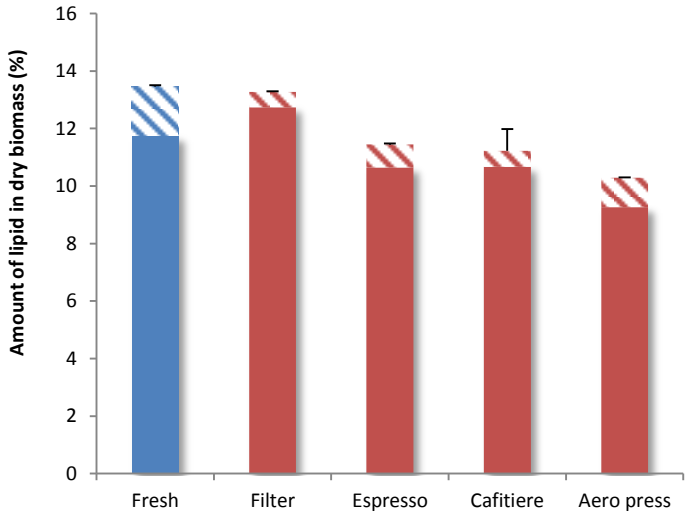

Figure 2.7 Oil extracted from the same type of coffee subjected to a number of brewing method. Blue bars indicate the amount of lipid extracted from FCG, red bars indicate the lipid extracted from SCG (as a percentage of the post-brewed dry coffee biomass). The filled area shows the level of saponifiable matter and the striped area, the unsaponifiable lipid.

For all brewing methods, the total lipid extracted decreased when compared to fresh. For fresh coffee, the level of lipid recovered was 13.5%, while the different brewing methods yielded between 10.3 to 13.3%. The filter coffee machine yielded the most oil, whilst AeroPress coffee maker yielded the least. SCG obtained by the filtered method had an oil content of 8.1%, 15.4% and 28.7% higher than SCG obtained by cafetière, espresso and AeroPress, respectively. Potentially this is due to the different pressures and temperatures the grounds are subjected to during the brewing process. However, for each method the percentage of unsaponifiables present in the overall lipid was lower than that for FCG, suggesting that they are more soluble than triglycerides. This is unsurprising, as many unsaponifiables reported to be present in coffee grounds (kahweol, cafestol and α-tocopherol) possess hydroxyl moieties in their structure.

For filter coffee, hot water is poured slowly over the fresh coffee, extracting the flavour as it runs through. There is no pressure higher than atmospheric involved in this process and therefore it is likely that the coffee grounds retain their oil more effectively using this method.[50] The higher pressures employed in the other

methods compresses the coffee grounds more effectively, resulting in superior extraction of the oils and more retention of unsaponifiable lipids.

2.3.2 Biodiesel Composition and Properties

The FAME profile of the biodiesel produced from each coffee was analysed via GC-MS (Table 2.1). The fuel properties and therefore suitability of an oil as a biodiesel feedstock are dependent on the FAME profile.[60] The composition of coffee lipid extracted in prior studies generally consists of four major fatty acids; palmitic acid (16:0, 32 - 51%), stearic acid (18:0, 7 - 8%), oleic acid (18:1, 0 – 9%) and linoleic acid (18:2, 40 – 46%).[32, 35-36, 48] Interestingly, there is little variation in the FAME profile of the oils examined, with palmitic acid ranging from 35.4 – 42%, stearic acid from 6.7 – 8.5%, oleic acid from 6.5 – 11.5%, and linoleic acid from 42.2 – 49.9%. Also identified were small amount of linolenic acid (18:3) and eicosenoic acid (20:0), each up to 1.5%. This is in direct contrast to terrestrial crops and microbial oils, where the FAME profile is highly variable and dependent on growth conditions.[61-63] One exception is the coffee sourced from Vietnam, where the lipids possess a significantly higher portion of monounsaturates (23.1% in FCG, 24.0% in SCG) than any other coffee in this study or reported previously. Though the coffee is advertised as a blend of Arabica and Robusta beans, Vietnamese coffee is well known for its use of artificial flavouring and enzymatic treatments to provide similar flavour to its famous 'Civet' coffee, which may affect the structure of the lipids.[64]

The FAME profiles of the FCG are very similar to the SCG, with no degradation of the unsaturated esters observed. This suggests that the resulting coffee oil is relatively stable. This is agreement with the literature, where waste coffee biodiesel was found to have a Rancimat score of 3.05,[32] a score comparable to palm oil methyl ester (at 3.52) and better than sunflower oil methyl ester (at 2.10).[65] However, it should be noted that for the minimum allowed according to the EU standard for biodiesel is 6, whereas for the US the minimum is 3.[66-67] Though the coffee oil is relatively stable, the process of brewing and (to a larger extent) roasting will have an effect on the stability of the oil. Therefore the effects of roasting and brewing on the stability of the resultant fuel should be determined.

Table 2.1 Weight percent FAME of the biodiesel produced from the coffee samples, FCG = fresh coffee grounds, SCG = spent coffee grounds, Tr = trace, less than 0.5%.

	Costa Rica		Honduras		Ethiopia		Indonesia		Kenya		Columbia		Brazil		Vietnam	
Type	**FCG**	**SCG**	**FCG**	**SCG**	**FCG**	**SCG**	**FCG**	**SCG**	**FCG**	**SCG**	**FCG**	**SCG**	**FCG**	**SCG**	**FCG**	**SCG**
16:0	36.9	35.4	37.2	35.4	36.4	36.4	36.8	36.9	38.1	41.4	36.5	36.7	36.7	37.1	41	40.4
18:0	6.7	6.7	7.3	6.7	7.4	7.4	7.4	7.5	7.4	8.2	7.0	7.6	8.2	8.5	12.1	13.5
18:1	6.6	6.7	6.8	6.7	7.4	7.4	6.6	6.6	6.7	7.1	6.7	7.9	8.2	8.3	23.1	24.0
18:2	48.5	49.9	47.4	49.9	46.4	46.4	46.5	46.2	45.3	42.2	47.1	45.1	45.6	44.7	22.9	22.0
18:3	Tr.	Tr.	Tr.	Tr.	1.4	1.4	1.4	1.4	1.4	Tr.	1.4	1.5	Tr.	Tr.	Tr.	Tr.
20:0	1.2	1.2	1.3	1.2	1.0	1.0	1.4	1.4	1.1	1.2	1.2	1.3	1.3	1.4	0.9	0

	Peru		Guatemala		India		100% Arabica		100% Robusta		95% Arabica		80% Arabica		70% Arabica	
Type	**FCG**	**SCG**	**FCG**	**SCG**	**FCG**	**SCG**	**FCG**	**SCG**	**FCG**	**SCG**	**FCG**	**SCG**	**FCG**	**SCG**	**FCG**	**SCG**
16:0	37.3	41.3	37	38.8	37.6	36.8	36.1	36	35.4	35.7	36.3	36.5	36.2	36.3	36.8	37
18:0	7.4	8.2	6.8	6.9	8.4	8.3	8.1	8.1	7.5	7.6	8.1	8.3	7.8	8.0	7.9	8.0
18:1	6.5	6.7	6.8	6.3	8.0	8.4	7.0	7.0	11.5	11.5	7.6	7.8	7.9	8.0	8.3	8.3
18:2	46.1	42.2	48.2	46.7	43.3	43.8	46.1	46.1	44.5	44	45.3	46.1	46.6	46.3	45.6	45.3
18:3	1.4	Tr.	Tr.	Tr.	1.4	1.3	1.4	1.4	Tr.	Tr.	1.4	Tr.	Tr.	Tr.	Tr.	Tr.
20:0	1.3	1.5	1.2	1.2	1.3	1.3	1.4	1.4	1.2	1.2	1.3	1.4	1.4	1.4	1.4	1.4

	Decaffeinated 1		Decaffeinated 2		Decaffeinated 3		Colombian FCG		Cafetière (Columbian)		Filter (Columbian)		Aeropress (Colombian)		Espresso (Colombian)	
Type	**FCG**	**SCG**	**FCG**	**SCG**	**FCG**	**SCG**	**FCG**	**SCG**	**FCG**	**SCG**	**FCG**	**SCG**	**FCG**	**SCG**	**FCG**	**SCG**
16:0	36.9	37.4	42	40.7	36.5	36.8	36.5			36.7		37		37.3		36.5
18:0	7.4	7.5	7.5	7.9	8.4	8.3	7.0			7.6		7.6		7.8		7.7
18:1	7.0	7.2	6.6	6.7	8.2	8.4	6.7			7.9		8.0		8.2		8.0
18:2	46.2	45.4	43.9	43.4	44.3	43.8	47.1			45.1		44.7		45.3		45.1
18:3	1.2	1.3	Tr.	Tr.	1.3	1.3	1.4			1.5		1.5		Tr.		1.5
20:0	1.3	1.3	Tr.	1.2	1.3	1.3	1.2			1.3		1.3		1.3		1.3

Another important factor is the presence of caffeine in the lipids. Caffeine is a xanthine based alkaloid, and as such contains four nitrogen atoms. Caffeine was found to be present in all the oils and biodiesels extracted from FCG, though was not observed in any of the SCG oil or biodiesel (Figure 2.8). This is an advantage of SCG-based fuel over FCG as the presence of nitrogen-containing compounds will, upon combustion, produce harmful mono-nitrogen oxides (NO_x) emissions which are heavily regulated.[68]

The amount of caffeine present can be calculated from the ^{1}H NMR spectroscopy, using the integration values for the FAME methoxy group (δ 3.6 ppm) and the shift for the aromatic proton in caffeine's structure (δ 7.45 ppm). For Arabica FCG biodiesel, the approximate amount of caffeine is 0.5 mol% (Figure 2.8). Caffeine would account for 0.32% of the weight of the fuel, or 4.3 g per litre^{-1}.

Current European standards quote the emission limits of a car in g km^{-1}. Assuming an average fuel consumption of a diesel car of 4.5 litres per 100km (combined fuel consumption of a 2014 Ford Focus 1.6 l TDCi), 0.045 litres of fuel would be combusted each km, in which 0.194 g of caffeine would be present. Assuming complete combustion of the caffeine, and that an even amount of NO and NO_2 are produced, this would equate to 0.182 g of NO_x per km. The current European legislation on emissions, Euro 5, allows only 0.180 g km^{-1} NO_x. Euro 5 is now being phased out, replaced by stricter emissions regulations (Euro 6), which allows for only 0.080 g km^{-1} NO_x. Irrespective of the level of NO_x produced from atmospheric nitrogen, caffeinated fuels would not be permissible in the EU. It is therefore necessary for coffee biodiesel to be solely produced from used coffee grounds and not from rejected beans or FCG.

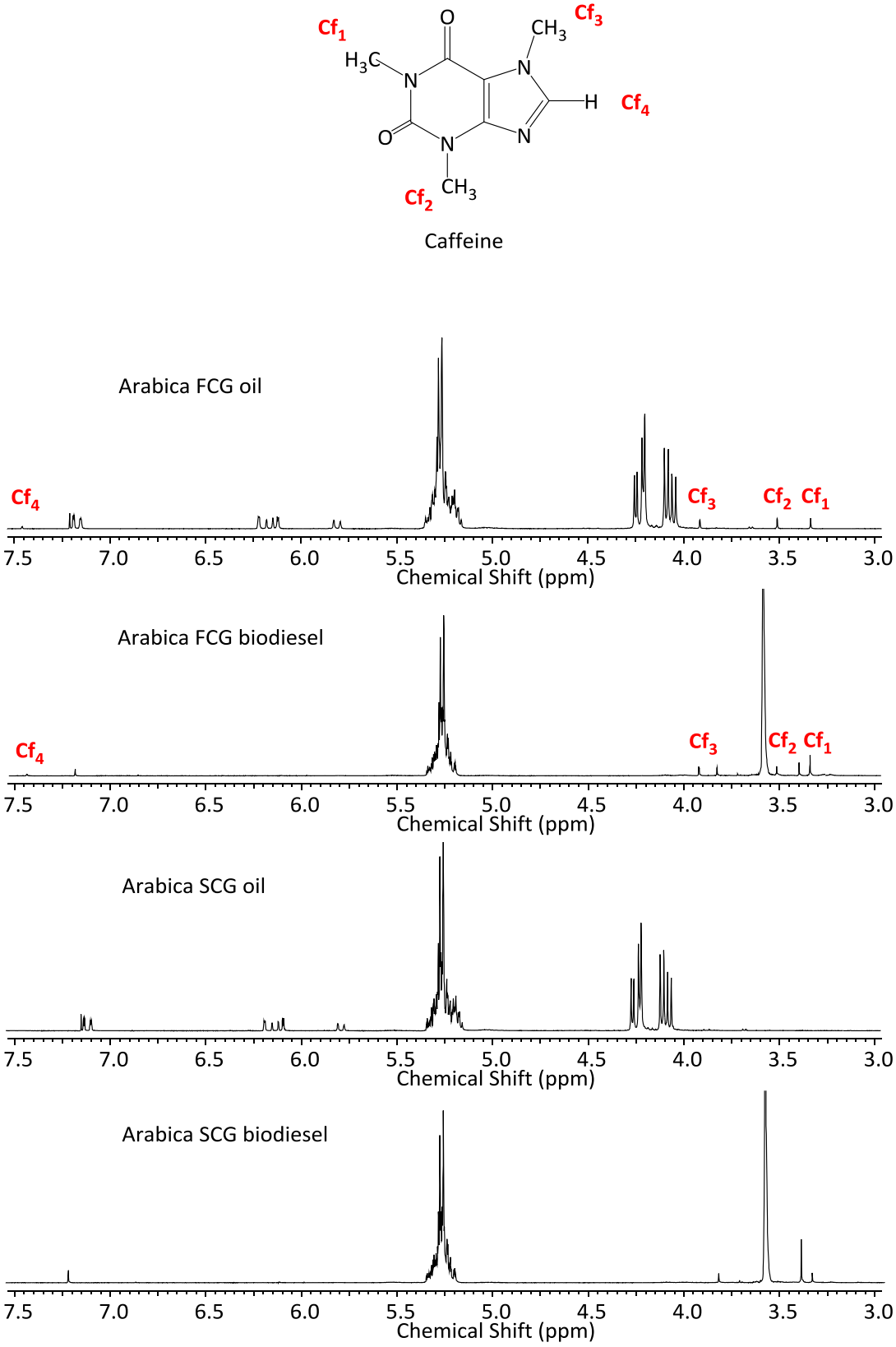

Figure 2.8 ^{1}H NMR Spectra of 100% Arabica coffee oil (from both fresh and spent) and biodiesel (from both fresh and spent), showing the proton shifts associated with caffeine.

Though a number of studies discuss the potentiality of waste coffee as a fuel source and investigate its lipid extraction and biodiesel production,[24, 69] little work has been published examining the resulting fuel properties of the biodiesel produced. Kondamudi, *et al.,* investigated the composition and properties of biodiesel produced from oil extracted from SCG derived from a commercial coffee shop. The FAME profile was found to contain 59% saturated esters and 40% linoleic acid, the resulting biodiesel had a viscosity of 5.8 mm^2s^{-1} at 40 °C, a cloud point of 11 °C and a pour point of 2 °C.[32] Oliveira *et. al.* determined that two types of fresh Brazilian bean, one deemed defective and the other suitable for coffee production, produced fuels with variable properties. The kinematic viscosity of the biodiesel produced from the defective beans was 3.1 mm^2s^{-1} at 40 °C, meanwhile the biodiesel from the non-defective beans was 4.9 mm^2s^{-1} at 40 °C. The densities of the biodiesel samples also varied being 894.1 and 892.5 kg m^{-3} respectively.[35] Most recently, Vardon, *et al.* produced biodiesel from collected spent coffee grounds from a local Starbucks. the biodiesel was shown to have a pour point of 13°C, viscosity of 5.2 mm^2s^{-1} at 40 °C and an acid value of 0.11 mg KOH/g (for which both the ASTM D6751 and the EN 14214 maximums are 0.50).[25]

The density of a fuel is an important property, directly affecting engine performance as fuel injection is controlled via a volumetric metering system,[70] and therefore can affect the vehicle range. Biodiesel tends to be of a higher density than that of conventional diesel (attributed to its longer chain length), and so is limited to a range of 860 – 900 kg m^{-3} by EN 14214 standard, though there is no official limit in ASTM D6751. The density of approximately half of the fuels produced from different geographical locations fell within the European standard (Figure 2.9) with the rest falling slightly above or below, the lowest being 841 kg m^{-3} and the highest being 926 kg m^{-3}. Similar results can be seen for the biodiesel produced from decaffeinated coffees, and those with varying levels of Robusta (Figure 2.10), with densities ranging between 844 kg m^{-3} to 927 kg m^{-3}. While there is a lot of variation between the samples, there is no clear pattern between the densities of biodiesel from FCG or SCG, caffeinated or decaffeinated or between different bean types.

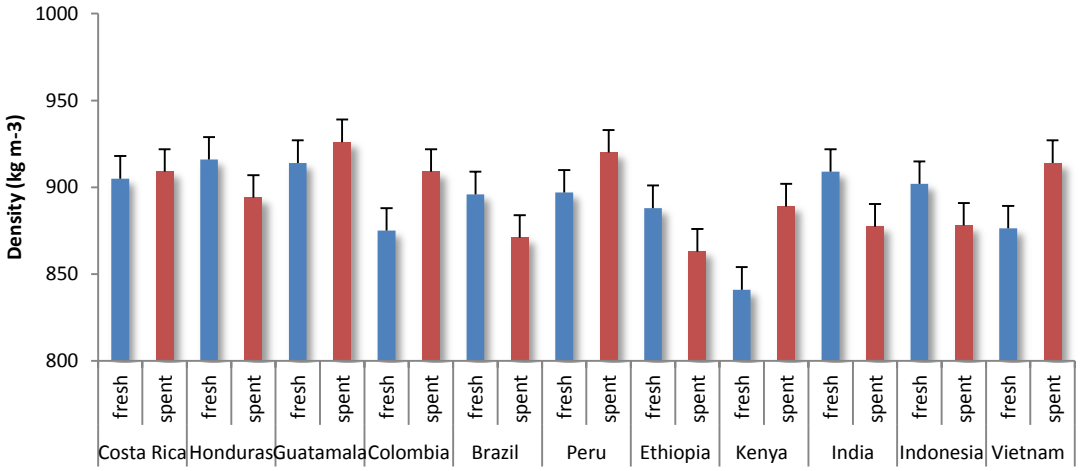

Figure 2.9 Densities of the FAME produced from coffee sourced from a range of geographical locations, blue bars indicate FCG, red bars indicate SCG. Error bars represent systematic error.

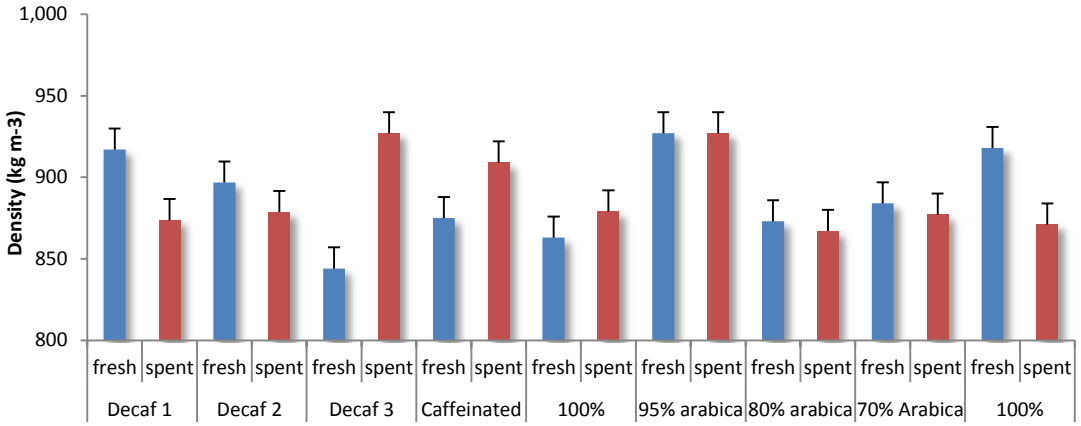

Figure 2.10 Densities of the FAME produced from coffee sourced from a range of different strength coffees including decaffeinated coffee. Blue bars indicate FCG, red bars indicate SCG. Error bars represent systematic error.

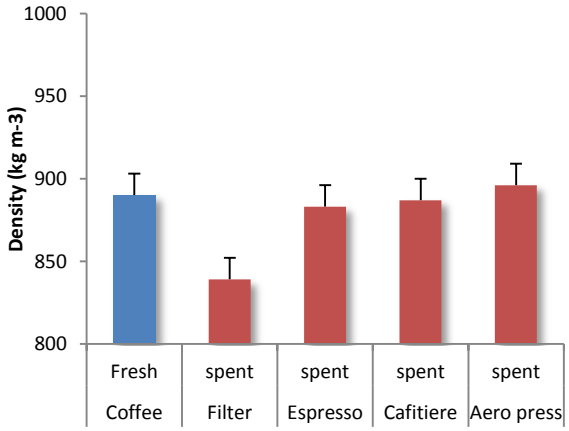

Figure 2.11 Densities of the FAME produced from the same type of coffee subjected to a number of brewing methods. Blue bars indicate from FCG, the red bars indicate from SCG. Error bars represent systematic error.

Comparing the different brewing methods, it was found that the density of the biodiesels for the Colombian FCG and SCG made from the espresso, cafetière and AeroPress methods were very similar, though filter produced a lower density fuel (Figure 2.11). This suggests that the pressures and temperatures associated with the other systems may be extracting biomolecules that were not using the filter machine.

The kinematic viscosity of the biodiesel is one of the most important parameters of a fuel, as it affects how the fuel flows around the engine, whether the atomisation from the injection is sufficient enough for uniform and efficient combustion and also can affect the effectiveness of seals. All biodiesel sold within the EU must have a kinematic viscosity of between 3.5 – 5.0 $mm^2 s^{-1}$ at 40 °C, according to EN 14214, whereas the ASTM standards are less restrictive, allowing biodiesel of kinematic viscosity between 1.9 and 6.0 $mm^2 s^{-1}$ at 40 °C. All the coffee biodiesel samples were analysed using a kinematic viscometer at 40 °C (Figs. 2.12 – 2.14). The biodiesel produced from the different regions generally lie between 3.5 and 5 $mm^2 s^{-1}$ and therefore would be able to be used in both Europe and the US, as well as being similar to previously published coffee-derived biodiesel.[32, 35] Biodiesel produced from Kenyan FCG and SCG, however, are significantly above the EU maximum at 5.89 and 5.59 mm^2s^{-1} respectively, and Honduras FCG is slightly below the EU minimum at 3.26 mm^2s^{-1}. All three, however, fall within US standards.

Those fuels produced from decaffeinated coffee and from the varying proportions of Arabica and Robusta possess similar viscosities. All fall within 3.5 and 5.0 mm^2s^{-1}, and therefore within the EU and US fuel standards, with the exception of one of the decaffeinated coffees which falls just above the EU maximum at 5.1 mm^2s^{-1}. The viscosity of the biodiesel increases slightly when a filter coffee maker is used as opposed to other methods. The harsher methods can be seen to reduce the viscosity slightly. This is likely due to different compounds, such as α-tocopherol, squalene and nonacosane (all reported to be present in coffee oil[49]), which affect the viscosity of the oil by being extracted into the coffee beverage under these harsher methods, and therefore not present in the oil or biodiesel. All, however, fall within the EU standard and therefore the US standards.

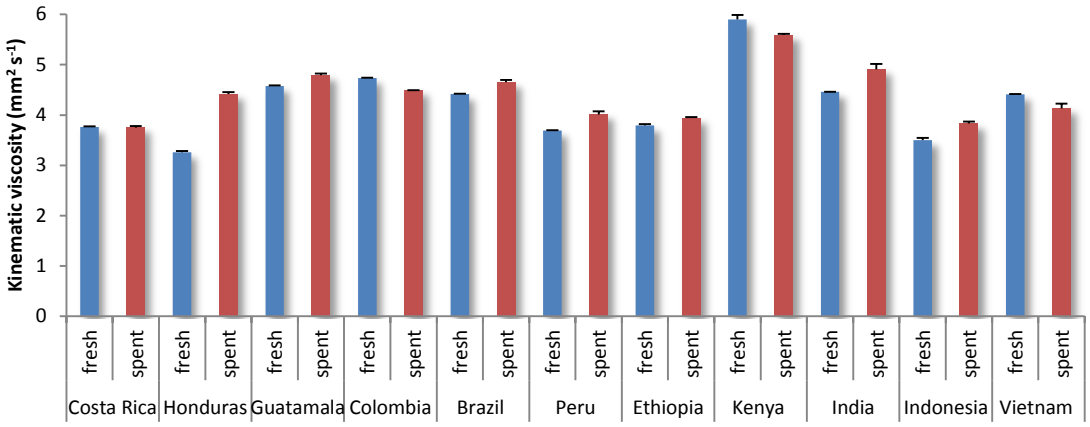

Figure 2.12 Kinematic viscosity of the FAME produced from coffee sourced from a range of geographical locations. Blue bars indicate the biodiesel was produced from FCG, red bars indicate from SCG.

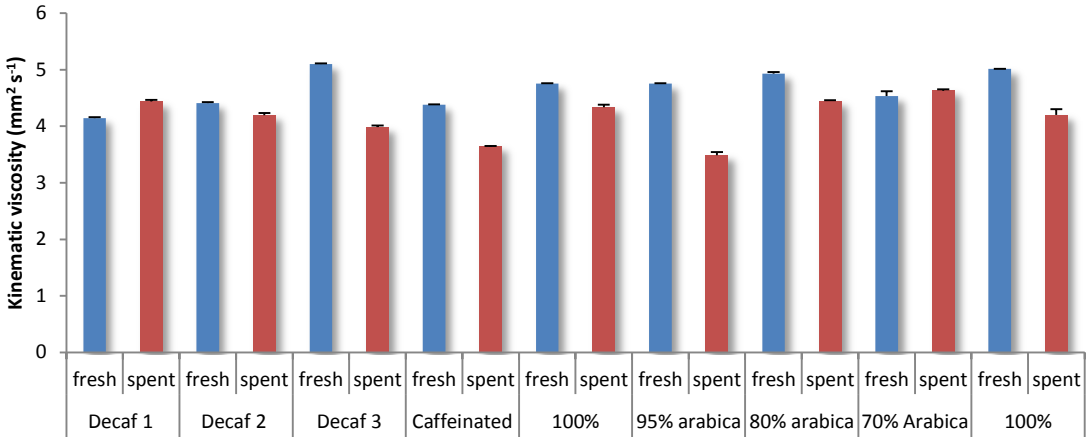

Figure 2.13 Kinematic viscosity of the FAME produced from coffee sourced from a range of different strength coffees including decaffeinated coffee. Blue bars indicate FCG, red bars indicate SCG.

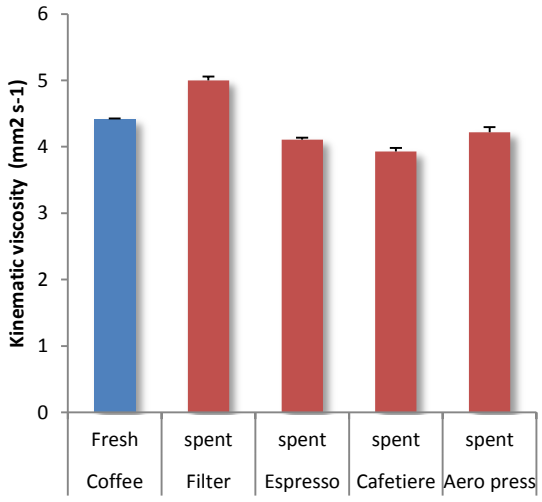

Figure 2.14 Kinematic viscosity of the FAME produced from the same type of coffee subjected to a number of brewing methods. Blue bars indicate from FCG, red bars indicate from SCG.

Pour point is also an important fuel property, as it dictates the environmental conditions in which it can be used. Biodiesel typically has a poor pour point when compared with conventional diesel and therefore cannot be used at high blends in winter conditions.

The pour point of biodiesel from fresh and spent coffee oil obtained from all the samples tested exhibited a significant variation, ranging from -1 – 16 °C (Figs. 2.15-2.17). Again, there is no clear trend between geographical location, decaffeination, varying bean type or brewing methods. It can be seen, however, that the pour points for SCG biodiesel are generally the same or lower than for FCG biodiesel. The coffee biodiesels produced have roughly 50% saturated esters. Based on this, it would be expected that the biodiesel would have a similar pour point to palm oil, which is between 10-16 °C.[60] While most samples are comparable, some have sub-zero pour points. This could be due to other biomolecules in the biodiesel disrupting the stacking between the saturated esters.

However, this is refuted by the pour points of the different brewing techniques. For the density and the viscosity, the three harsher techniques (espresso, cafetière and AeroPress) possess more similar densities and viscosities to the FCG biodiesel than the filter. This has been attributed to the filter method being more efficient at extracting other biomolecules into the beverage than the triglycerides, accounting for its significantly small percentage of the overall lipid. However, there is no substantial difference in the pour points of the different brewing techniques, with the pour point of filter SCG biodiesel being very similar to that of FCG, while there is significant variation across the geographical regions.

One potential reason for the difference could be the difference in the bean roasting, and therefore the difference in the other biomolecules present. A darker roast could potentially cause more unsaturated molecules (such as squalene) to break down to more water-soluble oxygenates, whereas a lighter roast may allow a higher proportion to remain, to be extracted with the organic solvent and the rest of the lipid, and therefore effect the other physical properties. This cannot be determined due to the lack of knowledge of the different roasting processes.

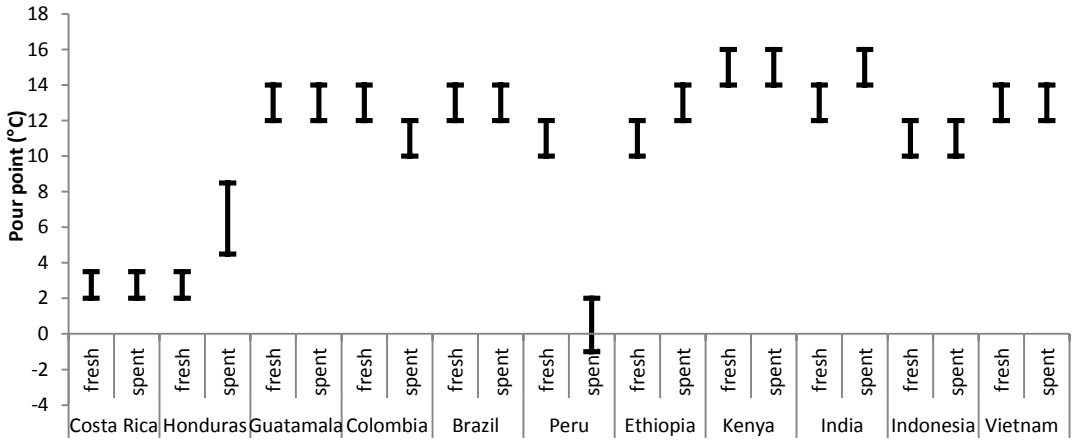

Figure 2.16 Pour points of the FAME produced from coffee sourced from a range of geographical locations.

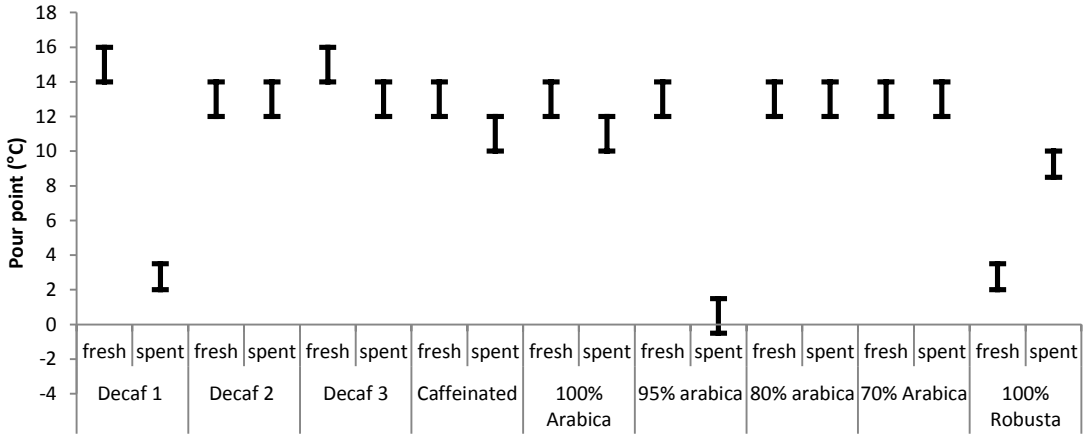

Figure 2.17 Pour points of the FAME produced from coffee sourced from a range of different strength coffees including decaffeinated coffee.

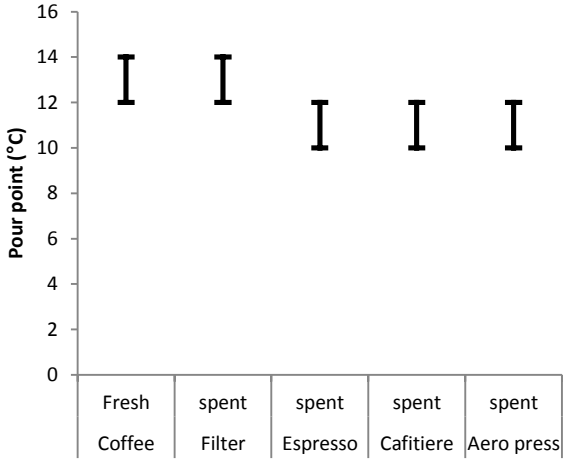

Figure 2.18 Pour points of the FAME produced from the same type of coffee subjected to a number of alternative brewing methods.

2.4 SUMMARY

In this investigation, oil extraction, saponifiable lipids and fatty acid profile of a range of coffees from different locations of origin, production process, and brewing techniques were assessed. Each oil was subsequently converted to biodiesel via transesterification and tested for key fuel properties, those being density, viscosity and pour point.

The coffee grounds used in this study contain between 7 - 14% lipids, with a relatively minor reduction in lipid portion (with respect to the dry coffee mass extracted) upon brewing. The lipid extracted contains a majority of saponifiable lipids that can be transesterified into biodiesel. The lipid can contain up to 40% unsaponifiable compounds though this is generally much lower. There is a large variability in the amount of lipid extracted from the grounds, but there was no clear trend when comparing geographical location or bean type. However, the overall proportion of unsaponifiable matter was lower in spent coffee than fresh, likely due to the brewing process extracting them more efficiently than glyceride species. The amount of biodiesel achieved, therefore, was similar for both fresh and spent grounds compared to the dry mass.

The fatty acid profile of all but one of the coffees studied was found to be highly similar, regardless of the geographical region, bean type, brewing method of whether the oil extracted was from spent or fresh coffee grounds. The majority of the fatty acids consisted of palmitic acid (35.4% – 42.0%) and linoleic acid (42.2 – 49.9%), with lower amounts of oleic, stearic, linolenic and eicosenoic acid. SCG oil (and the resulting biodiesel) was also found to contain significantly less caffeine than those derived FCG. This suggests that biodiesel produced from defective beans could potentially lead to increased NO_x emissions on combustion.

Despite little variability in the FAME profile, the key fuel properties – density, pour point and viscosity – were reasonably different. The density ranged from 841 - 927 kg m^{-3}, the kinematic viscosity ranged 3.26 - 5.89 $mm^2 s^{-1}$, and the pour point ranged from -1 - 16 °C. This is potentially due to the presence of other biomolecules

present in the oil and the biodiesel. This variability is undesirable as it could cause the fuel to fall out of specification. Therefore, the identification and removal of these biomolecules is vital to further assess the suitability of waste coffee biodiesel as a fuel, though this increased processing would result in increased costs. Furthermore, the effect of the level of roasting (i.e. lighter versus dark roast) on coffee beans on the biomolecules present and their stability should be investigated.

Irrespective of this variation, all the biodiesel fuels tested fell within the US standard for biodiesel, ASTM D6751, and the vast majority fell within the more restrictive European standard, EN 14214. This demonstrates that biodiesel produced from waste resources, irrespective of the source of the waste coffee, has potential to be used in the existing fuel infrastructure. However, coffee from biodiesel still suffers from the inherent issues associated with biodiesel (i.e. poor low temperature performance, poor oxidative stability), which are part of the reason it is restricted to 7 vol% blend in the EU, and 20 vol% in the US. Alternative chemical transformations of triglycerides to produce a fuel of improved physical properties, therefore, are desirable.

2.5 REFERENCES

1. Jenkins, R. W.; Stageman, N. E.; Fortune, C. M.; Chuck, C. J., Effect of the Type of Bean, Processing, and Geographical Location on the Biodiesel Produced from Waste Coffee Grounds. *Energy & Fuels* **2014,** *28* (2), 1166-1174.
2. Pugh, J., Coming soon, coffee that really does rev your engine. *Daily Mail* June 17, 2014.
3. Oasmaa, A.; Solantausta, Y.; Arpiainen, V.; Kuoppala, E.; Sipilä, K., Fast Pyrolysis Bio-Oils from Wood and Agricultural Residues. *Energy & Fuels* **2009,** *24* (2), 1380-1388.
4. Ho, D. P.; Ngo, H. H.; Guo, W., A mini review on renewable sources for biofuel. *Bioresource Technology* **2014,** *169* (0), 742-749.
5. Panda, A. K.; Singh, R. K., Thermo-catalytic degradation of low density polyethylene to liquid fuel over kaolin catalyst. *International Journal of Environment and Waste Management* **2014,** *13* (1), 104-114.
6. Lin, C. S. K.; Pfaltzgraff, L. A.; Herrero-Davila, L.; Mubofu, E. B.; Abderrahim, S.; Clark, J. H.; Koutinas, A. A.; Kopsahelis, N.; Stamatelatou, K.; Dickson, F.; Thankappan, S.; Mohamed, Z.; Brocklesby, R.; Luque, R., Food waste as a valuable resource for the production of chemicals, materials and fuels. Current situation and global perspective. *Energy & Environmental Science* **2013,** *6* (2), 426-464.
7. Food and Agricultural Organisation of the Nations, FAOSTAT - Green Coffee World Production Quanttity. 2012.
8. Mussatto, S.; Machado, E. S.; Martins, S.; Teixeira, J., Production, Composition, and Application of Coffee and Its Industrial Residues. *Food and Bioprocess Technology* **2011,** *4* (5), 661-672.
9. Verdcourt, B.; Bridson, D. M.; Herbarium, E. A., *Flora of tropical East Africa - Rubiaceae Volume 3 (1991)*. Taylor & Francis: 1991.
10. Zuorro, A.; Lavecchia, R., Spent coffee grounds as a valuable source of phenolic compounds and bioenergy. *Journal of Cleaner Production* **2012,** *34* (0), 49-56.
11. Wintgens, J. N., *Coffee: growing, processing, sustainable production : a guidebook for growers, processors, traders and researchers*. Wiley-VCH: 2004.
12. Bertrand, B.; Guyot, B.; Anthony, F.; Lashermes, P., Impact of the *Coffea canephora* gene introgression on beverage quality of *C. arabica*. *Theoretrical Applied Genetics* **2003,** *107* (3), 387-394.
13. Ramalakshmi, K.; Raghavan, B., Caffeine in Coffee: Its Removal. Why and How? *Critical Reviews in Food Science and Nutrition* **1999,** *39* (5), 441-456.
14. Bermejo, D. V.; Luna, P.; Manic, M. S.; Najdanovic-Visak, V.; Reglero, G.; Fornari, T., Extraction of caffeine from natural matter using a bio-renewable agrochemical solvent. *Food and Bioproduct Processing* **2013,** *91* (C4), 303-309.
15. International Coffee Organisation - Decaffeination http://www.ico.org/decaffeination.asp (accessed July 14th).
16. Bernstein, M. New biorefinery finds treasure in Starbucks' spent coffee grounds and stale bakery goods. http://www.acs.org/content/acs/en/pressroom/newsreleases/2012/august/new-biorefinery-finds-treasure-in-starbucks-spent-coffee-grounds-and-stale-bakery-goods.html (accessed July 22nd 2014).
17. Lin, C. S. K.; Leung, C. C. J.; Zhang, A. Y.; Han, W., Valorisation of coffee grinds and unconsumed bakery waste from Starbucks Hong Kong for the sustainable production of chemical and materials. *Abstracts of Papers of the Americal Chemical Society* **2012,** *244*.
18. Nestlé Recycling coffee grounds as fuel | Nestlé Global. http://www.nestle.com/csv/case-studies/AllCaseStudies/Recycling-coffee-grounds-fuel (accessed 22nd July 2014).

19. Kante, K.; Nieto-Delgado, C.; Rangel-Mendez, J. R.; Bandosz, T. J., Spent coffee-based activated carbon: Specific surface features and their importance for H_2S separation process. *Journal of Hazardous Materials.* **2012,** *201*, 141-147.
20. Castro, C. S.; Abreu, A. L.; Silva, C. L. T.; Guerreiro, M. C., Phenol adsorption by activated carbon produced from spent coffee grounds. *Water Sci. Technol.* **2011,** *64* (10), 2059-2065.
21. Arulrajah, A.; Maghoolpilehrood, F.; Disfani, M. M.; Horpihulsuk, S., Spent coffee grounds as a non-structural embankment fill material: engineering and environmental considerations. *Journal of Cleaner Production* **2014,** *72*, 181-186.
22. da Fonseca, B. S.; Vilao, A.; Galhano, C.; Simao, J. A. R., Reusing coffee waste in manufacture of ceramics for construction. *Advanced Applied Ceramics* **2014,** *113* (3), 159-166.
23. Sampaio, A.; Dragone, G.; Vilanova, M.; Oliveira, J. M.; Teixeira, J. A.; Mussatto, S. I., Production, chemical characterization, and sensory profile of a novel spirit elaborated from spent coffee ground. *LWT-Food Science and Technology* **2013,** *54* (2), 557-563.
24. Kwon, E. E.; Yi, H.; Jeon, Y. J., Sequential co-production of biodiesel and bioethanol with spent coffee grounds. *Bioresource Technology* **2013,** *136* (0), 475-480.
25. Vardon, D. R.; Moser, B. R.; Zheng, W.; Witkin, K.; Evangelista, R. L.; Strathmann, T. J.; Rajagopalan, K.; Sharma, B. K., Complete Utilization of Spent Coffee Grounds To Produce Biodiesel, Bio-Oil, and Biochar. *ACS Sustainable Chemistry and Engineering* **2013,** *1* (10), 1286-1294.
26. Cataluna, R.; Kuamoto, P. M.; Petzhold, C. L.; Caramao, E. B.; Machado, M. E.; da Silva, R., Using Bio-oil Produced by Biomass Pyrolysis as Diesel Fuel. *Energy & Fuels* **2013,** *27* (11), 6831-6838.
27. Zanella, E.; Della Zassa, M.; Navarini, L.; Canu, P., Low-Temperature Co-pyrolysis of Polypropylene and Coffee Wastes to Fuels. *Energy & Fuels* **2013,** *27* (3), 1357-1364.
28. Kan, T.; Strezov, V.; Evans, T., Catalytic Pyrolysis of Coffee Grounds Using NiCu-Impregnated Catalysts. *Energy & Fuels* **2014,** *28* (1), 228-235.
29. Yang, S. I.; Hsu, T. C.; Wu, C. Y.; Chen, K. H.; Hsu, Y. L.; Li, Y. H., Application of biomass fast pyrolysis part II: The effects that bio-pyrolysis oil has on the performance of diesel engines. *Energy* **2014,** *66*, 172-180.
30. Karmakar, A.; Karmakar, S.; Mukherjee, S., Properties of various plants and animals feedstocks for biodiesel production. *Bioresource Technology* **2010,** *101* (19), 7201-7210.
31. Al-Hamamre, Z.; Foerster, S.; Hartmann, F.; Kroeger, M.; Kaltschmitt, M., Oil extracted from spent coffee grounds as a renewable source for fatty acid methyl ester manufacturing. *Fuel* **2012,** *96* (1), 70-76.
32. Kondamudi, N.; Mohapatra, S. K.; Misra, M., Spent Coffee Grounds as a Versatile Source of Green Energy. *Journal of Agricultural and Food Chemistry* **2008,** *56* (24), 11757-11760.
33. Canakci, M., The potential of restaurant waste lipids as biodiesel feedstocks. *Bioresource Technology* **2007,** *98* (1), 183-190.
34. Kiss, A. A.; Dimian, A. C.; Rothenberg, G., Biodiesel by Catalytic Reactive Distillation Powered by Metal Oxides. *Energy & Fuels* **2007,** *22* (1), 598-604.
35. Oliveira, L. S.; Franca, A. S.; Camargos, R. R. S.; Ferraz, V. P., Coffee oil as a potential feedstock for biodiesel production. *Bioresource Technology* **2008,** *99* (8), 3244-3250.
36. Oliveira, L. S.; Franca, A. S.; Mendonça, J. C. F.; Barros-Júnior, M. C., Proximate composition and fatty acids profile of green and roasted defective coffee beans. *LWT - Food Science and Technology* **2006,** *39* (3), 235-239.
37. Chhetri, A.; Watts, K.; Islam, M., Waste Cooking Oil as an Alternate Feedstock for Biodiesel Production. *Energies* **2008,** *1* (1), 3-18.

38. Ahangari, B.; Sargolzaei, J., Extraction of lipids from spent coffee grounds using organic solvents and supercritical carbon dioxide. *Journal of Food Processing and Preservation* **2013,** *37* (5), 1014-1021.
39. Couto, R. M.; Fernandes, J.; da Silva, M. D. R. G.; Simões, P. C., Supercritical fluid extraction of lipids from spent coffee grounds. *The Journal of Supercritical Fluids* **2009,** *51* (2), 159-166.
40. Sarrazin, C.; Le Quéré, J.-L.; Gretsch, C.; Liardon, R., Representativeness of coffee aroma extracts: a comparison of different extraction methods. *Food Chemistry* **2000,** *70* (1), 99-106.
41. Araújo, J. M. A.; Sandi, D., Extraction of coffee diterpenes and coffee oil using supercritical carbon dioxide. *Food Chemistry* **2007,** *101* (3), 1087-1094.
42. de Azevedo, A. B. A.; Kieckbush, T. G.; Tashima, A. K.; Mohamed, R. S.; Mazzafera, P.; Melo, S. A. B. V. d., Extraction of green coffee oil using supercritical carbon dioxide. *The Journal of Supercritical Fluids* **2008,** *44* (2), 186-192.
43. Abdullah, M.; Bulent Koc, A., Oil removal from waste coffee grounds using two-phase solvent extraction enhanced with ultrasonication. *Renewable Energy* **2013,** *50* (0), 965-970.
44. de Melo, M. M. R.; Barbosa, H. M. A.; Passos, C. P.; Silva, C. M., Supercritical fluid extraction of spent coffee grounds: Measurement of extraction curves, oil characterization and economic analysis. *Journal of Supercritical Fluids* **2014,** *86*, 150-159.
45. Lercker, G.; Frega, N.; Bocci, F.; Rodriguez-Estrada, M. T., High resolution gas chromatographic determination of diterpenic alcohols and sterols in coffee lipids. *Chromatographia* **1995,** *41* (1-2), 29-33.
46. Bligh, E. G.; Dyer, W. J., A rapid method of total lipid extraction and purification. *Canadian Journal of Biochemistry and Physiology* **1959,** *37* (8), 911-917.
47. Takeuchi, Y.; Ono, Y.; Hisanaga, N.; Kitoh, J.; Sugiura, Y., A Comparative Study on the Neurotoxicity of N-Pentane, N-Hexane, and N-Heptane in the Rat. *British Journal of Industrial Medicine* **1980,** *37* (3), 241-247.
48. Khan, N. A.; Brown, J. B., The composition of coffee oil and its component fatty acids. *Journal of the American Oil Chemists Society* **1953,** *30* (12), 606-609.
49. Folstar, P.; Van der Plas, H. C.; Pilnik, W.; De Heus, J. G., Tocopherols in the unsaponifiable matter of coffee bean oil. *Journal of Agricultural and Food Chemistry* **1977,** *25* (2), 283-285.
50. Silva, J.; Borges, N.; Santos, A.; Alves, A., Method Validation for Cafestol and Kahweol Quantification in Coffee Brews by HPLC-DAD. *Food Analytical Methods* **2012,** *5* (6), 1404-1410.
51. Bengis, R. O.; Anderson, R. J., The chemistry of the coffee-bean: I. concerning the unsaponifiable matter of the coffee-bean oil. preparation and properties of kahweol. *Journal of Biological Chemistry* **1932,** *97* (1), 99-113.
52. D'Amelio, N.; De Angelis, E.; Navarini, L.; Schievano, E.; Mammi, S., Green coffee oil analysis by high-resolution nuclear magnetic resonance spectroscopy. *Talanta* **2013,** *110* (0), 118-127.
53. Dias, E.; Borém, F.; Pereira, R.; Guerreiro, M., Amino acid profiles in unripe Arabica coffee fruits processed using wet and dry methods. *European Food Research and Technology* **2012,** *234* (1), 25-32.
54. Selmar, D.; Bytof, G.; Knopp, S.-E., The storage of green coffee (*Coffea arabica*): Decrease of viability and changes of potential aroma precursors. *Annals of Botany London* **2008,** *101* (1), 31-38.
55. Jham, G. N.; Velikova, R.; Vidal Muller, H.; Nikolova-Damyanova, B.; Cecon, P. R., Lipid classes and triacylglycerols in coffee samples from Brazil: effects of coffee type and drying procedures. *Food Research International* **2001,** *34* (2–3), 111-115.

56. Aguiar, A. T. d. E.; Salva, T. d. J. G.; Fazuoli, L. C.; Favarin, J. L., Variação no teor de lipídios em grãos de variedades de *Coffea canephora*. *Pesquisa Agropecuária Brasileira* **2005,** *40*, 1251-1254.
57. Budryn, G.; Nebesny, E.; Żyżelewicz, D.; Oracz, J.; Miśkiewicz, K.; Rosicka-Kaczmarek, J., Influence of roasting conditions on fatty acids and oxidative changes of Robusta coffee oil. *European Journal of Lipid Science and Techology* **2012,** *114* (9), 1052-1061.
58. Chu, Y. F.; Technologists, I. o. F., *Coffee: Emerging Health Effects and Disease Prevention*. Wiley: 2012.
59. Petracco, M., Technology IV: Beverage Preparation: Brewing Trends for the New Millennium. In *Coffee*, Blackwell Science Ltd: 2008; pp 140-164.
60. Knothe, G.; Gerpen, J. H. V.; Krahl, J., *The biodiesel handbook*. AOCS Press: 2005.
61. Hoekman, S. K.; Broch, A.; Robbins, C.; Ceniceros, E.; Natarajan, M., Review of biodiesel composition, properties, and specifications. *Renewable and Sustainable Energy Reviews* **2012,** *16* (1), 143-169.
62. Ageitos, J. M.; Vallejo, J. A.; Veiga-Crespo, P.; Villa, T. G., Oily yeasts as oleaginous cell factories. *Applied Microbiology and Biotechnology* **2011,** *90* (4), 1219-1227.
63. Chisti, Y., Fuels from microalgae. *Biofuels* **2010,** *1* (2), 233-235.
64. Thout, B. M., Coffee in Vietnam: It's the shit. *The Economist* January 2012, 2012.
65. Knothe, G., Some aspects of biodiesel oxidative stability. *Fuel Processing Technology* **2007,** *88* (7), 669-677.
66. EN 14214:2008, Automotive fuels - Fatty acid methyl esters (FAME) for diesel engines - Requirements and test methods.
67. ASTM D6751:2008, Standard Specification for Biodiesel Fuel Blend Stock (B100) for Middle Distillate Fuels. ASTM International: 2008.
68. Mushrush, G. W.; Quintana, M. A.; Bauserman, J. W.; Willauer, H. D., Post-refining removal of organic nitrogen compounds from diesel fuels to improve environmental quality. *Journal of Environmental Science and Health, Part A* **2011,** *46* (2), 176-180.
69. Rocha, M. V. P.; de Matos, L.; de Lima, L. P.; Figueiredo, P. M. D.; Lucena, I. L.; Fernandes, F. A. N.; Goncalves, L. R. B., Ultrasound-assisted production of biodiesel and ethanol from spent coffee grounds. *Bioresource Technology* **2014,** *167*, 343-348.
70. Demirbas, A., *Biodiesel: A Realistic Fuel Alternative for Diesel Engines*. Springer: 2007.

CHAPTER 3

CROSS-METATHESIS OF RENEWABLE LIPID SOURCES FOR A DUAL FUEL PROCESS

In Chapter 2 the potential of producing biodiesel from waste coffee lipid was investigated. Though the biodiesel is produced from a sustainable resource, and thus satisfies one of the three desirable traits for a novel biofuel, biodiesel exhibits certain technical issues which limit its application. Additionally, there is simply not enough coffee lipid available to displace significant reserves of fossil fuels. Alternatively, microbial lipids have the potential to be produced on a larger scale, while alternative chemical transformations have the potential to produce biofuels with superior fuel properties. In this chapter, the cross-metathesis of biologically sourced lipids with ethene to produce a dual fuel stream – a hydrocarbon for aviation and shorter-chain ester for road transport – along with their suitability as replacement fuel in terms of their fuel properties is presented.

Parts of this study were presented in the EADS PhD showcase (Bristol, UK, May 28-29, 2012) in the form of a poster where it won the poster prize, and as posters in the Centre for Sustainable Chemical Technologies' Summer Showcases of 2012 and 2013. A manuscript for this work is currently being prepared for submission to the ACS journal *Sustainable Chemistry and Engineering*.

3.1 INTRODUCTION

One alternative chemical transformation of lipids is metathesis, which utilises the unsaturation of the fatty acid chain. Self-metathesis of the lipids can lead to oligomer formation which increases the viscosity of the oil significantly, making it unsuitable as a fuel.[1] Alternatively, the cross metathesis of the lipids with another alkene source has the potential to split the lipid into a shorter triglyceride, and three equivalents of shorter-chain alkene (Scheme 3.1). The most inexpensive alkene for this reaction would be ethene – potentially produced by the dehydration of bioethanol.[2-3]

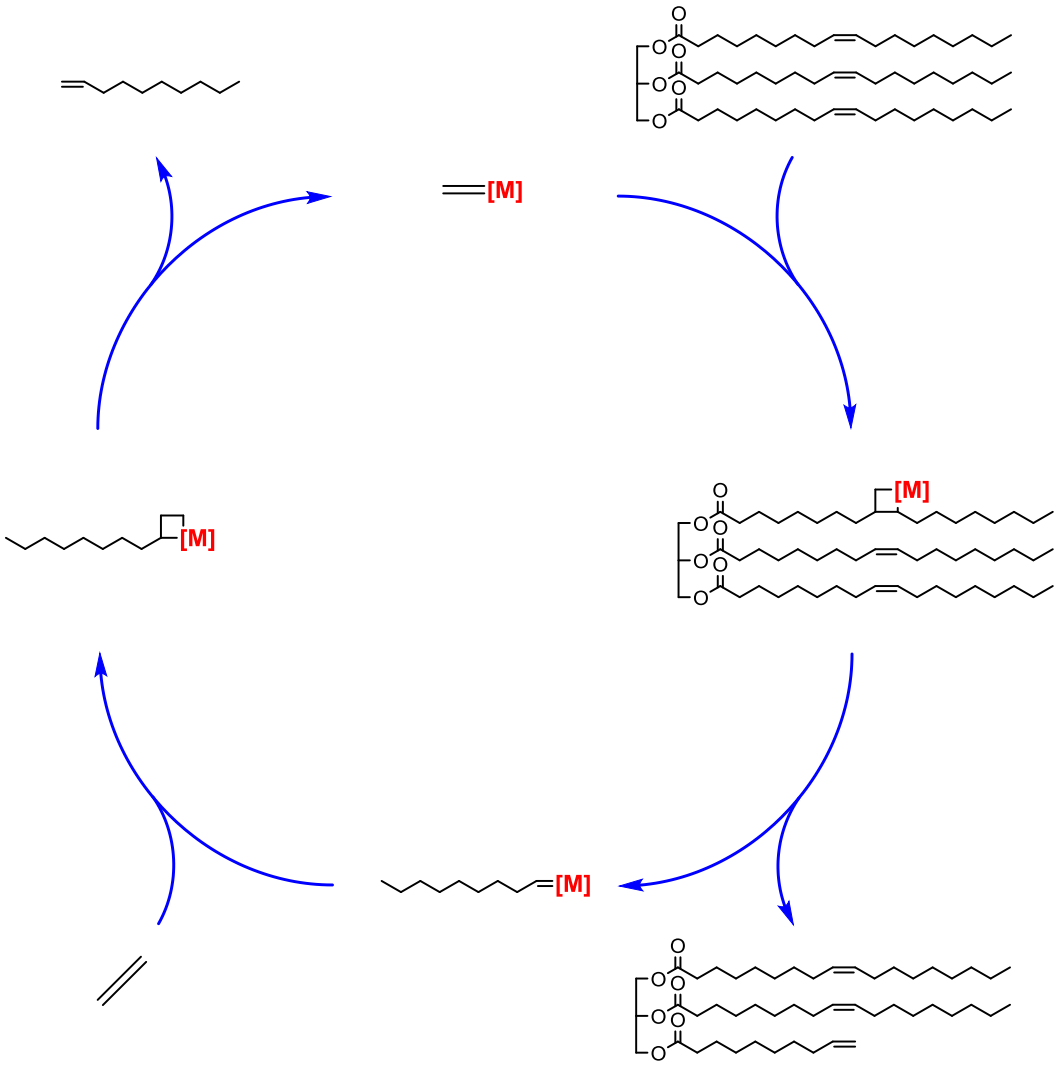

Scheme 3.1 The Chauvin mechanism, showing a potential step of cross-metathesis of glyceryl trioleate with ethene to produce 1-decene, a viable Jet A-1 replacement. Adapted from Hérisson and Chauvin.[4]

The primary products of the cross-metathesis of glyceryl trioleate with ethene (also known as "ethenolysis") are 1-decene and tridecenylglycerol, both of which have the potential to be suitable replacement fuels. The metathesis reaction has been considered previously as a method for refining biological lipids,[5] though there are few reports considering it for fuel production.[6-7] As far as the author is aware no fuel properties analysis has been undertaken on metathesis products, however, the physical properties of 1-decene fall almost exactly within the Jet A-1 aviation specification (Table 3.1). Similarly, the fuel properties of the resulting tridecenylglycerol have not been investigated, though due to their shorter chain length than most triglycerides may have potential as a diesel replacement even without subsequent transesterification. This chemical transformation, therefore, has the potential to produce two distinct liquid fuel streams.

Table 3.1 Physical properties of 1-decene and Jet A-1 Kerosene.[8-9] Kinematic viscosity of 1-decene was found experimentally.

	1-Decene	Jet A-1 Kerosene
Melting temperature / °C	-66.0	max -47.0
Boiling temperature / °C	171	140-280
Flash Point / °C	47.8	min 38
Density / g cm^{-3}	0.743	0.775-0.840
Kinematic Viscosity at -20 °C / mm^{2}s^{-1}	2.25	max 8.00

Natural triglycerides, however, are not all mono-unsaturated. The presence of poly-unsaturated fatty acid chains (i.e. with two or more double bonds) may lead to the production of short-chain alkenes. The cross-metathesis of linolenic acid with ethene, for example, would yield 1-butene and 1,4-pentadiene (Scheme 3.2). Though these would likely evolve from the reaction mixture as gases, if captured they have the potential as higher-value products. 1-butene is already known as an important petrochemical product as an initial component of a number of commercial processes for organic synthesis,[10] as well as successful monomer and co-monomer in the polymer industry.[11-12] Though 1,4-pentadiene is not known as a platform chemical for any known industrial process, as a diene it processes the functionalization to be used as a co-monomer in the polymer industry. Alternatively, through isomerisation it could be converted to 1,3-pentadiene

(piperylene), currently used as a monomer in the production of polymers, adhesives and resins, as well as having potential as a versatile chemical feedstock for conversion into higher value products via catalysis.[13] The metathesis of biological lipids, therefore, could form the basis of a biorefinery, by which the higher value products would help fund the expense of a higher-cost fuel production process. Excitingly, the proportions of the fractions could be tailored by a change in the feedstock, or by changing the reaction conditions.

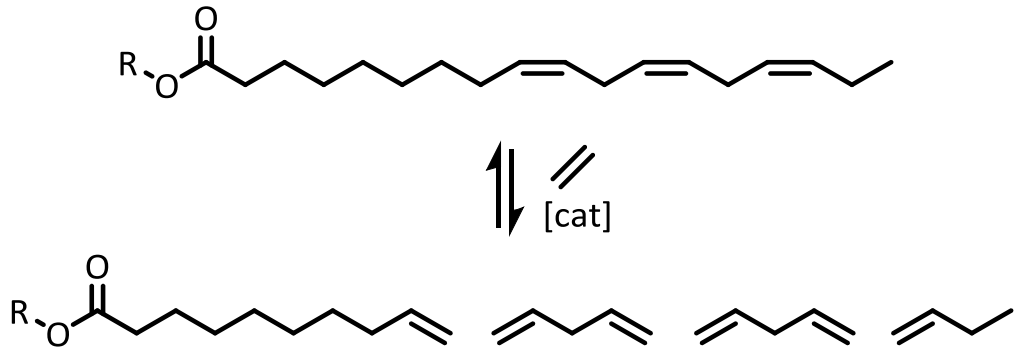

Scheme 3.2 Cross-metathesis of linolenic fatty acid chain with ethene

Altering the composition of these fractions, and therefore the properties of the cross-metathesis products, can also be done by varying the alkene source. While ethene is a promising reactant, alternative sustainable alkenes such as isoprene also have potential for this reaction. Isoprene is produced by plants and trees and accounts for the largest natural hydrocarbon emission into the atmosphere.[14] It is also liquid at ambient conditions, potentially leading to a simpler industrial process. Though isoprene is not symmetrical and would lead to the formation of larger number of products, it is more substituted, and as such should lead to less de-activation of the ruthenium-based Grubbs catalyst, as the ruthenium methylidene complexes formed as intermediates in ethenolysis are unstable.[15]

As well as Grubbs catalyst (and later iterations), other catalyst systems have proven to be active for the metathesis of lipids. The original catalyst system for lipid metathesis – $WCl_6/SnMe_4$ – has also been found to perform as a bifunctional catalyst, catalysing the transesterification reaction in the presence of methanol as well as the metathesis reaction.[16-17] This catalyst system is also considerably

cheaper than the ruthenium complexes. Therefore, optimizing this reaction to produce 1-decene for aviation fuel and a shorter FAME for diesel replacement purposes could provide an economical method of producing fuels via metathesis. One of the challenges to overcome with this particular catalyst system, however, is their susceptibility to poisoning and de-activation and need for very dry inert conditions in order to function.

In this study, the cross-metathesis of triglycerides with different alkene substrates and catalysts was investigated. The co-catalyst $SnMe_4$ is very toxic, and so the less toxic (though still active[18]) co-catalyst $SnBu_4$ was used in its place. Furthermore, the fuel properties of the resultant products of the cross-metathesis reaction with potential sustainable fuel feedstock triglycerides were assessed.

3.2 EXPERIMENTAL

3.2.1 MATERIALS

All solvents were purchased from Fisher, were reagent quality and were used without purification except when dried (as indicated) by passing through anhydrous alumina columns using an Innovative Technology Inc. PS-400-7 solvent purification system unless otherwise stated. Deuterated solvents ($CDCl_3$, D_2O) for ^1H NMR spectroscopic analysis were purchased from Fluorochem. Tungsten hexachloride (WCl_6), tetrabutyl tin ($SnBu_4$), Grubbs 1st generation catalyst, Hoveyda-Grubbs 2nd generation catalyst, glyceryl trioleate (technical grade), methyl oleate (technical grade), methyl oleate (99%), isoprene, 1-hexene, triethylamine and tris(hydroxymethyl)phosphine were all obtained from Sigma-Aldrich, UK and used without further purification unless otherwise stated. Rapeseed oil, sunflower oil and coffee grounds were purchased from a local supermarket and used without further purification. Ethene (Research grade, >99.99% purity) was obtained from BOC Ltd.

3.2.2 METHODS

3.2.2.1 GENERAL ANALYSIS

Analysis of the lipids and reaction mixtures was done by ^1H NMR spectroscopy and GC-MS. GC-MS analysis was carried out using the Agilent 7890B Gas Chromatograph equipped with a capillary column (30 m x 0.250 mm internal diameter) coated with DB-FFAP (nitroterephthalic-acid-modified polyethylene glycol) stationary phase (0.25 µm film thickness) and a He mobile phase (flow rate: 1.2 ml min^{-1}), coupled with an Agilent 5977A inert MSD with Triple Axis Detector. Approximately 50 mg of each sample was dissolved in 10 ml ethyl acetate or 1,4-dioxane and 1 µl of each solution was loaded onto the column, pre-heated to 40 °C. This temperature was held for 1 minute and then heated to 250 °C at a rate of 20 °C min^{-1} and then held for 10 minutes. NMR spectroscopic measurements were carried out at 298 K using a Bruker AV300 spectrometer, operating at 300.13 MHz for ^1H.

Typically samples were made up of 0.05 ml of the oil or biodiesel sample dissolved in 0.5 ml $CDCl_3$. ^1H spectra were typically acquired using a 30 degree excitation pulse and a repetition time of 4.2 sec. 0.3 Hz line broadening was applied before Fourier transform, and spectra were referenced to the residual $CHCl_3$ peak from the solvent (δ 7.26 ppm).

3.2.2.2 CATALYST SCREENING

Tungsten Hexachloride / Tetrabutyl Tin ($WCl_6/SnBu_4$)

For the reactions in air, catalyst WCl_6 (0.83g, 2.25×10^{-3} mol) was added to a round bottom flask. It was then charged with either technical grade glyceryl trioleate (11 ml, 10g, approx. 0.0011 mol) or technical grade methyl oleate (10 ml, 8.74 g, approx. 0.03 mol) and isoprene (6.2 ml, 4.2 g, 0.0678 mol for glyceryl trioleate, 8.19 ml, 5.58 g, 0.09 mol for methyl oleate). The co-catalyst, $SnBu_4$ (1.56g, 4.5×10^{-3} mol), was then added to the reaction mixture. This reaction mixture was then held as specified for the reaction period. After this period, the reaction mixture was quenched with water and allowed to settle to a biphasic system. The top organic later was then analysed by ^1H NMR spectroscopy.

For reactions in inert conditions, all experiments were carried out under standard Schlenk conditions under dry N_2 atmosphere. The catalyst WCl_6 (0.083g, 2.25×10^{-4} mol) was added to a Schlenk tube and evacuated. Either technical grade methyl oleate (1 ml, 0.874 g, approx. 0.003 mol) or 99% purity methyl oleate (1 ml, 0.874 g, 0.003 mol) and isoprene (0.819 ml, 0.558 g, 0.009 mol) or 1-hexene (0.370 ml, 0.252 g, 0.003 mol) were freeze thawed over several cycles before addition to the Schlenk tube reactor. Dry solvent, either hexane (10ml) or toluene (10 ml) was added. $SnBu_4$ (1.56g, 4.5×10^{-3} mol) was evacuated and dried before adding to the reaction mixture. This was then held as specified temperature for the reaction period. After this period, the reaction mixture was passed through a short silica plug to remove the catalyst, and excess solvent removed under reduced pressure. The resulting oil was then analysed by ^1H NMR spectroscopy, where isoprene was used, or by GC-MS when 1-hexene was used.

Grubbs 1st Generation Catalyst

For the reactions in air, Grubbs 1st generation catalyst (0.01 g, 1.1×10^{-5} mol) was added to a round bottom flask. It was then charged with either technical grade glyceryl trioleate (11 ml, 10g, approx. 0.0011 mol) or technical grade methyl oleate (10 ml, 8.74 g, approx. 0.03 mol) and isoprene (6.2 ml, 4.2 g, 0.0678 mol for glyceryl trioleate, 8.19 ml, 5.58 g, 0.09 mol for methyl oleate). This reaction mixture was then held as specified temperature for the reaction period. After this period, the reaction mixture was quenched with water and allowed to settle to a biphasic system. The top organic later was then analysed by ^{1}H NMR spectroscopy.

For reactions in inert conditions, all experiments were carried out under standard Schlenk conditions under dry N_2 atmosphere. Grubbs 1st generation catalyst (0.0025 g, 3×10^{-6} mol) was added to a Schlenk tube and the air removed under vacuum. Either technical grade methyl oleate (1 ml, 0.874 g, approx. 0.003 mol) or 99% purity methyl oleate (1 ml, 0.874 g, 0.003 mol) and isoprene (0.819 ml, 0.558 g, 0.009 mol) or 1-hexene (0.370 ml, 0.252 g, 0.003 mol) were freeze thawed over several cycles before addition to the Schlenk tube reactor. Dry solvent, either hexane (10ml) or toluene (10 ml) was added. This was then held as specified temperature for the reaction period. After this period, the reaction mixture was passed through a short silica plug to remove the catalyst, and excess solvent removed under reduced pressure. The resulting oil was then analysed by ^{1}H NMR spectroscopy, where isoprene was used, or by GC-MS where 1-hexene was used.

For reactions with ethene using the Parr bomb reactor, it was charged with technical grade methyl oleate (1 ml, 0.823 g, 0.003 mol), toluene (2 ml, 2.3 g, 0.025 mol), and Grubbs 1st generation catalyst (0.0025 g, 3×10^{-6} mol). This was then filled with 10 bar pressure of ethene. Under constant stirring, the reaction was held at 40 °C for two hours, after which the reaction mixture was passed through a silica plug and analysed by ^{1}H NMR spectroscopy and GC-MS.

For reactions with ethene in glassware, a three-necked round bottom flask was charged with technical grade methyl oleate (1.0 ml, 0.82 g, 0.0030 mol), toluene (10

ml, 9.2 g, 0.125 mol), and Grubbs 1st generation catalyst (0.0025 g, 3×10^{-6} mol). Ethene was pumped though the reaction mixture at a pressure of 1 bar. Under constant stirring, the mixture was held at 40 °C for 60 mins. After this time, the reaction mixture was the analysed by ^{1}H NMR spectroscopy.

Hoveyda-Grubbs 2nd Generation Catalyst

All experiments were carried out under standard Schlenk conditions under dry N_2 atmosphere. For the catalyst screening experiments, Hoveyda-Grubbs 2nd generation catalyst (9.4×10^{-4} g, 1.5×10^{-6} mol) was added to a Schlenk tube and evacuated. 99% purity methyl oleate (0.5 ml, 0.41 g, 0.0015 mol) and isoprene (0.41 ml, 0.28 g, 0.0045 mol) or 1-hexene (0.17 ml, 0.13 g, 0.0015 mol) were freeze thawed over several cycles before addition to the Schlenk tube reactor. Dry solvent, either hexane (10ml) in the case of isoprene or toluene (10 ml) in the case of 1-hexene, was added. This was then held as specified temperature for the reaction period. After this period, the reaction mixture was passed through a short silica plug to remove the catalyst, and excess solvent removed under reduced pressure. The resulting oil was then analysed by ^{1}H NMR spectroscopy, where isoprene was used, or by GC-MS where 1-hexene was used.

3.2.2.3 Optimisation of Lipid Metathesis with Ethene

In order to optimise the reaction for metathesis with ethene, a pressurised rig was designed around a Fisher Porter pressure reaction vessel, with sample port / canula and push-on tube attachment to allow for connection to the Schlenk line. This allowed for reactions under inert conditions.

Non-inert, comparison of pressures

To the Fisher Porter bottle, technical grade glyceryl trioleate (1.0 ml, 0.91 g, 0.00103 mol) was added, along with Hoveyda-Grubbs 2nd generation catalyst (0.0064 g, 1.03×10^{-5} mol). The mixture was heated (up to 60°C), pressurised with ethene (5 or 10 bar), and stirred (1200 rpm) for the reaction period. After the reaction the mixture was passed through a short silica plug, washed through with

DCM (3 ml) which was subsequently removed *in vacuo*. The resulting mixture was then analysed by ^{1}H NMR spectroscopy.

Inert, conformation of reaction with impure lipids

To ensure the reactions with microbial lipids would be active for the metathesis reaction despite the inherent impurities in them, to maximise yield, and to determine the optimum reaction time, preliminary reactions were carried out using the Fisher Porter bottle under inert conditions. Due to the limited amount of microbial oil available for the reaction the sample port was used. This reduced the amount of oil used with unnecessary batch reactions.

All reactions under inert conditions were carried out using standard Schlenk line techniques under dry Ar atmosphere. The triglyceride (glyceryl triolate [technical grade], glyceryl triolate [99%], rapeseed oil or *P. ellipsoida* oil) was added (1.0 ml, 0.91 g, 0.0010 mol) to the Fisher Porter Bottle and placed under vaccuum. Hoveyda-Grubbs 2nd generation catalyst (0.032 g, 5.1 x 10^{-5} mol) was added to a Schlenk tube under an inert atmosphere. Dry DCM (15 ml) was added to the Schlenk tube to solubilise the catalyst. The solution was immediately transferred to the Fisher Porter bottle, and the reaction mixture heated (60°C), pressurised with ethene (10 bar) and stirred (1200 rpm). Samples of the reaction mixture were taken at 15, 30, 45, 60, 90, 120, 180 and 240 mins, passed through a plug of silica, and the solvent removed *in vacuo*. The resulting mixture was then analysed via ^{1}H NMR spectroscopy.

3.2.2.4 Microbial and Waste Oil Cross-Metathesis

Lipid production / extraction

Coffee lipid was extracted and purified using the same procedure as presented in chapter two, section 2.2.2.3, with the only difference being the larger scale of the reactions, i.e. 227g of fresh Columbian coffee. Oil purity was determined by ^{1}H NMR spectroscopy and was found to be >99% triglyceride.

Cultivated samples of *Rhodotorula glutinis* 2439 and *Rhodotorula minuta* 62 biomass were provided by Lisa Sargeant, Dept. of Chemical Engineering, University of Bath. *Rhodotorula glutinis* 2439 and *Rhodotorula minuta* 62 were purchased from the National Collection of Yeast Cultures (Norwich, UK). The yeast was cultivated on glucose according to a literature method by Sargeant *et al.*[19] *Pseudochorisystis ellipsoidea* was sourced from the Dept. of Biology, University of Bath and was cultured in two 500 litre raceway ponds using a minimal media over 20 days. *Scenedesmus obliquus* strain CCAP 276/7 was sourced from the Dept. of Biology, University of Bath and was cultured using 1% anaerobic digestate concentrate in two 500 litre open ponds over 14 days. Chitosan (20 mg l^{-1}) was used as a flocculent; the biomass from both microalgae was harvested and freeze-dried prior to lipid extraction. *Metschnikowia pulcherrima* was sourced from the Dept. of Biology, University of Bath. The yeast was cultured on glycerol according to a literature method by Santomauro, *et al*.[20]

The microbial lipid was extracted from the biomass using a modified Bligh & Dyer literature method, using a chloroform : methanol mixture in a 2:1 volumetric ratio as the solvent.[21] The oil was washed three times with water to remove the methanol and any cellular residues, before the chloroform was removed *in vacuo*.

Metathesis and Work-up

The same reaction conditions presented in section 3.2.2.2 were used for the metathesis of the microbial sources. The resulting mixtures were purified according to the literature method given by Maynard and Grubbs.[22] Upon removal, the reaction mixture was added to a solution of tris(hydroxymethyl)phosphine ($P[CH_2OH]_3$, 0.13 g, 0.0010 mol) and triethylamine (Et_3N, 0.014 ml, 0.010 g, 1.0 x 10^{-4} mol) in DCM (20 ml) and stirred for 10 minutes. Distilled water (~30ml) was then added and the biphasic solution vigorously stirred for >15 minutes before the aqueous layer was separated. The mixture was then washed further with distilled water (2 x 30ml) before removing the solvent *in vacuo* to isolate the reaction mixture. The resulting mixture was then analysed via ^1H NMR spectroscopy and for its key fuel properties.

Fractional distillation

After fuel analysis, the metathesis products were distilled using a Schlenk vacuum and liquid N_2 trap. Under inert conditions, the metathesis product mixture was heated to 120 °C and subjected to reduced pressure over an hour. After this time, the vacuum was removed; the Schlenk line was allowed to reach ambient pressure before the liquid N_2 was removed from the trap and allowed to reach ambient temperature. The resulting condensate was transferred to a 100 ml round bottom flask with DCM which was subsequently removed *in vacuo*.

Transesterification of the metathesis residue

The residue remaining after the short-chain alkenes had been removed, was added to an excess of methanol (~25ml) and sulfuric acid (10 wt% in relation to the oil). The reaction mixture was refluxed for 24 hours. On completion of the reaction the mixture was allowed to cool to room temperature before being washed with distilled water (3 x 50ml) to remove the methanol, glycerol and acid catalyst. The glyceride to FAME yield was calculated using ^{1}H NMR spectroscopy (according to the Knothe equation[23]) to ensure that over 99% of the glyceride species had reacted.

3.2.2.4 Fuel properties

Where suitable, the viscosity was measured using Canon-Fenske capillary kinematic viscometer, in accordance with ASTM D445. Temperature modulation was achieved using a refrigeration/heating unit. Samples within the viscometer were allowed to rest at 40 °C or -20 °C as appropriate for a minimum of 5 minutes prior to viscosity measurement to allow temperature equilibration. However, due to their high viscosity of some samples, the time it took to flow through was impractical for repeated measurements to be taken (>30 minutes), and therefore a Bohlin C-VOR digital rheometer was used. The rheometer used was of the “cone and plate” variety, whereby the fluid is place on a plate and a shallow cone (in this case, 1 °) is lowered onto it. Subjecting the fluid to a specific shear stress, the

dynamic viscosity was determined and converted to kinematic viscosity using the density of the samples.

Pour points of the fuels were determined visually by cooling of approximately 0.5 ml samples in a digitally controlled low temperature freezer set to specific temperatures. The samples were allowed to rest at each temperature for a minimum of 60 minutes in order to allow equilibration, after which the samples were checked in order to see if their pour point had been reached. Energy densities were measured using the IKA C1 static jacket oxygen bomb calorimeter, in accordance with DIN 51900 and ISO 1928. Samples sizes of 0.3-0.5 g were used for each reading.

3.3 Results and Discussion

3.3.1 Catalyst screening

3.3.1.1 Tungsten Hexachloride / Tetrabutyl Tin (WCl_6/$SnBu_4$)

Initially, WCl_6/$SnBu_4$ was assessed for its ability as a robust bifunctional metathesis / transesterification catalyst system for the conversion of glyceryl trioleate (technical grade) and methyl oleate. Initially isoprene was screened due to its relative ease of use. The reactions were held at 100 °C, with reaction times ranging between 30 mins and 24 hours (Table 3.2, reactions 1-6). To assess the activity of the catalyst to also perform a transesterification, methanol was added to the system (Table 3.2, reactions 3-5). On work up water was added to the reaction mixture to quench the reaction and remove any glycerol. The organic layer was isolated and used for analysis. The successful cross-metathesis of isoprene would result in terminal alkenes, found between 4.6-6.0 ppm in the ^{1}H NMR spectra.[24] As such ^{1}H NMR spectroscopy was used to analyse the resulting product mixtures.

For all of the initial reactions using WCl_6/$SnBu_4$ and glyceryl trioleate, (Table 3.2, reactions 1-5) no metathesis activity was observed, irrespective of the conditions screened. In contrast, the catalyst did show a high activity for the transesterification reaction, with over 90% yield of FAME produced after 120 minutes when methanol was included in the original reaction mixture. Interestingly, if methanol was added after two hours, only a maximum of 72% FAME was recovered. This suggests that the catalyst is being deactivated under these reaction conditions. The WCl_6/$SnBu_4$ catalyst system was also inactive in the cross-metathesis of methyl oleate with isoprene under the same conditions (Table 3.2, reaction 6). The WCl_6/$SnBu_4$ catalyst system is known to be very sensitive to air, requiring use under inert conditions.[25] However, even under inert conditions using dry reagents and dry hexane as a co-solvent, no metathesis activity was observed (Table 3.2, reactions 7 & 8). Therefore, the inactivity could be due to the isoprene used, as it contains a polymerisation inhibitor – 4-*tert*-butylpyrocatechol – which contains hydroxyl groups and as such could poison and deactivate the catalyst. However, conjugated dienes themselves

are known to be difficult for cross-metathesis due to their tendency to strongly deactivate catalysts. The isoprene itself, therefore, could be deactivating the relatively sensitive $WCl_6/SnBu_4$ catalyst system. This was investigated by distilling the isoprene directly into the reaction vessel immediately before use (Table 3.2, reaction 8), though no metathesis conversion was observed. This supports the inference that isoprene is deactivating the catalyst.

To further investigate the effect of different alkene reagents, the cross-metathesis between methyl oleate (technical grade) and 1-hexene (in equimolar amounts) was investigated (Table 3.2, reaction 9). Though 1-hexene would not produce viable fuel molecules via metathesis with lipids and isn't obtained from sustainable sources, it is a liquid which isn't susceptible to polymerisation and therefore is a useful reagent for the optimisation of metathesis reactions. As the cross-metathesis of methyl oleate with 1-hexene will produce internal alkenes rather than terminal alkenes, GC-MS was used to analyse the product mixture. The GC-MS analysis of the reactions confirmed that neither cross- nor self-metathesis was observed using the $WCl_6/SnBu_4$ catalyst system.

While other organo-tin co-catalysts have been demonstrated to give a higher activity in the metathesis reaction (for example, $SnMe_4$, which is known to be a more active alkylating agent[26]) they tend to be extremely toxic and highly air-sensitive, thus alternative metathesis catalysts were investigated. Grubbs 1st generation catalyst (G1) – in contrast to $WCl_6/SnBu_4$ – is less sensitive to air and moisture, relatively benign and more active. However, the catalyst has not been reported for any activity in the transesterification reaction. Furthermore, G1 is sensitive to primary alcohols and is known to produce metathesis-inactive Ru-CO complexes in the presence of methanol,[27-28] therefore methanol was not used in the reaction mixture. The cross-metathesis of glyceryl trioleate and isoprene was investigated using G1 as a catalyst (Table 3.2, reactions 10-12). The reactions were carried out at more moderate temperatures, required to prevent catalyst deactivation (55-60 °C).[29]

Table 3.2 Table summarising selected cross-metathesis reactions involving the model lipids – glyceryl trioleate and methyl oleate – with isoprene and 1-hexene. All reactions were carried out in glassware in non-inert conditions unless otherwise stated. GT – Glyceryl trioleate. MO – methyl oleate. G1 – Grubbs 1st generation catalyst, HGII – Hoveyda-Grubbs 2nd generation catalyst.

Reaction #	Reagents			Catalyst	Catalyst loading / %	Time / mins	Temp / °C	Conversion (%)	
	1	2	3					Metathesis	FAME
1	Glyceryl trioleate	Isoprene	-	$WCl_6/SnBu_4$	20	60	100	0	-
2	Glyceryl trioleate	Isoprene	-	$WCl_6/SnBu_4$	20	1120	100	0	-
3[a]	Glyceryl trioleate	Isoprene	MeOH	$WCl_6/SnBu_4$	20	120	100	0	90
4[a]	Glyceryl trioleate	Isoprene	MeOH	$WCl_6/SnBu_4$	20	1440	100	0	95
5[b]	Glyceryl trioleate	Isoprene	MeOH	$WCl_6/SnBu_4$	20	120	100	0	72
6	Methyl oleate	Isoprene	-	$WCl_6/SnBu_4$	20	1120	100	0	-
7[c]	Methyl oleate	Isoprene	-	$WCl_6/SnBu_4$	20	120	100	0	-
8[c,d]	Methyl oleate	Isoprene	-	$WCl_6/SnBu_4$	20	120	100	0	-
9[c]	Methyl oleate	1-hexene	-	$WCl_6/SnBu_4$	20	1440	100	0[e]	-
10	Glyceryl trioleate	Isoprene	-	G1	0.1	30	55	0	-
11	Methyl oleate	Isoprene	-	G1	0.1	60	60	0	-
12[c]	Methyl oleate	Isoprene	Hexane[f]	G1	0.1	60	60	0	-
13[c]	Methyl oleate	1-hexene	Toluene[f]	G1	0.1	60	60	0[e]	-
14[c]	Methyl oleate	Isoprene	Hexane[f]	HGII	0.1	60	RT	0	-
15[c]	Methyl oleate	Isoprene	Hexane[f]	HGII	0.1	180	RT	0	-
16[c]	Methyl oleate	Isoprene	Hexane[f]	HGII	0.1	60	40	0	-
17[c]	Methyl oleate	Isoprene	Hexane[f]	HGII	0.1	180	40	0	-
18[c]	Methyl oleate	1-hexene	Toluene[f]	HGII	0.1	60	40	91[e]	-
19[c]	Methyl oleate	1-hexene	Toluene[f]	HGII	0.1	180	40	85[e]	-
20[c]	Methyl oleate	1-hexene	Toluene[f]	HGII	0.1	180	60	90[e]	-

a – Methanol added as part of original reaction mixture.

b – Methanol added after initial metathesis reaction period.

c – Inert conditions.

d – Isoprene purified by distillation immediately before use .

e – Calculated by GC-MS. Conversion (%) = 100 – (% of methyl oleate)

f – As co-solvent.

Similarly to the $WCl_6/SnBu_4$ catalyst system, G1 showed no activity for the cross-metathesis reaction between the model lipids and isoprene, even under inert conditions. Shortly after the reaction started, the reaction mixture changed from purple to brown, signifying a change in oxidation state. While this deactivation could be due to the isoprene, the cross metathesis with 1-hexene was also unsuccessful.

While both the cross- and self-metathesis have been reported under similar conditions with G1,[30] it was suspected that the catalyst was still highly sensitive to the conjugated double bonds found in isoprene, though similar inactivity was seen when using 1-hexene as the cross-metathesis reagent. In an attempt to address these issues Hoveyda-Grubbs 2nd generation catalyst (HGII) was examined. HGII is air and moisture stable and is reportedly more stable and selective in the production of terminal alkenes than G1.[31] Under an inert atmosphere, methyl oleate (>99%) and isoprene (3 molar equivalents) were reacted using 0.1% HG II at either ambient temperature or 40 °C, using dry hexane as a solvent. Ambient temperature was used to reduce the evaporation of the isoprene (Table 3.2, reactions 14-20). Like all attempted metathesis reactions using isoprene previously, no metathesis activity was observed. This is most likely due to the isoprene deactivating the ruthenium centre, as conjugated dienes have been reported as poisons for these catalysts previously. Patel, *et al.*, in a study of cross-metathesis of natural oils with 2-butene, attempted to use commercial-grade 2-butene as their scission reagent. Due to the trace levels of 1,3-butadiene (which is of a very similar structure to isoprene) present in the gas mixture, the reaction yielded poor results (using HGII), when compared to using pure 2-butene. This is also supported by a study reporting the vinyl-alkylidene-ruthenium complex produced by the addition of 1,3-butadiene to G1 being inactive for metathesis.[33]

However, HG II was found to be highly active in the cross-metathesis of 1-hexene and methyl oleate. The reaction resulted in two major cross-metathesis products: methyl mystriolate (14:1ω5) and methyl 9-decenoate (10:1ω1), though a range of other primary and secondary reaction products were also observed (Table 3.3). It

should be noted that certain products expected to be present in the reaction mixture, 5-decene and 1-decene, were not observed in the chromatogram. This is most likely due to their high volatility, leading to their elution with the GC-MS solvent. Due to the promising activity in using HGII with the model compounds, this catalyst was used for all the subsequent reactions using ethene.

Table 3.3 Metathesis products of the reaction between methyl oleate & 1-hexene, using 0.1% HG II catalyst, at 40 °C for 60 mins.

Metathesis Product	GC-MS % Area
5-Tetradecene (E + Z)	28.0
Methyl 9-decenoate (10:1)	15.5
5-Octadecene (E +Z)	9.4
Methyl myristoleate (14:1)	26.4
Z-Methyl oleate (18:1)	16.7
E-Methyl oleate (18:1)	3.3
Dimethyl octadec-9-enedioate	0.8

3.3.2 Optimisation of Lipid Metathesis with Ethene

To further assess the activity of HGII as a lipid metathesis catalyst with ethene, a Fisher Porter bottle (a glass pressure reactor vessel) rig was designed and built (Figure 3.1). The rig included a push-on tube fitting, allowing for connection to a Schlenk line and thus allowing reactions under inert conditions to take place; a thin, 1/16” sample tube, allowing for sample-taking and as a make-shift canula for the introduction of solvents and reagents while remaining under inert conditions; and needle valves before and after the reaction vessel, to allow for safe transfer of the pressure to/from the system. Due to the limited amount of microbial oil available for the reactions, and therefore the high value of it, a sample port was added to the rig in order to allow for sampling throughout a reaction. This reduces the amount of oil used with unnecessary batch reactions.

The reaction vessel itself was made of borosilicate glass, and this allowed a visual appraisal of the reaction. The reactor was rated to 13 bar, though as ethene is highly flammable, the highest operating pressure used in this investigation was 10 bar, with a safety valve attached preventing the system from exceeding 11 bar. This

allowed for determination of the metathesis reaction success under relatively facile conditions, as pressures as high as 100 bar have been reported for the complete ethenolysis of glyceryl trioleate.[34]

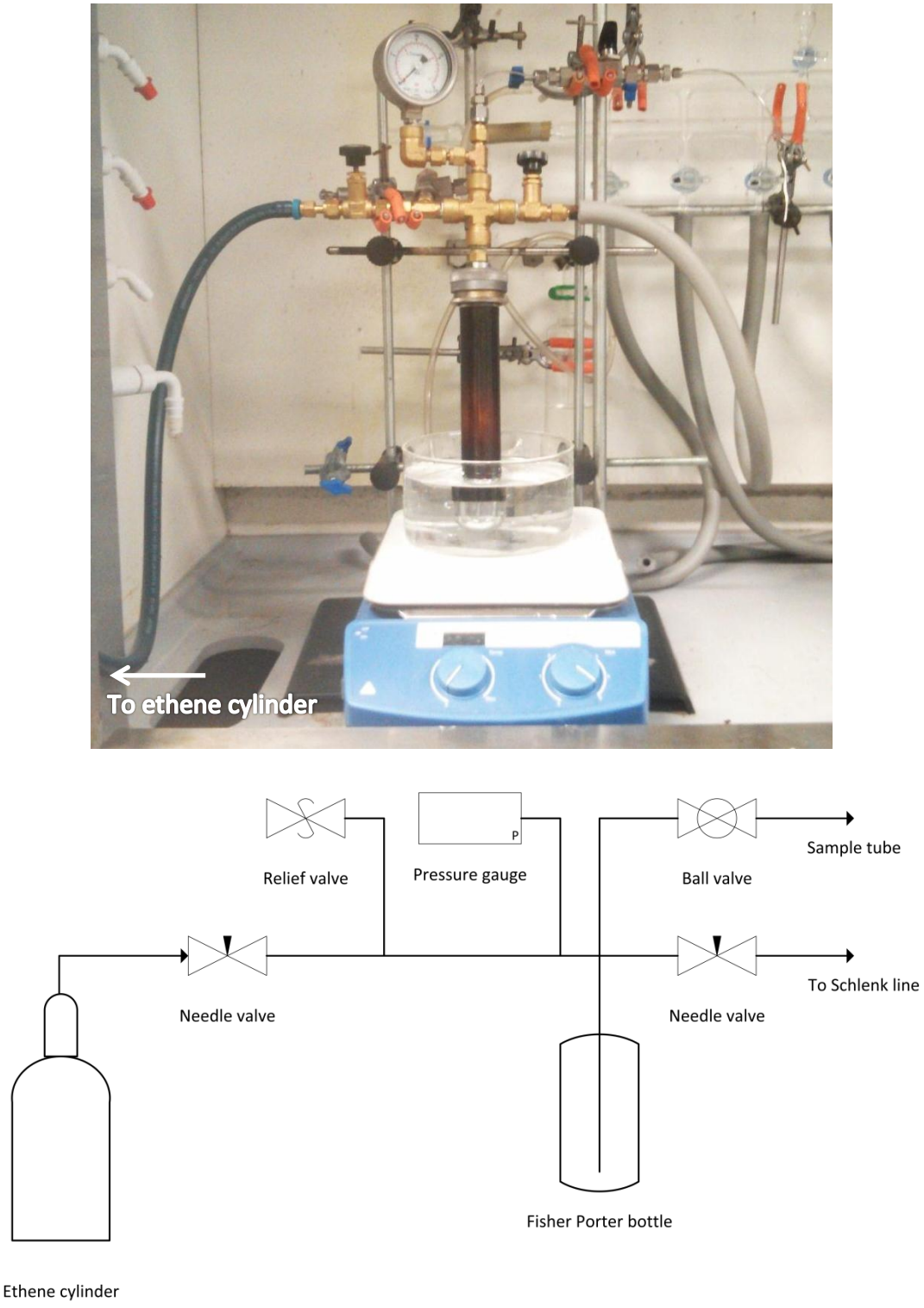

Figure 3.1 Photograph and simplified schematic of Fisher Porter bottle rig designed for pressurised metathesis reactions.

Firstly, to optimise the reaction, glyceryl trioleate (technical grade) was used. Experiments were carried out at two pressures (5 and 10 bar), at both room temperature and 60 °C and at reaction times between 0.5 to 4 hours. The reaction was carried out in atmospheric conditions without a co-solvent and 0.5 mol% HGII catalyst.

The activity was monitored by ^{1}H NMR spectroscopy (Figure 3.2). As the lipid is metathesized, the internal double bond protons (5.0-5.5 ppm) are consumed. The terminal alkenes that are produced are identified by the α-protons with a shift of 4.8 ppm, and the β-protons with a shift of 5.8 ppm, peaks that are not observed in the original spectra. As the glyceryl backbone of the triglyceride is present and unchanged in both, this can be used as the internal standard to determine the metathesis conversion. As the shift of the glyceryl backbone at 4.8 ppm corresponds to 4 protons, and a 100% conversion to 1-decene and tridecenylglycerol would produce 12 protons at a shift of 4.8 ppm (i.e. a ratio of 1:3), the selectivity for terminal alkenes (%) can be calculated according to equation (1).

$$Terminal\ Bond\ Selectivity\ (\%) = \left[\left(\frac{\int Terminal\ protons\ (4.8\ ppm)}{\int Glyceryl\ protons\ (4.2 ppm)}\right) \div 3\right] \times 100 \qquad \text{(eq. 1)}$$

Temperature had a significant effect on the production of terminal alkenes. The maximum selectivity for terminal alkenes at 5 bar is 10.5% at room temperature and 19.5% at 60 °C (Figure 3.3). At 10 bar, the selectivity peaks at 13.5% at room temperature and 23.3% at 60 °C. The effect of pressure on this selectivity, while not as significant as the temperature, still has an effect on conversion. At 60 °C, the yield was increased to 23.3 % at 10 bar from 19.5% at 5 bar. The maximum conversions to terminal alkenes were generally observed between 30 – 120 minutes, with lower conversions seen for longer reaction times. This could be due to the difference in kinetics of the cross-metathesis with ethene and self-metathesis, secondary metathesis side reactions, or isomerisation. Isomerisation of terminal alkenes has been observed previously by Lehman, *et al.*, on the metathesis of 1-octene with HGII.[35]

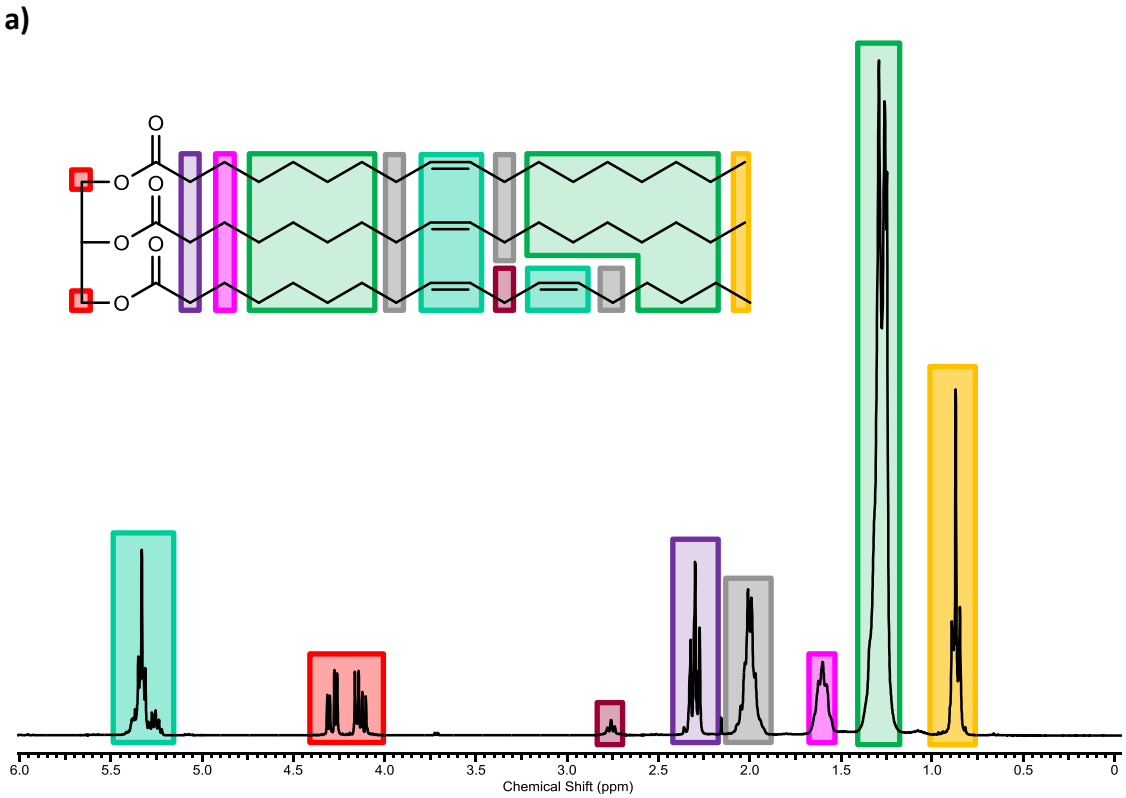

Figure 3.2 ^{1}H NMR Spectra of a) representative triglyceride substrate (glyceryl trioleate), and; b) corresponding representative metathesis product mixture, showing the associated proton shifts.

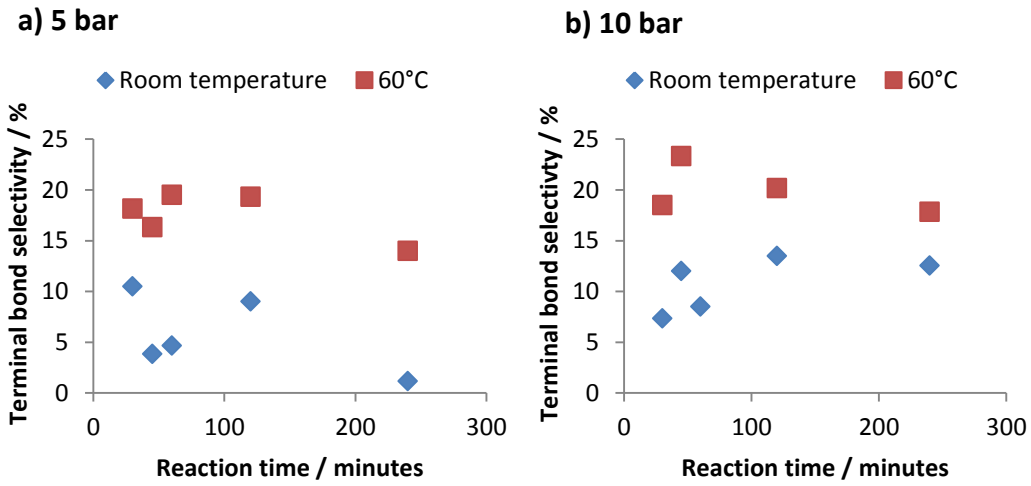

Figure 3.3 Terminal bond selectivity for the cross-metathesis of glyceryl trioleate in Fisher Porter pressurised rig at a) 5 bar, and; b) 10 bar of ethene.

However, these reactions were carried out in neat conditions. It has been previously been reported that ethenolysis reactions carried out under solvent-free conditions can depress the metathesis conversion and lower the selectivity to terminal alkenes when compared with the application of a co-solvent, due to the increased solubility of ethene when using solvents.[31] To increase the yield, therefore, all subsequent reactions were run using DCM as a co-solvent to increase the solubility of ethene, under inert atmosphere, and an increased catalyst loading (5 mol%) to counter the dilution of the oil. Samples were taken at 15, 30, 45, 60, 90, 120, 150, 180 and 240 minutes. Under these reaction conditions, both technical and >99% grade glyceryl trioleate reached conversions of over 55% terminal alkene selectivity within 1 hour (Figure 3.4). The metathesis of rapeseed oil and *Pseudochorisystis ellipsoidea* oil yielded lower levels of terminal alkenes, most likely due to the presence of saturates and impurities. Despite this, yields of over 40% were achieved for both oils. To limit the resulting secondary reactions, a reaction period of 60 minutes was used for all subsequent conversions.

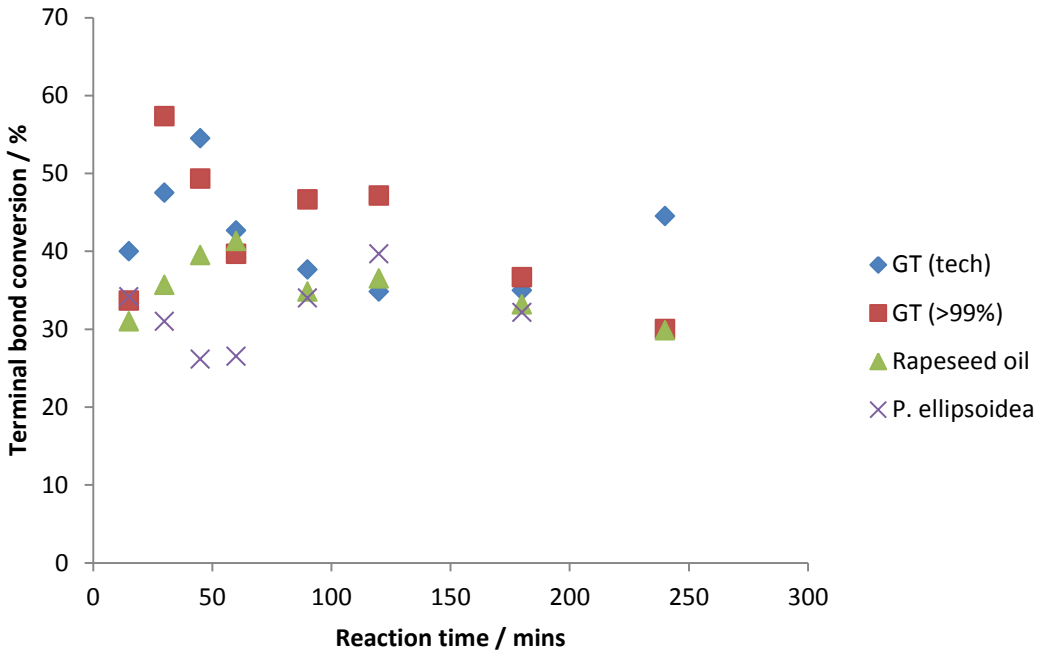

Figure 3.4 Terminal bond selectivity for the cross metathesis of model compounds and real-life oils under inert conditions.

3.3.3 Metathesis of Microbial Oils in a Biorefinery Context

A range of microbial oils from both heterotrophic and photoautotophic organisms were screened for their viability as ethenolysis reagents. While one product stream produced from metathesis is the short-chain hydrocarbons – potentially suitable as a replacement jet fuel – a short-chain triglyceride is also produced. Though its production has been reported in previous studies,[33] there is no information on this products fuel properties in the literature to date. If it possesses poor fuel properties, however, upon transesterification it would yield a short-chain FAME. Due to the shorter chains than is present in current biodiesel feedstocks, this fuel would potentially have superior low temperature properties and an elevated cetane number.[36]

Standard fuel properties (kinematic viscosity, energy density and pour point) were determined at each stage of the production process (Figure 3.5), as these are the properties most important in terms of the fuel's flow and combustion. Cetane analysis for the diesel replacements was unfortunately not possible due to the large amount needed for that analysis (500 ml), though shorter FAMEs tend towards a

higher cetane rating.[36] Purity is extremely important in producing fuels and determining the fuel properties. The HGII present in the reaction mixture, therefore, was removed by the quenching of the reaction in a solution of tris(hydroxymethyl)phosphine and triethylamine in DCM and vigorous stirring which lightened the colour of the reaction mixture from brown to yellow within 10 minutes in most cases (the potent colour associated with chorophyll present in the microalgae *P. ellipsoidea* and *S. obliquus* prevented observations of this colour change). The phosphine readily coordinates to the ruthenium centre, producing a water soluble complex. Washing with water then removes the vast majority of the ruthenium.[22]

The lower boiling alkenes potentially suitable as a jet fuel replacement (the aviation fuel fraction, AFF), were then distilled from this reaction mixture, leaving behind the 'metathesis residue'. After fuel analysis, this residue was transesterified to produce a mixture of FAME and higher boiling point alkenes (road transport fraction, RTF). A flow-diagram for the entire protocol for converting the oil to diesel and jet-fuel replacement fuels via metathesis (along with analysis) can be seen in figure 3.5.

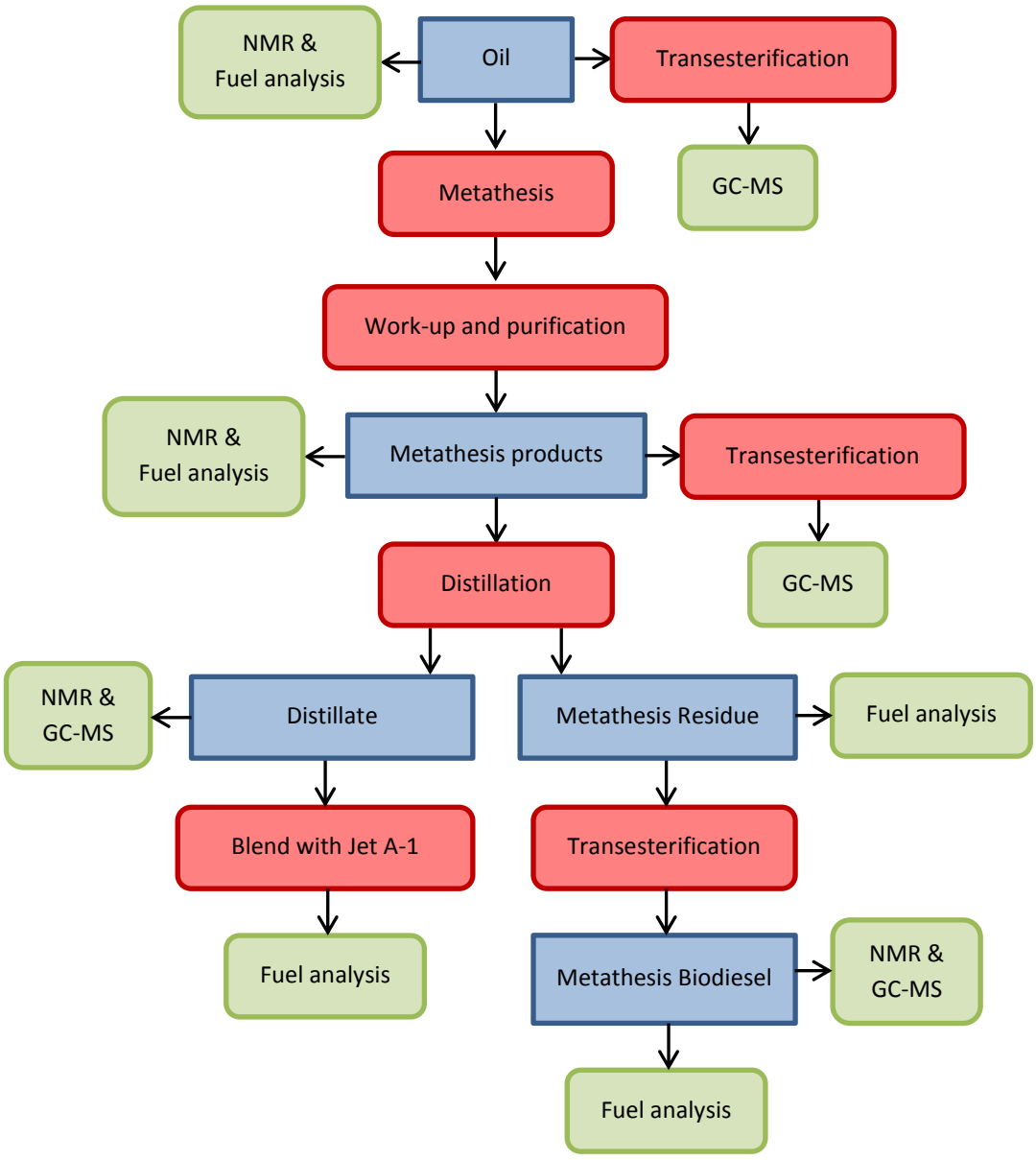

Figure 3.5 Metathesis flow chart to show the reactions and analysis of the oils and reaction products. Blue boxes represent a product or material, red boxes represent experiment work, and green boxes represent analysis

The microbial oils investigated were compared to two first generation biodiesel feedstocks: rapeseed oil (high in monounsaturates), and sunflower oil (high in polyunsaturates). Waste coffee oil was also screened, due to the potentiality as a suitable second generation waste oil resource. The microbial oils selected were from two microalga; *Pseudochoricystis ellipsoidea*, an extremophilic lipid producer[37] and *Scenedesmus obliquus*, currently used in waste water treatment and previously reported as having potential for oil production.[38] These were compared to *Rhodotorula glutinis* and *Rhodotorula minuta*, both oleaginous unicellular yeasts

identified as having potential for biofuel production[19, 39-40] and *Metschnikowia pulcherrima*, a unicellular yeast being considered for its lipid production, and high sterol content within this lipid.[20, 41] The original lipid profiles of the oils screened are given in table 3.4.

The rapeseed oil has a typical lipid profile for an EU biodiesel feedstock with a high proportion of 18:1 that provides reasonable low temperature properties, whilst maintaining good oxidative stability.[42] Due to the elevated levels of ω-9 monounsaturates, including 18:1 and 22:1, this would be advantageous for the production of 1-decene. The monounsaturated C_{20} fatty acid present in rapeseed and *P. ellipsoidea*, however, has been previously identified as gadoleic acid which possesses a double bond in the ω-11 position,[43-44] which would lead to the production of 1-dodecene. Though gadoleic acid is present in fairly small amounts in the oils screened (1.6% for rapeseed, 3.1% for *P. ellipsoidea*) it have been reported as high as 9.3% of the composition of some rapeseed oils.[45] Due to the slightly higher melting point of 1-dodecene (-35 °C),[8] this may have a negative effect on the aviation fuel fraction which is required to remain liquid down to -47 °C.[9]

There is also a significant amount of ω-6 and ω-3 fatty acids which, would lead to the production of 1-heptene, 1-butene, and 1-4-pentadiene. In comparison the sunflower oil has a higher proportion of polyunsaturates, and therefore the production of shorter, lower-boiling alkenes is more likely. The coffee oil has the highest amount of saturates out of all the oils tested. These saturates are not active for the metathesis reaction and therefore should remain in the final FAAE road transport fuel fraction.

The microbial oils, *P. ellipsoidea*, *R. glutinis* and *R. minuta* are relatively high in 18:1 (all around 50%) and have similar fatty acid profiles to rapeseed, with *R. glutinis* and *R. minuta* having a higher amount of polyunsaturates than rapeseed and *P. ellipsoidea* having a higher amount of saturates. However, both *S. obliquus* and *M. pulcherrima* display a huge variety of alternative fatty acid lipids and will potentially produce more complex product mixtures.

Table 3.4 Fatty acid profiles of the oils used in the metathesis

FAME	*Rapeseed Methyl Ester*	*Sunflower Methyl Ester*	*Coffee Methyl Ester*	*P. ellipsoidea methyl ester*	*S. obliquus methyl ester*	*R. glutinis methyl ester*	*R. minuta methyl ester*	*M. pulcherrima methyl ester*
14:0	0.0	0.0	0.0	0.0	1.8	0.0	0.0	0.9
16:0	4.9	16.9	38.1	22.8	24.3	1.5	20.9	12.3
16:1	0.0	0.0	0.0	0.0	7.7	0.0	0.0	2.7
16:2	0.0	0.0	0.0	0.0	3.1	0.0	0.0	1.2
16:4	0.0	0.0	0.0	0.0	4.8	0.0	0.0	0.0
17:0	0.0	0.0	0.0	0.0	3.1	0.0	0.0	1.0
17:1	0.0	0.0	0.0	0.0	2.9	0.0	0.0	2.4
17:2	0.0	0.0	0.0	0.0	4.8	0.0	0.0	0.0
18:0	1.7	3.5	7.8	8.9	2.4	5.9	3.6	21.0
18:1	61.9	26.3	9.1	51.9	25.2	51.7	47.4	6.7
18:2	19.5	53.2	41.4	6.5	14.5	28.9	28.1	39.9
18:3	9.3	0.0	1.1	6.8	4.0	0.0	0.0	11.9
20:0	0.6	0.0	2.5	0.0	1.6	12.0	0.0	0.0
20:1	1.6	0.0	0.0	3.1	0.0	0.0	0.0	0.0
22:1	0.6	0.0	0.0	0.0	0.0	0.0	0.0	0.0
Saturates	7.2	20.4	48.4	31.8	33.1	19.4	24.5	35.3
Monounsaturates	64.1	26.3	9.1	54.9	35.8	51.7	47.4	11.7
Polyunsaturates	28.8	53.2	42.5	13.3	31.2	28.9	28.1	53.0

While the glycerides are the predominant component of lipids, a range of other biological compounds are present in the oils screened. Figure 3.6 shows the ^{1}H NMR spectra of the oils used over the course of this study. Unsurprisingly, the edible oils, rapeseed and sunflower oil almost exclusively contain triglycerides. Interestingly, coffee oil and both *Rhodotorula* species are similarly pure. In the spectra of *P. ellipsoidea*, *S. obliquus* and *M. pulcherrima*, however, there are a number of peaks not assignable to triglycerides. This is likely to be due to other biological organic solvent-soluble materials such as sterols, cell residue and phospholipids. These compounds could potentially have a large effect on the catalyst activity, the down-stream processing or the fuel properties of the resulting fuels.

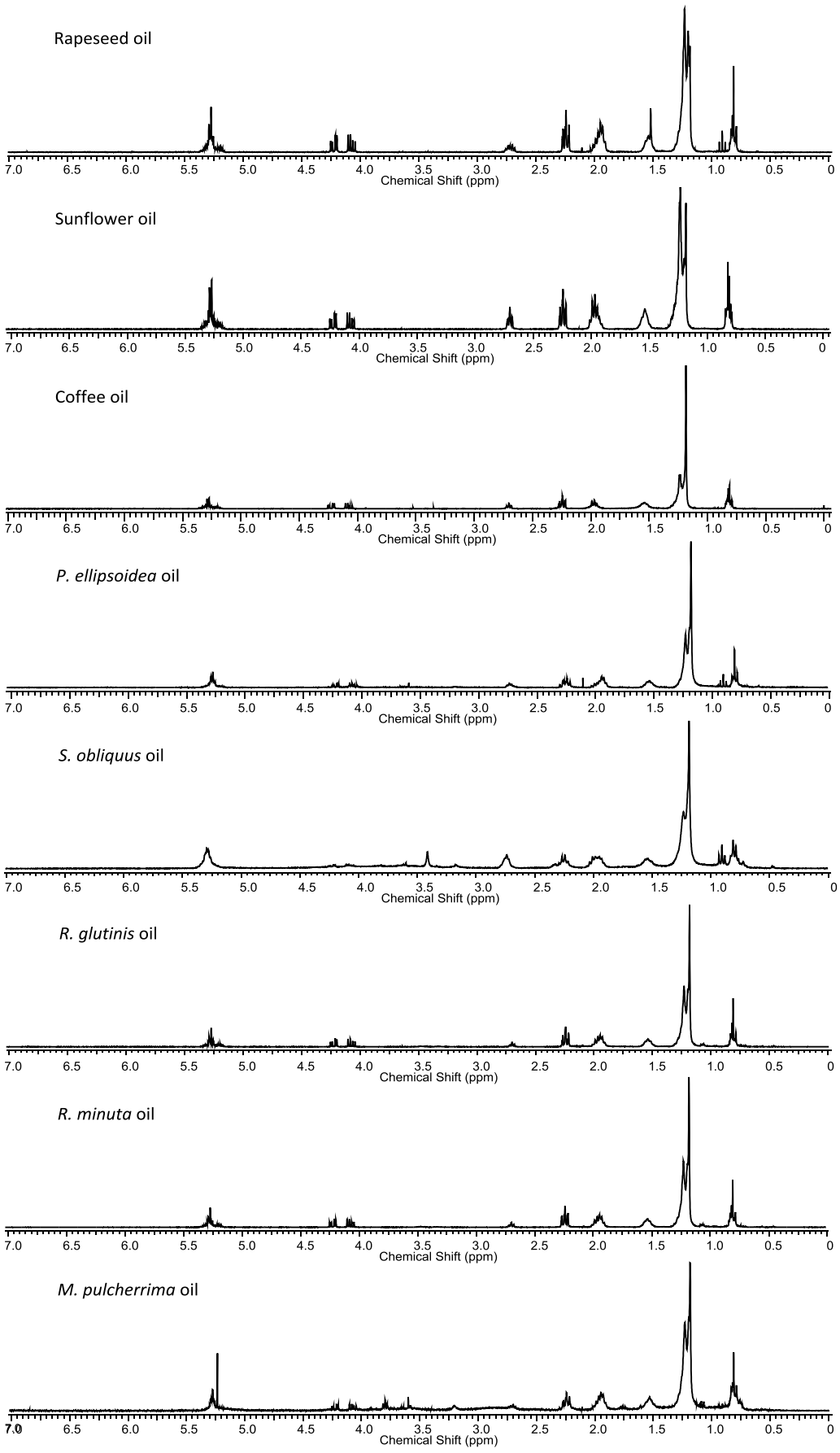

Figure 3.6 ^{1}H NMR spectra of oils used in metathesis experiments.

3.3.3.3 Metathesis Conversion & Products

To examine the properties of the resulting fuels, reactions were carried out on a 1 ml scale. To produce enough fuel for the properties testing each reaction was repeated between 3-10 times. The ratio of terminal alkenes produced was analysed by ^{1}H NMR spectroscopy (Figure 3.7). Rapeseed, sunflower, *P. ellipsoida* and *R. glutinis* oils all reached conversions between 35-40%, similar to the reaction optimisation reactions presented in figure 3.4. The conversion of the coffee oil was slightly lower at 28%, most likely due to the high amount of saturates present. A similarly low conversion was achieved for *S. obliquus* lipid. *R. minuta* and *M. pulcherima* achieved the lowest conversion at 23% and 24%, respectively. These conversions suggest that impurities in these oils could be deactivating the catalyst. However, the yields presented are calculated on that amount of product recovered. Certain impurities may have been discarded or degraded during the reaction or work-up, and subsequently lost from the purified product.

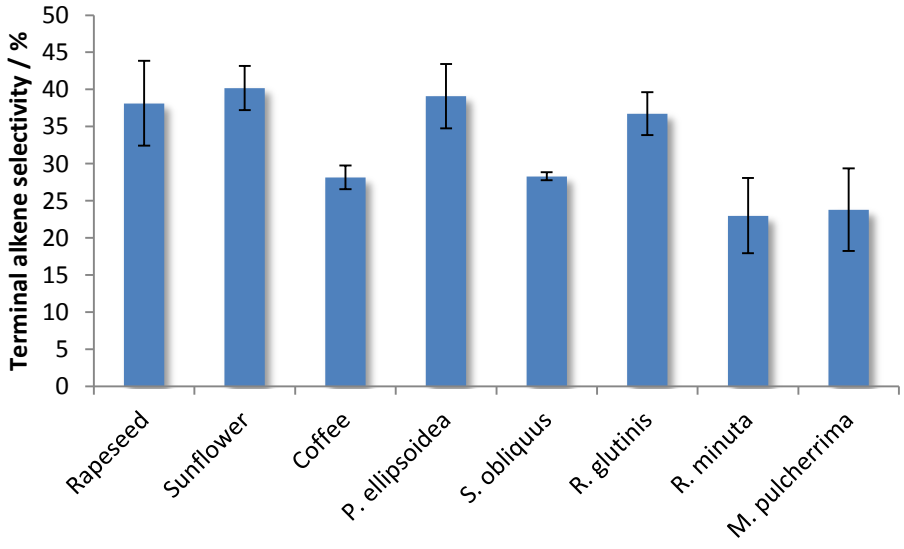

Figure 3.7 Terminal bond selectivity calculated by ^{1}H NMR spectroscopy.

The mass balance, as a % of the initial oil, was calculated on the total product produced (metathesized triglycerides and the resulting hydrocarbons), to assess the losses due to light fraction of alkene products (Figure 3.8). Generally, the recovered mass is between 70-75% of the starting mass for the oils under investigation. While

some of the mass will have been lost in the work up, more significant are the production of low-boiling volatiles during the reaction.

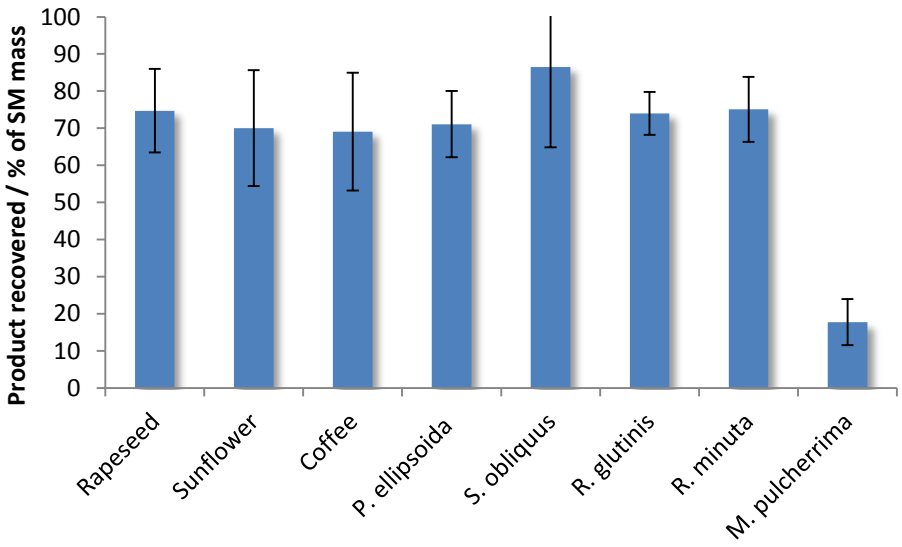

Figure 3.8 Metathesis product recovered, as a percentage of starting material (SM) mass

Polyunsaturated oils, depending on the positioning of the double bond, have the potential to be partially converted into 1-butene and 1,4-pentadiene (from cross-metathesis with ethene) and 3-hexene (from metathesis between two ω-3 fatty acids) which possess low boiling temperatures and are likely to evaporate from the reaction mixture during work-up. While around 70% of the mass was retained from the majority of the oils examined, only 15% mass was recovered from the initial *M. pulcherrima* lipid. The low recovery percentages for *M. pulcherrima* could potentially due to the water-soluble impurities in the original oil which are lost in the extensive work-up and purification.

In order to assess the products of the metathesis residue formed during the reaction, a small sample (0.1g) of the combined reaction mixtures was transesterified to allow for GC-MS analysis (Table 3.5).

Table 3.5 Composition of metathesis products, determined by GC-MS. Assigned "CX:Y", whereby X denotes carbon number and Y denotes number of double bonds. Different species that fall within the same label according to these rules (i.e. 1-decene and 2-decene) are grouped together. FADME = Fatty acid dimethyl ester.

		Rapeseed metathesis products	**Sunflower metathesis products**	**Coffee metathesis products**	***P. ellipsoida* metathesis products**	***S. obliquus* metathesis Products**	***R. glutinis* metathesis products**	***R. minuta* metathesis products**	***M. pulcherrima* metathesis products**
FAME / %	**C8:1**	0.0	0.0	0.0	2.3	1.0	0.0	0.0	0.0
	C9:1	1.0	0.8	0.0	0.3	2.1	0.3	0.7	0.0
	C10:1	54.4	56.3	12.5	55.8	25.0	42.3	21.0	14.1
	C11:1	1.3	1.1	0.0	0.3	0.0	0.5	0.0	0.0
	C12:1	3.6	0.9	4.3	2.5	3.2	0.3	0.0	0.0
	C14:0	0.0	0.6	0.0	1.9	3.6	1.2	2.1	1.7
	C15:1	1.9	4.3	1.5	0.0	2.8	1.9	1.8	4.1
	C16:0	7.5	8.8	51.0	0.0	36.7	24.4	21.2	22.7
	C16:1	2.3	1.4	6.2	1.6	2.4	0.2	0.0	1.9
	C17:0	0.0	0.0	0.0	0.0	0.0	0.4	0.0	0.0
	C17:1	0.0	0.0	0.0	0.0	0.0	0.0	0.0	0.0
	C18:0	2.4	5.0	10.4	12.6	3.7	6.0	5.2	9.5
	C18:1	6.0	3.5	0.7	0.5	4.4	4.6	8.3	13.3
	C18:2	0.0	1.0	0.2	0.0	0.0	0.7	0.0	6.5
	C20:0	0.0	0.4	3.4	1.0	1.0	0.4	0.0	1.4
	C20:1	0.0	0.0	0.0	0.0	0.0	0.0	0.0	0.0
	C22:0	0.0	0.9	0.7	0.0	1.5	0.3	0.0	0.0
	Total	80.4	85.1	90.9	78.7	87.4	83.4	60.2	75.3
Olefin / %	**C10:1**	4.7	4.0	3.9	0.7	0.0	3.9	1.8	0.0
	C11:1	0.5	0.2	0.0	0.0	0.0	0.0	0.0	0.0
	C12:1	0.8	1.3	0.2	0.7	0.7	0.2	0.0	0.0
	C13:1	0.0	0.0	0.0	0.0	0.0	0.0	0.0	0.0
	C14:1	0.0	0.0	0.0	0.0	0.0	0.0	0.0	0.0
	C15:1	2.3	2.3	0.3	0.8	0.0	1.0	1.5	0.0
	C16:1	0.0	0.2	0.0	0.0	0.0	0.0	0.0	0.0
	C17:1	0.0	0.0	0.0	0.0	0.0	0.0	0.0	0.0
	C18:1	4.8	1.5	0.0	2.8	1.1	1.1	2.0	0.6
	Total	13.1	9.5	4.4	5.1	1.7	6.2	5.2	0.6
C18:1 FADME / %		4.3	4.4	1.1	5.7	0.0	2.7	4.2	2.7
"Other" / %		0.7	1.0	3.5	10.5	10.9	7.7	30.3	20.6

The analysis shows a significant amount of variation in the resulting esters between the metathesis products, presumably due to the different fatty acid profiles of each oil. The reaction for those oils possessing a large proportion of unsaturates yielded a majority of mono-unsaturated C_{10} esters, accounting for over half of the esters present in the rapeseed, sunflower and *P. ellipsoida*'s composition. This is expected as most unsaturates, though they may possess more than one double bond, have a double bond in the C_9 position and are saturated upto the ester moiety. However, while the vast majority of these C_{10} mono-unsaturated esters were terminal alkenes (>90%), a number of alternative peaks associated with this species were also identified. Due to the lack of stereochemistry in terminal alkenes, it can therefore be inferred that isomerisation is taking place, moving the double bond up the carbon chain. This is typical of ruthenium catalysts in their hydride form,[35] the form that HGII is likely to be in its deactivated state.

Isomerisation in metathesis has been widely reported as a side-reaction in ruthenium-carbene catalysed metathesis, as well as being the strongly preferred or even exclusively observed pathway,[46] due to the *in situ* formation of ruthenium-hydride species. The metathesis, and specifically ethenolysis, of triglycerides and fatty acid chains has been a subject of research due to its potential production of terminal alkenes, which can be further functionalised and used as intermediates for the production of lubricants, surfactants and polyesters.[31, 47-49] However, the isomerisation associated with fatty acid ethenolysis using ruthenium-carbide catalysts produces unwanted internal alkenes which are difficult to separate via standard purification techniques and is the main limitation of its industrial application.[25] Some methods have been developed to inhibit or reduce this isomerisation, such as the additions of catalytic amounts (10 mol%) of 1,4-benzoquinones or acetic acid,[50] or the use of lower temperatures.[51] However, these would increase the cost of the products due to the need of further reagents and increased reaction time associated with lower temperatures, unsuitable for a fuel-production process. There may, however, be little need to inhibit the isomerisation. The presence of internal alkenes should have a minimal effect on the general fuel properties of the molecules, and the stability of the fuel could be increased, as

terminal alkenes are generally more reactive due to their inherent lack of steric hindrance.[52] This isomerisation is potentially the reason for the presence of fatty acids and alkenes otherwise unexpected from the oils, such as C_9 and C_{11} fatty acid alkenes, and C_{11} and C_{12} alkenes (Scheme 3.1).

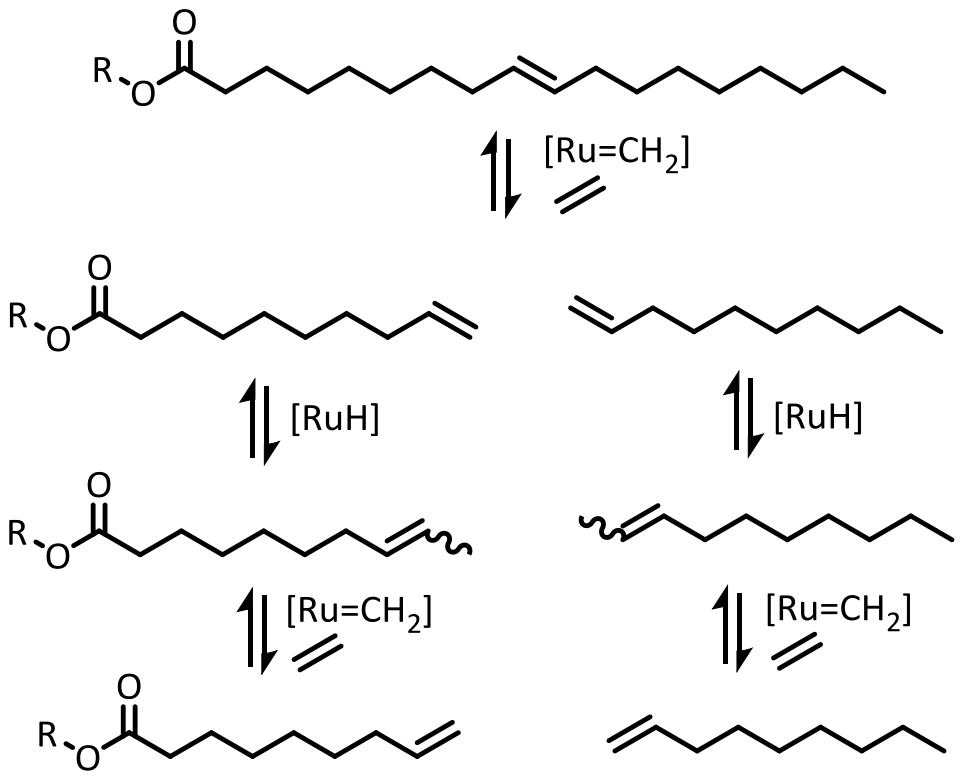

Scheme 3.3 The metathesis of oleic fatty acid with ethene catalysed with ruthenium-carbene catalyst, and the potential isomerisation of the products with ruthenium-hydride catalysts**.**

In all reaction mixtures there are small amounts of unreacted mono-unsaturated fatty acids, which are expected due to the equilibrium associated with Ru-based metathesis catalysts at lower pressures.[53] However, the polyunsaturates are significantly decreased due to the probability of each double bond being consumed, along with the potential production of 1,4 pentadiene which would partition into the gas phase, thus significantly reducing the rate at which it would react.

The lack of polyunsaturates would also increase the oxidative stability of any fuel produced by this method.[41] At higher pressures of ethene, the presence of these species would likely decrease. Due to the lack of double bonds saturated fatty acid chains are also present in the final reaction mixtures. Interestingly, a dimethyl ester

(octadec-9-enedionic acid methyl ester) was observed in up to 5.7% of the final composition. This is most likely produced between two C_{18} fatty acid chains with a double bond in the 9-position, on either the same or different triglyceride species, or the product of a two terminally unsaturated C_{10} fatty acids (produced from the reaction of the triglyceride with ethene) reacting with each other, or between one terminally unsaturated C_{10} fatty acid and one C_{18} fatty acid chains with a double bond in the 9-position.

Five olefins were detected by GC-MS in the product mixtures analysed. Surprisingly there is a relatively small amount of 1-decene and other diesel / kerosene carbon range (C_{12} and below), with the maximum being 6% (rapeseed). This is most likely due to the relatively low pressure of ethene, leading to significant reaction of the unsaturated triglyceride fatty acid chains with one another. It should be noted, however, that the metathesis of *S. obliquus* didn't produce any 1-decene and only dodecene is present. Though the double bond position is unclear, it is likely that the dodecene is 6-dodecene, produced from the cross-metathesis of ω-6 fatty acids. Therefore, due to the lack of 1-decene in both *S. obliquus* and *M. pulcherimma*, it can be said that the cross-metathesis reaction between their triglycerides and ethene is not favoured. Other olefins present in all but *S. obliquus* and *M. pulcherimma* are pentadecene (the likely cross metathesis product between ω-6 and ω-9 fatty acids), and octadecene (the likely cross metathesis product between two ω-9 fatty acids).

Due to the lack of short-chain alkenes present in the metathesis products it seems that *S. obliquus* and *M. pulcherrima* are not suitable as potential metathesis fuel feedstocks and therefore were not further examined. Due to the higher yields *R. glutinis* was selected over *R. minuta* as the most suitable oleaginous yeast for further study.

3.3.3.4 Aviation Fuel Fraction (AFF)

The volatile olefin fraction, termed aviation fuel fraction (AFF) was isolated and purified using a Schlenk line. The metathesis mixture was heated to 120 °C, subjected to vacuum and held for 60 minutes. The liquid nitrogen cold trap was allowed to warm to room temperature before washing out with DCM, which was subsequently removed *in vacuo*. The masses recovered – between 2.1% - 5.4% – are consistent with the amount of short-chain olefins present in the metathesis product mixtures (Figure 3.9).

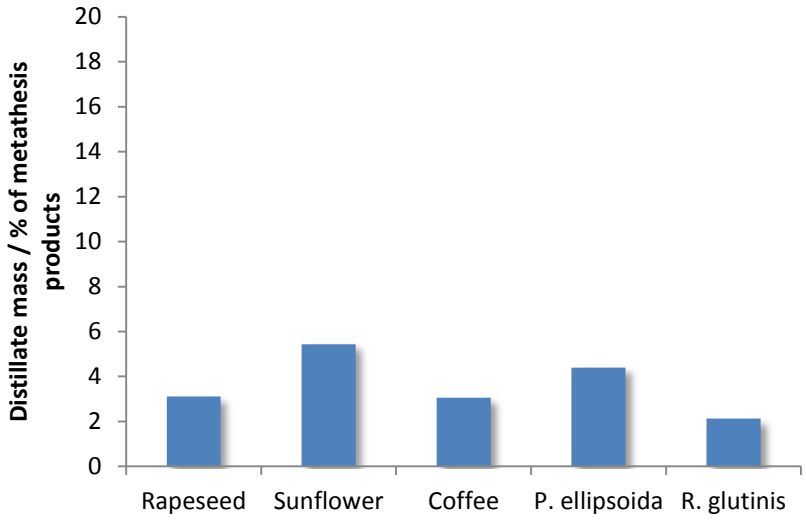

Figure 3.9 Distillate mass recovered, as a percentage of the metathesis product mass.

The AAF was analysed by GC-MS (Figure 3.10). The major product from this reaction is 1-decene, which increases from 58.1% of the distillate for coffee oil, to 92.0% for *P. ellipsoida*. The rest are made up of a small amount of decene isomers, most likely isomerised 1-decene from the deactivated ruthenium complexes; an even smaller amount of undecene isomers, most likely produced from the decene isomers and ω-3 fatty acids; and dodecane isomers, which accounts for the second-largest proportion of all olefins in the distillate. These longer alkenes may potentially have negative effects on the fuel properties of the distillate, when compared to pure 1-decene, as longer alkenes have higher melting points and generally higher viscosities.[8] Surprisingly, there was no 1-heptene present (likely produced between

ω-6 fatty acids and ethene) in the distilled fraction, most likely due to losses in the work-up.

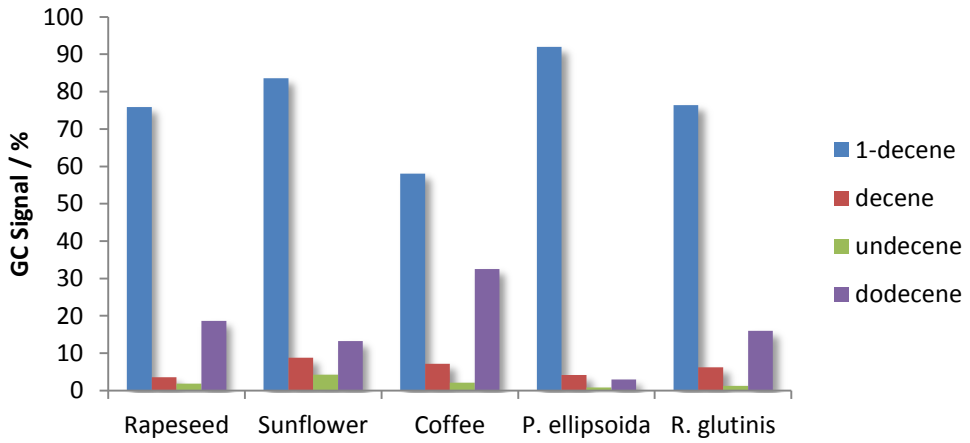

Figure 3.10 Proportion of olefins present in metathesis distillate from the cross-metathesis products of various oils.

3.3.3.5 Road Transport Fuel (RTF)

After distillation of the lower-boiling alkenes from the metathesis product mixture, the residue left was analysed for its fuel properties, before the glycerides present were fully transesterified to give the Road Transport Fuel (RTF). The composition for the fuel is roughly the same as for the metathesis product, apart from the absence of the low-boiling alkenes (Table 3.6). No oxidation products were formed during the distillation of the C_{12} and lower olefins. This is likely to be, in part, due to the lack of free oxygen in the mixture due to being subjected to vacuum, but also potentially due to the increased stability of the mixture due to the lack of polyunsaturated species in the product mixtures.

Table 3.6 Composition of the Road Transport Fraction (analysed by GC-MS), formed via the transesterification of the residue left after removal of the aviation fuel fraction.

		Rapeseed metathesis RTF	Sunflower metathesis RTF	Coffee metathesis RTF	*P. ellipsoida* metathesis RTF	*R. glutinis* metathesis RTF
FAME / %	C8:1	0.2	0.0	0.0	2.5	0.0
	C9:1	2.3	0.7	0.3	0.0	0.7
	C10:1	51.4	60.7	35.6	39.2	40.8
	C11:1	2.4	0.9	0.0	0.0	1.0
	C12:1	4.1	0.8	0.3	2.0	0.3
	C14:0	0	0.0	0.0	0.0	0.5
	C16:0	7.1	9.8	45.1	21.8	26.6
	C16:1	0.8	0.3	0.6	1.1	0.4
	C17:0	0	0.0	0.0	0.0	0.4
	C17:1	1.2	0.1	0.0	0.0	0.0
	C18:0	2.4	6.0	9.9	9.2	6.7
	C18:1	7.7	4.3	0.9	7.2	5.2
	C20:0	0.8	0.4	3.0	0.6	0.4
	C20:1	0.5	0.2	0.0	0.0	0.1
	Total	80.9	84.2	95.8	83.8	83.2
Olefin / %	C14:1	0.1	0.0	0.0	0.0	0.0
	C15:1	1.3	0.3	0.0	0.0	1.1
	C16:1	0.4	0.0	0.0	0.0	0.0
	C17:1	0.4	0.0	0.0	0.0	0.1
	C18:1	2.7	0.4	0.0	2.3	0.3
	Total	4.9	0.7	0.0	2.3	1.5
C18:1 FADME / %		6.4	4.5	1.5	5.2	5.2
"Other" / %		7.8	10.6	3.6	8.7	10.4

3.3.3.6 Higher Value Product Fraction

To qualify the products being produced in the gas fraction, an experiment was carried out using sunflower oil (the most polyunsaturated oil), under the same conditions. Once the reaction time was complete, the pressure was released through a gas-trap, 50 cm^3 of which was analysed via GC-MS (Appendix). As predicted, 1-butene (from the cross-metathesis of ethene and a ω-3 fatty acid), 1,4-pentadiene (from the cross-metathesis of a polyunsaturated fatty acid and two

molecules of ethene), 1-heptene (from the cross-metathesis of ethene and a ω-6 fatty acid) and 3-hexene (from the cross-metathesis of two ω-3 fatty acids) were observed. However, many isomers of butane and pentadiene were seen. This supports the inference that ruthenium hydride complexes, formed by the deactivation of the HGII, are acting as isomerisation catalysts. This is further supported by the significant presence of propene, only achievable via the isomerisation of 1-alkenes to the more stable 2-alkenes and subsequent cross-metathesis with ethene.

These terminal alkenes, as well as the di-enes, are suitable higher values products that can act as co-monomers in polymer production. These side-products, therefore, could support the fuel production process and make it more economically viable.

3.3.3.6 Fuel Properties

To assess the suitability of the metathesis of lipids to produce suitable fuels, the energy density, kinematic viscosity and freezing point of the reaction mixtures were examined.

Kinematic Viscosity

The viscosity of the oils converted, along with the total metathesis products, RTF and AFF analysed. For products with a low viscosity (less than 10 mm^2s^{-1}), a kinematic viscometer was used, and with highly viscous oils (above 10 mm^2s^{-1}) the dynamic viscosity was measured using a spinning disk rheometer then converted to the kinematic viscosity using the oil's density.

All the oils tested (i.e. prior to metathesis) had a viscosity of above 20 mm^2s^{-1} at 40 °C (Figure 3.11), in agreement with reported values.[54] Sunflower oil exhibited the lowest viscosity (21.9 mm^2s^{-1}), presumably due to its high amount of polyunsaturates. Correspondingly the viscosity of the oleic acid rich rapeseed and *R. glutinis* oils were slightly higher at 24.2 and 25.4 mm^2s^{-1} respectively. Unsurprisingly, the highly-saturated coffee oil had a higher viscosity than the yeast

oils (31.1 mm^2s^{-1}), though the viscosity of *P. ellipsoida* lipid was significantly higher at 109 mm^2s^{-1}, presumably due to impurities present in the oil which possess strong intermolecular bonding.

When metathesized, the viscosity of the mixtures drops significantly due to the presence of shorter-chain alkenes. The presence of these short-chain alkenes, however, is not enough to change the viscosity to a level that would allow this to be used as a fuel – the lowest viscosity of these products is 15.1 mm^2s^{-1} (sunflower) at 40 °C, whereas the maximum allowed for biodiesel is 5.0 mm^2s^{-1} for the EU[55] and 6.0 mm^2s^{-1} for the US.[56] After the shorter-chain alkenes were distilled off, the viscosity of the mixture (the "metathesis residue") generally increases to a similar level of the original oil.

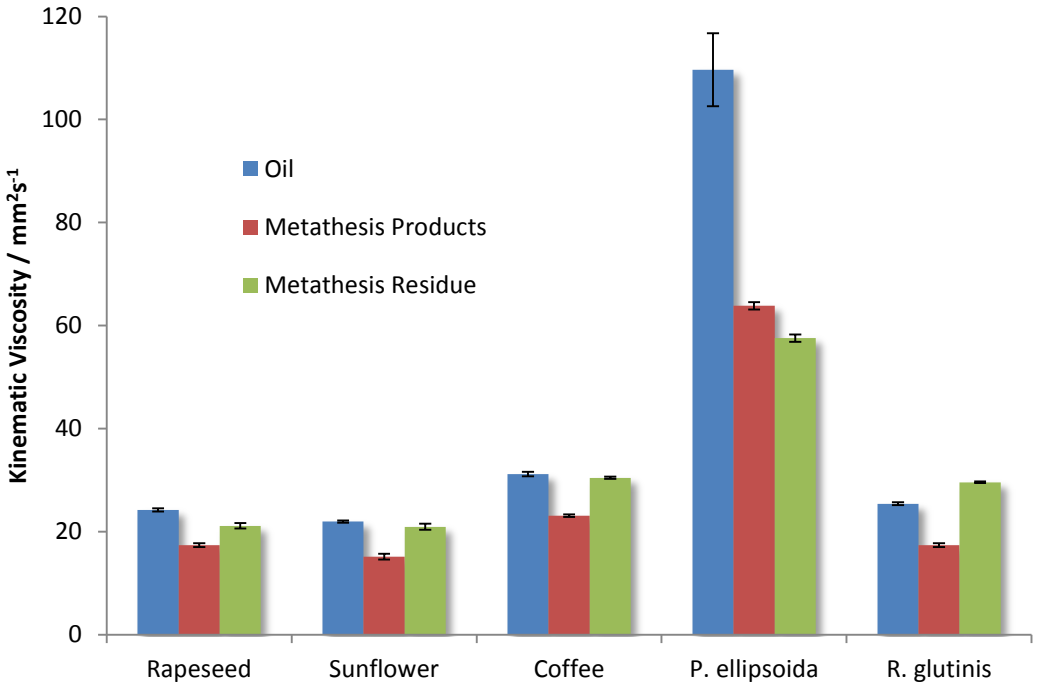

Figure 3.11 Viscosity of the oils used, metathesis products, metathesis residue at 40 °C.

This demonstrates that creating short chain triglycerides is not enough to reduce the viscosity of the oil to required levels, and the additional transesterification step is indeed necessary to produce a suitable road transport fuel. The kinematic viscosity of the RTF follows the same trend as for the parent oils;

sunflower < rapeseed < *R. glutinis* < coffee < *P. ellipsoida*

R. glutinis RTF is the only sample that would pass European standards for biodiesel (Figure 3.12), with rapeseed and sunflower RTF falling below the minimum, and coffee and *P. ellipsoida* RTF being above the maximum. It should be noted that the viscosity for rapeseed RTF and sunflower RTF fall within the viscosity range outline for diesel (2.00-4.50 mm^2s^{-1}). Furthermore, all samples analysed fall within the US standard for biodiesel (range 1.9-6.0 mm^2s^{-1}). Coffee metathesis biodiesel is actually more viscous than the biodiesel produced from coffee oil without metathesis. In chapter two, the same oil (SCG, Columbian coffee) was converted to biodiesel in the conventional manner and found to have a viscosity of 4.5 mm^2s^{-1}. This is likely due to the high proportion of saturates in the coffee metathesis biodiesel (55%), compared to the conventional coffee biodiesel (44.7%).

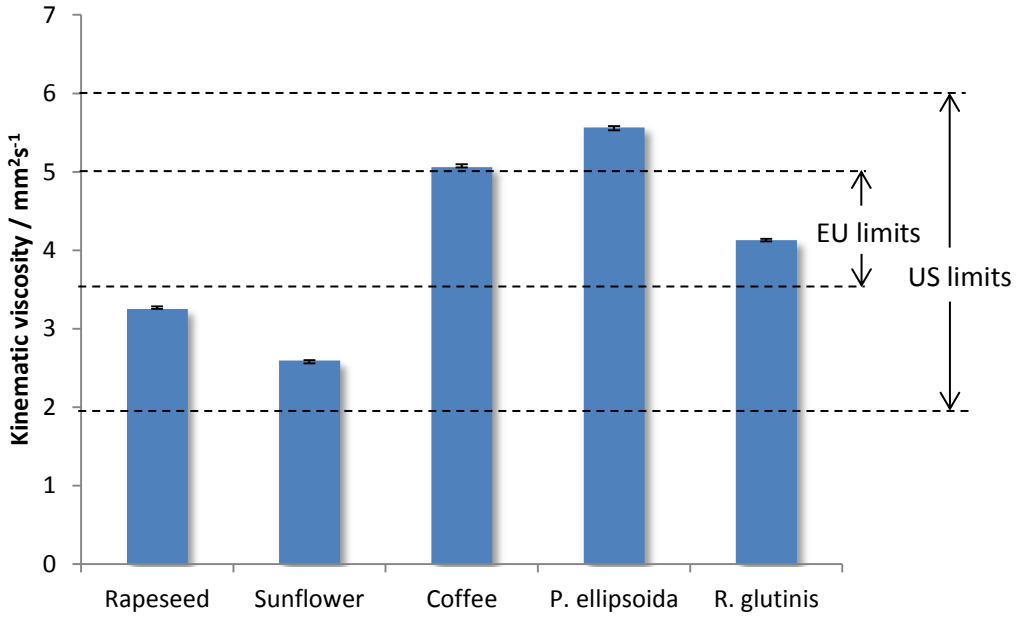

Figure 3.12 Kinematic viscosity of the RTF at 40 °C, showing the limits of biodiesel viscosity outlined in EN 14214 (EU) and ASTM D6751 (US).

Unfortunately, due to the low percentage of distillate recovered from the metathesis mixtures, it was impossible to determine the viscosity of the distillate themselves due to the minimum volume requirement of the viscometers (*ca.* 0.5 ml). Therefore, the distillate from each of the metathesis products was blended 20 vol% with Jet A-1 aviation fuel. From this point on, these blends will be referred to as "RMD-20" (rapeseed oil metathesis distillate blended 20 vol% with jet-fuel),

"SMG-20" (sunflower oil metathesis distillate blended 20 vol% with Jet A-1), "CMG-20" (coffee oil metathesis distillate blended 20 vol% with Jet A-1), "RgMG-20" (*R. glutinis* oil metathesis distillate blended 20 vol% with Jet A-1), and "PMG-20" (*P. ellipsoida* oil metathesis distillate blended 20 vol% with Jet A-1). As a comparison, a representative model mixture (AFF model) of the distillates was made from blending the individual olefins (purchased commercially), using an approximate average of the AFFs produced (i.e. 80 vol% decene, 5 vol% undecene, 15 vol% dodecene).

At 40 °C, the blending of AFF does not significantly alter the viscosity of the Jet A-1 (Figure 3.13). The viscosity of Jet A-1 used in this study was 1.17 mm^2s^{-1}, at 40 °C, whereas the blends with 20 vol% distillate ranged from 1.12 mm^2s^{-1} (rapeseed) to 1.29 mm^2s^{-1} (coffee). The increased viscosity of the CMD-20 is presumably due to the high proportion of dodecene. In the Jet A-1 fuel standards, the fuel is required to have a viscosity of 8 mm^2s^{-1} or below at -20 °C. At this temperature, all samples tested were found to be significantly below this maximum. The blends with 20 vol% distillate ranged from 4.00 to 4.18 mm^2s^{-1}, significantly lower than Jet A-1's value of 4.68 mm^2s^{-1}. This is unsurprising as 1-decene and the AAF model mixture have a considerably lower viscosity of 2.52 mm^2s^{-1} and 2.41 mm^2s^{-1}, respectively. These lower viscosities are most likely due to the lower proportion (or complete lack, in the case of 1-decene and AAF model) of aromatics.

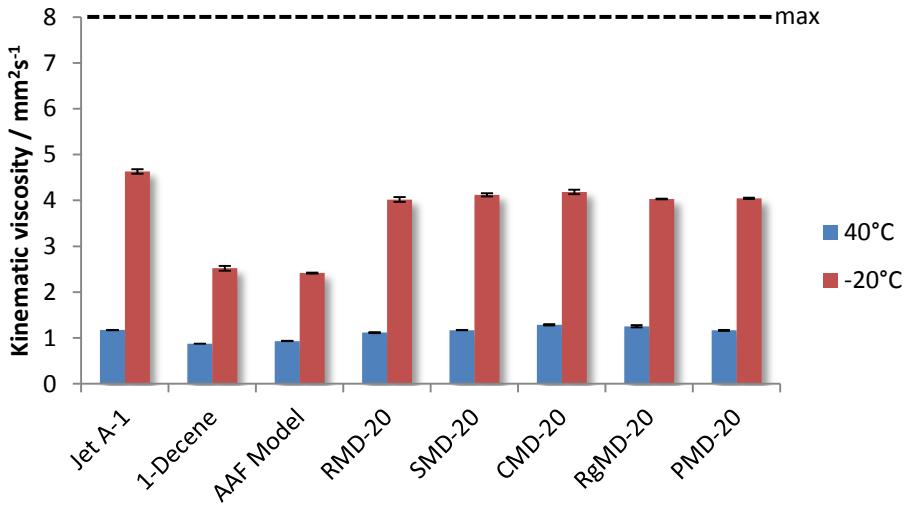

Figure 3.13 Viscosity of the distillate, blending with jet fuel (20:80), showing the maximum allowed viscosity at -20 °C for both ASTM and DEF STAN standards.

Energy density

The energy density of each stage of the metathesis protocol was measured using an IKA C1 static jacket oxygen bomb calorimeter (Figure 3.14). The oils all possessed similar energy densities, similar to those in literature, of around 40 MJ kg^{-1}.[54] Coffee, *R. glutinis* oil and *P. elipsoidea* have slightly lower energy densities (37.7 MJ kg^{-1} and 38.2 MJ kg^{-1}, respectively) than rapeseed and sunflower oil (39.7 MJ kg^{-1} and 40.1 MJ kg^{-1}, respectively), likely due to the slightly higher amount of oxygenated impurities.

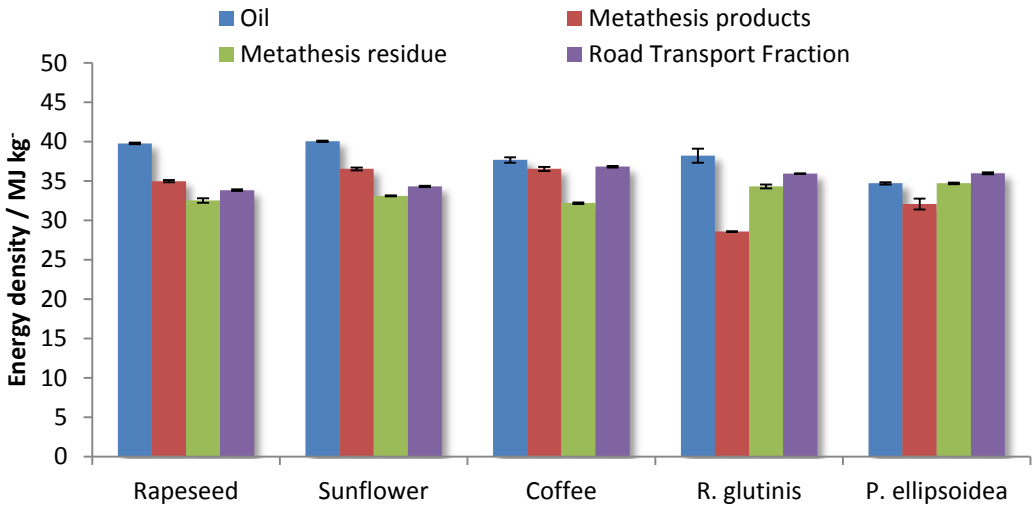

Figure 3.14 Energy density of oil, metathesis products and metathesis residue and RTF

Upon metathesis, the energy density of all the oils (bar *P. ellipsoidea*) decreased. This is slightly counter intuitive, as cross-metathesizing the mixture with ethene adds carbon, leading to an increase in the C/O and H/C ratio (i.e. more C-H bonds available for combustion) of the overall mixture. Though it is a small difference, both are associated with an increase in energy density. The conversion of polyunsaturated fatty acids, however, leads to the production of volatile alkenes such as 1-butene, 1,4 pentadiene, and 3-hexene, which are removed from the reaction mixture upon work-up. This removes carbon originating from the fatty acids themselves, decreases the C/O and H/C ratios and therefore decreases the energy density.

Distilling the lower-boiling hydrocarbons decreased C/O and H/C ratios and thus the decreased energy density of the residue that remained was observed for all metathesis residue samples. Transesterifying this residue to the RTF introduces three methyl groups (i.e 9 C-H bonds) per triglyceride rather than a glyceryl moiety (i.e. 5 C-H bonds), which should increase the energy density slightly. This was observed for RTF samples. Interestingly the RTF for *P. ellipsoidea* exhibits a higher energy density than its original oil – likely due to the amount of oxygenated impurities present in the oil which have since been lost in the extensive processing and work-up. The energy densities for all RTF fractions were between 33.8 and 36.8 MJ kg^{-1} which is lower than diesel and biodiesel at approximately 45 and 40 MJ kg^{-1}, respectively.

The energy densities for the metathesis distillate mixtures, along with Jet A-1, 1-decene and the AAF model were measured (Figure 3.16). The AAF model and 1-decene exhibited the highest energy density at 47.0 and 46.9 MJ kg^{-1}, significantly larger than Jet A-1 at 44.7 MJ kg^{-1}. This is unsurprising due to the aromatic proportion present in Jet A-1, significantly reducing the H/C ratio of the fuel. The energy densities for the distillate mixtures were lower than the AAF model and 1-decene and higher than Jet A-1 with a range between 45.2 and 46.0 MJ kg^{-1}. All fuels were above the minimum set by ASTM and DEF STAN standards (42.8 MJ kg^{-1}).

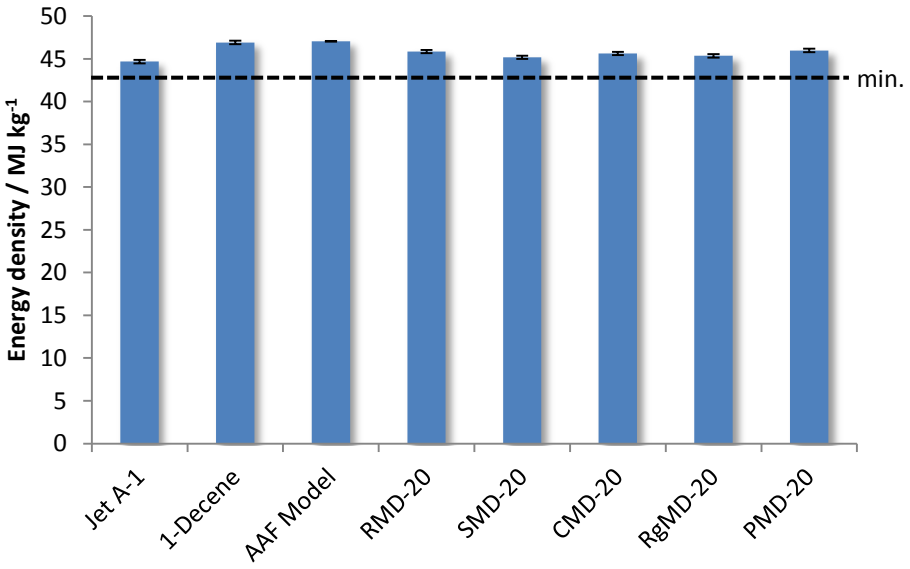

Figure 3.15 Energy densities of Jet A-1, 1-decene, AAF model and all metathesis distillate mixtures, showing the minimum outlined in ASTM and DEF STAN standards.

Pour point

The pour point of a fuel is important as it must flow down to the lowest operational temperature. The pour points of the oils, metathesis products, metathesis residue and RTF were assessed (Figure 3.17). For the oils, a wide range of pour points was observed, from as low as -8 - -7 °C for rapeseed oil, to as high as 8-10 °C for *P. ellipsoidea* oil, likely due to the difference in saturation and impurity. Interestingly, different effects were seen with each stage of the process.

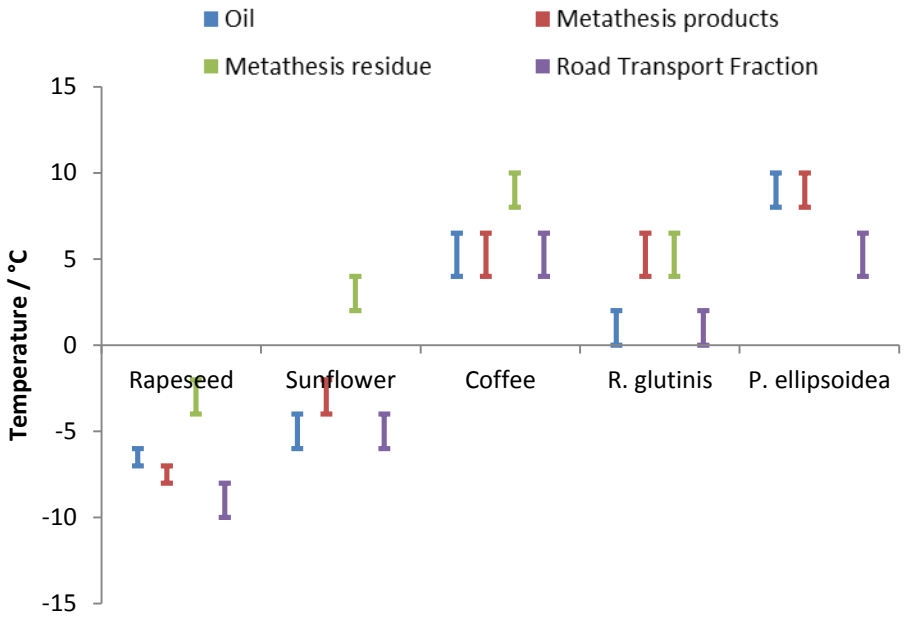

Figure 3.16 Pour points of the oil, metathesis products, metathesis residue and RTF

One would expect the pour point of an oil to decrease upon cross-metathesis due to the production of lower mass and therefore lower pour point species. This was observed for rapeseed oil, though not for any other oil tested. Coffee oil and *P. ellipsoidea* oil do possess the same pour point range as their metathesis products. For sunflower and *R. glutinis*, however, the pour points of the metathesis products increased. This presumably demonstrates enhanced molecular interactions between the products. Upon distilling the short-chain hydrocarbons out of the mixture, the pour point decreased for all the samples apart from *R. glutinis*, though any small difference is masked by the 2 °C range. Interestingly, the metathesis residue for *P. ellipsoida* gelled at room temperature.

Transesterifying the residue led to the RTF pour point lowering, to the same range or lower than that of the original oil in all cases. Rapeseed was the lowest pour point range, between -10 and -8 °C, with coffee and *P. ellipsoidea* the highest at between 4 and 6.5 °C. These are all comparable with pour points for conventional biodiesel, likely due to the presence of saturated long chains FAMEs. Therefore, production of a RTF of improved low temperature properties would require a feedstock low in saturates.

The Jet A-1 standard sets a minimum freezing point of -47 °C. The freezing point of the Jet A-1 used in this study was found to be -51 °C. The metathesis distillates were still liquid at this temperature while the blended distillates were all found to flow up to -51 °C.

Stability

The AFF produced contains a significant portion of terminal alkenes and a small portion of internal alkenes due to the isomerisation activity of the deactivated metathesis catalyst. Though this is not a problem for the fuel properties, the catalyst is a significant portion of the cost of fuel production, and so its replacement / rejuvenation will add cost to the process. Ideally the catalyst would be robust and selective for terminal alkene production. A high portion of terminal bonds, however, may reduce the stability of the fuel due to their higher reactivity compared with internal double bonds.[52]

To assess the stability of a fuel with a high portion of terminal double bonds, technical grade 1-decene was subjected to Rancimat conditions (110 °C, airflow 10 l h^{-1}), and samples taken regularly between 1-72 hours and analysed by ^{1}H NMR spectroscopy (Figure 3.15). For the first 24 hours of the experiment little change was observed. At 48 hours, however, there is significant difference. The peaks associated with the terminal double bond (δ 4.9 ppm & 5.8 ppm) are noticeably decreased, and there is a range of peaks from 2.0 – 4.5 ppm which are indicative of a range of oxygenated species, including alcohols & carbonyl species.[57] At 72 hours, the double bonds were almost completely been consumed, and from 2.0 – 4.5 ppm

there are wide, overlapping peaks which suggest a number of different oxygenated species. The study shows, however, that 1-decene is stable at Rancimat conditions for at least 24 hours, significantly more than Jet A-1 which undergoes significant chemical changes after 1 hour.[58]

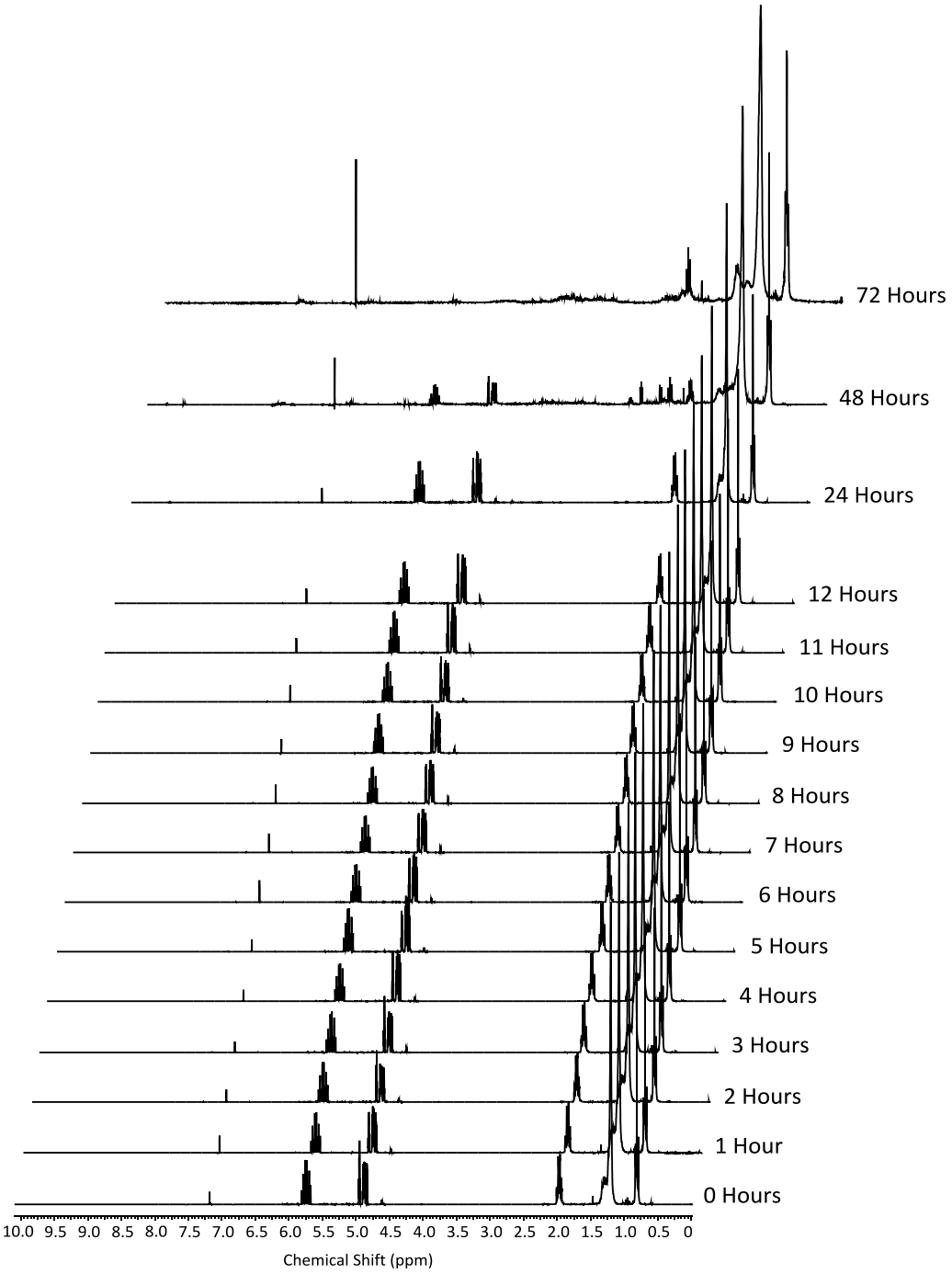

Figure 3.17 ^{1}H NMR spectra of 1-decene samples subjected to Rancimat conditions (110 °C, 10 l h^{-1} airflow)

3.4 SUMMARY

Cross-metathesis of natural triglycerides high in oleic acid with a short-chain alkene source has the potential to produce two fuels from the same source – a shorter chain triglyceride that can be transesterified into a shorter-chain FAME (and therefore improved physical properties to conventional biodiesel), and a short-chain hydrocarbon fraction potentially suitable for aviation. Though losses could be formed in the form of gas if a polyunsaturated triglyceride was used, these short chain alkenes have potential as higher value products, particularly as co-monomers in the polymer industry. A range of cross-metathesis alkene sources, as well as different metathesis catalyst systems, were investigated.

Initially, the bi-functional $WCl_6/SnBu_4$ catalyst system was compared to Grubbs 1st and Hoveyda-Grubbs 2nd generation catalysts, using different cross-metathesis substrates (isoprene, hexane), temperatures, and reaction times with model fatty acid esters. None of the catalysts were active for the cross-metathesis with isoprene under any conditions, even when the reagent was distilled prior to the reaction. This was most likely due to the isoprene itself deactivating the catalytic metal centres. Only HGII was found to possess a suitable activity for the cross-metathesis of microbial oils. Upon optimising the reaction conditions the cross-metathesis reactions of glyceryl trioleate with ethene, 57% terminal bond selectivity was reached with model compounds while 41% terminal bond selectivity was reached with unrefined triglyceride sources. The suitable reaction conditions were determined to be 10 bar ethene, 60 °C and 1 hour, under inert conditions.

Lipids from first generation (rapeseed, sunflower), second generation (SCG oil) and third generation (algae and yeast) feedstocks were tested for their suitability as a feedstock for the process. The oils screened contained a wide range of fatty acids, differing largely in saturation. Lipids from rapeseed, sunflower, *P. ellipsoidea* and *R. glutinis* all achieved similar terminal bond selectivity as the model glyceride components (35-40%), though *M. pulcherrima* and *S. obliquus* performed worse due to their higher saturation or impurity. Upon GC-MS analysis, the conversion for 1-decene production was considerably low (<1%) for *S. obliquus* and *M.*

pulcherimma, and therefore their distillates could not be isolated to a significant enough amount to determine their fuel properties.

The metathesis products of rapeseed, sunflower, coffee, *P. ellipsoidea* and *R. glutinis* were subjected to distillation, separating the AFF and metathesis residue, which was then transesterified to give the RTF. The viscosity of the RTF produced was found to be within the limits for the US biodiesel, though there was significant range between the different RTFs that all but one fell within the stricter viscosity limits set out in European standards. This range is presumably due to the different levels of saturates in the RTF products. The viscosity of the AAF-jet-A1 blends and AAF model, however, fall well within the maximum value for Jet-A1. Interestingly, it was found that the metathesis of the oil reduced the energy density of the mixture significantly due to the loss of short chain alkenes which are lost from the reaction mixture during work-up. Upon distillation and removal of the hydrocarbons produced it was reduced even further. Tranesterifying this residue to produce the RTF increased the energy density slightly, with the RTF energy densities ranging between 33.8-36.8 MJ kg^{-1}. Though significantly lower than conventional diesel and biodiesel, improved physical properties such as stability and low temperature performance increase the viability of uptake. The AAF-Jet-A1 blends and AAF model mixture, however, showed higher energy density than that of Jet A-1, assumed to be due to a decrease in aromatics and therefore an increase in C-H bonds available for combustion. The pour points of the RTF produced were comparable to those of conventional biodiesel.

Therefore, it has been shown that the metathesis of biologically sourced lipids with ethene has good potential to produce multiple fuels from one feedstock, with the expense being somewhat mitigated by the production of higher-value products. The usage of a lipid feedstock leaves behind a significant amount of biomass, which could undergo fermentation. Ethanol, the most significant fuel produced via fermentation, exhibits a number of undesirable physical properties. Therefore, alternative products from fermentation should be assessed for their viability as a fuel.

3.5 REFERENCES

1. Mol, J. C.; Buffon, R., Metathesis in Oleochemistry. *J. Braz. Chem. Soc.* **1998,** *9*, 1-11.
2. Christensen, C. H.; Rass-Hansen, J.; Marsden, C. C.; Taarning, E.; Egeblad, K., The Renewable Chemicals Industry. *ChemSusChem* **2008,** *1* (4), 283-289.
3. Van Uytvanck, P. P.; Hallmark, B.; Haire, G.; Marshall, P. J.; Dennis, J. S., Impact of Biomass on Industry: Using Ethylene Derived from Bioethanol within the Polyester Value Chain. *ACS Sustainable Chemistry and Engineering.* **2014,** *2* (5), 1098-1105.
4. Jean-Louis Hérisson, P.; Chauvin, Y., Catalyse de transformation des oléfines par les complexes du tungstène. II. Télomérisation des oléfines cycliques en présence d'oléfines acycliques. *Die Makromolekulare Chemie* **1971,** *141* (1), 161-176.
5. Chikkali, S.; Mecking, S., Refining of Plant Oils to Chemicals by Olefin Metathesis. *Angew. Chem.-Int. Edit.* **2012,** *51* (24), 5802-5808.
6. Marvey, B. B., Sunflower-based feedstocks in nonfood applications: Perspectives from olefin metathesis. *International Journal of Molecular Sciences* **2008,** *9* (8), 1393-1406.
7. Holser, R.; Doll, K.; Erhan, S., Metathesis of methyl soyate with ruthenium catalysts. *Fuel* **2006,** *85* (3), 393-395.
8. Scifinder, and references found therein.
9. British Ministry of Defence, DEF STAN 91-91 Turbine Fuel, Kerosine Type, Jet A-1. MOD: Glasgow, 2011.
10. Kotov, S. V.; Kankaeva, I. N., Commercial production and principal trends in the use of 1-butene. *Chemistry and Technology of Fuels and Oils* **1994,** *30* (5-6), 240-245.
11. Marega, C.; Spataro, S.; Fassone, E.; Camurati, I.; Marigo, A., Self-welding 1-butene/ethylene copolymers from metallocene catalysts: Structure, morphology, and mechanical properties. *Journal of Applied Polymer Science* **2014,** *131* (8)..
12. Natta, G.; Corradini, P.; Bassi, I., Crystal structure of isotactic poly-alpha-butene. *Il Nuovo Cimento (1955-1965)* **1960,** *15*, 52-67.
13. Behr, A.; Neubert, P., Piperylene—A Versatile Basic Chemical in Catalysis. *ChemCatChem* **2014,** *6* (2), 412-428.
14. Sharkey, T. D.; Monson, R. K., The future of isoprene emission from leaves, canopies and landscapes. *Plant, Cell & Environment* **2014,** *37* (8), 1727-1740.
15. Thomas, R. M.; Keitz, B. K.; Champagne, T. M.; Grubbs, R. H., Highly Selective Ruthenium Metathesis Catalysts for Ethenolysis. *Journal of the American Chemical Society* **2011,** *133* (19), 7490-7496.
16. Nordin, N. A. M.; Yamin, B. M.; Yarmo, M. A.; Pardan, K.; Alimuniar, A. B., Metathesis of palm oil. *Journal of Molecular Catalysis* **1991,** *65* (1-2), 163-172.
17. Ahmad, F.; Hamdan, S.; Yarmo, M.; Alimunir, A., Co-metathesis reaction of crude palm oil and ethene. *Journal of the American Oil Chemists' Society* **1995,** *72* (6), 757-758.
18. Ichikawa, K.; Fukuzumi, K., Metathesis of 1-alkene. *The Journal of Organic Chemistry* **1976,** *41* (15), 2633-2635.
19. Sargeant, L. A.; Chuck, C. J.; Donnelly, J.; Bannister, C. D.; Scott, R. J., Optimizing the lipid profile, to produce either a palm oil or biodiesel substitute, by manipulation of the culture conditions for *Rhodotorula glutinis*. *Biofuels* **2014,** *5* (1), 33-43.
20. Santamauro, F.; Whiffin, F. M.; Scott, R. J.; Chuck, C. J., Low-cost lipid production by an oleaginous yeast cultured in non-sterile conditions using model waste resources. *Biotechnology for biofuels* **2014,** *7* (1), 34.
21. Bligh, E. G.; Dyer, W. J., A rapid method of total lipid extraction and purification. *Canadian Journal of Biochemistry and Physiology* **1959,** *37* (8), 911-917.
22. Maynard, H. D.; Grubbs, R. H., Purification technique for the removal of ruthenium from olefin metathesis reaction products. *Tetrahedron Letters* **1999,** *40* (22), 4137-4140.
23. Knothe, G., Monitoring a progressing transesterification reaction by fiber-optic near infrared spectroscopy with correlation to 1H nuclear magnetic resonance spectroscopy. *Journal of the American Oil Chemists' Society* **2000,** *77* (5), 489-493.
24. Kalsi, P. S., *Spectroscopy of Organic Compounds*. New Age International (P) Limited: 2004.

25. Dragutan, V.; Demonceau, A.; Dragutan, I.; Finkelshtein, E. S., *Green Metathesis Chemistry: Great Challenges in Synthesis, Catalysis and Nanotechnology*. Springer: 2009.
26. İmamoğlu, Y., *Metathesis Polymerization of Olefins and Polymerization of Alkynes*. Kluwer Academic: 1998.
27. Trnka, T. M.; Morgan, J. P.; Sanford, M. S.; Wilhelm, T. E.; Scholl, M.; Choi, T.-L.; Ding, S.; Day, M. W.; Grubbs, R. H., Synthesis and Activity of Ruthenium Alkylidene Complexes Coordinated with Phosphine and N-Heterocyclic Carbene Ligands. *Journal of the American Chemical Society* **2003,** *125* (9), 2546-2558.
28. Dinger, M. B.; Mol, J. C., Degradation of the First-Generation Grubbs Metathesis Catalyst with Primary Alcohols, Water, and Oxygen. Formation and Catalytic Activity of Ruthenium(II) Monocarbonyl Species. *Organometallics* **2003,** *22* (5), 1089-1095.
29. Ulman, M.; Grubbs, R. H., Ruthenium Carbene-Based Olefin Metathesis Initiators: Catalyst Decomposition and Longevity. *The Journal of Organic Chemistry* **1999,** *64* (19), 7202-7207.
30. Dinger, M. B.; Mol, J. C., High Turnover Numbers with Ruthenium-Based Metathesis Catalysts. *Advanced Synthesis & Catalysis* **2002,** *344* (6-7), 671-677.
31. van der Klis, F.; Le Notre, J.; Blaauw, R.; van Haveren, J.; van Es, D. S., Renewable linear alpha olefins by selective ethenolysis of decarboxylated unsaturated fatty acids. *Europeane Journal of Lipid Science and Technology* **2012,** *114* (8), 911-918.
32. Patel, J.; Mujcinovic, S.; Jackson, W.R.; Robinson, A.J.; Serelisb, A.K., Such, C., High conversion and productive catalyst turnovers in cross-metathesis reactions of natural oils with 2-butene. *Green Chemistry* **2006**, 8, 450-454.
33. Schwab, P.; Grubbs, R. H.; Ziller, J. W., Synthesis and Applications of $RuCl_2(CHR')(PR_3)_2$: The Influence of the Alkylidene Moiety on Metathesis Activity. *Journal of the American Chemical Society* **1996,** *118* (1), 100-110.,
34. Zlatanić, A.; Petrović, Z. S.; Dušek, K., Structure and Properties of Triolein-Based Polyurethane Networks. *Biomacromolecules* **2002,** *3* (5), 1048-1056.
35. Lehman Jr, S. E.; Schwendeman, J. E.; O'Donnell, P. M.; Wagener, K. B., Olefin isomerization promoted by olefin metathesis catalysts. *Inorganica Chimica Acta* **2003,** *345* (0), 190-198.
36. Knothe, G., Dependence of biodiesel fuel properties on the structure of fatty acid alkyl esters. *Fuel Processing Technology* **2005,** *86* (10), 1059-1070.
37. Adachi, K.; Matsuda, S.; Sato, A.; Sekiguchi, H.; Kurano, N.; Atsumi, M. (2009), *Novel microalgae and process for producing hydrocarbon*. US Patent: US 20090115140A1.
38. Mandal, S.; Mallick, N., Waste utilization and biodiesel production by the green microalga Scenedesmus obliquus. *Applied and Environmental Microbiology* **2011,** *77* (1), 374-377.
39. Ageitos, J. M.; Vallejo, J. A.; Veiga-Crespo, P.; Villa, T. G., Oily yeasts as oleaginous cell factories. *Applied Microbiology and Biotechnology* **2011,** *90* (4), 1219-1227.
40. Saxena, V.; Sharma, C. D.; Bhagat, S. D.; Saini, V. S.; Adhikari, D. K., Lipid and fatty acid biosynthesis by *Rhodotorula minuta*. *Journal of the American Oil Chemists' Society* **1998,** *75* (4), 501-505.
41. Chuck, C.; Santomauro, F.; Scott, R. (2014), *Method of increasing lipid accummulation in Metschnikowia pulcherrima cells*. World patent: WO 2014122539A1.
42. Chuck, C. J.; Jenkins, R. W.; Bannister, C. D.; Lowe, J. P., Design and preliminary results of an NMR tube reactor to study the oxidative degradation of Fatty Acid Methyl Ester. *Biomass and Bioenergy* **2012,** *47*, 188-194.
43. Satoh, A.; Kato, M.; Yamato, K.; Ishibashi, M.; Sekiguchi, H.; Kurano, N.; Miyachi, S., Characterization of the lipid accumulation in a new microalgal species, Pseudochoricystis ellipsoidea (Trebouxiophyceae). *日本エネルギー学会誌* **2010,** *89* (9), 909-913.
44. Baliga, M. N.; Hilditch, T. P., The component acids of rape seed oil. *Journal of the Society of Chemical Industry* **1948,** *67* (6), 258-262.
45. Ramos, M. J.; Fernández, C. M.; Casas, A.; Rodríguez, L.; Pérez, Á., Influence of fatty acid composition of raw materials on biodiesel properties. *Bioresource Technology* **2009,** *100* (1), 261-268.
46. Schmidt, B., Catalysis at the Interface of Ruthenium Carbene and Ruthenium Hydride Chemistry: Organometallic Aspects and Applications to Organic Synthesis. *European Journal of Organic Chemistry* **2004,** *2004* (9), 1865-1880.
47. Thurier, C.; Fischmeister, C.; Bruneau, C.; Olivier-Bourbigou, H.; Dixneuf, P. H., Ethenolysis of Methyl Oleate in Room-Temperature Ionic Liquids. *ChemSusChem* **2008,** *1* (1-2), 118-122.

48. Mandelli, D.; Jannini, M. D. M.; Buffon, R.; Schuchardt, U., Ethenolysis of esters of vegetable oils: Effect of B_2O_3 addition to $Re_2O_7/SiO_2.Al_2O_3$-$SnBu_4$ and $CH_3ReO_3/SiO_2.Al_2O_3$ metathesis catalysts. *Journal of the American Oil Chemists Society* **1996,** *73* (2), 229-232.
49. Yadav, G. D.; Doshi, N. S., Development of a green process for poly-α-olefin based lubricants. *Green Chemistry* **2002,** *4* (6), 528-540.
50. Hong, S. H.; Sanders, D. P.; Lee, C. W.; Grubbs, R. H., Prevention of Undesirable Isomerization during Olefin Metathesis. *Journal of the American Chemical Society* **2005,** *127* (49), 17160-17161.
51. Pederson, R. L.; Fellows, I. M.; Ung, T. A.; Ishihara, H.; Hajela, S. P., Applications of Olefin Cross Metathesis to Commercial Products. *Advanced Synthesis & Catalysis* **2002,** *344* (6-7), 728-735.
52. Clayden, J.; Greeves, N.; Warren, S., *Organic Chemistry*. OUP Oxford: 2012.
53. Park, C. P.; Van Wingerden, M. M.; Han, S.-Y.; Kim, D.-P.; Grubbs, R. H., Low Pressure Ethenolysis of Renewable Methyl Oleate in a Microchemical System. *Organic Letters* **2011,** *13* (9), 2398-2401.
54. Demirbas, A., Relationships derived from physical properties of vegetable oil and biodiesel fuels. *Fuel* **2008,** *87* (8–9), 1743-1748.
55. EN 14214:2008, Automotive fuels - Fatty acid methyl esters (FAME) for diesel engines - Requirements and test methods.
56. ASTM D6751:2008, Standard Specification for Biodiesel Fuel Blend Stock (B100) for Middle Distillate Fuels. ASTM International: 2008.
57. Fulmer, G. R.; Miller, A. J. M.; Sherden, N. H.; Gottlieb, H. E.; Nudelman, A.; Stoltz, B. M.; Bercaw, J. E.; Goldberg, K. I., NMR Chemical Shifts of Trace Impurities: Common Laboratory Solvents, Organics, and Gases in Deuterated Solvents Relevant to the Organometallic Chemist. *Organometallics* **2010,** *29* (9), 2176-2179.
58. Spellman, J. *Screening the Oxidative Stability of Novel Fuel Blends Under Accelerated conditions (M.Eng research project)*; University of Bath: 2014.

CHAPTER 4

THE IDENTIFICATION AND ENGINE TESTING OF POTENTIAL RENEWABLE OXYGENATED BIOFUELS FROM FERMENTATION

In Chapter 3, microbial lipids were converted into fuels via metathesis. However, the usage of lipids leaves behind a significant amount of biomass, which could be converted to useful fuel products. An alternative method for fuel production from biomass is biological transformation using fermentation. Fermentation products have the advantage that they are unimolecular and so would possess predictable fuel properties. There are a number of inherent issues associated with further ethanol utilisation, and therefore in this chapter a range of short-chain mono-, di- and tri- esters were assessed for their suitability as replacements to traditional fossil fuels. This was achieved by comparing their key molecular, physical and fuel properties. The fermentation product deemed most feasible as a diesel replacement, diethyl succinate, was then tested on a chassis dynamometer. The emissions and performance of these fuels were compared to their fossil fuels counterparts.

This identification of fermentation products was published in the Elsevier journal *Fuel*,[1] while the engine testing portion of the study, discussed later in the Chapter, has been submitted to the ACS journal *Environmental Science & Technology*, and is currently under review.[2]

4.1 INTRODUCTION

Fermentation allows the production of specific, unimolecular compounds to be produced from heterogeneous biomass sources. Ethanol fermentation by yeast is the largest industrial fermentation process for fuel production.[3] However, the low combustion energy and high purification cost inhibit its further use. The use of ethanol in current SI engines, with no modification can also lead to increased corrosion and engine damage from the stiffening and swelling of non-metallic seals.[4] A potential alternative is butanol, produced primarily from the ABE process, which, due to its lower oxygen content, has a higher combustion energy and lower corrosiveness.[5] However, there are considerable issues associated with its production, including the higher amount of energy and sugar feedstock required for production and the acute toxicity of butanol to the microbes that produce it. This increases the cost of its production beyond what is viable as a transport fuel at present. To reduce this cost, research in this area is focussed on genetic engineering to increase microbial resistance and selectivity for butanol in fermentation broths.[6] Genetic engineering has also been considered as a method to produce new fuel molecules by alteration of microbial metabolic flux, including higher alcohols, terpenoids and alkanes.[3, 7] Despite these developments, the scale-up of these processes to industrial levels is challenging due to poor microbial activity in large bioreactors and the inherently low cost of the biofuels produced.[8]

A range of different oxygenated species have the potential produced on a large scale that are already produced by microbes which can be produced, or have the potential to be produced, from fermentation (Table 4.1). These are largely organic acids, and as such could not be used as fuels themselves as they are corrosive and most are solid at ambient conditions. However, the esters, produced in the fermentation or esterified with an alcohol prior to use have potential.

Table 4.1 Some possible fermentation products from cellulosic biomass

Product	**Structure**	**Example organism**
Acetic acid	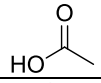	*Acetobacter aceti*[9]
Propionic acid	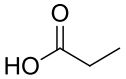	*Propionibacterium freudenreichii*[10]
Butyric acid	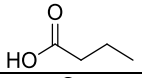	*Clostridium tyrobutyricum*[11]
L-Lactic acid	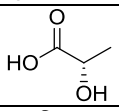	*Rhizopus oryzae*[12]
Oxalic acid	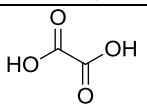	*Aspergillus niger*[13]
Malonic acid	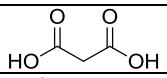	*Cerrena unicolor*[14]
Succinic acid	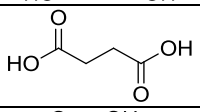	*Actinobacillus succinogenes*[15]
Malic acid	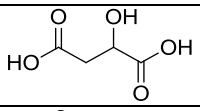	*Aspergillus flavus*[16]
Itaconic acid	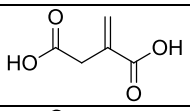	*Aspergillus terreus*[17]
Fumaric acid	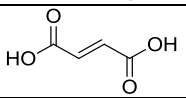	*Rhizopus arrhizus*[18]
Citric acid	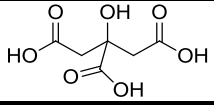	*Aspergillus niger*[19]

While fatty acid alkyl esters (biodiesel) have been heavily researched as alternative fuels, short chain esters can also possess desirable physical properties. Levulinic acid, for example, has been identified by the US Department of Energy as one of the top 12 value added bio-based chemicals,[20] can be produced from the acid-catalysed dehydration and hydrolysis of C_6 sugars from lignocellulosic biomass resources.[21] Production of levulinate esters has been carried out using the pure levulinic acid and appropriate alcohol using heterogeneous catalytic systems,[22-24] though Hishikawa, *et al.*, have shown that the direct preparation of butyl levulinate from a single solvolysis process of cellulose is possible, reaching up 60% yield of butyl levulinate in 5 hours at 130 °C in the presence of sulfuric acid catalyst.[25] The upgrading of levulinic acid to resins, polymers, pharmaceutical agents, chemical

intermediates and alternative species has been reported.[26] While the chemical conversion of levulinic acid to liquid hydrocarbons has been investigated,[27] potentially the most promising route to a fuel is by using the alkyl esters of the acid.

Christensen, *et al.*, tested the effects of methyl, ethyl and butyl levulinate esters (amongst other oxygenates), for their blending effects with gasoline (at 10 vol%).[28] Methyl and butyl levulinate were deemed unsuitable as a gasoline blending additive, as methyl levulinate separates from gasoline below 0 °C, and butyl levulinate significantly raised distillation temperatures beyond the ASTM US standard for gasoline. Ethyl levulinate, however, was acceptable in all properties assessed, and therefore has potential as a gasoline additive. Christensen *et al.* also tested the properties of levulinate esters (ethyl and butyl) blends with diesel.[29] Ethyl levulinate was found to have a lower potential as a diesel additive, due to the higher cloud point of the blend and the separation of the fuels at relatively high temperatures. Butyl levulinate, however, had little effect on the cloud point up to a blend level of 20 vol%.

Levulinic acid can also be further processed into other ester fuels, such as γ-valerolactone (via dehydration and reduction steps[30-31]) and valeric acid (via the hydrogenation of γ-valerolactone[32]). Valeric acid can then be esterified to suitable fuel molecules. Lange, *et al.* produced valeric acid esters from cellulose, and evaluated them for their fuel compatibility by assessing the polarity, energy content, boiling point, octane number (for petrol) and cetane number (for diesel), oxidative stability, fouling tendency, corrosion, lubricity, water affinity and response to conventional fuel additives.[32] All the valeric acid esters tested (methyl, ethyl, propyl, and pentyl) possessed more acceptable energy densities and polarities than alternative potential biofuels such as ethanol, *n*-butanol, ethyl levulinate, γ-valerolactone and methyl-tetrahydrofuran, and were found to have good potential as fuel replacements.

While the physical properties of a fuel are indicative of the behaviour in the environment, to determine the true environmental impact evaluation of

performance via engine testing is vital. The complete combustion of any hydrocarbon (or oxygenated hydrocarbon) fuel leads to the formation of carbon dioxide and water. However, complete combustion is rarely achieved, and so products of incomplete combustion are observed in the exhaust emissions of an internal combustion engine. These include carbon monoxide (CO), total hydrocarbons (THC), and particulate matter (PM). The high temperatures of combustion also lead to reaction with nitrogen, producing mono-nitrogen oxide species (NO_x). In Europe, these emissions are controlled and regulated by the European Emissions standards. The maximum allowed emissions for a passenger car or light commercial vehicle is shown in Table 4.2.[33]

Table 4.2 The current emissions limits for spark and compression ignition engines from the European emissions standard "Euro 6".[33] M = passenger car, N_I = light commercial vehicles (I = less than 1350 kg, II = 1350 – 1750 kg, III = more than 1750 kg)

	Class		CO / mg km^{-1}	THC / mg km^{-1}	NO_x / mg km^{-1}	Combined THC and NO_x / mg km^{-1}	PM / mg km^{-1}
Diesel	**M**		500	-	80	170	5
	N_I	**I**	500	-	80	170	5
		II	630	-	105	195	5
		III	740	-	125	215	5
Petrol	**M**		1000	100	60	-	5
	N_I	**I**	1000	100	60	-	5
		II	1810	130	75	-	5
		III	2270	160	82	-	5

The majority of biofuels have a very different molecular structure to their hydrocarbon counterparts – specifically the presence of oxygen – which leads to altered fuel performance and emissions. In spark ignition engines, it is generally believed that ethanol reduces CO, THC and NO_x emissions for equivalent engine speeds when compared to gasoline.[34-35] The decrease in NO_x is potentially due to the high latent heat of vaporisation of ethanol, which lowers the flame temperature, reducing the amount of NO_x produced from atmospheric nitrogen as it requires considerable energy to reach the activation energy of NO_x formation. With biodiesel, most studies have shown reduced levels of CO, THC and PM emissions due to a more complete, cleaner combustion, though NO_x emissions are

generally increased when compared to mineral diesel.[36] While these effects increase with higher blend ratios,[37] the emissions profile is also highly dependent on the FAME profile of the biodiesel.[38]

Ethyl esters of three acids potentially obtainable from fermentation (acetic, propionic and butyric) have been tested on a homogeneous charge compression ignition (HCCI) engine.[39] Ethyl butyrate was found to increase ignition delay whereas ethyl acetate decreases it. Ethyl propionate demonstrated very similar ignition properties to reference gasoline fuel. In an engine testing study of levulinate esters, ethyl levulinate was found not to significantly alter the PM, CO, THC and NO_x emissions when used in a 10% volumetric blend with diesel (EL10) when compared to the pure diesel.[29] On using a 20% volumetric blend of butyl levulinate with diesel (BL20) it was found that while the PM, CO and THC emissions do not alter significantly, NO_x did increase by 4.5%. Due to the oxygen content of the fuels, and therefore the reduced energy densities, EL10 and BL10 led to an increased brake-specific fuel consumption of 5.1% and 7.6% respectively. In two separate studies by Contino, *et al.*, the engine testing for a 20 vol% blend of two separate gasoline-suitable valeric esters (methyl and ethyl) was carried out on an SI engine,[40] while a 20 vol% diesel-suitable valeric esters (butyl and pentyl) were tested on a CI engine.[41] For the gasoline-suitable valeric esters, the difference between the oxygenated fuels and the gasoline used were largely within error, however an increase in CO_2 and a small decrease in NO_x was observed. The 20 vol% butyl and pentyl valerate blends with diesel have lower cetane numbers, and therefore a longer ignition delay, however when tested on a CI engine, the emissions and performance did not change significantly. Most notably there was very little change in NO_x at a range of loads, explained by the competing effects of the lower adiabatic flame temperature (associated with NO_x decrease), and the lower cetane number which increases pressure and temperature, and the increases oxygen availability (associated with NO_x increase).

In this study, a range of products were synthesised through the esterification of acids and alcohols obtainable from fermentation. These were then compared to

current fossil and biofuels, by assessing their physical properties. The most promising fuel in terms of their physical properties and economic viability was then tested on-engine to determine its effect on performance and emissions.

4.2 EXPERIMENTAL

4.2.1 MATERIALS

All solvents were of reagent quality and purchased commercially and were used without purification except when dried (as indicated) by passing through anhydrous alumina columns using an Innovative Technology Inc. PS-400-7 solvent purification system. Deuterated solvents ($CDCl_3$, D_2O) for ^1H NMR spectroscopy were purchased from Fluorochem.

For the identification of the potential fermentation product fuels acetic acid, propionic acid, butyric acid, oxalic acid, malonic acid, succinic acid, malic acid, itaconic acid, fumaric acid, citric acid, ethanol, *n*-butanol, ethyl acetate, ethyl butyrate, butyl butyrate, ethyl levulinate, butyl levulinate, butyl lactate, butyl butyl lactate and sulfuric acid were purchased from Sigma–Aldrich, UK and were used without further purification. Aviation Jet A-1 kerosene, mineral diesel and petrol were provided from standard fuel suppliers.

For the engine testing of the potential fermentation product fuels, EN 590-compliant winter-grade ultra-low sulfur diesel (ULSD) supplied by the Ford motor company. Dimethyl succinate, ethanol and sulfuric acid were all purchased from Sigma Aldrich, UK and used without further purification.

4.2.2 METHODS

4.2.2.1 GENERAL ANALYTICAL METHODS

NMR spectra were recorded on Bruker Avance 250 or Bruker Avance 300 spectrometers. GC-MS analysis was carried out using the same equipment and method as is outlined in Chapter 2, section 2.2.2.4.

4.2.2.2 Fermentation Products

Esterification

Diethyl fumarate, diethyl malate, diethyl malonate, diethyl succinate, diethyl oxalate, ethyl propionate and triethyl citrate were synthesised according to the following method. A round bottom flask was charged with the appropriate organic acid (0.3 mol), ethanol (138 g, 175 ml, 3 mol) and 3 wt% (with respect to the starting organic acid) of H_2SO_4 as a catalyst. The reaction mixtures were stirred under reflux for 24 h. On reaction completion, the mixtures were washed with distilled water (4 × 50 ml) to remove the sulfuric acid as well as any unreacted acid and ethanol. The resulting fuel was purified by removing any excess alcohol or water under reduced pressure. The product was established by ^{1}H NMR spectroscopy to be >99% pure. Butyl acetate, butyl propionate, dibutyl fumarate, dibutyl itaconate, dibutyl malate, dibutyl malonate, dibutyl succinate dibutyl oxalate and tributyl citrate were synthesised in an identical manner, with the substitution of *n*-butanol (222.2 g, 274 ml, 3 mol) instead of ethanol.

To test their cetane number and tribology properties, dibutyl fumarate, dibutyl malonate, and dibutyl succinate were synthesised on a ~1 l scale via a simple esterification reaction. A 2 l round bottom flask was charged with the appropriate organic acid (5.85 mol), *n*-butanol (962 g, 1190 ml, 13 mol), and approximately 3 wt% (with respect to the organic acid) of H_2SO_4. The reaction mixtures were left heating under reflux overnight. The mixtures were washed with distilled water (4 × 250 ml) to remove the sulfuric acid as well as any unreacted acid. The resulting fuel was purified by removing any excess alcohol or water under reduced pressure. The product purity (>99%) was establish by ^{1}H NMR spectroscopy. Diethyl succinate was synthesised in an identical manner, except for the addition of ethanol (598 g, 758 ml, 13 mol) instead of *n*-butanol.

Kinematic Viscosity

The kinematic viscosities of all promising esterified fuel products were measured with calibrated Canon-Fenske Routine Viscometers No. 75 and 150, in accordance

with standard test methods set out in ASTM D445 and ISO 3104 at 40 °C or -20 °C where appropriate.

Blending Studies

The esterified fuel products were mixed in a 50:50 blend with the relevant hydrocarbon fuel to determine miscibility. Those found not to be miscible with current fuels were added drop wise until the mixture became translucent to determine their solubility in the relevant hydrocarbon fuel. On establishing that the fuels were miscible the fuel mixtures were held in a cold bath and the temperature reduced by 5 °C and held for 10 min until the cloud point of the relevant hydrocarbon fuel was reached.

Energy Content

The energy content of promising fuels products (specifically diethyl succinate, dibutyl succinate, dibutyl malonate, dibutyl oxalate, dibutyl fumarate, butyl lactate, butyl butyrate and butyl butyryllactate) were measured using a Parr 1341 Plain Oxygen Bomb Calorimeter, in accordance with testing method ASTM D240.

Oxidation Studies

A 10 ml round bottom flask was charged with 5 ml of the fuel. These were dibutyl succinate, diethyl succinate, dibutyl itaconate, dibutyl fumarate and rapeseed methyl ester. The flask was placed in an oil bath at the required temperature (110 °C) and the compounds were mechanically stirred at a constant rate, subjected to constant light intensity and constant airflow for 24 h. The resulting mixture was analysed by ^{1}H NMR spectroscopy and GC–MS.

Cetane Number, Octane Number and Lubricity

Cetane number (CN) analysis and tribology studies were conducted by Saybolt, United Kingdom Ltd. The cetane number was ascertained using a Co-operative Fuel Research (CFR) engine in accordance with the testing standard ISO 5165. The lubricity was ascertained by using a High Frequency Reciprocating Rig (HFRR) and

measuring the corrected wear scar diameter at 60 °C, in accordance to the test method ISO 12156-1. The research octane number (RON) of butyl butyrate was conducted by Intertek testing, UK on a RON engine in accordance with the testing standard EN ISO 5164.

4.2.2.3 Engine Testing

Diethyl Succinate Production

To provide the 5 litres of diethyl succinate needed for the engine testing, the following reaction was repeated four times. Dimethyl succinate (955 ml, 1095 g, 7.5 mol) and ethanol (1750 ml, 1380 g, 30 mol) were added together in a large glass reactor with 3 wt% H2SO4 (30 ml, 55.2 g, 0.56 mol) and heated to reflux overnight. This mixture was then split into 3 equal amounts, each washed thoroughly with water (4 × 250 ml) to remove unreacted alcohol and acid. Any remaining water was then removed under reduced pressure. The product was established by ^{1}H NMR spectroscopy to be >99% pure.

Pure diethyl succinate was then blended with petrodiesel in a 20% blend (DES20), along with a small amount of cetane improver in accordance with Christensen, *et al*. The fuel properties of DES20 and diesel were assessed using the following methods. Densities were determined via the blending of fuels to the desired composition in a quantity of no less than 40.0 cm^3 ± 0.1 and weighing to an accuracy of ±0.00005 g. The kinematic viscosities were measured with calibrated Canon-Fenske Routine Viscometers No. 75 and 150, in accordance with standard test methods set out in ASTM D445 and ISO 3104 at 40 °C. Flash points of each sample were determined in accordance with ASTM D56/IP 170 using a Stanhope-Seta 99880-0 Flashcheck, tag, closed cup flash point machine. Energy content of fuels was determined in accordance with ASTM D3338 using of a Parr 1341 plain jacket adiabatic bomb calorimeter using a Parr 1108 oxygen combustion bomb. Approximately 0.3 g of each sample (weighed accurately to 4 significant figures) was placed in the crucible within the bomb and the bomb then filled with oxygen to a pressure of approximately 25 bar. The temperature change of the water within

the stirred calorimeter was determined to an accuracy of ±0.0005 °C. The cetane number analysis was carried out by Intertek Commodities, using a Co-operative Fuel Research (CFR) engine in accordance with the testing standard ISO 5165.

Engine Testing Methodology

The chassis dynamometer facility used in this study consists of a Zollner 48in roller with two independent 126 kW d.c. machines housed within a climatically controlled environment with a temperature range from -10-50 °C. The facility was equipped with two Horiba MEXA 7000 emissions analysers for pre-catalyst and post-catalyst continuous sampling and 'bag' emissions via a constant-volume sampling (CVS) system. The vehicle used in this study utilised a 2.0 l turbocharged EURO 3-compliant light commercial vehicle equipped with a direct-injection common-rail fuel injection system (Table 4.3).

Table 4.3 Vehicle description

Factor	**Description**
Manufacturer	Ford Motor Company
Type	Transit van 125 T260
Mean vehicle inertia	2025 kg
Engine	DuraTorq TDCi – 125PS
Fuel injection equipment	Delphi common rail (production)
Transmission	Front-wheel drive, five-speed, manual
ECU	DPC-801 (development ECU)
Emissions level	EURO 3 (category N1 – III)
Registered	2002
Catalyst	DOC (close coupled)
Diesel particulate filter	None

Pseudo steady-state testing was carried out, whereby the vehicle speed was held constant by the dynamometer and the pedal demand ramped up over a 5 minute period, using a specifically designed manual rig. The vehicle speed was kept constant by the dynamometer controller gradually increasing torque from the chassis dynamometer. The engine speeds investigated were 1200, 1500, 2000, 2500, 3000, 3500 and 4000 rpm. The two fuels used were diesel and a 20% (by volume) blend of diethyl succinate with diesel (DES20), with small amount of cetane improver (2-ethylhexyl nitrate, 1600 ppm), in accordance with Christensen, *et al.*[29]

4.3 RESULTS AND DISCUSSION

4.3.1 POTENTIAL OXYGENATED FERMENTATION FUELS

A number of oxygenated acids potentially obtainable from the fermentation of biomass were esterified with ethanol or *n*-butanol. The resulting esters were assessed for their potential as fuel replacements by comparison with fossil fuels and conventional biofuels. The esters fell into two main groups: mono-esters, the ethyl and butyl esters of acetic, propionic, butyric and lactic acid; and di-esters, the ethyl and butyl esters of oxalic, malonic, succinic, malic, itaconic and fumaric acid. Also included in the study are the esters of levulinic acid, a product of acid hydrolysis of cellulose and a possible diesel replacement;[29] and citric acid, which is a tri-carboxylic acid currently produced via fermentation on a million tonne+ scale per year.[42]

4.3.1.1 PHYSICAL PROPERTIES OF THE PURE COMPOUNDS

Ideally potential fuel replacements would have similar physical properties to the current fuels to allow use of the existing infrastructure, which are defined in the current legal specifications (Appendix A). Common molecular and physical properties, such as melting and boiling temperature, flash point and density were obtained from the scientific database Scifinder. Using these properties an initial screening was performed to determine which esters were suitable for further investigation. The properties for all compounds considered are shown in Tables 4.4 and 4.5.

Flash point is a measure of the lowest temperature at which liquid vapours form an ignitable mixture with air. For SI engines, this is required to be relatively low. For all the esters considered, the flash points were at least 40 °C above that of gasoline (approx. -43 °C) and are therefore unsuitable as gasoline replacements. The flash points for butyl acetate, ethyl propionate, butyl propionate and ethyl butyrate were below the minimum allowed flash points for diesel (55 °C) and aviation kerosene (38 °C). Butyl butyrate possessed a flash point of 49 °C, above the allowed minimum

for kerosene but below that of diesel, all other esters exhibit flash points higher than the minimum required for diesel. This is unsurprising due to the presence of oxygen, associated with an increase in local polarity and therefore an increase in intermolecular forces.

Table 4.4 Physical properties of mono-ester fermentation products possibly derived from cellulosic biomass, and levulinate esters.[43]

Compound	Flash point / °C	Melting temperature / °C	Boiling temperature / °C	Density at 15°C / g cm^{-3}
Ethyl acetate	-3.3	-84	77	0.91
Butyl acetate	22	-78	126	0.87
Ethyl propionate	12	-73	95	0.89
Butyl propionate	38	-90	146	0.88
Ethyl butyrate	19	-98	122	0.87
Butyl butyrate	49	-91	165	0.87
Ethyl levulinate	78	<-60	206	1.01
Butyl levulinate	98	<-60	238	0.97
Ethyl lactate	55	-26	154	1.03
Butyl lactate	69	-28	170	0.98

Table 4.5 Physical properties of di-ester fermentation products possibly derived from cellulosic biomass, and citrate esters.[43]

Compound	Flash point / °C	Melting temperature / °C	Boiling temperature / °C	Density at 15°C / g cm^{-3}
Diethyl oxalate	76	-41	185	1.07
Dibutyl oxalate	108	-30	240	1.05
Diethyl malonate	100	-50	199	1.05
Dibutyl malonate	117	-83	252	1.00
Diethyl succinate	100	-21	218	1.04
Dibutyl succinate	123	-29	274	0.99
Diethyl malate	85	N/A	281	1.15
Dibutyl malate	121	N/A	344	1.06
Diethyl itaconate	108	58	228	1.04
Dibutyl itaconate	142	N/A	307	0.99
Diethyl fumarate	93	1	214	1.07
Dibutyl fumarate	136	-18	280	1.00
Triethyl citrate	96	-55	294	1.18
Tributyl citrate	121	-20	390	1.08

The melting point is affected by intermolecular forces, such as hydrogen bonding and dipole interactions. Therefore fuels without hydroxyl groups and longer alkyl chains possess lower melting temperatures. This metric is extremely important for aviation kerosene replacements, as they must have a maximum melting temperature of -47 °C; a safety feature ensuring that the fuel will still be

operational at altitude. Though a number of fuels tested had appropriate low temperature properties only butyl butyrate, ethyl and butyl levulinate, diethyl and dibutyl malonate and triethyl citrate had flash points that fall within the Jet A-1 standard also.

In terms of diesel replacement, the melting temperature can be compared to the cloud point of diesel i.e. the point at which components within the diesel start to precipitate. While no limit is given in the EN 590 standard, typical values range from -5 – -20 °C, depending on the additives, geographical location, season and source). Comparing the fuels with an appropriate flash point, ethyl and butyl levulinate, ethyl and butyl lactate, diethyl and dibutyl oxalate, diethyl and dibutyl malonate, diethyl and dibutyl succinate, triethyl and tributyl citrate all had melting points below this lower limit. Dibutyl fumarate, with a melting point of -18 °C, was low enough to justify further testing.

Boiling temperatures of the fermentation products with appropriate flash point and melting temperature fall largely within the ranges of their fossil fuel counterparts, apart from in the case of tributyl citrate which was considerably higher. The density ranges outlined in the international standards are ranges specifically for petroleum products to assure their quality. Therefore, though all the esters had a density outside of standard ranges, it was not considered a significant enough issue to deem the esters unsuitable as replacement fuels.

4.3.1.2 KINEMATIC VISCOSITY

The kinematic viscosity of a fuel is extremely important as the fuel must flow well and atomise sufficiently in the combustion chamber of an engine for optimal operation. Fuels of too low viscosity are also undesirable as they can leak from pumps and injectors, and cause abnormal amounts of wear in the engine. The kinematic viscosity range for diesel according to the European standard (EN 590) is 2.00-4.50 mm^2s^{-1} at 40 °C. The kinematic viscosities of the fermentation fuels (those still deemed suitable after comparison with fossil fuel physical properties) are shown in Figure 4.1.

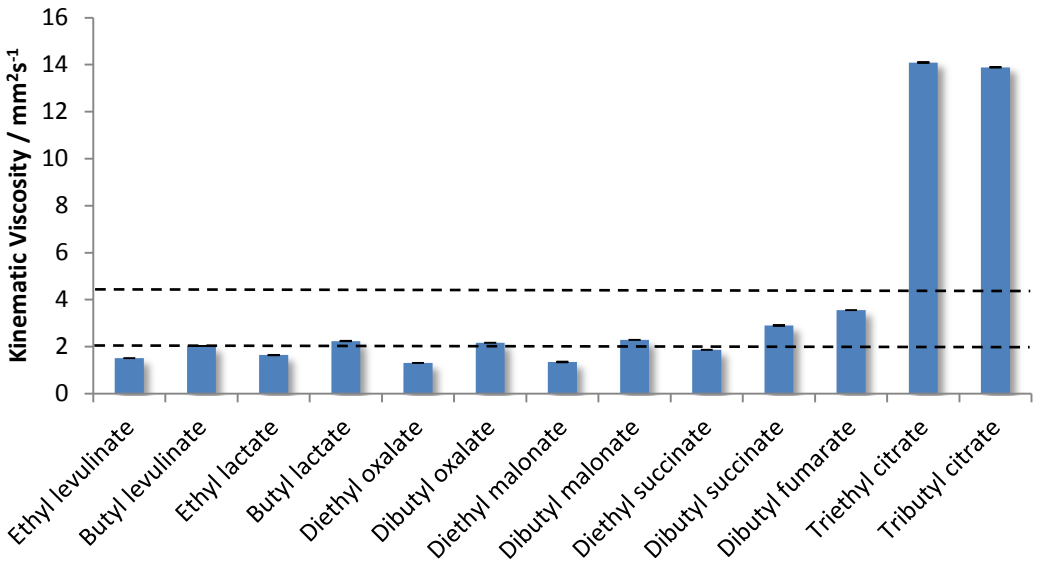

Figure 4.1 Kinematic viscosities (measured at 40 °C) of potential fuels from fermentation, with the range for diesel (2.00-4.50 mm^2s^{-1}), according to the EN 590 standard shown.

A number of fuels fell outside the range set in the EN 590 European standards. Ethyl levulinate, ethyl lactate, diethyl oxalate and diethyl malonate all have viscosities that were well below the minimum of 2 mm^2s^{-1}. Triethyl and tributyl citrate have viscosities much higher than the upper limit at 14.10 mm^2s^{-1} and 13.88 mm^2s^{-1}, respectively. This is most likely due to their increased hydrogen bonding of the hydroxyl group present. Butyl lactate, butyl levulinate, dibutyl oxalate, dibutyl malonate, dibutyl succinate, diethyl fumarate and dibutyl fumarate all fell within the standard range and so were investigated further. Diethyl succinate, with a viscosity of 1.86 mm^2s^{-1} was deemed close enough to the lower limit to justify further testing.

The maximum kinematic viscosity of aviation kerosene allowed in the Jet A-1 standard is 8.00 mm^2s^{-1} at -20 °C. The citrate esters were deemed unsuitable aviation fuel prior to this analysis, as their viscosities at 40 °C were higher than the allowed maximum at -20 °C (Figure 4.2). The viscosities of butyl levulinate and dibutyl malonate were found to be above the allowed maximum, and are therefore not suitable as aviation fuels without blending. Only ethyl levulinate, diethyl malonate, and butyl butyrate fell within the Jet A-1 specification.

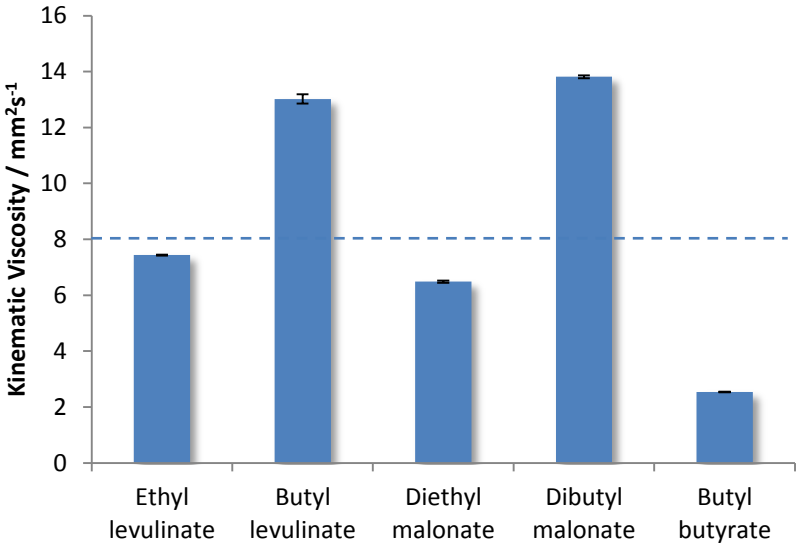

Figure 4.2 Kinematic viscosities (measured at -20 °C) of potential fuels from fermentation, with the maximum allowed value (8.00 mm^2s^{-1}) according to the Jet A-1 standard shown.

4.3.1.3 Blending Studies

Current biofuels are used in blends with their fossil fuel counterparts. Therefore any novel fuel developed must possess significant solubility with the fuel it is displacing, and ideally be miscible with the appropriate hydrocarbon. Their aqueous solubility is also an important factor, as high solubility in water can lead to high energy processes needed for their production, as well as solubilising water from the atmosphere which can lead to wet corrosion in engines. The mass solubility of the potential fuels in conventional fuels and water are shown in Table 4.6.

Table 4.6 Solubility of the potential fermentation fuel in the appropriate hydrocarbon fuel. - = Not applicable, M = miscible. Water solubility found in Scifinder, and references found within.[43]

Compound	Solubility at 25 °C		
	Diesel / g l^-	Kerosene / g l^-	Water (pH 7) / g l^-
Butyl butyrate	-	M	1.9
Ethyl levulinate	152	7.5	30
Butyl lactate	M	-	38
Dibutyl oxalate	M	-	0.93
Dibutyl malonate	M	M	0.91
Diethyl succinate	M	-	10
Dibutyl succinate	M	-	0.48
Dibutyl fumarate	M	-	0.43

At room temperature, all the fuels identified were completely miscible with the appropriate hydrocarbon fuel with the exception of ethyl levulinate. This may be due to the shorter alkyl chains, which decreases the lipophilicity of the molecule. Ethyl levulinate would only be able to be used in blends of 15% or below and was therefore dismissed as a potential replacement fuel.

As well as the solubility at room temperature, a suitable replacement fuel must remain fully miscible at the lowest operational temperature of the hydrocarbon fuel. The fuels that were found to be miscible were mixed with the appropriate fuel in a 50% volumetric blend and cooled to -20 °C or -47 °C, respectively, and remaining at the temperature for 10 minutes. All the di-esters were miscible down to -20 °C, the cloud point of the diesel used in this study. Butyl butyrate remained miscible with kerosene down to -47 °C where the cloud point of the fuel was reached. Dibutyl malonate, however, did not remain in solution at sub-zero temperatures and is therefore not suitable as an aviation fuel substitute.

All of the fuels exhibited very low solubility in water, with the dibutyl esters showing less than 0.1% solubility, and diethyl ester showing 1% solubility. Butyl lactate was the most water-soluble at 38 g l^{-1}, and so was dismissed from further study. However, it should be noted that the solubility of *n*-butanol is 48 g l^{-1}, while ethanol is completely miscible with water.

4.3.1.4 Energy Density

Current biofuels exhibit lower energy densities than the conventional fossil fuels. This is mainly due to the higher oxygen content of these fuels. However, these fuels also tend to have higher densities than their fossil fuel counterparts, and therefore the difference in volumetric energy density is less than the difference in energy density per unit mass. The potential fermentation fuels considered appropriate were measured for their energy densities in a bomb calorimeter, in accordance to ASTM D240. These, as well as the energy densities of fossil fuels (lowest allowable values) and current biofuels are shown in Figure 4.3.

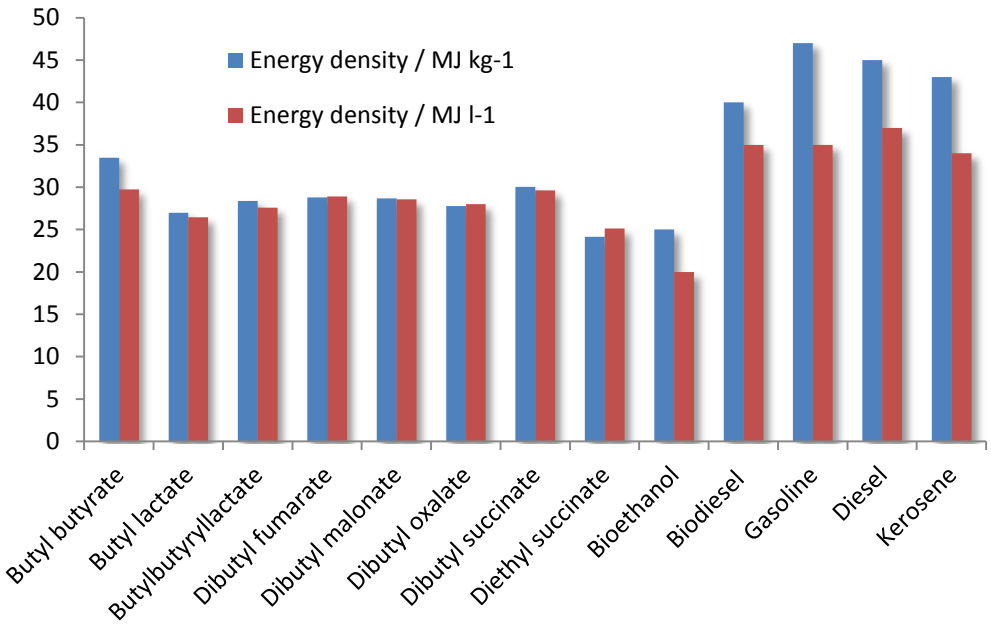

Figure 4.3 Energy densities of suitable fermentation fuels, current biofuels and traditional fossil fuels.

The diester fuels under consideration all exhibit energy densities between 27 and 30 MJ, per unit kg and per unit litre. The diethyl succinate, due to the higher proportion of the fuel being oxygen, has slightly lower energy density, at 24.1 MJ kg^{-1} (25.1 MJ l^{-1}). While these values are higher than bioethanol, due to the lower proportion of oxygen they are lower than biodiesel. Butyl butyrate had an energy density closer considerable close to that of kerosene, showing 77% of the energy density of kerosene per unit mass, and 87% of the energy density of kerosene per unit volume.

4.3.1.5 Oxidative Stability

For biodiesel, polyunsaturation leads to poor oxidative stability as the bis-allylic protons present on the biodiesel can be abstracted by a radical species and, via a complex mechanism, can form a range of oxygenated species. Eventually oligomers are formed, which increases the viscosity and can adversely affect the operation of an engine. Other species, including volatile species such as aldehydes and organic acids are also produced. The oxidative stability of biodiesel was measured by the Rancimat test, whereby a sample of biodiesel (3 g) was subjected to temperature (110 °C) and airflow (10 l h^{-1}). The airflow, along with the volatile components given

off by the oxidising biodiesel, was bubbled through 60 ml deionised water which was fitted with an electrode to measure conductivity.[44] This ultimately leads to a value which represents the point at which the conductivity increase decelerates and increases continuously, i.e. the "induction period". For biodiesel, in the EN14214 standard this induction period must be ≥ 6 hours.

Though none of the fuels being considered contain any polyunsaturated components, the molecular structure of two of the potential fuels contains a double bond – One between the alpha and beta carbons of both carbonyl groups (dibutyl fumarate), and one with a terminal double bond and double bond in the alpha carbon of one of the carbonyl groups (dibutyl itaconate). Both, therefore, could undergo conjugate addition. To examine the oxidative stability, the unsaturated fuels were held under Rancimat conditions for 24 hours, and analysed by ^{1}H NMR spectroscopy. The stability was then compared to rapeseed methyl ester (RME) under the same conditions (Figure 4.4). After 24 hours, the structure of the fermentation esters was unchanged, whereas 90% of the unsaturated components of RME had degraded. The absence of polyunsaturated components in the fuels being studied makes them much more stable than the polyunsaturated fatty acid chains in lipids.

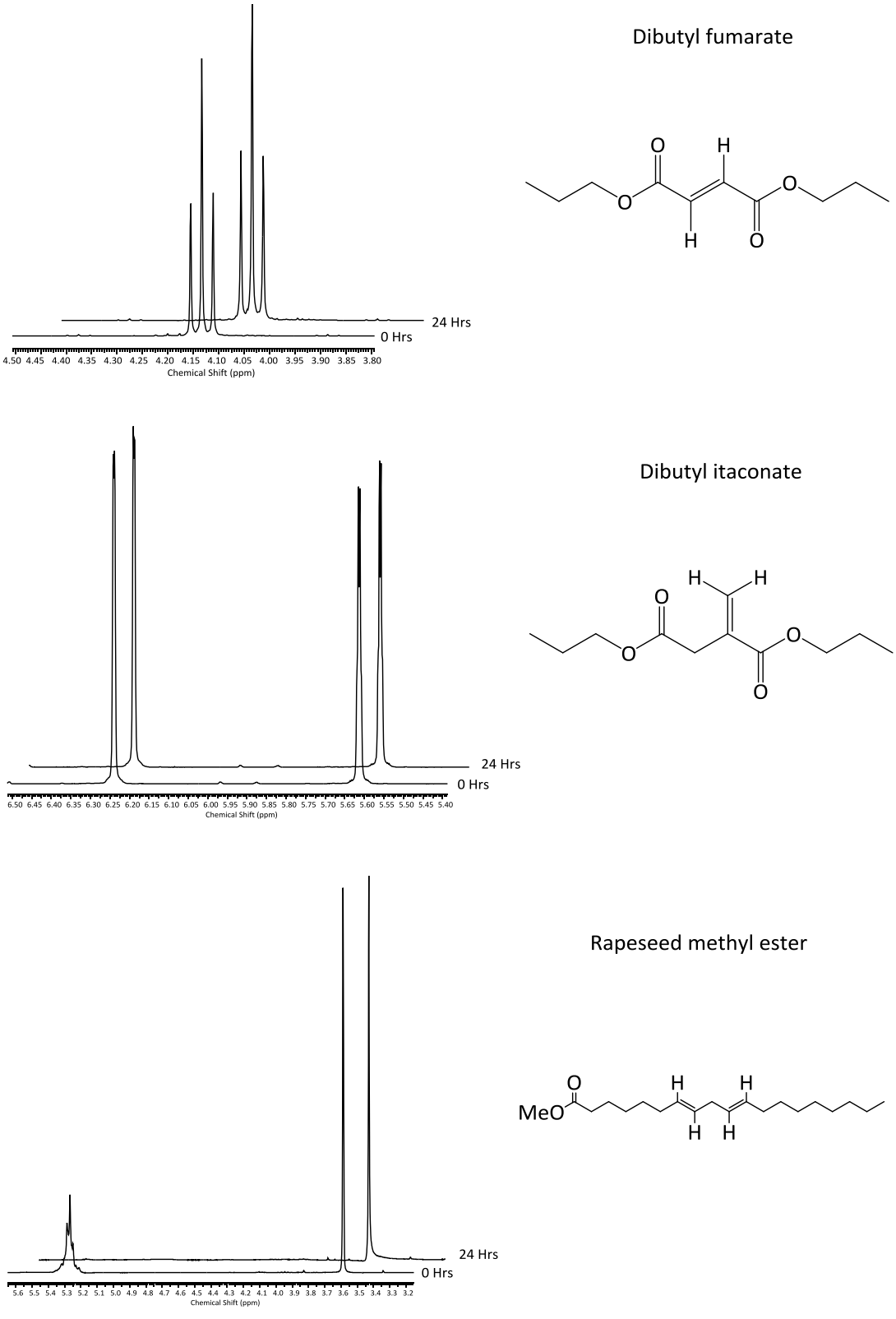

Figure 4.4 ^{1}H NMR spectra showing the degradation of the peak assignable to the double bonds in oxidation of dibutyl fumarate (δ 4.1ppm), dibutyl itaconate (δ5.8 & 6.4 ppm) and rapeseed methyl ester (δ 5.3ppm) after 24 hours at 110 °C.

4.3.1.6 TOXICITY

There is no aspect of the international standards for fossil fuels that covers toxicity and environmental impacts of the fuels themselves before combustion; however fossil-derived fuels are known to contain a number of carcinogens. Therefore, in the development of novel fuels toxicity should also be considered. The fuels were compared to conventional fossil fuels by using their material safety datasheets (MSDS). All the esters, bar dibutyl oxalate, were found to be more benign than diesel or kerosene. However, dibutyl oxalate can cause skin irritation, serious eye damage and respiratory irritation and was therefore judged to be unsuitable for further study.

4.3.1.7 LUBRICITY

Lubricity is a measure of how well a material reduces friction. It is an important aspect of diesel fuel as the fuel itself lubricates the engine. If a fuel exhibits low lubricity, it can lead to abnormal engine wear. The property of lubricity, however, cannot be measured directly. For the international standards for diesel fuel lubricity, ASTM D6079 and EN 590, it is measured using a High Frequency Reciprocating Rig (HFRR). In this method, a steel test plate is submerged in a small sample of the fuel held at 60 °C. A vibrator arm, holding a hardened non-rotating ball is loaded with a 200 g mass is lowered until it makes contact with the steel test plate. It is then vibrated across the steel plate in a 1 mm stroke, at a frequency of 50 Hz for 75 mins. Once this time is complete, the ball is removed and the wear scar diameter on the steel test plate is recorded.[45] The maximum allowed wear scar outlined in EN 590 is 460 µm, whereas for ASTM D6079 is it 520 µm. The lubricity of the four potential diesel replacement fuels was measured with a HFRR in accordance with ISO 12156-1 (Figure 4.5).

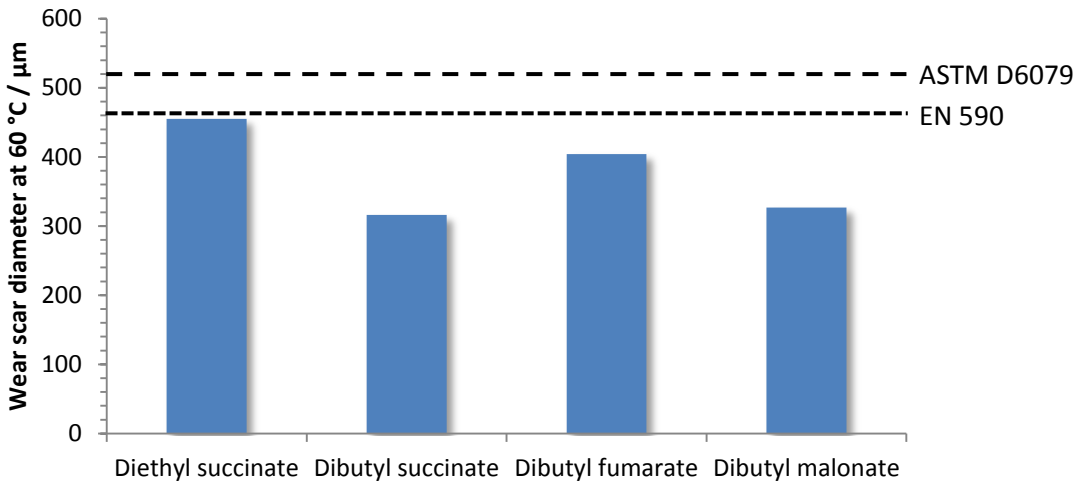

Figure 4.5 Wear scar diameter of the four potential fermentation fuels, as measured by HFRR. The maximum allowed levels for this test method for ASTM D6079 and EN 590 are shown.

A molecule must have at least two features to possess sufficient lubricity. The first is a polarity-imparting heteroatom such as oxygen, which can interact with the metal or metal oxide layer of the surface of any engine / test rig components, and the second is a carbon chain of sufficient length. These are two features present in biodiesel, and can be used to restore the poor lubricity of ultra-low sulfur diesel.[46] These features are also present in the fermentation fuels being investigated, but the chain length is significant shorter. All the fuels tested fall within the international standards, with the dibutyl esters exhibiting slightly better lubricity than diethyl esters most likely due to the increased lipophilicity of the butyl moiety compared with the ethyl moiety. Dibutyl fumarate exhibited a lower lubricity, possibly due to the lack of flexibility inherent with the double bond present in its molecular structure. Dibutyl succinate exhibited the best lubricity and could potentially be used as a lubricity additive.

4.3.1.8 Cetane and Octane Numbers

Cetane number is an important metric in determining the effectiveness of diesel fuels, as it is a measurement of the fuels ignition delay, and shows how readily the fuel undergoes autoignition. The cetane number is calculated using a CFR engine by comparison with cetane (hexadecane) and isocetane (2,2,3,4,6,8,8-heptamethylnonane). The higher the number is, the more readily the fuel autoignites, which is required in a diesel engine. The minimum values given in

ASTM D975 and EN 590 are 40 and 51, respectively. The cetane numbers of the four potential diesel fuel replacements were measured in accordance with ISO 5165 (Figure 4.6).

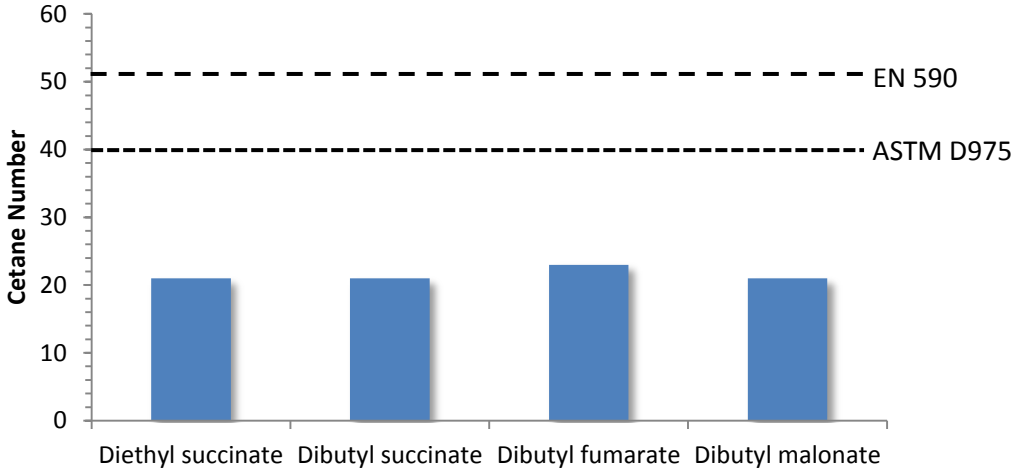

Figure 4.6 Cetane number of the four potential fermentation fuels. The minimum allowed levels for this test method for ASTM D975 and EN 590 are shown.

The cetane number is mainly due to the molecular structure of the fuel. It was found that, for biodiesel, cetane number rises significantly with longer chains.[47] However, there was no increase with increasing carbon number of the four fuels studied, as dibutyl and diethyl succinate exhibited the same cetane number.

The four fuels studied have significantly lower cetane numbers (ranging from 21-23) than is allowed in the international standard. The cetane number of a fuel can cause a number of issues. Fuels of significantly low cetane number can lead to considerable 'diesel knock' (a shock wave produced by a sudden rise in pressure in the cylinder), excessive engine deposits and NO_x and PM emissions.[48] However it is important to note that ethyl levulinate and butyl levulinate, previously identified as possible diesel fuel, possess even lower cetane numbers at 5 and 14, respectively.[29] Even on blending to 20% with diesel, butyl levulinate still was below the minimum allowed cetane number, and a cetane improver (2-ethylhexylnitrate [2-EHN]) was added in order for the fuel to meet ASTM standards. Similar methods, therefore, would most likely be required for the diester fuels in this study.

The octane number is a measurement of how a fuel resists autoignition and its performance in a SI engine. It is, therefore, inversely proportional to cetane number and is an important metric for assessing gasoline and aviation fuels. Though no fermentation fuel was found to be suitable as a gasoline replacement, due to their considerably higher flash points, they may be used as gasoline additives. Butyl butyrate, the most promising aviation fuel replacement had an octane number of 97.3, higher than the minimum allowed value of 95 as set by EN 228, though further study is needed to determine its suitability as a gasoline additive, due to the difference in flash point.

4.3.1.9 Further Considerations of Fermentation Product Fuels

Throughout this study, the physical properties of fermentation fuels have been compared to those of their fossil fuel counterparts. However, though the fuels have proven to have technical potential, there are other factors that must be considered for a viable fuel replacement. The fuels must be inexpensive to manufacture, and exhibit high yields in the fermentation process so to be economically competitive with fossil fuels.

Three of the diesel replacement fuels use fumaric and succinic acid, which are both important platform chemicals for a number of industries, including food additives, plasticisers, and polymers. However, both of these acids are largely produced from maleic anhydride, itself produced from the oxidation of *n*-butane (a petrochemical). Recently, advances in the fermentation technology have produced fumaric and succinic acid in approximately 85-95% yields from glucose (per unit weight).[49-50] Yields in this region vastly decrease the raw material cost of producing the acids, as glucose is a third of the price of maleic anhydride. The potential for lower costs can also come from the economics of scale, one report estimates that the cost of succinic acid could reduce from its current price – US $ 5.90-9.00 kg^{-1} – to a more feasible US $ 0.50-1.00 kg^{-1}.[51] Further research and development is being carried out to increase the viability of scaling up fumaric acid fermentation.[52] However, it should be noted that the production of these acids uses glucose as a feedstock. To

produce truly sustainable fuels from these acids the microbes, which metabolise them must be cultivated on feedstocks that do not derive from food crops.

The esters were produced using two different alcohols, ethanol and *n*-butanol. Though the butyl esters exhibited slightly more favourable fuel properties, ethanol production is more cost-effective than butanol production. Therefore, diethyl succinate was chosen as the most promising fuel replacement suitable for further evaluation on engine.

4.3.2 Engine Testing of Diethyl Succinate (DES)

4.3.2.1 Properties of DES, DES20 and Diesel

The properties of DES, a 20% blend of DES with diesel (DES20) and mineral diesel were compared with international standards (Table 4.7). As DES possesses a low cetane number, the cetane improver (2-ethyl hexyl nitrate) was added to bring the blended fuel into specification as outlined by Christensen *et al.*[29] Interestingly, though the energy density for DES was lower than the typical value for diesel (approximately 45 MJ kg^{-1} [53]) there is no specific lower limit for diesel or biodiesel for both international standard agencies.

Table 4.7 Properties of DES, DES20, and diesel used compared with the European and US standards for diesel and biodiesel.

Physical property	**DES**	**DES20**	**Diesel**	**EN 590 (Diesel)**	**EN 14214 (Biodiesel)**	**ASTM D 975 (Diesel)**	**ASTM D 6751 (Biodiesel)**
Boiling point / °C	218	n/a	n/a	n/a	n/a	n/a	n/a
Flash point / °C	100	65	65	55 min	101 min	52 min	93 min
Density @ 15 °C / g cm^{-3})	1.04	0.873	0.833	820-845	860-900	n/a	n/a
Kinematic Viscosity @ 40 °C / mm^2s^{-1}	1.86	2.30	2.746	2.0-4.5	3.5-5.0	1.9-4.1	1.9-6.0
Energy density / MJ kg^{-1}	24.2	40.49	42.59	n/a	n/a	n/a	n/a
Cetane Number	21	45.1	52.8	51 min	51 min	40 min	47 min

The physical properties of the fuel blend, DES20, were reasonably similar to diesel. The flash point remained within specification and was unchanged, due to the continued presence of volatile species in the fuel. The density increased by 4.8%, falling outside of the EU standard for diesel, though the importance of this aspect is questionable as no limit is set in the ASTM standard. The kinematic viscosity, 2.30 mm^2s^{-1}, fell comfortably within both EU and US standards. The energy density of DES was 24.2 MJ kg^{-1}, considerably lower than diesel. Subsequently the DES20 had only 95% of the gravimetric energy density of the diesel used in this study. The cetane number was also considerably lower than that given in the EN 590 specification, though above the ASTM minimum. DES20, therefore, fell within ASTM standards though not EN 590. As such the DES20 fuel blend fell within the ASTM specification for road transport diesel, and as such could potentially be used in the US with no change to the current infrastructure.

4.3.2.2 Engine Performance & Emissions

The tests were carried out on a Ford Transit van on a rolling road (chassis dynamometer (Figure 4.7). The vehicle was held in a series of "steady state" tests, where the emissions of diesel versus DES20 were compared under defined engine conditions.

Figure 4.7 Chassis dynamometer

The steady state tests were carried out by setting the engine speed to a specific value and the increasing the pedal demand slowly from 0%-100% over the course of approximately 5 minutes using a specially designed manual rig. Therefore at any point the engine state was defined as steady.

The engine speeds tested were: 1200, 1500, 2000, 2500, 3000, 3500, and 4000 rpm. The pedal demand is directly linked to the amount of fuel injected, and thus this is how the power output is managed. At the same pedal position, the same volumetric amount of fuel will be injected into the cylinder, so that fuels of differing energy density will give differing power output. The engine speed was kept constant due to the increasing torque provided by the chassis dynamometer.

Fuel Demand

For each pseudo-steady state test, the volumetric fuel injection per stroke was measured, and converted to mass fuel consumption by using the densities of each fuel. The fuel demand of diesel, DES20 and a plot demonstrating the difference at varying speed and the position of the accelerator pedal (pedal demand) is shown in Figure 4.8. As pedal demand was increased and the engine speed was kept constant (by the chassis dynamometer increasing the rolling resistance), the fuel demand increased for both fuels, until around 60% pedal demand due to the fuel delivery quantity reaching its maximum. In the majority of engine states, the fuel demand for DES20 was higher than that of diesel, the difference peaking at 3.5-4 mg per stroke at and engine speed of 3000 rpm engine speed and 55-65% pedal demand. This corresponds to a 7.2-9.2% increase in demand under these conditions. After this peak the difference reduced to 1.5-2 mg per stroke (or 3.1-4.9%), close to the increase in the density of the fuel (4.8%). It therefore seems likely that the fuel demand is dependent on an aspect other than the density of the fuel.

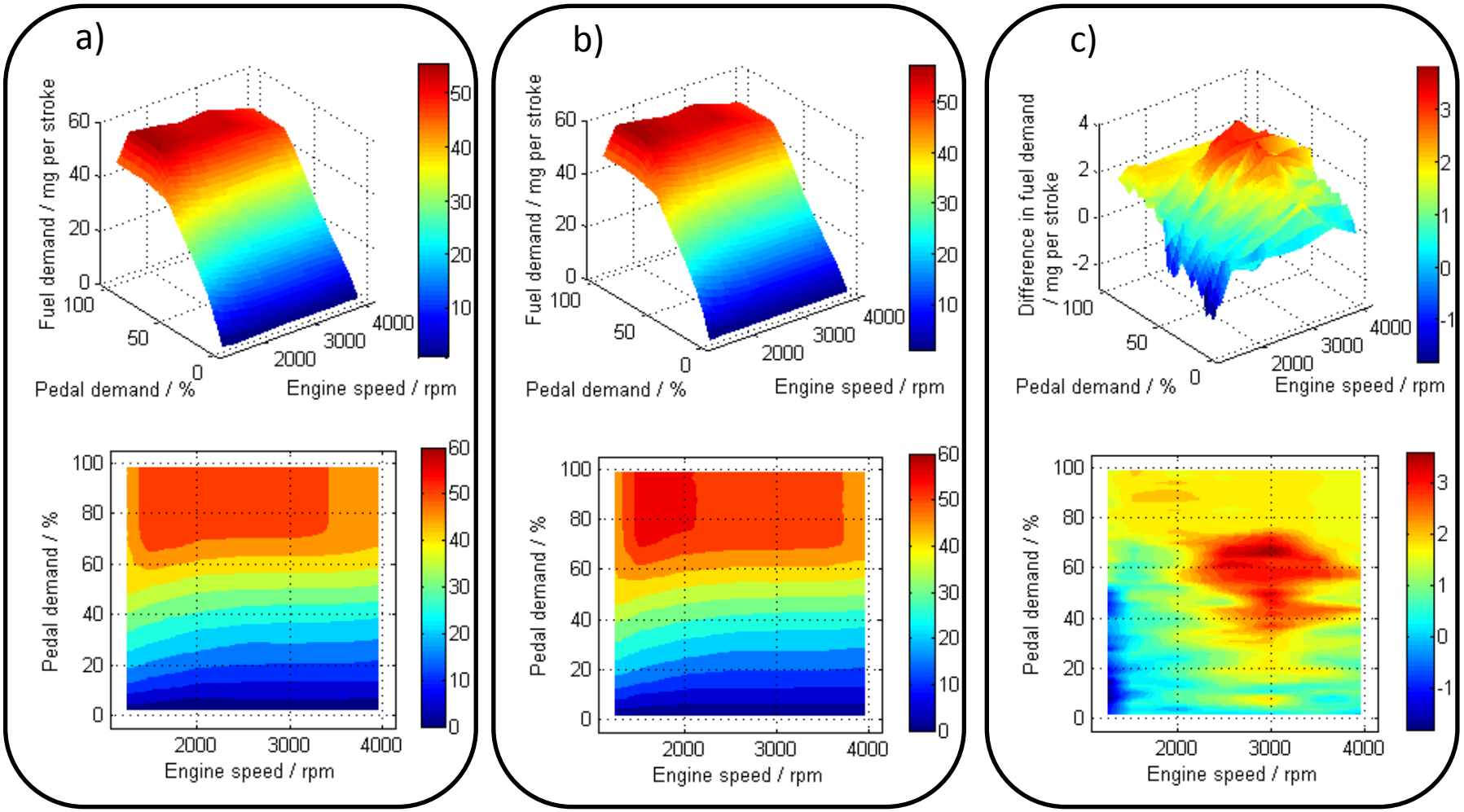

Figure 4.8 Fuel demand at varying pedal demand and engine speed for; a) Diesel, b) DES20, c) Difference between the two.

The amount of fuel injected is calibration specific, though is carefully controlled by the Engine Control Unit (ECU) on-engine. In a common-rail injection system, the injector pressure is kept constant, generated independently of engine speed and load, and so the volume of the fuel injected is determined by the injection period. This injection period is primarily controlled by the position of the accelerator pedal, though the ECU records many operational conditions which can affect engine operation and carries out calculations to adjust the quantity of fuel delivered accordingly.[54] These conditions include pressures and temperatures throughout the engine, the vehicle speed, the movement of the injector itself as well as the pedal position.

The increase in fuel demand at certain conditions beyond what is predicted by the change in density could be due to a number of external conditions. Most important of these is temperature. A reduction in temperature, due to either a cooler engine environment or the lower energy of combustion of a fuel, has a knock-on effect. If the exhaust temperature is lower, the exhaust gas is of a lower pressure and contains less energy, and therefore would lead to a lower boost pressure generated by the turbocharger. This could lead to an increase in fuel demand in an attempt to increase the turbo. The decrease in exhaust temperature would have an effect via the exhaust has recirculation system. The lower the temperature of the gas being recirculated leads to a lower air charge temperature (with a corresponding increase in air density), which in turn could lead to a higher fuel demand in an attempt to compensate for this temperature difference. Also, the gas being recirculated – as a result of being lower in temperature – is denser and therefore has a higher concentration of oxygen. This increases the amount of fuel able to be practically injected, while maintaining complete combustion, and therefore leads to an increase in fuel demand.

Exhaust Temperature

Exhaust temperature is an indirect measurement of the amount of energy produced from a specific volume of fuel, due to the direct correlation between pedal demand and volume of fuel injected. Generally, the exhaust temperatures increase with increasing pedal demand – due to the higher volume of fuel being injected – and with increasing engine speed – due to the higher amount of fuel being injected per unit of time.

On combustion of DES20, there was a significant decrease in temperature at most engine conditions (Figure 4.9). At low engine speeds, where the difference in fuel consumption is lowest, this decrease was between 0-20 °C. As pedal demand – and therefore fuel consumption – increases, this difference became more pronounced. The magnitude of this decrease in exhaust temperature was also seen to increase with increasing engine speed, especially at high pedal demand. At the most extreme conditions, between 90-100% pedal demand and 4000 rpm, the exhaust temperature for DES20 was 80 °C lower than for diesel. This is potentially due to the lower energy density of the fuel. When it combusts, DES20 transfers less energy to the environment than the same volume of diesel, and therefore the exhaust gas is cooler. As the engine speed and pedal demand increase, more of the fuel is burned, and the difference in energy released by the fuel per unit time increases, amplifying the difference in temperature. In addition at high pedal demand there will be no exhaust gas recirculation used, preventing increased fuelling rates due to the lower air charge temperature.

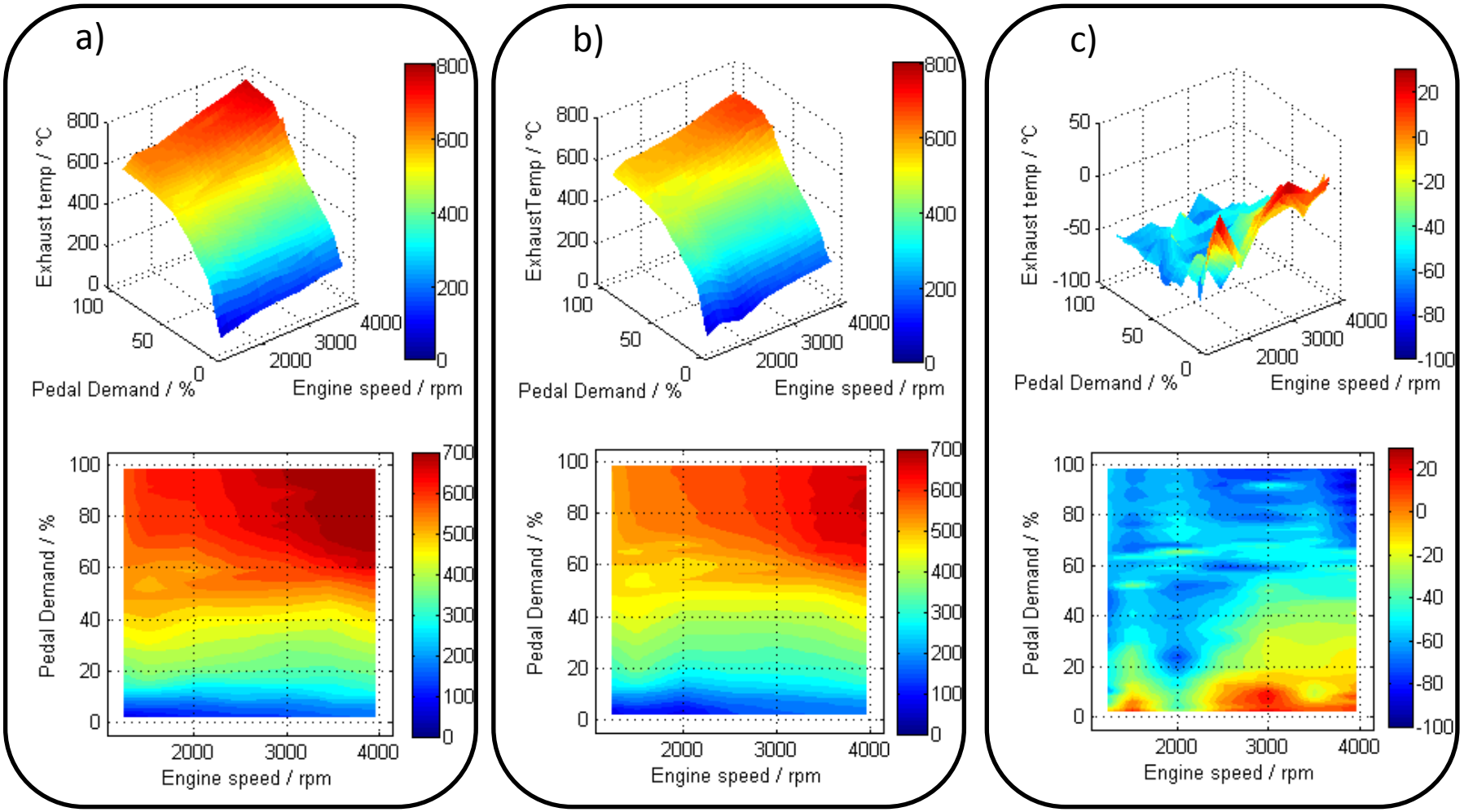

Figure 4.9 Temperature of exhaust fumes at varying engine speeds and pedal demand for a) diesel, b) DES20 and c) Difference between the two.

Wheel Force

The wheel force, or tractive force, is the total force that is parallel to the direction of motion or in this case the total force the vehicle exerts on the surface of the rolling road. The wheel force for each fuel followed a similar trend to that of fuel demand (Figure 4.10). At the beginning of each experiment, where the pedal demand was zero, the chassis dynamometer was driving the wheels, i.e. similar to a vehicle going down a hill whilst in gear. For all of the engine speeds at zero pedal demand the wheel force was therefore negative. As the pedal demand increases the amount of wheel force produced by the engine increases, and therefore decreases the amount of force required by the chassis dynamometer to keep the engine speed constant. Eventually there is a point whereby the wheel force produced by the engine overcomes the need for the wheels to be driven and so to keep the engine at the same speed the chassis dynamometer must provide negative force, i.e. resistance against the wheel. This point, where the wheel force crosses zero, was seen for both fuels at low pedal demands (between 0-20%), though the pedal demand required to overcome the driving of the chassis dynamometer increased with increasing engine speed, due to the higher amount of force needed. With increasing pedal demand, the amount of resistance required from the chassis dynamometer increases, until eventually it reaches a plateau at the same time as the maximum for fuel delivery is reached.

Over the majority of engine conditions, the wheel force was lower for DES20 than it was for diesel, with the difference increasing as pedal demand increased. This was due to the increasing disparity of fuel demand with increasing pedal demand, leading to an increasing difference in energy and therefore force.

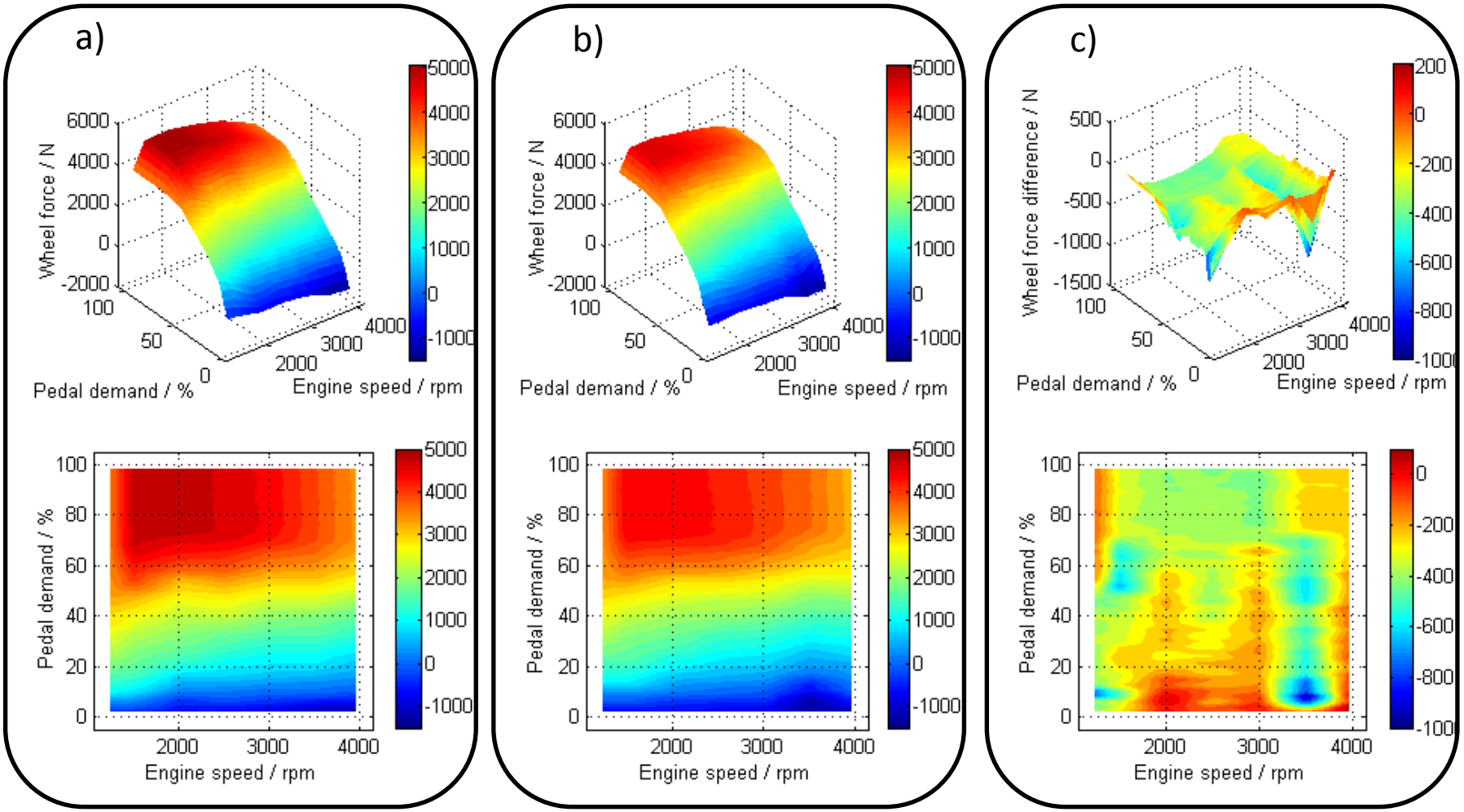

Figure 4.10 Wheel force produced at varying engine speeds and pedal demand for a) diesel, b) DES20 and c) Difference between the two.

Carbon Monoxide (CO) Emissions

Carbon monoxide (CO) and carbon dioxide (CO_2) emissions are closely related to the quality of combustion. The complete combustion of hydrocarbons and oxygenated hydrocarbons forms CO_2, whereas CO is produced only when the combustion is incomplete. While CO is only a weak greenhouse gas, it has the potential to react with hydroxyl radicals in the atmosphere that reduce more potent GHG such as methane. Carbon monoxide is also extremely toxic and has been linked with numerous localized health effects.[55] At low engine speed, 1200 rpm, the level of CO emitted at low pedal demand (0-40%) was similar for diesel and DES20, being relatively low in both cases (Figure 4.11). However, at higher pedal demand (and therefore higher torque) the amount of CO emissions rose dramatically. This was most likely caused by low boost pressure – due to the lightness of the load – and the high fuelling requirement, which leads to considerable incomplete combustion. At more moderate speeds, between 2000 and 3000 rpm, peaks in CO emissions were observed for both diesel and DES20 at lower pedal positions, between 0 and 20 %. Small fuel quantities lead to cycle-to-cycle combustion variability as the engine transitions from negative to positive torque, and therefore incomplete combustion can occur. CO emissions lowered as the speed rose (signifying more complete combustion). It was observed again, however, that the combustion of DES20 under the conditions investigated emitted much lower CO than diesel. At higher engine speeds of 3500 and 4000 rpm, the trend matched that seen at lower engine speeds, i.e. with relatively low CO emissions at low to moderate pedal demand (0-60%), with a sharp increase to a plateau. These high plateaus are somewhat masked by the considerably higher plateau at 1200 rpm. These plateaus are reached due to the fuel delivery quantity reaching its maximum.

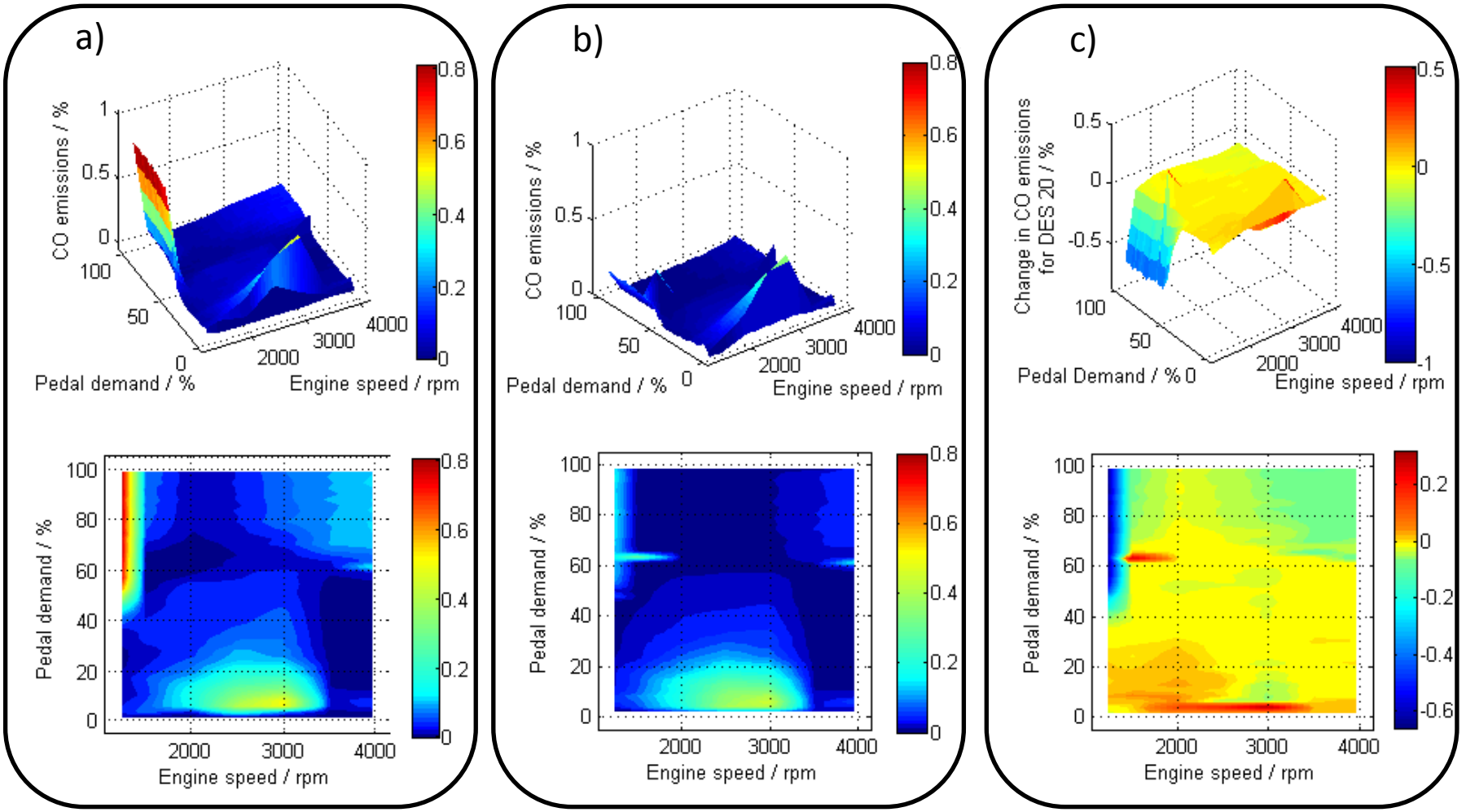

Figure 4.11 CO emissions at varying pedal demand and engine speed for; a) Diesel, b) DES20, c) Difference between the two.

The difference of CO emissions between diesel and DES20 is given in Figure 4.11 c. Though the CO emissions plateaued at the same degree of pedal demand, the plateau was found to be lower for DES20. At low engine speed this decrease was 0.6%. Potentially the more complete combustion observed was due to the higher oxygen content of the fuel compared to diesel. Over most other engine conditions CO emissions for DES20 were lower than diesel but to a lesser degree, generally around 0-0.2% less than diesel. This is in agreement with emissions data published for other oxygenated fuels such as biodiesel, levulinate esters, valerate esters and dimethyl ether.[29, 36, 41, 56] At specific engine conditions, however, the CO emissions for DES20 were higher, as can be seen at moderate engine (2000-3500 rpm) speed and a low pedal demand (0-5%). Potentially this is due to the lower cetane number of the fuel, reported to cause a significant amount of incomplete combustion at low loads, due to the long ignition delay.

Total Hydrocarbon (THC) Emissions

Another group of compounds indicative of poor combustion is the presence of unburnt hydrocarbons in the emissions (Figure 4.12). Hydrocarbon emissions are particularly problematic as they can react with nitrogen oxides in the presence of sunlight, forming ground level ozone, a major source of smog and localized urban pollution.[55] The total hydrocarbon (THC) content in the pre-catalyst emissions was highest at the lower pedal demands (0-20%), as was also the case for CO emissions. This early peak was most probably due to the poor, unstable combustion resulting from poor turbine performance and low boost pressures, similar to what is observed when using biodiesel.[36] However, at low and high engine speeds, this maximum was of a lower level (in the range of 150-400 ppm for 1200, 1500, 3500, and 4000 rpm). The high maxima of THC at moderate speeds are in agreement with the maxima for CO under the same conditions, unsurprising as both are caused by incomplete combustion.

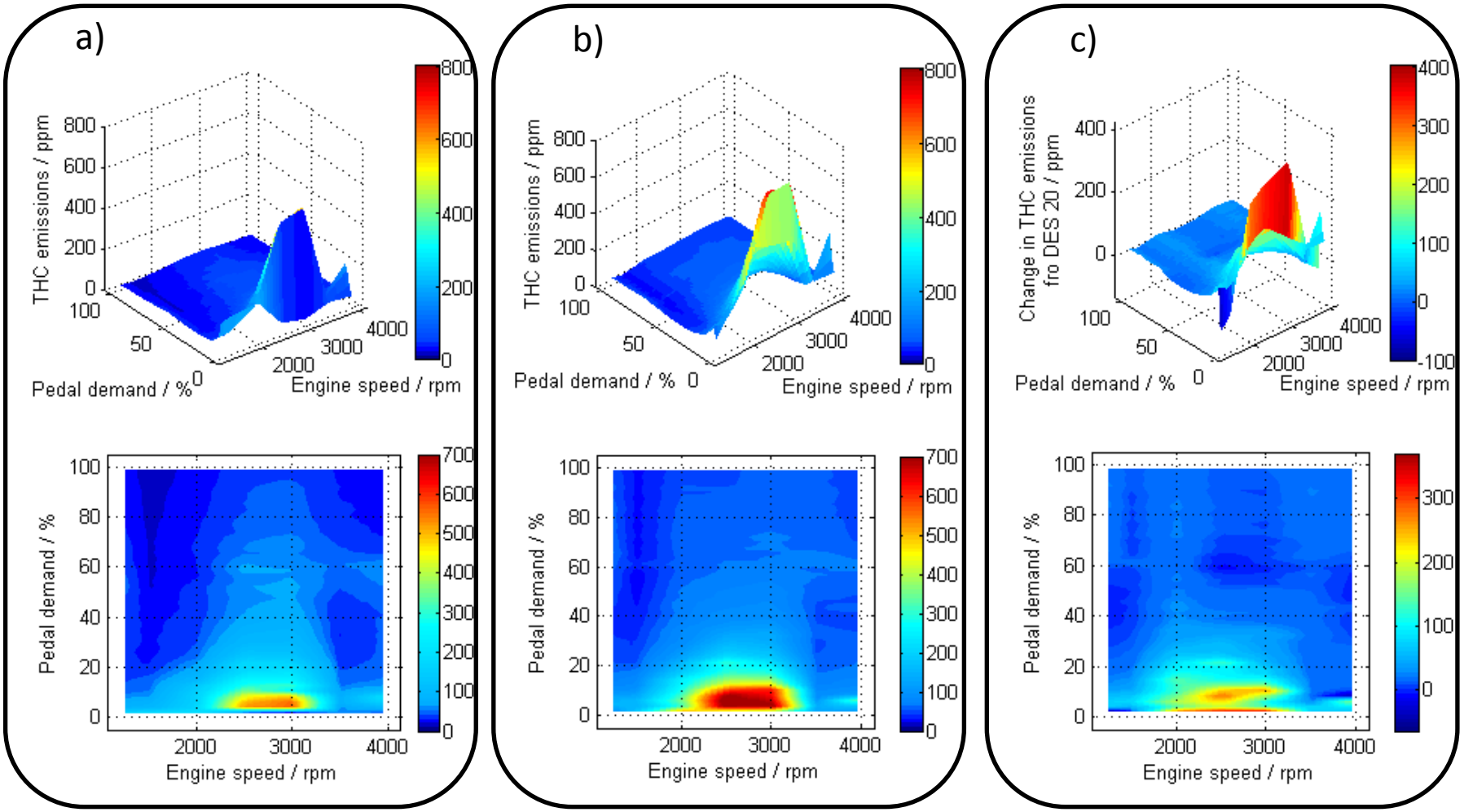

Figure 4.12 THC emissions at varying pedal demand and engine speed for; a) Diesel, b) DES20, c) Difference between the two.

However, under low loads the THC emissions were considerably higher, up to 300 ppm, for DES20 than for diesel. This was presumably caused by the lower cetane number of the fuel, which (at low loads) leads to long ignition delay leads to a higher amount of unburnt fuel.[36, 57] This was supported by the maxima seen for CO at the same conditions. However, while it was expected that the high oxygen content of DES would lead to more complete combustion, as suggested by the general reduction of CO emissions at medium and high engine loads, and that was observed with the vast majority of biodiesel engine testing studies,[56] it can be seen that THC emissions were slightly higher overall engine conditions. It must be noted, however, that the structure of DES has a considerably higher amount of oxygen per molecule of biodiesel and therefore it is likely that the unburnt hydrocarbons themselves may have a lower C/O ratio. As the detector responsible for recording hydrocarbons, flame-ionisation detection is known to be sensitive to changes in molecular make-up, and the increase observed could be due to higher response factor of the exhaust hydrocarbon species when using DES20 rather than diesel. This difference, however, was almost negligible (>20 ppm) due to the very small amount of THC being produced at these conditions for both fuels, close to the lower detection limit of the analyser detectors.

Mono-Nitrogen Oxide (NO_x) Emissions

Mono-nitrogen oxides (NO_x) are potent GHG and can react with other compounds in the exhaust to produce localized urban pollution.[55] For both fuels investigated, over all engine speeds examined, NO_x increased with increased pedal demand (Figure 4.13). As more fuel is injected into the combustion chamber to meet higher power demand the in-cylinder temperature and pressure increase, increasing the production of NO_x. The NO_x production for both fuels reached a plateau when the fuel delivery reached its maximum at 60% pedal demand, similar to the CO emissions.

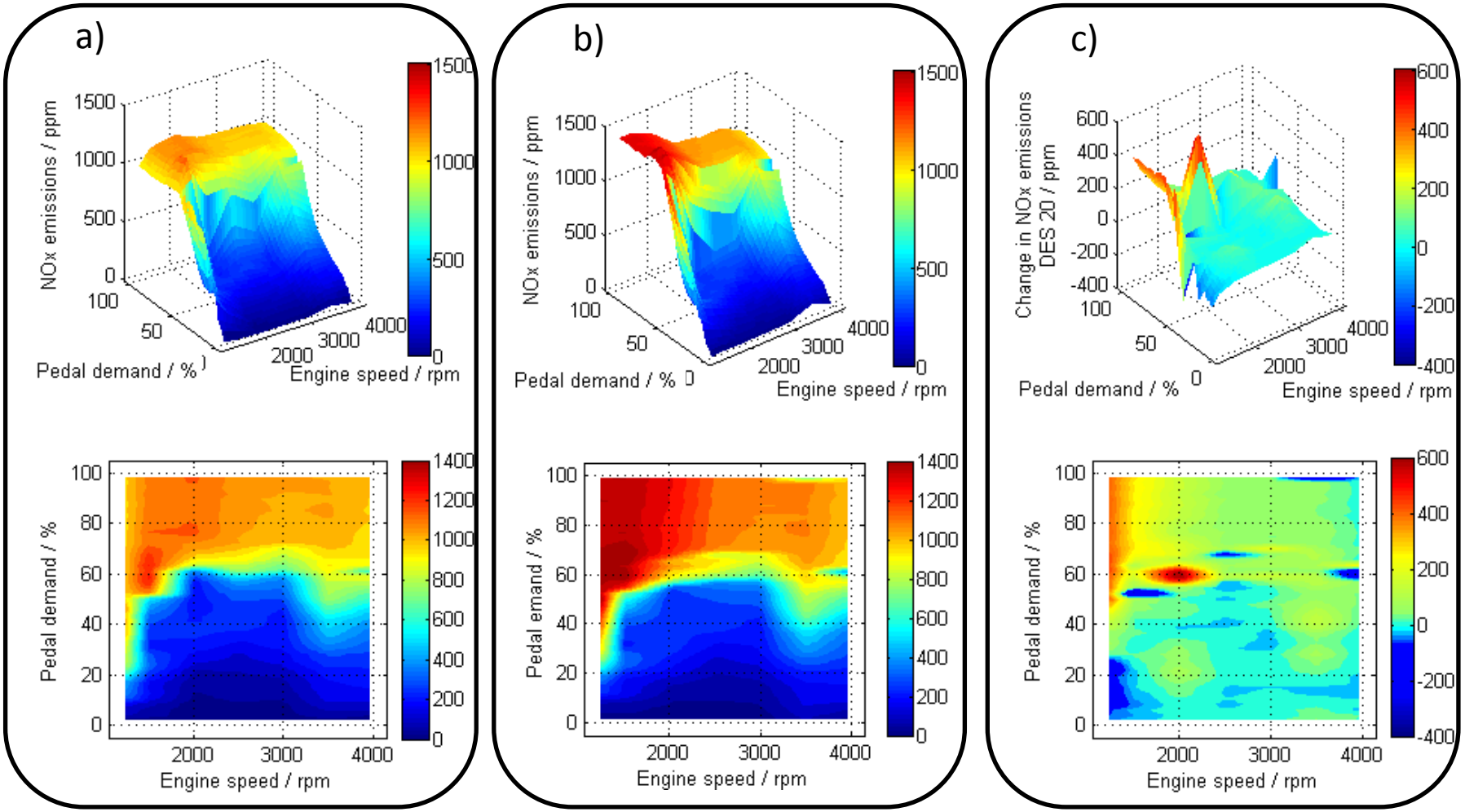

Figure 4.13 NO_x emissions at varying pedal demand and engine speed for; a) Diesel, b) DES20, c) Difference between the two.

On using DES20 at low engine speed (1200 rpm) and maximum fuel delivery there was a significant increase (around 400 ppm) over the diesel. This was likely caused by more complete combustion, inferred from significantly reduced CO, leading to higher combustion temperature and pressures, conditions which favour NO_x production. Increased NO_x emissions (50-150 ppm) were also observed for the DES20 over the majority of all engine conditions. Various factors can contribute to an increase in NO_x emissions when using oxygenated fuels, especially biodiesel. This can be due to the difference in the physical properties of the fuel, such as viscosity, density and compressibility, which effects how the fuel flows, injects and combusts.[58] One possibility is the higher density of DES20. As pedal demand is in direct correlation with the volume of fuel injected, there is potentially a higher number of moles of carbon per volumetric unit of the fuel, leading to increased temperatures. However, as can be seen in the exhaust temperatures, DES20 produced cooler exhaust gases. This would lead to lower NO_x emission, the opposite of what it observed. An increase in density alone, however, cannot account for an increase in the amount of fuel injected. The injection line pressure, and therefore the speed in which the fuel is injected into the combustion chamber, is affected by the viscosity and the compressibility of the fuel.[59, 60] DES20, however, was a lower viscosity than diesel. It has been found that fuel of lower viscosity tend to decrease injection volume[60] and therefore an increase in fuel injection must be attributed to another aspect of the fuel's properties.

Outside the effects of the injection, properties of the fuel can affect the combustion. The lower cetane number of the DES20 was likely to be linked to increased NO_x emissions. Cetane number can affect NO_x emissions in two ways. Generally, when a cetane number of a fuel decreases, ignition delay increases. After this ignition delay period, there are two further periods within the overall combustion cycle: the pre-mixed combustion period and the diffusion combustion period. During the pre-mixed combustion period, fuel and air that have already mixed ignite, causing a rapid rise in temperature and pressure. The longer the ignition delay, more fuel is injected and mixed with the air before ignition occurs. This leads to more extreme temperature and pressure increases, conditions with

favour NO_x formation. Cetane number can also effect the duration of the combustion, which in turn effects NO_x formation. A longer residence time at elevated temperatures will increase it.[58] Determining the true effects of the cetane number on the combustion characteristics require further in-chamber analysis.

4.4 SUMMARY

An investigation of alternative fermentation-derived fuels produced by microbes has been carried out. A range of organic acids products potentially obtained from fermentation were identified, the ethyl and butyl esters of which were compared to current transportation fuels in terms of their physical and fuel properties, including melting temperature, flash point, density, kinematic viscosity, water and fossil fuel solubility, energy density, oxidative stability, toxicity, lubricity, cetane and octane number. All esters identified were found to be unsuitable as gasoline replacements due to their significantly high flash points, though four were deemed as potential diesel substitutes: diethyl succinate, dibutyl succinate, dibutyl fumarate and dibutyl malonate. The low cetane numbers, however, would necessitate the use of a cetane improver additive. On consideration of the availability and cost the most viable diesel replacement fuel was determined to be diethyl succinate. Only butyl butyrate was suitable as a potential kerosene replacement.

To further assess the suitability of diethyl succinate, a blend with diesel was tested in a common rail injection engine on a chassis dynamometer. The 20 vol% diethyl succinate was tested at a range of engine speeds (1200 -4000 rpm) against pedal demand and compared to diesel. Under most engine conditions, an increase in fuel demand, a decrease in wheel force and exhaust temperature, a decrease in CO, and a marginal increase in NO_x were observed. These emissions and the performance were similar to other ester fuels, in particular biodiesel, levulinate and valerate esters.[29, 36, 41] However, an unexpected increase in THC was also observed; though this increase is negligible and is likely due to the lack of instrumentation optimisation of the oxygenated fuel.

Therefore DES could be used in blends with diesel without significant changes to the emissions or performance under a range of conditions and therefore represents a suitable fuel blending agent. Fermentation, however, does not utilize the entirety of the biomass. Fuel production technologies which are of higher carbon efficiency should be investigated, such as thermochemical conversion.

4.5 REFERENCES

1. Jenkins, R. W.; Munro, M.; Nash, S.; Chuck, C. J., Potential renewable oxygenated biofuels for the aviation and road transport sectors. *Fuel* **2013,** *103*, 593-599.
2. Jenkins, R. W.; Chuck, C. J.; Bannister, C. D., Emissions and performance of diethyl succinate in a diesel fuel blend. *Environmental Science and Technology* **2014,** *under review*.
3. Hollinshead, W.; He, L.; Tang, Y., Biofuel Production: an odyssey from metabolic engineering to fermentation scale-up. *Frontiers in Microbiology* **2014,** *5*.
4. Surisetty, V. R.; Dalai, A. K.; Kozinski, J., Alcohols as alternative fuels: An overview. *Applied Catalysis A: General* **2011,** *404* (1-2), 1-11.
5. Jin, C.; Yao, M.; Liu, H.; Lee, C.-f. F.; Ji, J., Progress in the production and application of n-butanol as a biofuel. *Renewable and Sustainable Energy Reviews* **2011,** *15* (8), 4080-4106.
6. Kumar, M.; Gayen, K., Developments in biobutanol production: New insights. *Applied Energy* **2011,** *88* (6), 1999-2012.
7. Peralta-Yahya, P. P.; Zhang, F.; del Cardayre, S. B.; Keasling, J. D., Microbial engineering for the production of advanced biofuels. *Nature* **2012,** *488* (7411), 320-328.
8. Lamonica, M., Why the promise of cheap fuel from super bugs fell short. Cambridge, MA: MIT Technology Review: 2014.
9. Matsushita, K.; Inoue, T.; Adachi, O.; Toyama, H., Acetobacter aceti possesses a proton motive force-dependent efflux system for acetic acid. *Journal of Bacteriology* **2005,** *187* (13), 4346-4352.
10. Feng, X.-H.; Chen, F.; Xu, H.; Wu, B.; Yao, J.; Ying, H.-J.; Ouyang, P.-K., Propionic acid fermentation by Propionibacterium freudenreichii CCTCC M207015 in a multi-point fibrous-bed bioreactor. *Bioprocess Biosystems Engineering* **2010,** *33* (9), 1077-1085.
11. Wu, Z.; Yang, S.-T., Extractive fermentation for butyric acid production from glucose by Clostridium tyrobutyricum. *Biotechnology and Bioengineering* **2003,** *82* (1), 93-102.
12. Yin, P.; Nishina, N.; Kosakai, Y.; Yahiro, K.; Pakr, Y.; Okabe, M., Enhanced production of l(+)-lactic acid from corn starch in a culture of Rhizopus oryzae using an air-lift bioreactor. *Journal of Fermentation and Bioengineering* **1997,** *84* (3), 249-253.
13. Allsopp, A., The formation of oxalic acid by aspergillus niger. *New Phytologist* **1937,** *36* (4), 327-356.
14. Galkin, S.; Vares, T.; Kalsi, M.; Hatakka, A., Production of organic acids by different white-rot fungi as detected using capillary zone electrophoresis. *Biotechnology Techniques* **1998,** *12* (4), 267-271.
15. Zeikus, J. G.; Jain, M. K.; Elankovan, P., Biotechnology of succinic acid production and markets for derived industrial products. *Applied Microbiology and Biotechnology* **1999,** *51* (5), 545-552.
16. Peleg, Y.; Barak, A.; Scrutton, M.; Goldberg, I., Malic acid accumulation by Aspergillus flavus. *Applied Microbiology and Biotechnology* **1989,** *30* (2), 176-183.
17. Okabe, M.; Lies, D.; Kanamasa, S.; Park, E., Biotechnological production of itaconic acid and its biosynthesis in *Aspergillus terreus*. *Applied Microbiology and Biotechnology* **2009,** *84* (4), 597-606.
18. Kenealy, W.; Zaady, E.; du Preez, J. C.; Stieglitz, B.; Goldberg, I., Biochemical Aspects of Fumaric Acid Accumulation by Rhizopus arrhizus. *Applied and Environmental Microbiology* **1986,** *52* (1), 128-133.
19. Lopez-Garcia, R., Citric Acid. In *Kirk-Othmer Encyclopedia of Chemical Technology*, John Wiley & Sons, Inc.: 2000.
20. Werpy, T.; Petersen, G.; Aden, A.; Bozell, J.; Holladay, J.; White, J.; Manheim, A.; Eliot, D.; Lasure, L.; Jones, S. *Top value added chemicals from biomass. Volume 1-Results of screening for potential candidates from sugars and synthesis gas*; DTIC Document: 2004.
21. Nemoto, K.; Tominaga, K.-i.; Sato, K., Straightforward Synthesis of Levulinic Acid Ester from Lignocellulosic Biomass Resources. *Chemistry Letters* **2014,** *43* (8), 1327-1329.
22. Yan, K.; Wu, G.; Wen, J.; Chen, A., One-step synthesis of mesoporous $H_4SiW_{12}O_{40}$-SiO_2 catalysts for the production of methyl and ethyl levulinate biodiesel. *Catalysis Communications* **2013,** *34* (0), 58-63.

23. Yadav, G. D.; Yadav, A. R., Synthesis of ethyl levulinate as fuel additives using heterogeneous solid superacidic catalysts: Efficacy and kinetic modeling. *Chemical Engineering Journal* **2014,** *243* (0), 556-563.
24. Fernandes, D. R.; Rocha, A. S.; Mai, E. F.; Mota, C. J. A.; Teixeira da Silva, V., Levulinic acid esterification with ethanol to ethyl levulinate production over solid acid catalysts. *Applied Catalysis A: General* **2012,** *425–426* (0), 199-204.
25. Hishikawa, Y.; Yamaguchi, M.; Kubo, S.; Yamada, T., Direct preparation of butyl levulinate by a single solvolysis process of cellulose. *Journal of Wood Science* **2013,** *59* (2), 179-182.
26. Rackemann, D. W.; Doherty, W. O. S., The conversion of lignocellulosics to levulinic acid. *Biofuels, Bioproducts and Biorefining* **2011,** *5* (2), 198-214.
27. Braden, D. J.; Henao, C. A.; Heltzel, J.; Maravelias, C. T.; Dumesic, J. A., Production of liquid hydrocarbon fuels by catalytic conversion of biomass-derived levulinic acid. *Green Chemistry* **2011,** *13* (7), 1755-1765.
28. Christensen, E.; Yanowitz, J.; Ratcliff, M.; McCormick, R. L., Renewable Oxygenate Blending Effects on Gasoline Properties. *Energy & Fuels* **2011,** *25* (10), 4723-4733.
29. Christensen, E.; Williams, A.; Paul, S.; Burton, S.; McCormick, R. L., Properties and Performance of Levulinate Esters as Diesel Blend Components. *Energy & Fuels* **2011**, *25* (11), 5422-5428.
30. Gürbüz, E. I.; Alonso, D. M.; Bond, J. Q.; Dumesic, J. A., Reactive Extraction of Levulinate Esters and Conversion to γ-Valerolactone for Production of Liquid Fuels. *ChemSusChem* **2011,** *4* (3), 357-361.
31. Bozell, J. J.; Moens, L.; Elliott, D. C.; Wang, Y.; Neuenscwander, G. G.; Fitzpatrick, S. W.; Bilski, R. J.; Jarnefeld, J. L., Production of levulinic acid and use as a platform chemical for derived products. *Resources, Conservation and Recycling* **2000,** *28* (3–4), 227-239.
32. Lange, J.-P.; Price, R.; Ayoub, P. M.; Louis, J.; Petrus, L.; Clarke, L.; Gosselink, H., Valeric Biofuels: A Platform of Cellulosic Transportation Fuels. *Angewandte Chemie International Edition* **2010,** *49* (26), 4479-4483.
33. Regulation (EC) No 715/2007 of the European Parliament and of the Council of 20 June 2007 on type approval of motor vehicles with respect to emissions from light passenger and commercial vehicles (Euro 5 and Euro 6) and on access to vehicle repair and maintenance information.
34. Koç, M.; Sekmen, Y.; Topgül, T.; Yücesu, H. S., The effects of ethanol–unleaded gasoline blends on engine performance and exhaust emissions in a spark-ignition engine. *Renewable Energy* **2009,** *34* (10), 2101-2106.
35. Al-Hasan, M., Effect of ethanol–unleaded gasoline blends on engine performance and exhaust emission. *Energy Conversion and Management* **2003,** *44* (9), 1547-1561.
36. Xue, J. L.; Grift, T. E.; Hansen, A. C., Effect of biodiesel on engine performances and emissions. *Renewable & Sustainable Energy Reviews* **2011,** *15* (2), 1098-1116.
37. Environmental Protection Agency *A comprehensive analysis of biodiesel impacts on exhaust emissions. Draft Technical Report EPA420-P-02-001*; Assessment and Standards Division, Office of Transportation of Air Quality, United States Environmental Protection Agency: 2002.
38. Hellier, P.; Ladommatos, N.; Allan, R.; Rogerson, J., The Influence of Fatty Acid Ester Alcohol Moiety Molecular Structure on Diesel Combustion and Emissions. *Energy & Fuels* **2012,** *26* (3), 1912-1927.
39. Contino, F.; Foucher, F.; Mounaïm-Rousselle, C.; Jeanmart, H., Combustion Characteristics of Tricomponent Fuel Blends of Ethyl Acetate, Ethyl Propionate, and Ethyl Butyrate in Homogeneous Charge Compression Ignition (HCCI). *Energy & Fuels* **2011,** *25* (4), 1497-1503.
40. Contino, F.; Foucher, F.; Halter, F.; Dayma, G.; Dagaut, P.; Mounaïm-Rousselle, C. *Engine performances and emissions of second-generation biofuels in spark ignition engines: The case of methyl and ethyl valerates*; SAE Technical Paper: 2013.
41. Contino, F.; Dagaut, P.; Dayma, G.; Halter, F.; Foucher, F.; Mounaïm-Rousselle, C., Combustion and Emissions Characteristics of Valeric Biofuels in a Compression Ignition Engine. *Journal of Energy Engineering* **2013**, A4014013.
42. Singh Dhillon, G.; Kaur Brar, S.; Verma, M.; Tyagi, R., Recent Advances in Citric Acid Bio-production and Recovery. *Food and Bioprocess Technology* **2011,** *4* (4), 505-529.
43. Scifinder, and references found therein.

44. Jain, S.; Sharma, M. P., Review of different test methods for the evaluation of stability of biodiesel. *Renewable & Sustainable Energy Reviews* **2010,** *14* (7), 1937-1947.
45. Totten, G. E.; Westbrook, S. R.; Shah, R. J., *Fuels and Lubricants Handbook: Technology, Properties, Performance, and Testing*. ASTM International: 2003.
46. Knothe, G.; Steidley, K. R., Lubricity of Components of Biodiesel and Petrodiesel. The Origin of Biodiesel Lubricity†. *Energy & Fuels* **2005,** *19* (3), 1192-1200.
47. Knothe, G., Dependence of biodiesel fuel properties on the structure of fatty acid alkyl esters. *Fuel Processing Technology* **2005,** *86* (10), 1059-1070.
48. Wellington; Asmus, A., *Diesel engines and fuel systems*. Longman: 1995.
49. Roa Engel, C.; Straathof, A. J.; Zijlmans, T.; Gulik, W.; Wielen, L. M., Fumaric acid production by fermentation. *Applied Microbiology and Biotechnology* **2008,** *78* (3), 379-389.
50. Song, H.; Lee, S. Y., Production of succinic acid by bacterial fermentation. *Enzyme and Microbial Technology* **2006,** *39* (3), 352-361.
51. Beauprez, J. J.; De Mey, M.; Soetaert, W. K., Microbial succinic acid production: Natural versus metabolic engineered producers. *Process Biochemistry* **2010,** *45* (7), 1103-1114.
52. Xu, Q.; Li, S.; Huang, H.; Wen, J., Key technologies for the industrial production of fumaric acid by fermentation. *Biotechnology Advances*, **2012**, *30* (6), 1685-1696.
53. Song, C., *Chemistry of Diesel Fuels*. Taylor & Francis: 2000.
54. Zhao, H., *Advanced Direct Injection Combustion Engine Technologies and Development: Diesel Engines*. Elsevier Science: 2009.
55. Wallington, T. J.; Kaiser, E. W.; Farrell, J. T., Automotive fuels and internal combustion engines: a chemical perspective. *Chemical Society Reviews* **2006,** *35* (4), 335-347.
56. Lapuerta, M.; Armas, O.; Rodriguez-Fernandez, J., Effect of biodiesel fuels on diesel engine emissions. *Progress in Energy and Combustion Science* **2008,** *34* (2), 198-223.
57. Kidoguchi, Y.; Yang, C.; Kato, R.; Miwa, K., Effects of fuel cetane number and aromatics on combustion process and emissions of a direct-injection diesel engine. *JSAE Review* **2000,** *21* (4), 469-475.
58. Hoekman, S. K.; Robbins, C., Review of the effects of biodiesel on NO_x emissions. *Fuel Processing Technology* **2012,** *96* (0), 237-249.
59. Monyem, A.; Van Gerpen, J. H., The effect of biodiesel oxidation on engine performance and emissions. *Biomass and Bioenergy* **2001,** *20* (4), 317-325.
60. Tat, M. E.; Van Gerpen, J. H., Measurement of biodiesel speed of sound and its impact on injection timing. NREL, Ed. Golden, CO, 2003.

CHAPTER 5

UPGRADING BIOMASS PYROLYSIS VAPOUR MODEL COMPOUNDS OVER METAL-IMPREGNATED ZEOLITE CATALYSTS

In previous chapters, the production of liquid transportation fuels from biological sources has concentrated on the use or conversion of specific portion of the biomass. In Chapters 2 and 3 this portion was the triglycerides, in an attempt to produce more sustainable biofuel via the use of waste resources or an alternative transformation. In Chapter 4, the portion was that which can be fermented, i.e. sugars, starches and cellulose. However, this does not utilise the entirely of the biomass produced. Pyrolysis, the thermal decomposition of organic matter in the absence of oxygen, converts all biomass to different gas, liquid and solid fractions. Shorter reaction times maximise the liquid yield (bio-oil), which is mainly composed of oxygenated species. These must be chemically upgraded, deoxygenated and refined to produce suitable fuel molecules.

In order to understand the mechanistic changes that occur during bio-oil upgrading, and therefore be able to tailor the final products towards desirable species, the reactivity of key components of the bio-oil during upgrading must be determined. In this study, the catalytic upgrading of a model compound representative of the ketonic portion of bio-oil – mesityl oxide – was carried out, using a range of different metal-supported HZSM-5 zeolite catalysts.

Work carried out in this study was carried out in the National Renewable Energy Laboratory (NREL) in Golden, Colorado, USA, as part of the international internship programme available through the CSCT, and is to be included in an NREL report for the United States Department of Energy.

5.1 INTRODUCTION

Pyrolytic conversion of renewable biomass and subsequent upgrading is one of the potential technologies to produce truly sustainable, drop-in biofuels. It is one of the most carbon-efficient methods, producing up to 75 wt% bio-oil.[1] Much work has been carried out on the conversion of lignocellulosic biomass via pyrolysis, using a number of different conditions, processes and catalysts.[2] However, one of the main issues associated with the catalytic upgrading of pyrolysis oil is the deactivation of the catalysts, due to the formation and deposition of coke. This is generally attributed to the condensation of phenolic species which can consist of up to 30 wt% of the bio-oil.[3] The rest of the pyrolysis oil is composed of a range of alcohols, aldehydes, ketones and acids.[3-4] Generally the bio-oil is composed of over 400 compounds,[5] the concentrations and ratios of which depend heavily on the feedstock, pyrolysis conditions and catalyst used. Due to this wide range of molecules, the directed upgrading of bio-oil to specific fuel molecules is a considerable challenge.

In many biorefinery processes, the bio-oil is condensed to its liquid form. Liquid bio-oil which hasn't been upgraded has a high proportion of oxygen (35-40%) due to the oxygenated feedstock, and therefore has a high viscosity, high acidity, low energy density, and is reasonably unstable.[1] This severely limits its application and long-term storage potential. One promising process for the production of more stable bio-oils is catalytic fast pyrolysis, whereby the pyrolysis oil is upgraded prior to downstream refinement using a deoxygenation catalyst. This comes in two forms: *in situ*, whereby the deoxygenation catalyst is within the pyrolysis reactor itself and the pyrolysis vapour is deoxygenated as it is produced; and e*x situ,* whereby the deoxygenation catalyst is external to the pyrolysis reactor and the pyrolysis vapour produced is separated from the char and solids produced before being passed through the catalyst (Figure 5.1).[6]

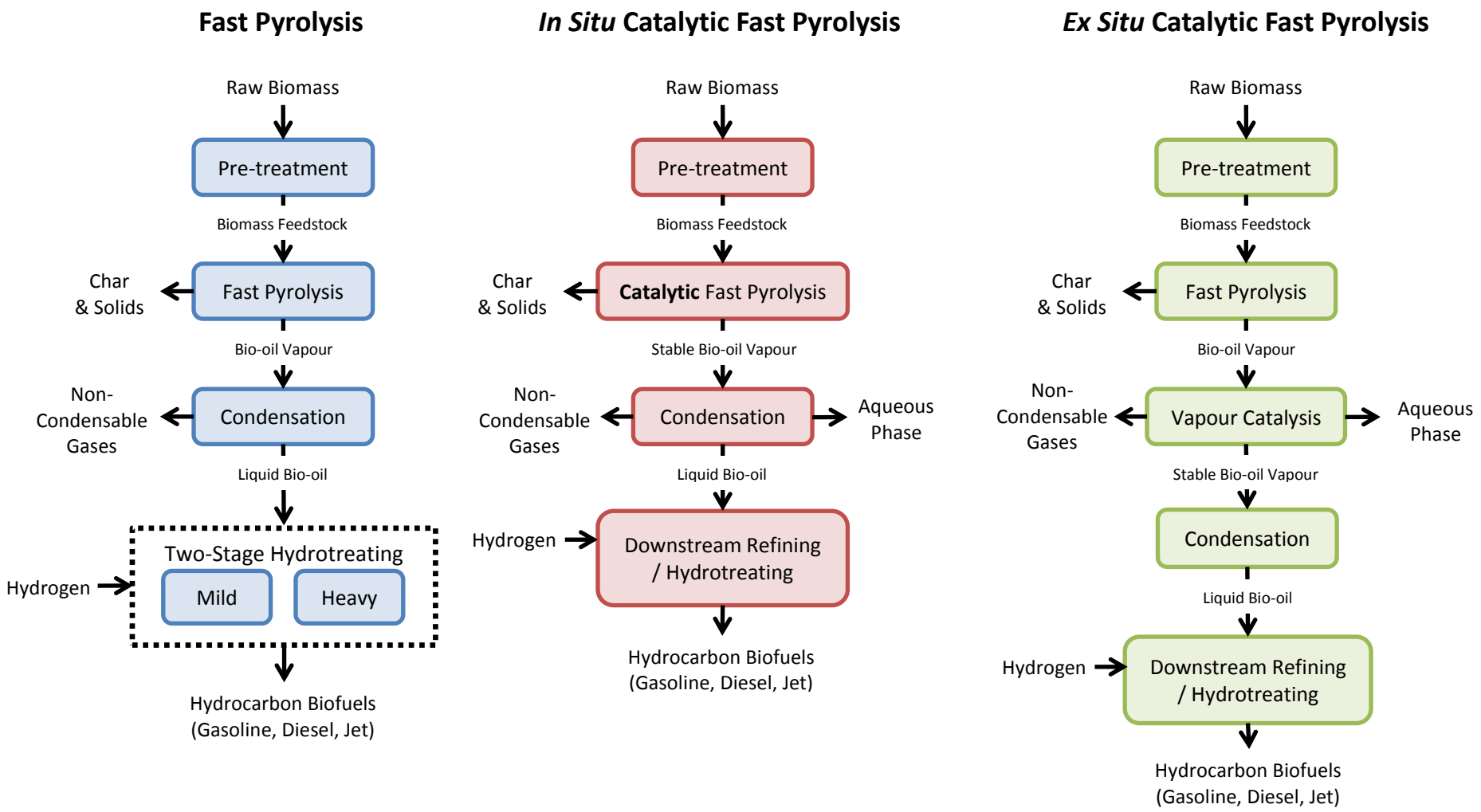

Figure 5.1 Process flow diagrams for fast pyrolysis pathways. Adapted from Ruddy, *et al.*[6]

In order to establish optimum conditions for pyrolysis oil upgrading, the mechanisms by which the different key components of the complex pyrolysis vapours should be determined. The *ex situ* catalytic fast pyrolysis pathway, therefore, lends itself to research in this area due to the ability to analyse the vapour pre- and post-upgrading.

The most promising catalysts for bio-oil upgrading are zeolite based systems, as these react with oxygenated hydrocarbons and reject the oxygen as CO_2 ('zeolite cracking').[7] A report published by Hydrocarbon Processing for the future of fluidic catalytic cracking states that

"*Biomass-derived oils are generally best upgraded by HZSM-5 or ZSM-5, as these zeolite catalysts promote high yields of liquid products and propylene. Unfortunately, these feeds tend to coke easily, and high TANs (total acid number) and undesirable byproducts such as water and CO_2 are additional challenges.*"[2]

Zeolites occur naturally in geological formation, with over 40 naturally occurring forms known such as mordenite, natrolite and faujasite. Specifically, a zeolite is a crystalline, microporous aluminosilicate material consisting of interconnecting SiO_4 and AlO_4 tetrahedra. In these forms, silicon has a +4 charge, while alumina has a +3 charge, and so the AlO_4 tetrahedron carries an overall negative charge. The interconnecting tetrahedra form a three-dimensional framework, with uniform pores of roughly molecular dimensions that run through the structure. As such, monopositive cations can be accommodated in these pores, cancelling out the AlO_4 negative charge and allowing the overall structure to remain electoneutral.[8] Due to their unique combination of chemical nature and pore structure, zeolites have found many uses, including gas physisorption, liquid adsorption, molecular sieves, and catalytic applications.

The most prevalent and widely researched zeolite is ZSM-5. It is called due to its original synthesis by Mobil scientists (Zeolite Socony Mobil-5). It's structure has been well defined in literature,[9] containing straight and sinusoidal channels of *ca.* 5.5 Å diameter, and pores of *ca.* 8 Å (Figure 5.2). Commercially ZSM-5 is generally

obtained in its ammonium form. Upon calcination, however, the ammonium ion breaks down, ammonia is given off leaving behind a proton, and HZSM-5 is produced. HZSM-5 can exhibit both Brønsted acidity and – when a Brønsted acid site is dehydrated – Lewis acidity, and can be characterised by its silicon to alumina ratio (SAR). A higher SAR signifies less negatively charged AlO_4 tetrahedrons which need to be neutralised by cations, and therefore is less acidic overall, leading to a lower reactivity.

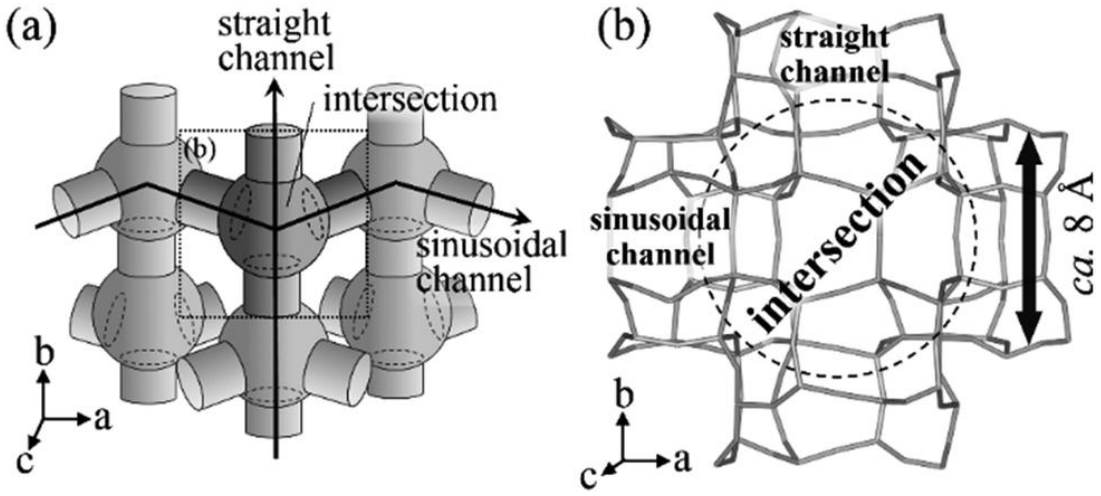

Figure 5.2 Channel system of ZSM-5, showing a) Schematic representation of pore structure, and; b) Intersection-centred framework with adjoining channels. Taken from Fujiyama, *et al.*[10]

ZSM-5 is an effective dehydration, isomerisation and oligomerisation catalyst. It is most significantly used to produce synthetic gasoline via the methanol-to-gasoline process, whereby two moles of methanol are dehydrated to form dimethyl ether, before being further dehydrated to C_2-C_5 olefins and eventual oligomerisation to a mixture of alkanes, cycloalkanes, alkenes and aromatics.[11]

A number of biomass-derived oxygenates have also been investigated for their reactivity over HZSM-5.[11-13] Gayubo, *et al.* carried out a thorough investigation of the different components found in biomass pyrolysis vapour, including *n*- and *iso*-alcohols, phenols, aldehydes, ketones and carboxylic acids.[3, 4] The authors concluded that alcohols dehydrate to the corresponding alkenes at relatively low temperatures (200 °C), with *iso*-alcohols dehydrating faster than *n*-alcohols, and with minimal coking.

The upgrading of 2-methoxyphenol over HZSM-5 showed little activity for hydrocarbon production, and formed a significant amount of thermal coke. Acetaldehyde exhibited a similar low reactivity, and noticeable deactivation caused by coke formation, attributed to the formation of trimethyltrioxane and its subsequent oligomerisation. Thermal coking of the catalyst does not necessarily deactivate the catalyst, though it does block the micropores of the catalyst bed, therefore blocking flow of the vapour and access to the active catalytic sites while catalytic coking can deactivate the catalyst, due to the chemisorption onto the active sites. Regeneration of the catalyst is possible by burning the coked catalyst in air or oxygen, producing CO_2. The pyrolysis of acetone over HZSM-5 was found to be less reactive than for alcohols, requiring higher temperatures and residence times to dehydrate to its initial dehydration product, *iso*-butene. Above 350 °C, this *iso*-butene was found to form C_{5+} alkanes and aromatics, though the proportion of aromatics was much higher than for alcohols. The initial pyrolysis product of acetic acid is acetone, and therefore it was found to react in a very similar way. Deactivation by catalyst coking was found to be considerably higher for acetone and acetic acid than for alcohols as aromatic species fuse and oligomerise, eventually forming graphitic coke.

As the conversion of alcohols is facile and leads to the formation of desirable products, investigations into the catalytic upgrading and conversion of acetone and related ketonic species are vital for the understanding of fundamental catalytic requirements and efficient conversion of complex pyrolysis vapour deoxygenation.

The catalytic conversion of acetone over HZSM-5 follows a well-defined conversion pathway, undergoing acid-catalysed aldol condensation and, if the reaction occurs at sufficiently high temperature, aromatisation to mesitylene (1,3,5-trimethylbenzene).[11] However, the overall reaction is a complex mechanism involving cross- and self-condensation of a number of ketonic species, leading to a range of products (Scheme 5.1). However, the final product mixture can be directed by altering the reaction conditions. Salvapati, *et al.*, reviewed the methods by which product selectivity could be achieved, concentrating on the effect of different catalysts.[14]

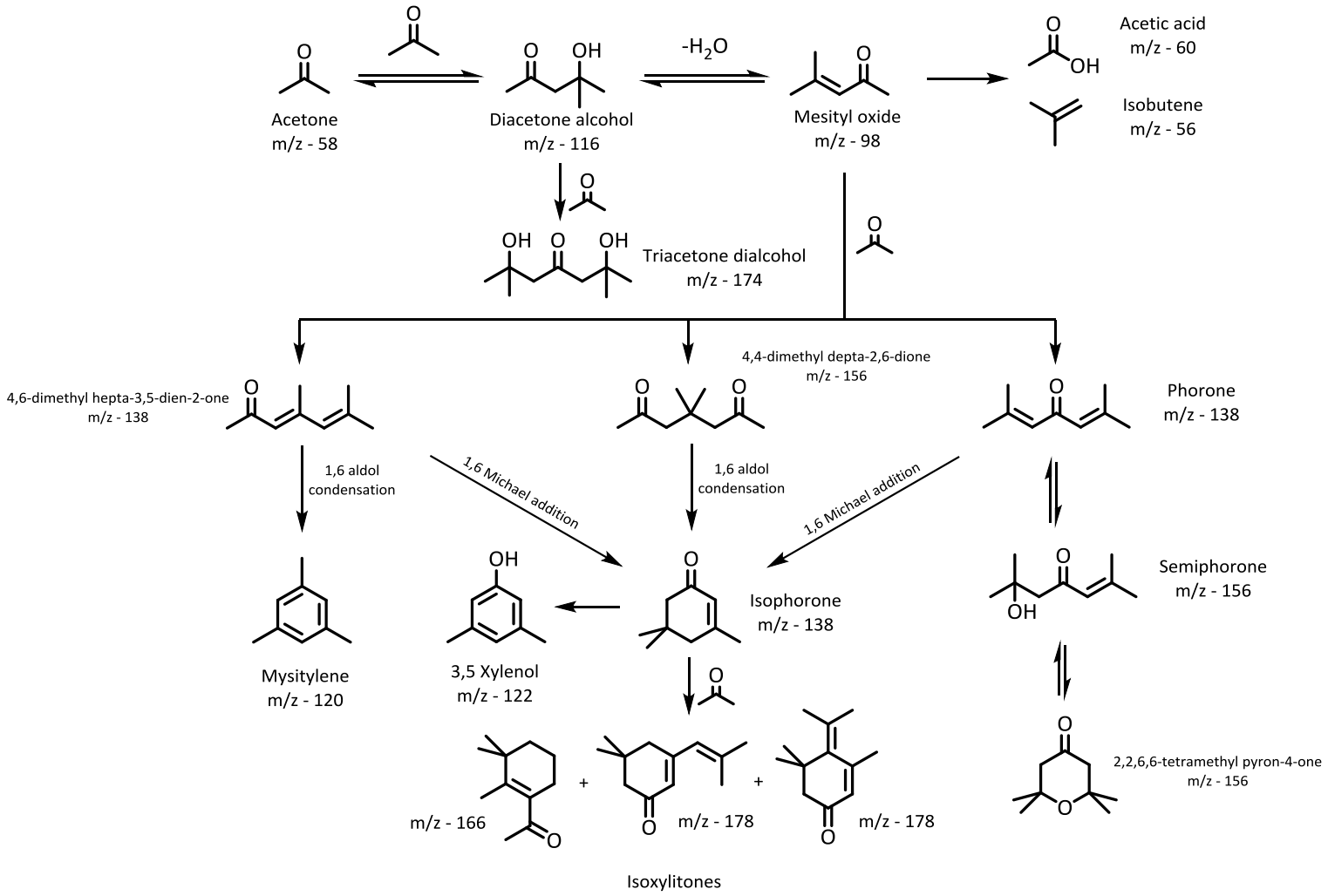

Scheme 5.1 Reaction products formed in the acid-catalysed condensation of acetone. Adapted from Salvapati, *et al.*[14]

Scheme 5.1, however, is not a complete scheme for all the reactions which lead to aromatic formation and therefore coking of the ZSM-5 catalyst. For example, *iso*-butene can undergo secondary reactions, such as oligomerisation, aromatisation and cracking.[15] To successfully produce fuel molecules from ketonic species, therefore, aromatisation needs to be reduced. There are alterations to the reaction conditions with ZSM-5 based catalyst systems that have been reported to inhibit the production of aromatics.

Metal ion-exchange, the replacement of protons present in HZSM-5 with metal ions, reduces the secondary reactions which produce aromatic species in biomass vapour pyrolysis. Transition metal-exchanged zeolites are effective catalysts for certain applications, often more effective than their protonic forms.[16] The presence of a metal centre on the zeolite changes the reaction mechanism and therefore the products formed. Cruz-Cabeza*, et al.,* investigated the conversion of acetone using a range of metal-supported β-zeolites. Despite lowering the conversion at 400 °C from 96.8% with H-β zeolite to 58.5% with Cu-β zeolite, a considerably higher proportion of the converted products observed were aliphatic species (71 wt%).[17] Furthermore, no aromatic species were observed with Cu-β zeolite, while they were observed with H-β zeolite and all other metal-supported β zeolites tested. However, the effect of Cu-supported ZSM-5 on acetone and related ketonic species has not been reported.

All mechanisms in the condensation of acetone that lead to aromatisation require carbon-carbon double bonds to form. One method that blocks the formation of aromatics and the subsequent graphitic coke, therefore, is the hydrogenation of the pyrolytic products. Palladium-supported heterogeneous catalysts are well known for their activity in hydrogenation and carbon-carbon coupling reactions.[18, 19] Specifically, Pd-supported ZSM-5 acts as a bifunctional catalyst in the production of methyl *iso*-butyl ketone (MIBK) from acetone. The reaction occurs by the condensation of acetone to diacetone alcohol, followed by its dehydration to mesityl oxide, and finally by the selective hydrogenation of the carbon-carbon double bond, to form MIBK.[20-24] This selective hydrogenation is unsurprising as

carbon-carbon double bonds require lower temperatures to be reduced by hydrogen than carbonyl groups or alcohols (Figure 5.3).[25]

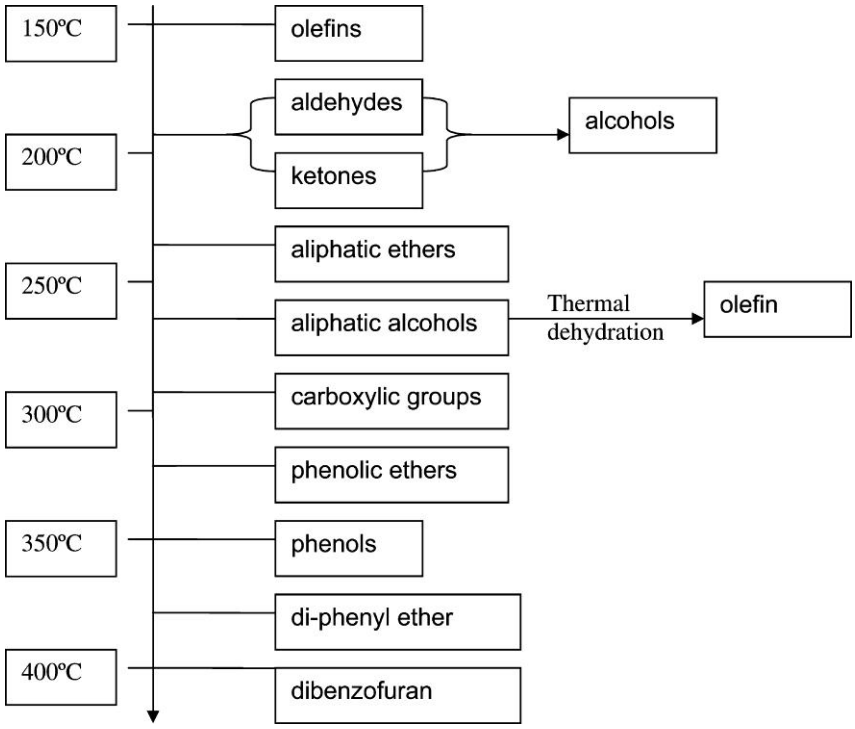

Figure 5.3 Reactivity scale of oxygenated groups under hydrotreatment conditions. Taken from Elliot, *et al.*[25]

These studies have reported selectivity to methyl *iso*-butyl ketone which, if further hydrotreated, would lead to the formation of 2-methyl butane which is unsuitable as a liquid transport fuel. However, MIBK is still active for the aldol condensation. For example, Yang, *et al.* used Pd-supported ZSM-5 as a catalyst for the one-step synthesis of MIBK from acetone, but also produced up to 1.5 wt% of di-*iso*-butyl ketone (DIBK).

It is possible therefore, that metal-supported ZSM-5 could produce a higher amount of oxygenated non-aromatic hydrocarbons that could be hydrotreated further to produce fuel-suitable hydrocarbons (Scheme 5.2). The oligomerisation of acetone self-condensation products formed, however, depends on the initial production of mesityl oxide, one of the first stable products to be produced via the acetone condensation reaction. It is reported as being produced with 100% selectivity in literature,[26] and its subsequent hydrogenation product (MIBK) has been reported as being produced with 95.9% selectivity.[24]

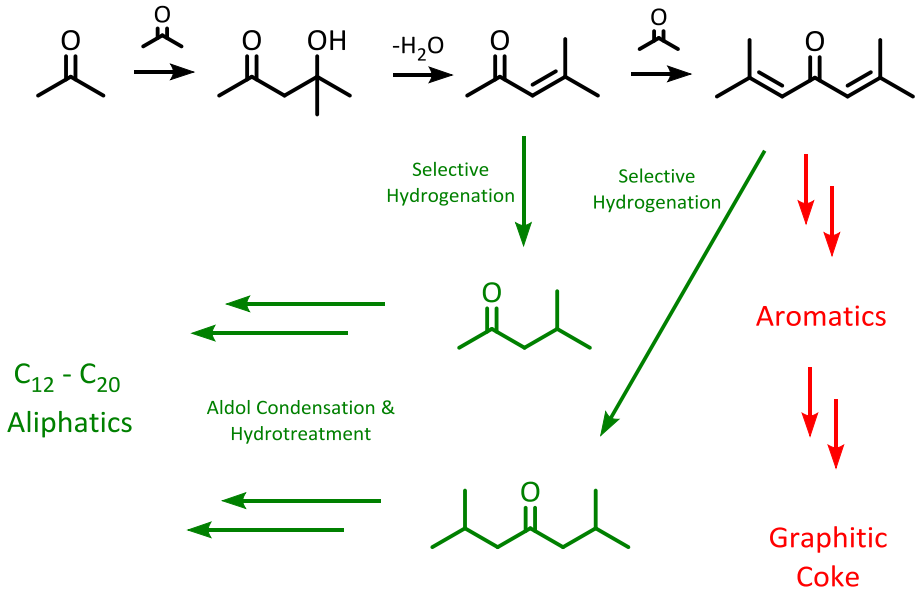

Scheme 5.2 Reaction products potentially formed by the selective hydrogenation of acetone self-condensation products

In this study the catalytic fast-pyrolysis of mesityl oxide with HZSM-5 and metal-exchanged ZSM-5 was examined so as to increase knowledge of the reaction and optimize the biomass-to-liquid fuel pyrolysis pathway. Product distribution of the upgraded vapours was monitored using a molecular beam mass spectrometer (MBMS) and, as such, were identified by their mass to charge ratio (*m/z*).

5.2 EXPERIMENTAL

5.2.1 MATERIALS

Ammonium ZSM-5 (SAR 30) zeolite powder was provided by Nexceris. Ammonium ZSM-5 (SAR 80 and 280) are proprietary commercial catalysts. Copper (II) nitrate hydrate, palladium (II) nitrate hydrate and mesityl oxide were provided by Sigma Aldrich, USA and used without further purification.

5.2.3 METHODS

5.2.3.1 CATALYST {REPARATION

HZSM-5

The acid form of ZSM-5 was achieved via calcination in flowing air. The catalyst was heated to 550 °C at a temperature ramp rate of 2 °C min^{-1} and held for 4 hours before being cooled to room temperature.

Metal-supported ZSM-5

Metal-supported ZSM-5 catalysts were prepared by incipient-wetness impregnation. The appropriate amount and concentration of metal nitrate solution was added to HZSM-5 to form a slurry which was allowed to dry overnight, prior to calcination of the same protocol as described for HZSM-5. The metal loadings were controlled at 0.2, 0.5 and 1 wt% for both copper and palladium.

5.2.3.2 CATALYTIC FAST PYROLYSIS

The reactor used for the reaction was a horizontal quartz annular flow tube reactor within a ceramic furnace coupled with an MBMS (Figure 5.4). The catalyst (0.5 g) was supported on quartz wool and packed into the inner tube of the reactor. The flow of mesityl oxide was controlled by a gas tight 5 ml syringe attached to an Orian Sage Model 365 syringe pump. For all reactions, mesityl oxide was injected at a flow of 0.12 ml min^{-1}, equal to 9.0% (x 1/100) flow set on the syringe pump. Upon

entering the reactor, the mesityl oxide was vapourised and carried over the catalyst with a flow of He (0.4 standard litres per minute, SLM), where the experiments were carried out in a helium environment, or a mixed flow of 0.2 SLM He & 0.2 SLM H_2 for those carried out in hydrogen-rich environments. This was then diluted with the outer flow of the reactor of 4 SLM He, along with a small flow of argon (0.04 SLM) as a reference gas for the MBMS. This flow was then sampled at the MBMS orifice.

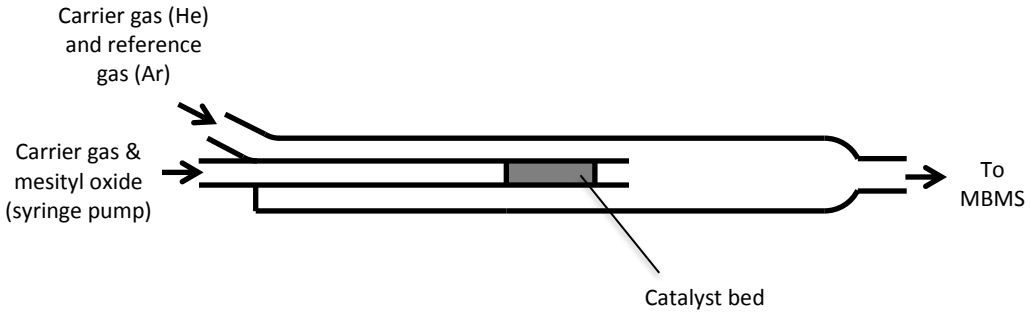

Figure 5.4 Simplified schematic of the horizonatal quartz annular flow tube reactor used in the catalytic fast pyrolysis reactions

The MBMS has been extensively reported as an effective method of biomass pyrolysis vapour analysis.[27] Upon sampling of the upgraded pyrolysis vapour through a 250 µm orifice, the gas undergoes adiabatic expansion in a vacuum chamber held at ~0.13 mbar. The cooled gas is then skimmed into a molecular beam and subjected to an electron ionisation source (22.5 eV). This produces positive ions which were analysed via a quadrupole mass spectrometer. Ions of mass 10-500 were collected and recorded at a rate of 1 Hz.

For each reaction, the carrier gases were allowed to flow with no mesityl oxide for 1 minute to provide a background spectrum for the experiment. After this time, the flow of mesityl oxide was started. The reaction period ended once the *m/z* for mesityl oxide (98) began to dominate to spectrum, or after 30 minutes of mesityl oxide flow.

5.3 Results and Discussion

5.3.1 Effect of Metal Loaded ZSM-5 (SAR 30) on the Conversion of Mesityl Oxide

5.3.1.1 HZSM-5 (SAR 30)

Helium atmosphere

Figure 5.5 shows mass spectra averaged over the period from which mesityl oxide was initially flowed through the system to the point where it was the dominant peak, for 150 °C, 250 °C and 350 °C under a helium atmosphere. At 150 °C, the majority of peaks seen were mesityl oxide (*m/z* 98), fragments of mesityl oxide (*m/z* 83, 55 and 43) and four species, peaks at *m/z* 119, 121, 134 and 136, that are not observed in the condensation of acetone, or classic pyrolysis compounds of species in this mass range. Though further qualitative analysis is required to identify these species it is possible that the species of *m/z* 119 and 121 are fragments of the species *m/z* 134 and 136, at a *m/z* difference of 15 is indicative of a methyl fragment loss. There was also a peak observed at *m/z* 178, likely to be due to the presence of isoxylitones, reported at being present in the condensation of acetone.[14] Increasing this temperature to 250 °C changes the product distribution. The starting material was still dominant, though peaks at *m/z* 56 and 41 were observed, likely due to butene and its associated fragment. The peaks *m/z* 119, 121 134 and 136 observed at 150 °C were not observed, suggesting that these products have reacted further or the temperature is high enough for an alternative pathway to dominate. The peak observed at *m/z* 196, not observed at 150 °C could potentially be due to the dimer of mesityl oxide. The dimerisation of mesityl oxide has been previously reported by Braude, *et al.* in 1956, whereby the reaction of mesityl oxide with *tert*-butyllithium produced 2-acetyl-1,3,3,5-tetramethylcyclohex-6-en-1-ol[28] (Figure 5.6), which has a mass of 196. The peak at *m/z* 153 would support this analysis, as the loss of the acetyl fragment (*m/z* 43), on the parent molecule would lead to this fragment.

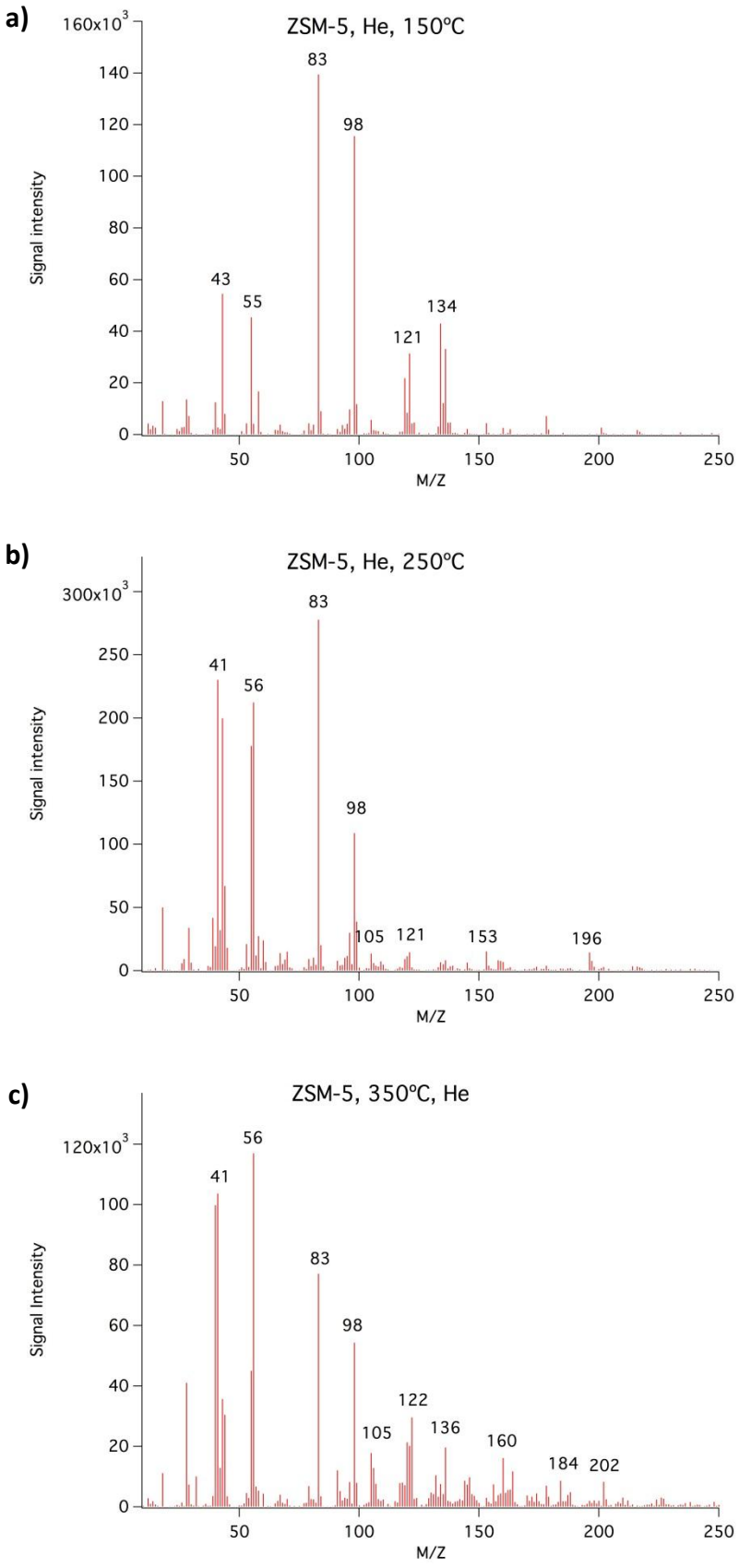

Figure 5.5 Mass spectrum of mesityl oxide vapours upgraded over HZSM-5 (SAR 30) in a He atmosphere at a) 150 °C, b) 250 °C and c) 350 °C

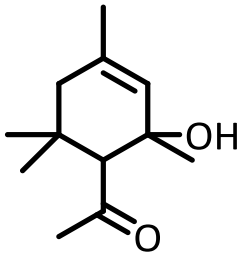

Figure 5.6 Mesityl oxide dimerisation product, 2-acetyl-1,3,3,5-tetramethylcyclohex-6-en-1-ol

Raising the temperature to 350 °C, produces a considerably larger amount of molecules (Figure 5.5, c). Though the starting products were still present, butene and its fragments dominate the spectrum. Aromatisation increased, as can be observed by the *m/z* values for toluene (*m/z* 91), xylene (*m/z* 106), mesitylene (*m/z* 120), dimethyl phenol (*m/z* 122), and trimethyl phenol (*m/z* 136). A wide number of larger molecules were also observed, particularly at *m/z* 164, 180 and 202. Though these require the further qualitative analysis to determine their structure, the mass *m/z* 202 could be due to the presence of pyrene, i.e. four fused aromatic rings, suggesting the beginning of aromatic oligomerisation and therefore graphitic coke production.[29] The production of fuel using HZSM-5 under these conditions, therefore, does not show much promise as ketonic species will not oligomerise efficiently.

Hydrogen atmosphere

The same technique was used to assess the reaction under a hydrogen atmosphere, over the same temperature range (Figure 5.7). Overall, there was little difference in the product distribution when compared to helium. However, at lower temperatures (150 °C and 250 °C), the presence of hydrogen seemed to inhibit the production of larger molecules. At 350 °C, this reduction of larger molecules was again observed, though there was a significantly larger proportion of smaller *m/z* aromatics (toluene, *m/z* 91; xylene *m/z* 106) than in the helium atmosphere. It seems likely that hydrogen potentially reduces coking, however, there was no significant production of non-aromatic oligomers, and so HZSM-5 is unsuitable for the upgrading of ketonic species.

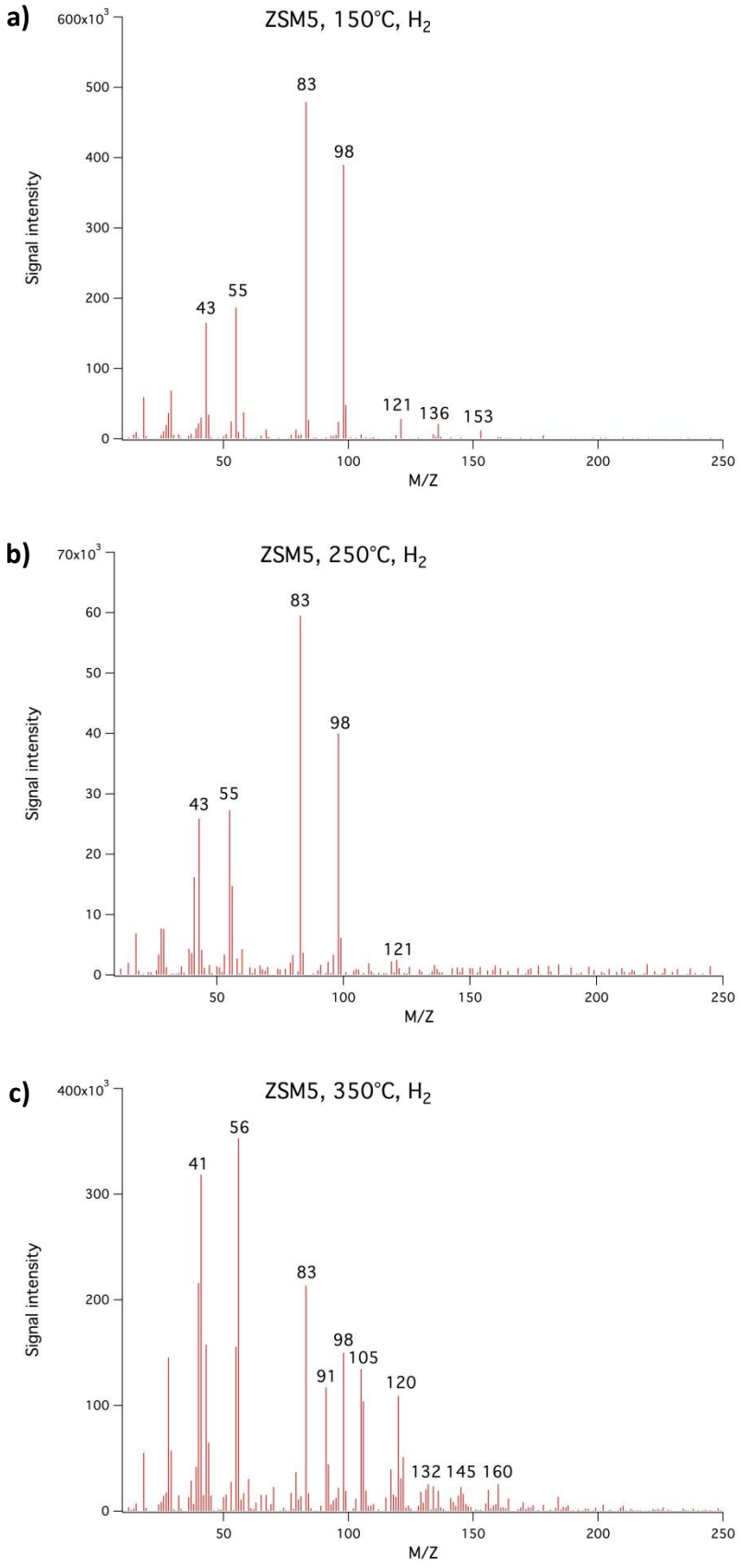

Figure 5.7 Mass spectrum of mesityl oxide vapours upgraded over ZSM-5 (SAR 30) in a H_2 atmosphere at a) 150 °C, b) 250 °C and c) 350 °C

5.3.1.2 Pd ZSM-5 (SAR 30)

Palladium-supported catalysts are well established hydrogenation catalysts,[30] as well as bifunctional catalysts for the condensation reaction of acetone.[20, 23, 24] As such, palladium-supported ZSM-5 catalysts were investigated for their potential to produce oligomeric species from mesityl oxide. Three different Pd loadings (0.2 wt%, 0.5 wt% and 1 wt%) were produced via incipient wetness, assuring that all the palladium added was present in the catalyst structure.

Helium atmosphere

Figure 5.8 shows the mass spectra averaged over the period from which mesityl oxide was initially flowed through the system (containing a packed bed of Pd [0.2 wt%] ZSM-5) to the point where mesityl oxide was the dominant peak, in a helium atmosphere. For the cases where the *m/z* for mesityl oxide did not become dominate, the flow was stopped after 30 minutes of continuous flow. The mass spectrums for the higher palladium loadings can be seen in appendices C.1 and C.2.

At lower temperatures (150 °C and 250 °C), there was no significant difference in the products formed than on using HZSM-5. There were, however, a lower proportion of larger molecules, as well as a lower proportion of butene (and associated fragments), produced. This was similarly seen for Pd (0.5 wt%) ZSM-5 and Pd (1 wt%) ZSM-5, though the production of butene increased with increasing Pd wt%. At 350 °C with Pd (0.2 wt%) ZSM-5, however, very little starting product was observed. At this temperature, the vast majority of the products were common aromatic pyrolysis products, benzene (*m/z* 78), toluene (*m/z* 91), xylene (*m/z* 106), mesitylene (*m/z* 120), as well as resultant products of aromatic cracking, ethene (*m/z* 28) and butene (*m/z* 56). This was similarly seen for Pd (0.5 wt%) ZSM-5 and Pd (1 wt%) ZSM-5, though the catalyst completely coked within 30 minutes and so there is a considerable about of starting product present.

For Pd (0.2 wt%) ZSM-5, however, other peaks were also observed. The peak at *m/z* 156 could be due to the presence of semiphorone, present in the condensation of acetone, or it's cyclisation product, 2,2,6,6-tetramethyl pyron-4-one.

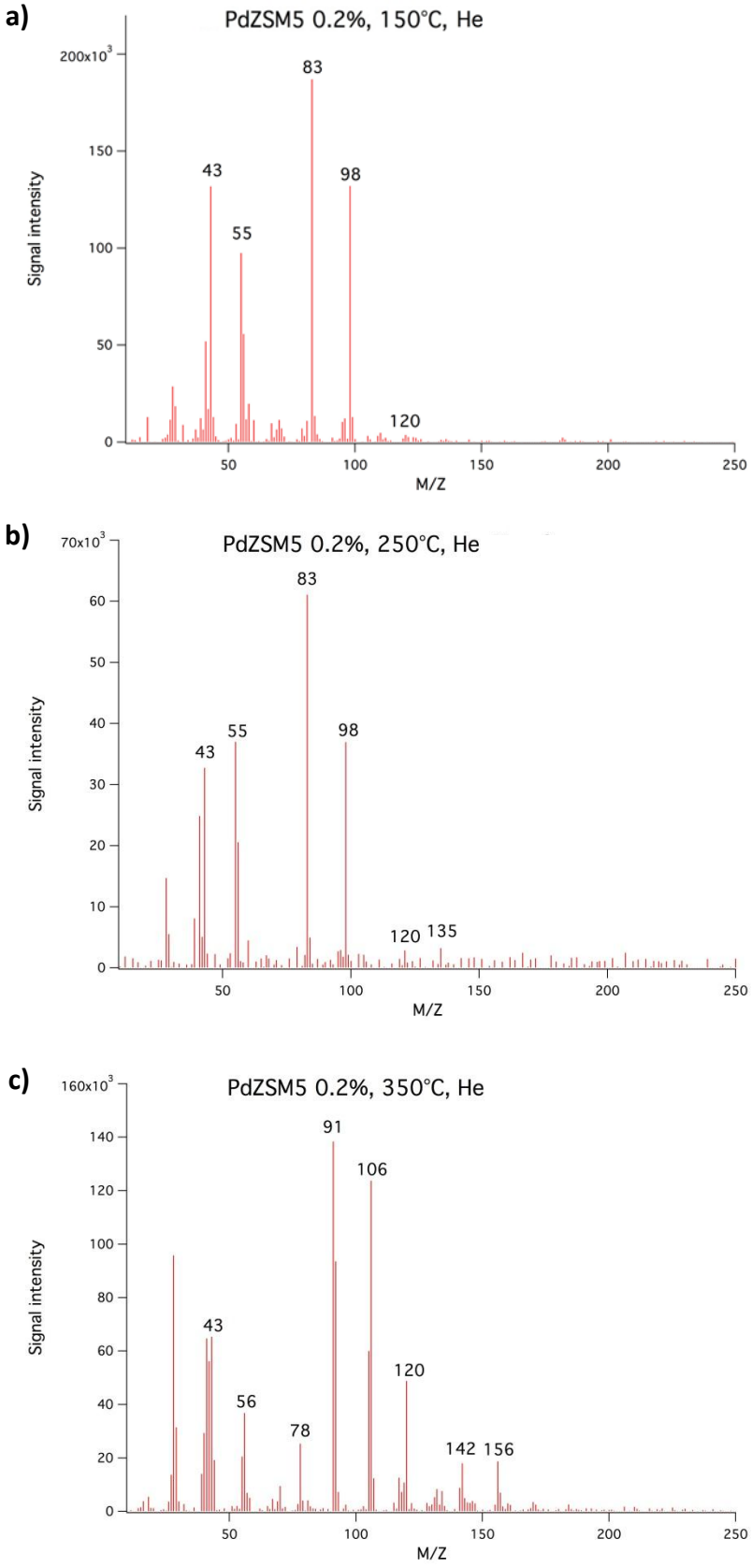

Figure 5.8 Mass spectrum of mesityl oxide vapours upgraded over Pd (0.2 wt%) ZSM-5 (SAR 30) in a He atmosphere at a) 150 °C, b) 250 °C and c) 350 °C

Hydrogen atmosphere

The same experimental set-up was used to assess the effect of hydrogen on the reaction products.

At 150 °C, Pd (0.2% wt) ZSM-5 hydrogenated the vast majority of mesityl oxide to MIBK, *m/z* 100 (Figure 5.9, a). The majority of the mass spectrum under these conditions is from MIBK and its fragments (*m/z* 43, 58, 85). Small peaks at *m/z* 158 and 200, however, were observed. The peak at *m/z* 200 could potentially be due to the dimer of MIBK. As has been previously discussed, the dimerisation of mesityl oxide has been reported to yield 2-acetyl-1,3,3,5-tetramethylcyclohex-6-en-1-ol (*m/z* 196) (Figure 5.6). This molecule, however, only possesses one carbon to carbon double bond. If it underwent selective hydrogenation in the same manner of MIBK (i.e. only olefinic double bonds), the resultant molecule would be of *m/z* 198 rather than the *m/z* 200 observed in the mass spectrum. The carbonyl present would also have to undergo hydrogenation to an alcohol moiety to produce a molecule of *m/z* 200, though carbonyl hydrogenation is unlikely at this temperature.[25] Furthermore, if the carbonyl was hydrogenated to an alcohol, fragmentation would lead to a significant peak at *m/z* 155, rather than the peak at *m/z* 158 observed. Assuming the peak at *m/z* 158 is a fragment of the parent molecule at *m/z* 200, the difference (42) is indicative of an acetyl fragment, further suggesting that carbonyl bonds have remained intact. This would suggest, therefore, that the dimer must have a double bond. Proposed mechanisms for this dimerisation and subsequent hydrogenation have been proposed in figure 5.10. Firstly, via acid-catalysed aldol condensation, the 6-hydroxy-2,6,8-trimethyl-4-nonanone is produced, and secondly via Michael addition, 8-hydroxy-2,6,6-trimethyl-4-nonanone is produced.

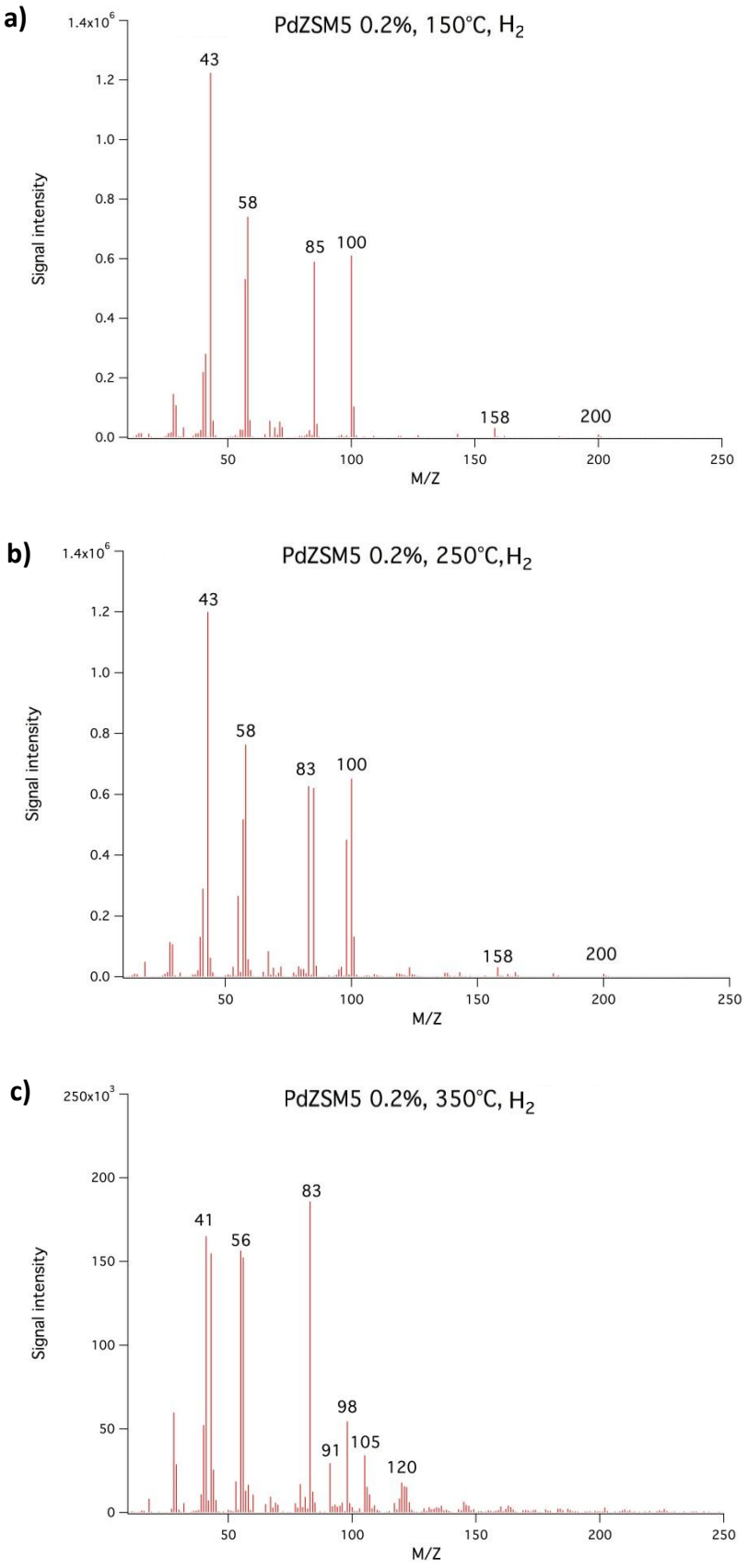

Figure 5.9 Mass spectrum of mesityl oxide vapours upgraded over Pd (0.2 wt%) ZSM-5 (SAR 30) in a H_2 atmosphere at a) 150 °C, b) 250 °C and c) 350 °C

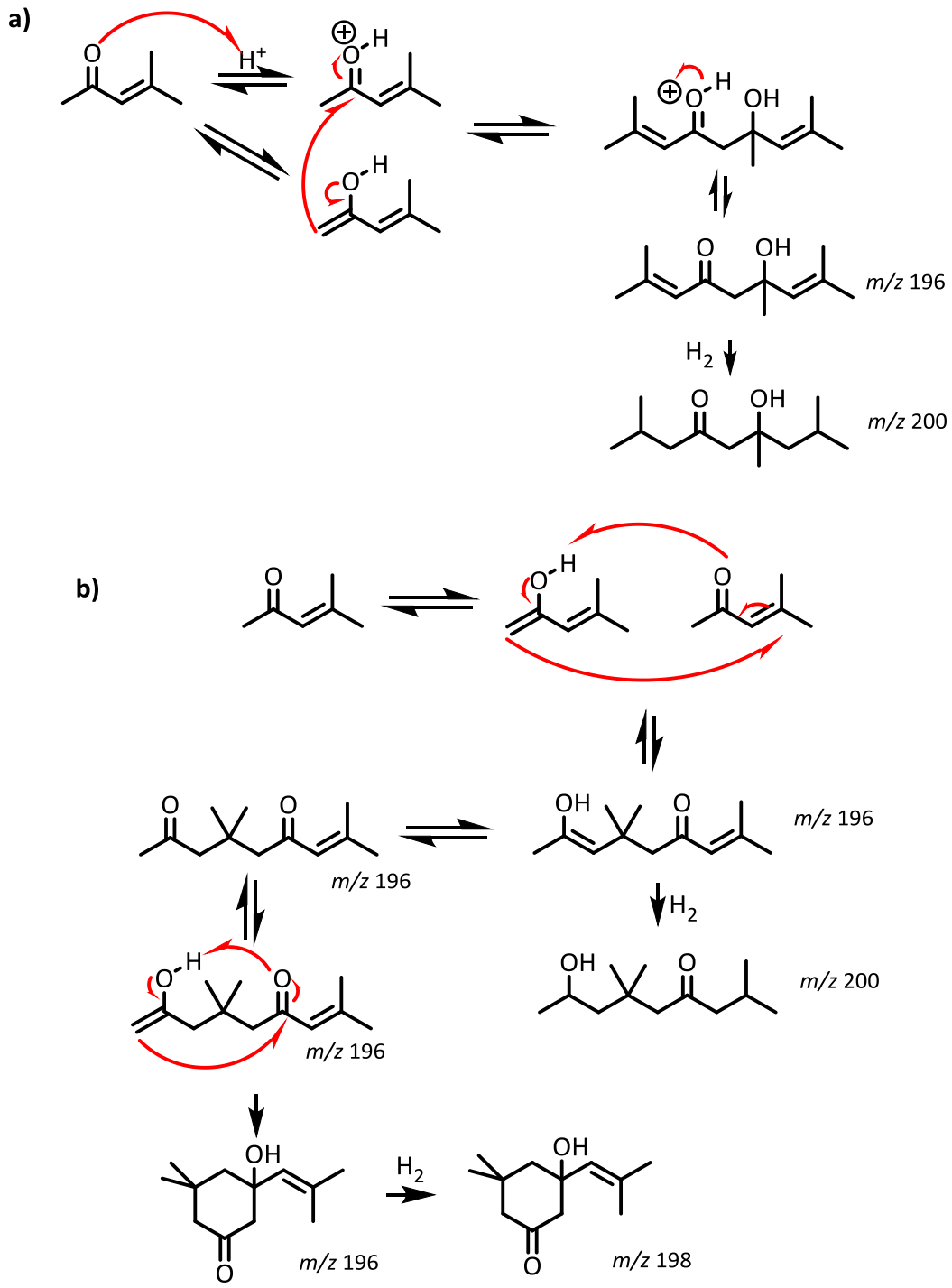

Figure 5.10 Proposed possible mechanisms for the production of molecule of *m/z* 200. a) Aldol condensation, b) Michael addition

Identification of these products (and therefore the reaction mechanism) would require further qualitative analysis (such as GC-MS). The mechanisms in figure 5.10 are not the only possible reactions. It is possible that the mesityl oxide is hydrogenated to MIBK before dimerisation. The lack of dimerisation present in a

helium atmosphere would support this, though dimers of mesityl oxide were observed using only HZSM-5. As the dimer of MIBK was not identified specifically, it will be referred to as di(methyl *iso*-butyl ketone), or DMIBK.

Increasing the temperature of the reaction to 250 °C (Figure 5.9, b) decreases the conversion of mesityl oxide to MIBK, as a proportional amount of starting product (*m/z* 98), and its fragments were observed. DMIBK and its assumed fragment at *m/z* 158, however, were still observed in small amounts. At 350 °C (Figure 5.9, c), the hydrogenation of mesityl oxide to MIBK, as well as the dimerisation and subsequent hydrogenation to DMIBK were not observed. The spectrum was dominated by mesityl oxide and butene, as well as aromatisation products toluene, xylene and mesitylene.

Increasing the palladium loading to 0.5 wt% and 1 wt% had little effect at 150 °C, with the only peaks observed being those of MIBK, DMIBK and their associated fragments (Appendices C.4 and C.5). No significant difference to the product distribution was observed. At 250 °C, however, with Pd (0.5 wt%) ZSM-5, all of the mesityl oxide was converted over the limited reaction time of 30 minutes. Pd (1 wt.%) ZSM-5, however, converted some of the mesityl oxide to MIBK though some mesityl oxide was observed throughout the reaction. Due to the presence of mesityl oxide through the reaction, rather than a change in production over the reaction period, this would be due to a poorly packed catalyst bed, allowing the mesityl oxide a path through without contact with the catalyst. At 350 °C, for both Pd (0.5 wt%) ZSM-5 and Pd (1 wt.%) ZSM-5, no hydrogenation products nor starting materials were observed. The mass spectrums are dominated by butene, and the aromatic products toluene, xylene, mesitylene and tetramethyl benzene (*m/z* 134). It should be noted that there was little oligomerisation of the aromatic species observed at these conditions, and therefore less coking.

Pd-supported ZSM-5 catalysts, therefore, can hydrogenate mesityl oxide (as has been reported previously) and to a limited extend, produce dimers of hydrogenated mesityl oxide. To produce more suitable fuel molecules, however, the competing oligomerisation reactions need to be more prevalent.

5.3.1.3 Cu ZSM-5 (SAR 30)

In an attempt to increase the production of oligomers rather than direct hydrogenation of mesityl oxide, Cu-supported ZSM-5 catalysts were investigated for their activity in the reactions with mesityl oxide. Three loadings were used etc.etc.… Cu-supported zeolites have been reported as active for aliphatic production from acetone, though not in the presence of hydrogen.[17] Cu-supported catalysts, however, have been reported as being active for hydrogenation of acetone self-condensation products, though these were supported on MgO.[31]

Helium atmosphere

Similarly to the Pd impregnated catalyst runs, the Cu ZSM-5 was loaded on in a packed bed and the reactions run to the point where mesityl oxide was the dominant peak. Mass spectrums for higher copper loadings can be seen in the appendices C.5 and C.6.

At 150 °C, very little difference from HZSM-5 was observed, however there were less peaks at *m/z* 119, 121, 134 and 136 (Figure 5.11). At this temperature the mass spectrum is dominated by the starting products and their fragments, though a small number of higher molecular weight products at *m/z* 153 and 178 (indicative of isoxylitones) were observed. At higher copper loadings a similar trend was observed, though at 1 wt% copper even less of the peaks at *m/z* 119, 121, 134 and 136, and as well as less of the peaks at *m/z* 153 and 178 than at lower loadings. Similar observations were made at all catalyst loadings at 200 °C.

Little difference was observed upon increasing the reaction temperature to 250 °C over all the copper loadings tested, though a small amount of aromatic species was produced, including toluene, xylene and mesitylene. The presence of copper seemed to inhibit the production of butene, at these temperatures.

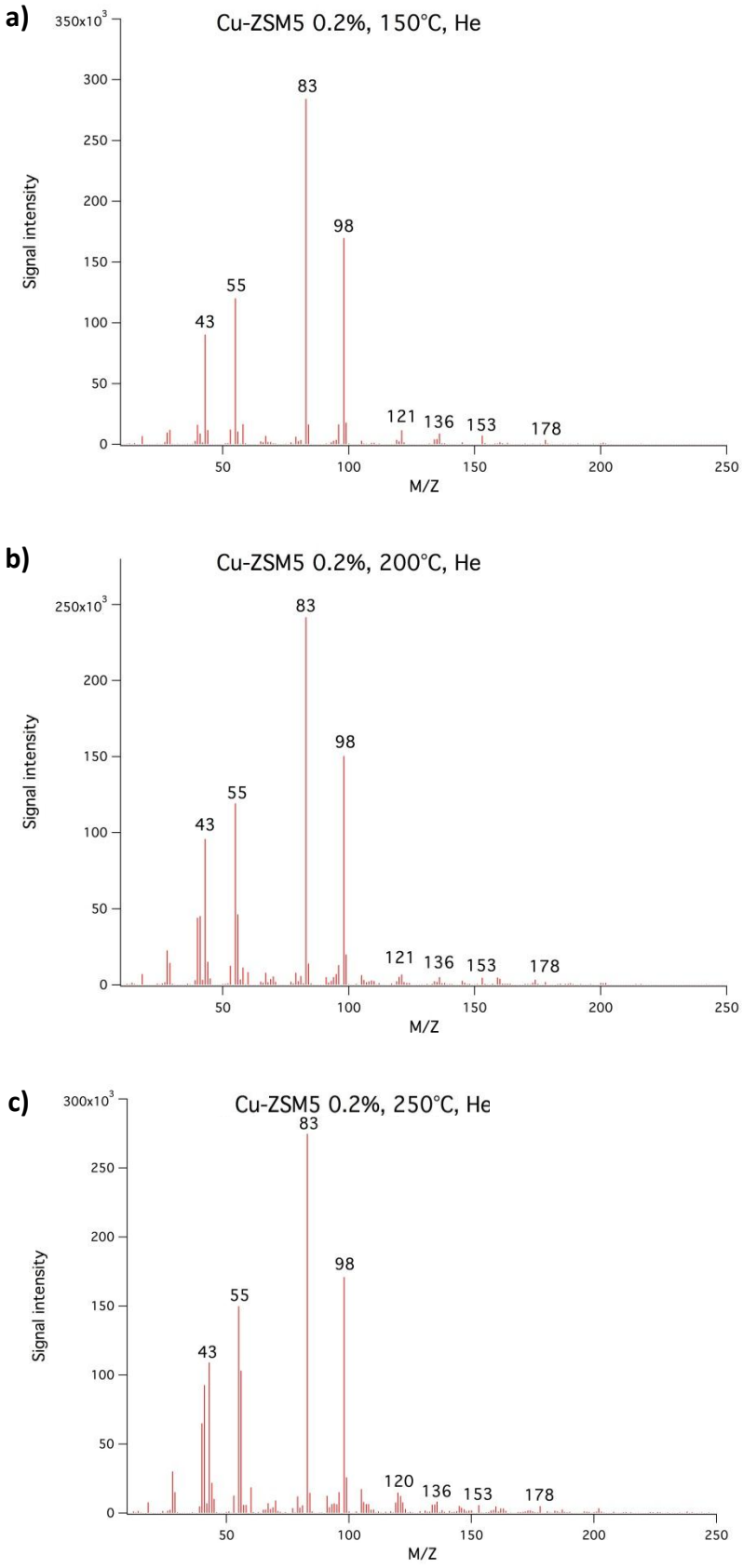

Figure 5.11 Mass spectrum of mesityl oxide vapours upgraded over Cu (0.2 wt%) ZSM-5 (SAR 30) in a He atmosphere at a) 150 °C, b) 200 °C and c) 250 °C

Hydrogen atmosphere

Copper-supported ZSM-5 catalysts were assessed for their activity for mesityl oxide conversion in the presence of hydrogen. Similar conditions to previous experiments were used. These experiments, using a copper loading of 0.2% wt on ZSM-5 can be seen in figure 5.12, while larger copper loadings can be found in appendices C.7 and C.8.

Little difference was observed between using the Cu ZSM catalysts under a hydrogen atmosphere when compared to a helium atmosphere. The mass spectrums for all copper catalysts used at 150 °C and 200 °C are dominated by the starting materials and their associated fragments, as well as very small amounts of larger reactants. With increasing reaction temperature, the amount of *iso*-butene produced increases. At 250 °C, aromatic species for all catalysts tested were observed in small amounts. Due to the inactivity of copper for the conversion or hydrogenation of mesityl oxide, it was not tested at temperatures above 250 °C.

Copper-supported ZSM-5 catalysts appear inactive for the desired oligomerisation reactions, though are also inactive for the undesirable aromatisation. This inactivity towards aromatic production has been attributed to the altered ratio between the Lewis and Brønsted acid sites.[17] For example, Cu-supported β-zeolites have been reported as having prominent Lewis acids of medium strength, while possessing only a few strong Brønsted sites, required for these reactions. The inactivity of copper hydrogenation is also unsurprising, as the only previously reported hydrogenation reaction by copper is the selective hydrogenation of CO_2 to methanol, supported on either ZnO or Cr_2O_3.[32]

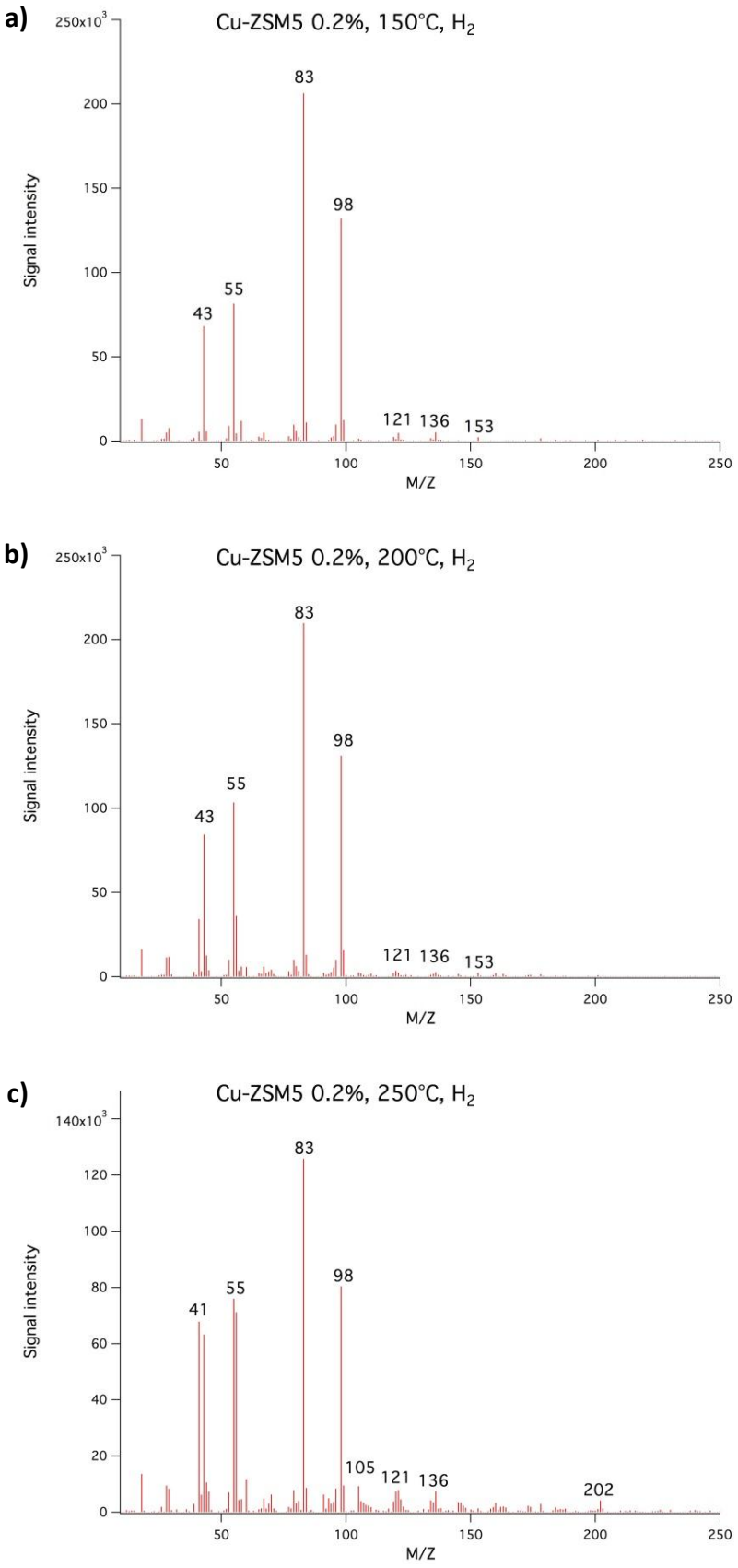

Figure 5.12 Mass spectrum of mesityl oxide vapours upgraded over Cu (0.2 wt%) ZSM-5 (SAR 30) in a H_2 atmosphere at a) 150 °C, b) 200 °C and c) 250 °C

5.3.2 Effect of Silicon / Alumina ratio on Pd-supported ZSM-5

The altering of the SAR of a zeolite changes the acidity of the overall structure and therefore its reactivity. In an attempt to alter the balance between hydrogenation and desirable oligomerisation, the reaction was carried out using Pd-supported ZSM-5 (0.2 wt%, 0.5 wt% and 1 wt%) of higher SAR. An identical reaction set up was used for the higher SAR zeolites as presented previously. All mass spectra discussed in this section are presented in appendices C.9 to C.14.

5.3.2.1 Pd ZSM-5 (SAR 80)

Helium atmosphere

At 150 °C, little conversion of the mesityl oxide was observed over all the palladium loadings tested. At 250 °C, Pd (0.2 wt%) ZSM-5 showed a small amount of *m/z* 153 being produced. Increasing the palladium loading, however, seems to promote aromatisation, as toluene and xylene were observed with Pd (0.5 wt%) ZSM-5 and toluene, xylene, mesitylene and tetramethylbenzene observed with Pd (1 wt%) ZSM-5. Increasing the temperature to 350 °C drastically increased the amount of larger molecules produced for all palladium loadings, with significant amounts of aromatics being produced.

Hydrogen atmosphere

At 150 °C, for Pd (0.2 wt%) ZSM-5, all mesityl oxide was converted, the vast majority of which was converted to MIBK, with a small amount of DMIBK also observed. This was similarly the case for Pd (0.5 wt%) ZSM-5 and Pd (1 wt%) ZSM-5 at this temperature. Upon increasing the reaction time to 250 °C, proportional amounts of starting material were seen with Pd (0.2 wt%) ZSM-5 and Pd (0.5 wt%) ZSM-5, though near-complete conversion of mesityl oxide was observed with Pd (1 wt%) ZSM-5, and of similar product distribution to 150 °C.

Interestingly, increasing the temperature to 350 °C reduced the conversion of mesityl oxide substantially, for Pd (0.2 wt%) ZSM-5 and Pd (0.5 wt%) ZSM-5. For Pd (0.2 wt%) ZSM-5, no aromatic species were observed, though Pd (0.5 wt%) ZSM-%

exhibited small amounts of toluene and xylene. This is significantly different to the catalysts of lower SAR, where a considerable amount of aromatic species were observed at this temperature. For Pd (1 wt%) ZSM-5, a small amount of conversion to MIBK was observed though the spectrum is dominated by aromatic species and cracking products. This is different to the catalyst of lower SAR, however, where only aromatic species were observed.

Increasing the SAR of the catalyst to 80 did not significantly increase the amount of useful aliphatic oligomerisation, however it did reduce aromatisation. The reduction of aromatic hydrocarbons with increasing SAR has been observed with previous reports.[33-34] This is presumably due to a reduction in the acidity of the catalyst overall, and therefore the reactivity. Reactions with require higher activation energies, therefore, are also significantly reduced.

5.3.2.2 Pd ZSM-5 (SAR 280)

The SAR of the catalyst was increased to 280 in an attempt to increase useful aliphatic oligomerisation. The reaction was carried out using Pd-supported ZSM-5 (0.2 wt%, 0.5 wt% and 1 wt%) as presented above. An identical reaction set up was used, all mass spectra discussed in this section are presented in appendices C.15-C.20.

Helium atmosphere

For all catalyst loadings, over all the temperatures examined, there was little conversion observed. The spectrums were dominated by mesityl oxide and its fragments. The only peak observed larger than mesityl oxide was *m/z* 153, and was observed in higher amounts than has been seen previously. Though this has been previously suggested as a fragment of the dimer of mesityl oxide, the lack of a peak at *m/z* 196 seems to indicate that this is a different, stable species.

Hydrogen atmosphere

At 150 °C, as with catalysts of lower SAR, the vast majority of mesityl acetone is reduced to MIBK, with a small amount of conversation to DMIBK. Palladium loading

does not seem to have a significant effect on the product distribution. Increasing this temperature to 250 °C, near-complete conversion was similarly observed across all palladium loadings. At 350 °C, however, the spectrums for Pd (0.2 wt%) ZSM-5 and Pd (0.5 wt%) ZSM-5 exhibit little conversion, similar to the catalysts of lower SAR. For Pd (1 wt%) ZSM-5 the conversion of mesityl oxide to MIBK is still observed, though proportional amounts of starting material are also present. Unlike catalysts with low SAR, little aromatic species were produced. This is, again, likely to be due to the reduced activity associated with fewer acidic sites.

5.4 SUMMARY

In this study, an investigation into the production of aliphatic oligomers via selective hydrogenation and oligomerisation of the initial self-condensation product of acetone – mesityl oxide – was carried out, using HZSM-5, Pd-ZSM-5 and Cu-ZSM-5. The aim of the study was to further understand the mechanistic changes of ketonic species present in biomass pyrolysis vapours, and investigate the viability of these catalysts as hydrogenation and oligomerisation catalysts whilst simultaneously reducing aromatisation.

Upon using HZSM-5, little useful conversion to known oligomers was observed. However, at lower temperatures, conversion to molecules of *m/z* 119, 121, 134 and 136 were observed. Though these are *m/z* assignable to aromatic species typically found in pyrolysis vapours, aromatic species are usually not seen at these lower temperatures. A species of *m/z* 196 was identified at 250 °C, likely due to the dimerisation of mesityl oxide, though elucidation of its structure would require further analysis. Increasing the temperature of the reaction led to a significant production of aromatic and graphitic coke precursors. Under a hydrogen atmosphere similar products were observed.

PdZSM-5 (SAR 30) showed significant amounts of hydrogenation of mesityl oxide to MIBK, and small amounts of dimerisation, though further work is needed to qualify the species. The mass of the dimer along with the temperature at which the hydrogenation took place suggest that is it unlikely that the dimer is the result of a cyclisation reaction as has been reported previously. Whether it is a result of hydrogenation to MIBK followed by aldol condensation, or the result of oligomerisation followed by hydrogenation, is unclear and requires further analysis to determine. Increasing the temperature of the reaction, the selectivity for hydrogenation decreased and the amount of aromatics produced increased. Similarly, increasing the palladium loading increased the selectivity for aromatic and cracking species at high temperatures, though inhibited the production of graphitic coke precursors.

Due to the small amount of oligomerisation with PdZSM-5 (SAR 30) when compared with the hydrogenation, CuZSM-5 (SAR 30) was investigated. However, for all catalyst loadings over all temperatures, little conversion of mesityl oxide was observed. The presence of copper on the zeolite seems to inhibit the reactions that mesityl oxide would otherwise undergo.

Increasing the SAR to 80 and 280 for PdZSM-5 was then investigated. Interestingly, for SAR 80, all catalysts hydrogenated mesityl oxide to MIBK at 150 °C (with small amounts of dimerisation), though this hydrogenation decreased as the temperature increased. For 0.2 and 0.5 wt% Pd, the mass spectrums at 350 °C were dominated by the starting material, whereas 1 wt% was selective for aromatisation. Increasing the SAR further to 280, little conversion for all catalyst loadings over all temperatures in helium was seen. Under a hydrogen atmosphere, however, hydrogenation was the prevalent reaction at higher temperatures, without significant amounts of competing aromatisation. Near-complete hydrogenation of mesityl oxide to MIBK was observed for all catalysts up to 250 °C, though the mass spectrums are dominated by the starting material for 0.2 and 0.5 wt% Pd. At 1 wt%, Pd, however, proportional amounts of starting material and hydrogenated MIBK were observed with minimal aromatisation. Though significant production of fuel-like carbon-number molecules was not achieved, directed catalytic fast pyrolysis of biomass remains an interesting and challenging subject of research and warrants further investigation.

5.5 REFERENCES

1. Bridgwater, A. V., *Fast Pyrolysis of Biomass: A Handbook*. CPL Press: 2005.
2. Bridgwater, A. V., Review of fast pyrolysis of biomass and product upgrading. *Biomass and Bioenergy* **2012,** *38*, 68-94.
3. Gayubo, A. G.; Aguayo, A. T.; Atutxa, A.; Aguado, R.; Olazar, M.; Bilbao, J., Transformation of Oxygenate Components of Biomass Pyrolysis Oil on a HZSM-5 Zeolite. II. Aldehydes, Ketones, and Acids. *Industrial & Engineering Chemistry Research* **2004,** *43* (11), 2619-2626.
4. Gayubo, A. G.; Aguayo, A. T.; Atutxa, A.; Aguado, R.; Bilbao, J., Transformation of Oxygenate Components of Biomass Pyrolysis Oil on a HZSM-5 Zeolite. I. Alcohols and Phenols. *Industrial & Engineering Chemistry Research* **2004,** *43* (11), 2610-2618.
5. Suib, S. L., *New and Future Developments in Catalysis: Catalysis for Remediation and Environmental Concerns*. Elsevier Science: 2013.
6. Ruddy, D. A.; Schaidle, J. A.; Ferrell Iii, J. R.; Wang, J.; Moens, L.; Hensley, J. E., Recent advances in heterogeneous catalysts for bio-oil upgrading via "ex situ catalytic fast pyrolysis": catalyst development through the study of model compounds. *Green Chemistry* **2014,** *16* (2), 454-490.
7. Rahimi, N.; Karimzadeh, R., Catalytic cracking of hydrocarbons over modified ZSM-5 zeolites to produce light olefins: A review. *Applied Catalysis A: General* **2011,** *398* (1–2), 1-17.
8. Jacobs, P. A.; Flanigen, E. M.; Jansen, J. C.; van Bekkum, H., *Introduction to Zeolite Science and Practice*. Elsevier Science: 2001.
9. Olson, D. H.; Kokotailo, G. T.; Lawton, S. L.; Meier, W. M., Crystal structure and structure-related properties of ZSM-5. *The Journal of Physical Chemistry* **1981,** *85* (15), 2238-2243.
10. Fujiyama, S.; Seino, S.; Kamiya, N.; Nishi, K.; Yoza, K.; Yokomori, Y., Adsorption structures of non-aromatic hydrocarbons on silicalite-1 using the single-crystal X-ray diffraction method. *Physical Chemistry Chemical Physics* **2014,** *16* (30), 15839-15845.
11. Chang, C. D.; Silvestri, A. J., The conversion of methanol and other O-compounds to hydrocarbons over zeolite catalysts. *Journal of Catalysis* **1977,** *47* (2), 249-259.
12. Ramasamy, K. K.; Gerber, M. A.; Flake, M.; Zhang, H.; Wang, Y., Conversion of biomass-derived small oxygenates over HZSM-5 and its deactivation mechanism. *Green Chemistry* **2014,** *16* (2), 748-760.
13. Fuhse, J.; Bandermann, F., Conversion of organic oxygen compounds and their mixtures on H-ZSM-5. *Chemical Engineering & Technology* **1987,** *10* (1), 323-329.
14. Salvapati, G. S.; Ramanamurty, K. V.; Janardanarao, M., Selective catalytic self-condensation of acetone. *Journal of Molecular Catalysis* **1989,** *54* (1), 9-30.
15. Tago, T.; Konno, H.; Sakamoto, M.; Nakasaka, Y.; Masuda, T., Selective synthesis for light olefins from acetone over ZSM-5 zeolites with nano- and macro-crystal sizes. *Applied Catalysis A: General* **2011,** *403* (1–2), 183-191.
16. Grassian, V. H., *Environmental Catalysis*. Taylor & Francis: 2005.
17. Cruz-Cabeza, A. J.; Esquivel, D.; Jiménez-Sanchidrián, C.; Romero-Salguero, F. J., Metal-Exchanged β Zeolites as Catalysts for the Conversion of Acetone to Hydrocarbons. *Materials* **2012,** *5* (1), 121-134.
18. Nishimura, S., *Handbook of Heterogeneous Catalytic Hydrogenation for Organic Synthesis*. Wiley: 2001.
19. Yin, L.; Liebscher, J., Carbon-carbon coupling reactions catalyzed by heterogeneous palladium catalysts. *Chemical Reviews* **2007,** *107* (1), 133-173.
20. Chen, P.; Chu, S.; Chang, N.; Chuang, T.; Chen, L., A New Catalyst for Mibk Synthesis—Palladium on ZSM-5 Zeolites. *Studies in Surface Science and Catalysis* **1989,** *46*, 231-239.
21. Chang, N. S.; Chen, P. Y.; Chen, C. C.; Chu, S. J.; Chuang, T.; Lin, W. C. (1991), *Preparation of methyl isobutyl ketone*. US Patent: US5059724A.
22. Chen, P.; Chu, S.; Lin, W.; Wu, K.; Yang, C., The synthesis of methyl isobutyl ketone over palladium supported zeolites. *Studies in Surface Science and Catalysis* **1994,** *83*, 481-488.
23. Bombos, D.; Bozga, G.; Bombos, M.; Stefan, A.; Stanciu, I., Reductive Condensation of Acetone to Methyl Isobutyl Ketone on a Bifunctional Catalyst. C*hemical Papers-Slovak Academy of Sciences* **2000,** *54* (3), 171-176.

24. Yang, P.; Shang, Y.; Wang, J.; Yu, J.; Wu, T., Effect of acidic and metallic sites on the catalytic performance of Pd/ZSM-5 catalysts in the one-step synthesis of mibk. *Reaction Kinetics and Catalysis Letters* **2007,** *91* (2), 391-398.
25. Elliott, D. C., Historical Developments in Hydroprocessing Bio-oils. *Energy & Fuels* **2007,** *21* (3), 1792-1815.
26. Al-Hazmi, M.; Choi, Y.; Apblett, A., Acetone Condensation Over Sulfated Zirconia Catalysts. *Catalysis Letters* **2013,** *143* (7), 705-716.
27. Mukarakate, C.; Zhang, X.; Stanton, A. R.; Robichaud, D. J.; Ciesielski, P. N.; Malhotra, K.; Donohoe, B. S.; Gjersing, E.; Evans, R. J.; Heroux, D. S., Real-time monitoring of the deactivation of HZSM-5 during upgrading of pine pyrolysis vapors. *Green Chemistry* **2014,** *16* (3), 1444-1461.
28. Braude, E. A.; Gofton, B. F.; Lowe, G.; Waight, E. S., 782. The dimerisation of mesityl oxide. A novel type of diene addition. *Journal of the Chemical Society (Resumed)* **1956,** (0), 4054-4060.
29. Eisenbach, D.; Gallei, E., Infrared spectroscopic investigations relating to coke formation on zeolites: I. Adsorption of hexene-1 and n-hexane on zeolites of type Y. *Journal of Catalysis* **1979,** *56* (3), 377-389.
30. Aboul-Gheit, A. K.; Aboul-Fotouh, S. M.; Aboul-Gheit, N. A. K., Hydroconversion of cyclohexene using catalysts containing Pt, Pd, Ir and Re supported on H-ZSM-5 zeolite. *Applied Catalysis A: General* **2005,** *283* (1–2), 157-164.
31. Chikán, V.; Molnár, Á.; Balázsik, K., One-Step Synthesis of Methyl Isobutyl Ketone from Acetone and Hydrogen over Cu-on-MgO Catalysts. *Journal of Catalysis* **1999,** *184* (1), 134-143.
32. Twigg, M. V.; Spencer, M. S., Deactivation of supported copper metal catalysts for hydrogenation reactions. *Applied Catalysis A: General* **2001,** *212* (1–2), 161-174.
33. Mukarakate, C.; Watson, M. J.; ten Dam, J.; Baucherel, X.; Budhi, S.; Yung, M. M.; Ben, H.; Iisa, K.; Baldwin, R. M.; Nimlos, M. R., Upgrading biomass pyrolysis vapors over β-zeolites: role of silica-to-alumina ratio. *Green Chemistry* **2014**, *16*, 4891-4905.
34. Ben, H.; Ragauskas, A. J., Influence of Si/Al Ratio of ZSM-5 Zeolite on the Properties of Lignin Pyrolysis Products. *ACS Sustainable Chemistry and Engineering* **2013,** *1* (3), 316-324.

CHAPTER 6

CONCLUSIONS AND FUTURE WORK

6.1 CONCLUSIONS

The overall aim of this thesis was to compare and contrast a number of biofuel technologies in terms of their potential to produce fuels of enhanced sustainability, physical properties, and ability to be produced by a process for which the product distribution could be tailored.

The first technology assessed was the production of biodiesel from spent coffee, examining the variability between the different geographic origins, bean types and brewing processes of the coffee. The oil yield was comparable to that of current biodiesel feedstocks, and the fatty acid profile of these oils differed little. Despite this, there was notable variation in the physical properties of the coffee biodiesel, presumably due to the presence of different biomolecules which affect the intermolecular interactions. Regardless of the variation, all biodiesel samples fell within the physical property range outlined by international standards. However, the fuel produced possessed all the technical issues that are inherent to biodiesel, and therefore the alternative chemical transformation of metathesis on triglycerides was assessed.

Cross-metathesizing triglyceride model compounds with a range of potentially sustainable alkene sources and catalyst systems led to the conclusion that Hoveyda Grubbs 2nd generation catalyst and ethene was the best option for the production of fuels from the triglycerides. Subsequent to reaction condition optimisation, a variety of natural triglycerides were cross-metathesized with ethene. From this reaction both an aviation transport fuel fraction and a road transport fuel fraction were produced. The road transport fuel fraction fell within the US standard for biodiesel and the physical properties were similar to those of common biodiesels. Though the fuel contained a significant proportion of short-chain FAMEs, it contained an even higher proportion of saturates than would have been present had the oils been transesterified directly, leading to little improvement in the physical properties. Furthermore, the lower C/O ratio caused the road transport fractions to be lower in energy density than conventional biodiesel. However, the stability of the fuel is assumed to have increased due to the removal of

polyunsaturated components. Upon comparison with the production of biodiesel from coffee, there is little improvement of the road transport fraction from metathesis. However, the production of the aviation fuel fraction, which possessed a higher energy density and lower viscosity of Jet A-1, as well as a volatile hydrocarbon fraction that could be used to produce higher value products such as polymers, show that the process as a whole could have the potential for an economically viable biorefinery. Additionally, the adjustment of reaction conditions such as ethene pressure could adjust the size and composition of each fraction, allowing some level of control over the ultimate fuel structure.

Upon removal of the lipids from any biological source, however, a significant amount of biomass remains which could be fermented. Fermentation is an attractive method for the production of specific fuels, due to the inherent selectivity of metabolic pathways. Bioethanol, the standard fuel from fermentation, possesses a number of undesirable properties. Therefore, a range of alternate products which could potentially be produced by fermentation were assessed for their fuel properties and compared to the international standards. Butyl butyrate was deemed a suitable Jet A-1 replacement, while four were considered to be suitable as diesel replacements: diethyl succinate, dibutyl succinate, dibutyl fumarate and dibutyl malonate. Diethyl succinate (DES) was determined to be the most economically viable. In comparison with previously investigated fuel technologies, it does not possess ideal physical properties to be used as a straight replacement for diesel, due to its low cetane number. However, the purity of DES allows for precise alteration of properties of the fuel blend regardless of the feedstock, not possible with coffee biodiesel or metathesis road transport fraction.

To further examine the suitability of DES as a road transport fuel, a 20 vol% blend of DES (DES 20) was tested on engine. The fuel was tested across a range of engine speeds and pedal demands, and compared to diesel. A general increase in fuel demand, decrease in wheel force and exhaust temperature, decrease in CO, and marginal increase in NO_x were observed, in line with what has been observed with other short chain esters. DES could be used in blends with diesel without significant

changes to the emissions or performance under a range of conditions and therefore represents a suitable fuel blending agent.

However, fermentation does not use all of the carbon available from waste biomass. For complete biomass utilization, thermochemical conversions such as pyrolysis potentially offer a more suitable solution. Pyrolysis converts 100% of the biomass, though maximising the bio-oil fraction and subsequent effective upgrading to liquid fuels is challenging due to the huge range of oxygenated species within it. Investigating the upgrading of specific molecules present in pyrolysis vapour is important for the understanding of mechanistic changes, and thus the ability to direct the production towards desired products.

The catalytic fast pyrolysis of mesityl oxide over different ZSM-5 catalysts, therefore, was investigated. It was found that HZSM-5 and CuZSM-5 catalysts were inactive for the effective upgrading to non-aromatic species in both helium and hydrogen atmospheres. PdZSM-5, however, effectively hydrogenated mesityl oxide to methyl *iso*-butyl ketone and produced a small amount of the non-aromatic dimerised species. Though this is difficult to compare to the previous fuels discussed as no specific fuel was produced for analysis, it represents an important step towards the control and direction of this technology. Further development could potentially allow for tailored processes by which the amount of each fuel for specific application (gasoline, diesel, jet) within the bio-oil is controlled.

6.2 FUTURE WORK

In Chapter 2, spent coffee grounds were assessed as a biodiesel feedstock. The oil extracted, and subsequently the biodiesel, contained biomolecules which could not be identified by GC-MS nor ^{1}H NMR spectroscopy. Therefore, the identification and removal of these biomolecules is vital to further assess the suitability of waste coffee biodiesel as a fuel. Furthermore, the effect of the level of roasting (i.e. lighter versus dark roast) on coffee beans on the biomolecules present and their stability should be investigated. This study has considered coffee purchased and brewed for domestic use. While other studies have considered waste coffee from high street coffee chains, which largely use espresso machines of more extreme pressures, one waste coffee source which has not been assessed is from instant, soluble coffee producers. Due to the large amounts of coffee used (and thus waste produced), the issue of collecting the waste is alleviated. Instant coffee production, however, is brewed at much more extreme conditions (up to 180 °C, 20 atm), leading to 40-60% of the mass of the coffee solubilised in the aqueous phase.[1] The effect these extreme conditions have on the amount, structure and stability of the lipid in the coffee beans is unknown.

In Chapter 3, the cross-metathesis of triglycerides with an alternative ethene source was investigated. Though fuels of acceptable physical property were produced, the variation of structure due to the ruthenium-hydride catalysed isomerisation reduced the control over the final product distribution. Therefore, alternative catalyst systems, or methods to reduce this isomerisation should be considered, such as the addition of catalytic amounts of acetic acid and benzoquinones.[2] Furthermore, all metathesis reactions carried out in this thesis use homogeneous catalysts which would require recovery before this could be considered a viable option, economically. Investigations into heterogeneous catalysts on the production of metathesis fuels, therefore, should be considered. Such examples include ruthenium complexes supported on mesoporous silica,[3] rhenium oxide supported on alumina[4] and, most recently, tungsten hydride species supported on alumina.[5] Upon the determination of the most suitable heterogeneous catalyst a

continuous process should be investigated, and the product achieved should be tested for its fuel properties, engine and infrastructure material compatibility, and engine performance.

In Chapter 4, diethyl succinate was deemed a suitable diesel blending agent in terms of its physical properties. However, though there is evidence that the cost of DES could potentially reduce to a more feasible level for fuel production (US $ 0.50-1.00 kg^{-1} [6]), further study into the feasibility of producing it on the substantial scale that would be required should be carried out, for example with an in-depth life cycle assessment. The emissions and performance of diethyl succinate-diesel blend were also tested via a chassis dynamometer engine test. Further engine testing studies require focus on in-chamber combustion experiments to determine the changes in pressure and combustion duration in order to further explain the changes in emissions and performance and to optimise the injection timing for future testing. Compatibility studies with the various materials present in engine fuel delivery systems and infrastructure should also be considered.

In Chapter 5, a small amount of mesityl oxide oligomerisation was achieved when using Pd-supported ZSM-5 catalysts. The production of fuel-like molecule ranges from pyrolytic vapours containing a significant amount of ketonic species is challenging, due to their tendency to form aromatics and graphitic coke precursors. If, however, optimisation of the oligomerisation is possible, there could be potential for a step-wise upgrading system by which oligomerisation precedes selective hydrogenation, producing species which could undergo further oligomerisation. This would allow for control of the carbon range. The production of a sole catalyst which allows for this step-wise synthesis, however, is a considerable challenge due to the effect that environmental conditions have on catalyst reactivity. The development of a step-wise system, whereby oligomerisation and hydrogenation occur using different catalyst systems, therefore, may be a potential step for further work.

Much further work is needed to determine the effects of metal-exchanged ZSM-5 on the dimerisation and hydrogenation of mesityl oxide and, by extension, related

ketonic species presence in pyrolysis vapours. First and foremost is catalyst characterisation. Though catalysts were prepared by incipient wetness in order to control the amount of metal present in the catalyst overall, the effect of this loading on the catalyst itself has not been determined. Therefore, X-ray diffraction should be carried out to determine the effect of the metal loading on the purity and crystallinity of the catalyst, NH_3 temperature controlled absorption should be carried out in order to quantify the number of acid sites present on the catalysts, and pyridine-IR will allow for comparative characterisation of the Brønsted and Lewis acid sites.

6.3 REFERENCES

1. Tzia, C.; Liadakis, G., *Extraction Optimization in Food Engineering*. Taylor & Francis: 2003.
2. Hong, S. H.; Sanders, D. P.; Lee, C. W.; Grubbs, R. H., Prevention of Undesirable Isomerization during Olefin Metathesis. *Journal of the American Chemical Society* **2005,** *127* (49), 17160-17161.
3. Li, L.; Shi, J.-l., A Highly Active and Reusable Heterogeneous Ruthenium Catalyst for Olefin Metathesis. *Advanced Synthesis & Catalysis* **2005,** *347* (14), 1745-1749.
4. Sibeijn, M.; Mol, J. C., Ethenolysis of methyl oleate over supported Re-based catalysts. *Journal of Molecular Catalysis* **1992,** *76* (1-3), 345-358.
5. Mazoyer, E.; Szeto, K. C.; Merle, N.; Norsic, S.; Boyron, O.; Basset, J.-M.; Taoufik, M.; Nicholas, C. P., Study of ethylene/2-butene cross-metathesis over W-H/Al_2O_3 for propylene production: Effect of the temperature and reactant ratios on the productivity and deactivation. *Journal of Catalysis* **2013,** *301*, 1-7.
6. Beauprez, J. J.; De Mey, M.; Soetaert, W. K., Microbial succinic acid production: Natural versus metabolic engineered producers. *Process Biochemistry* **2010,** *45* (7), 1103-1114.

APPENDIX

APPENDIX A - FUEL STANDARDS

APPENDIX A.1 - EN 228 (PETROL)

Property	Units	Min.	Max.	Test methods
Density at 15°C	kg m^{-3}	720	775	EN ISO 3675
Research octane number, RON	-	95	-	EN 25164
Motor octane number, MON	-	85	-	EN 25163
Vapour pressure, VP				EN 13016-1
summer	kPa	45	60	
winter	kPa	60	90	
Distillation (1013 mbar)				ISO 3405
evaporated at 100°C	% vol.	46	71	
evaporated at 150°C	% vol.	75	-	
Distillation residue	% vol.	-	2	ISO 3405
Final boiling point, FBP	°C	-	210	ISO 3405
Volatility, VLI (10 VP + 7 E70)				Calculation
summer	-	-	-	
winter	-	1000	1250	
Copper strip corrosion (3 h at 50 °C)	rating	Class 1		EN ISO 2160
Oxidation stability	hrs	6	-	EN ISO 7536
Hydrocarbons				ASTM D 1319
Olefins	% vol.	-	18	
Aromatics	% vol.	-	35	
Benzene	% vol.	-	1	
Oxygen	% wt.	-	2,7	EN 1601, EN 13132
Oxygenates				EN 1601, EN 13132
Methanol	% vol.	-	3	
Ethanol	% vol.	-	5	
Iso-propyl alcohol	% vol.	-	10	
Iso-butyl alcohol	% vol.	-	10	
Tert-butyl alcohol	% vol.	-	7	
Ethers (5 or more C atoms)	% vol.	-	15	
Other oxygenates	% vol.	-	10	
Sulphur	mg kg^{-}	-	10	EN ISO 20846
Lead	mg l^{-}	-	5	EN 237
Gums	mg/100 ml	-	5	EN ISO 6246
Appearance	-	Clear and bright		Visual inspection

APPENDIX A.2 - ASTM 4814 (GASOLINE)

Property	Units	Min.	Max.	Test methods
Maximum vapour pressure at 37.8°C	kPa	54	103	ASTM D5190
Distillation temperature				
10 vol% recovered	°C	-	50-70	ASTM D86
50 vol% recovered	°C	66-77	110-121	ASTM D86
90 vol% recovered	°C	-	185-190	ASTM D86
Distillation temperature for end point	°C	-	225	ASTM D86
Distillation residue	% vol.	-	2	ASTM D86
Max Driveability Index (DI)	°C	-	569-597	ASTM D86
Vapour-lock protection	°C	35	60	ASTM D5188
Copper strip corrosion (3 h at 50 °C)	rating	no. 1		ASTM D130
Silver corrosion (3 h at 50°C)	rating	1		ASTM D4814 (A1)
Oxidation stability	mins	240	-	ASTM D525
Lead content	g l^{-}	-	0.013	ASTM D3237
Sulfur content	mass%	-	0.0080	ASTM D381
Solvent-washed gum content	mg/100ml	-	5	ASTM D5453

APPENDIX A.3 - EN 590 (DIESEL)

Properties	**Units**	**Min.**	**Max.**	**Test Methods**
Cetane index		46.0	-	EN ISO 4264
Cetane number		51.0	-	EN ISO 5165
Density at 15°C	kg m^{-3}	820	845	EN ISO 3675, EN ISO 12185
Polycyclic aromatic hydrocarbons	% wt.	-	11	EN ISO 12916
Sulphur content	mg kg^{-}	-	10	EN ISO 20846, EN ISO 20884
Flash point	°C	55	-	EN ISO 2719
Distillation residue	% wt.	-	0.30	EN ISO 10370
Ash content	% wt.	-	0.01	EN ISO 6245
Water content	mg kg^{-}	-	200	EN ISO 12937
Total contamination	mg kg^{-}	-	24	EN ISO 12662
Copper strip corrosion (3 hours at 50 °C)	rating	Class 1	Class 1	EN ISO 2160
Oxidation Stability	g m^{-3}	-	25	EN ISO 12205
Lubricity, corrected wear scar diameter at 60 °C	µm	-	460	EN ISO 12156-1
Viscosity at 40 °C	mm^2s^{-1}	2.00	4.50	EN ISO 3104
Distillation (vol. % recovered)	°C			EN ISO 3405
65%		250	-	
85%		-	350	
95%		-	360	
Fatty acid methyl ester content	% vol.	-	7	EN 14078

APPENDIX A.4 - ASTM D975 (DIESEL)

Property	**Units**	**Min.**	**Max.**	**Test methods**
Flash point	°C	52	-	ASTM D93
Distillation temperature				
10 vol% recovered	°C	-	190	ASTM D86
50 vol% recovered	°C	-	221	ASTM D86
90 vol% recovered	°C	-	329	ASTM D86
95 vol% recovered	°C	-	355	
Distillation residue	% vol.	-	2	ASTM D86
Kinematic viscosity	mm^2s^{-1}	1.9	4.1	ASTM D86
Ash	mass%	-	0.01	ASTM D482
Trace sediment	vol%	-	<0.05	ASTM D2709
Cetane number	-	40		ASTM D613
API gravity at 15°C	-	34	38	ASTM D287
Ramsbottom Carbon Residue on 10% distillation residue	mass%	-	0.35	ASTM D524
Copper corrosion, 3 hours at 100°C	rating	-	No. 3A	ASTM D130
Lubricity, wear scar with HFRR @ 60°C	µm	-	520	ASTM D6079

APPENDIX A.5 - EN 14214 (BIODIESEL)

Properties	Units	Min.	Max.	Test-Method
Ester content	% wt.	96.5	-	EN 14103
Density at 15 °C	kg m^{-3}	860	900	EN ISO 3675 / EN ISO 12185.
Viscosity at 40 °C	mm^2s^{-1}	3.5	5	EN ISO 3104
Flash point	°C	101	-	EN ISO 2719 / EN ISO 3679.
Sulfur content	mg kg^{-}	-	10	- EN ISO 20846 / EN ISO 20884.
Distillation residue	% wt.	-	0.3	EN ISO 10370
Cetane number	-	51	-	EN ISO 5165
Sulfated ash content	% wt.	-	0.02	ISO 3987
Water content	mg kg^{-}	-	500	EN ISO 12937
Total contamination	mg kg^{-}	-	24	EN 12662
Copper band corrosion (3h at 50 °C)	rating	Class 1	Class 1	EN ISO 2160
Oxidation stability, 110 °C	hours	6	-	EN 15751 / EN 14112
Acid value	mg KOH/g	-	0.5	EN 14104
Iodine value	-	-	120	EN 14111
Linolenic Acid Methyl ester	% wt.	-	12	EN 14103
Polyunsaturated (4 Double bonds) Methyl ester	% wt.	-	1	EN 14103
Methanol content	% wt.	-	0.2	EN 14110l
Monoglyceride content	% wt.	-	0.8	EN 14105
Diglyceride content	% wt.	-	0.2	EN 14105
Triglyceride content	% wt.	-	0.2	EN 14105
Free Glycerine	% wt.	-	0.02	EN 14105 / EN 14106
Total Glycerine	% wt.	-	0.25	EN 14105
Group I metals (Na & K)	mg kg^{-}	-	5	EN 14108 / EN 14109 / EN 14538
Group II metals (Ca & Mg)	mg kg^{-}	-	5	EN 14538
Phosphorus content	mg kg^{-}	-	4	EN14107

APPENDIX A.6 - ASTM D6751 (BIODIESEL)

Property	**Units**	**Min.**	**Max.**	**Test methods**
Flash point	°C	93	-	ASTM D93
Sodium and Potassium, combined	ppm	-	5	EN 14538
Calcium and Magnesium combined	ppm		5	EN 14538
Monoglycerides	mass%	-	0.4	ASTM D6584
Methanol content	mass%	-	0.2	EN 14110
Water and sediment	vol%	-	0.05	ASTM D2709
Sulfur	mass%	-	0.00015	ASTM
Distillation	°C	-	360	ASTM D1160
Kinematic viscosity	mm^2s^{-1}	1.9	6	ASTM D86
Acid number	mg KOH/g	-	0.5	ASTM D664
Free glycerin	mass%	-	0.02	ASTM D6584
Total glycerin	mass%	-	0.024	ASTM D6584
Cetane number	-	47	-	ASTM D613
Phosphorus content	mass%	-	0.001	ASTM D4951
Carbon Residue	mass%	-	0.05	ASTM D4530
Copper corrosion, 3 hours at 100°C	rating	-	No. 3	ASTM D130
Oxidation stabiltiy	hours	3	-	EN 15751

APPENDIX A.7 - DEF STAN 91-91 TURBINE FUEL, KEROSINE TYPE, JET A-1

Properties	**Units**	**Min.**	**Max.**	**Test-Method**
Appearance		Clear, bright and visually free from solid matter and undissolved water		Visual
Total Acidity	mg KOH/g	-	0.015	IP 354 / ASTM D3242
Total Aromatics	% vol.	-	26.5	IP 436 / ASTM 1319
Total Sulfur	% wt.	-	0.3	IP 336
Density at 15 °C	kg m^{-3}	775	840	IP 365 / ASTM D4052
Viscosity at -20 °C	mm^2s^{-1}	-	8	IP 71 / ASTM D445
Specific Energy	MJ kg^{-}	42	-	ASTM 1840
Freezing point	°C	-	-47	IP 16 / ASTM D2386
Flash point	°C	-	38	IP 170
Distillation (vol. % recovered)	°C			IP 123 / ASTM D86
10%		205	-	
100%		-	300	
Existent Gum	mg / 100ml	-	7	IP 540
Electrical Conductivity	pS m^{-1}	50	600	IP 274 / ASTM D2624
Lubricity wear scar diameter	mm	-	0.85	ASTM D5001
Copper strip	Class	-	Class 1	IP 154

APPENDIX A.8 - BIOETHANOL & BIOBUTANOL PHYSICAL PROPERTIES

Properties	**Bioethanol**	**Biobutanol**
Flash point / °C	8.9	35
Melting point / °C	-114	-90
Boiling point / °C	73	118
Kinematic viscosity at 40 °C / $mm^2 s^-$	1.13	2.22
Density at 15 °C / g cm^3	0.794	0.814
Energy Density / MJ kg^-	25	36
Energy Density / MJ l^-	20	29
Mass solubility in water / g l^-	Miscible	48
Lubricity (wear scar diameter) at 60 °C / mm	1057	591
Cetane Number	8	17

APPENDIX B – GC-MS TIC FOR GAS FRACTION OF SUNFLOWER OIL CROSS-METATHESIS WITH ETHENE

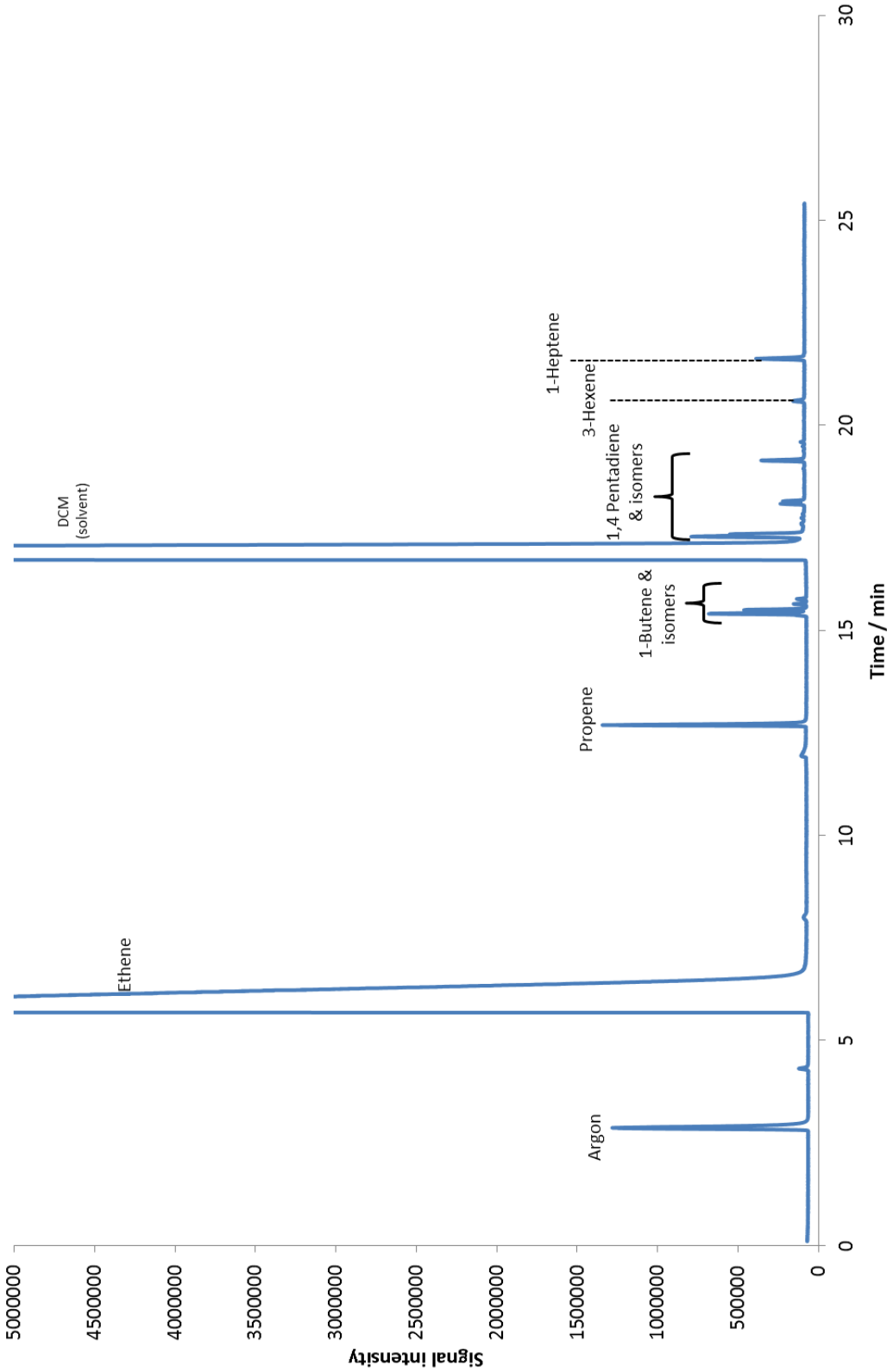

APPENDIX C – MASS SPECTRUMS FOR ZSM-5 DERIVED CATALYTIC FAST PYROLYSIS OF MESITYL OXIDE

APPENDIX C.1 - PD (0.5 WT%) ZSM-5 (SAR 30), HELIUM ATMOSPHERE

a) 150 °C

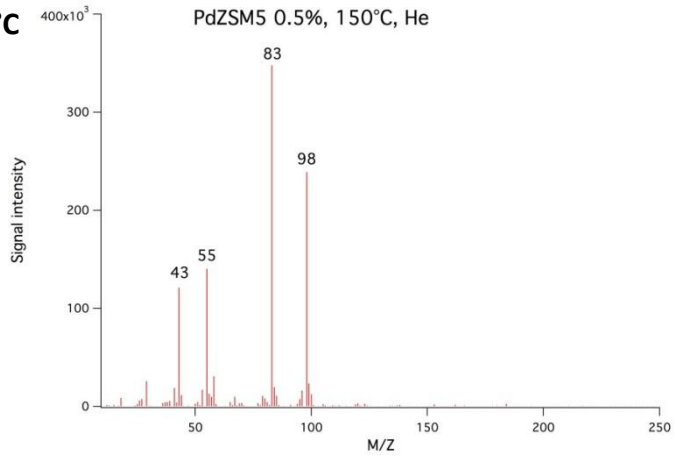

b) 250 °C

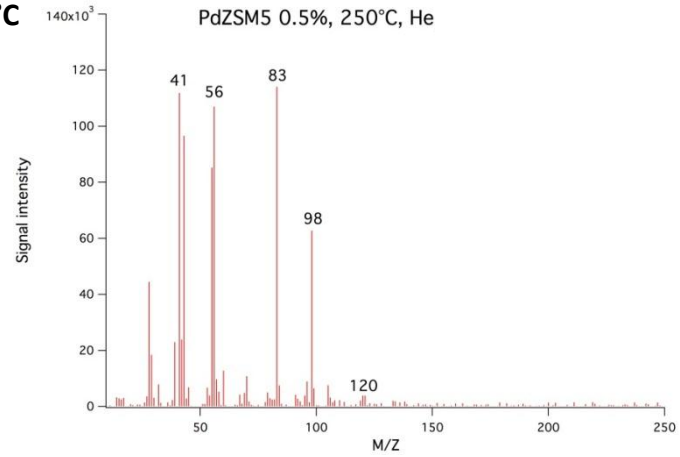

c) 350 °C

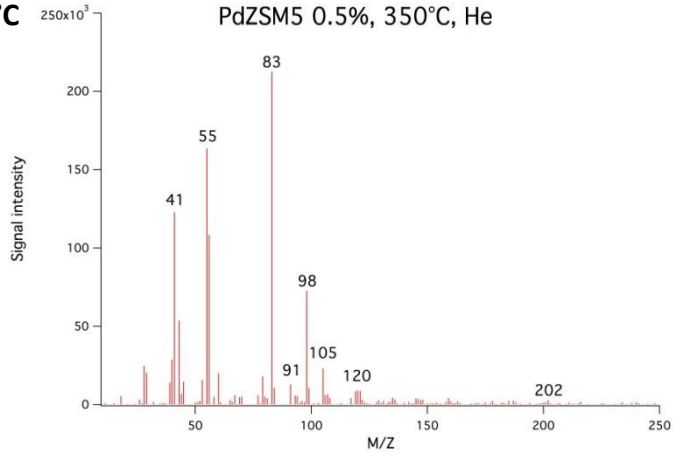

APPENDIX C.2 - PD (1 WT%) ZSM-5 (SAR 30), HELIUM ATMOSPHERE

a) 150 °C

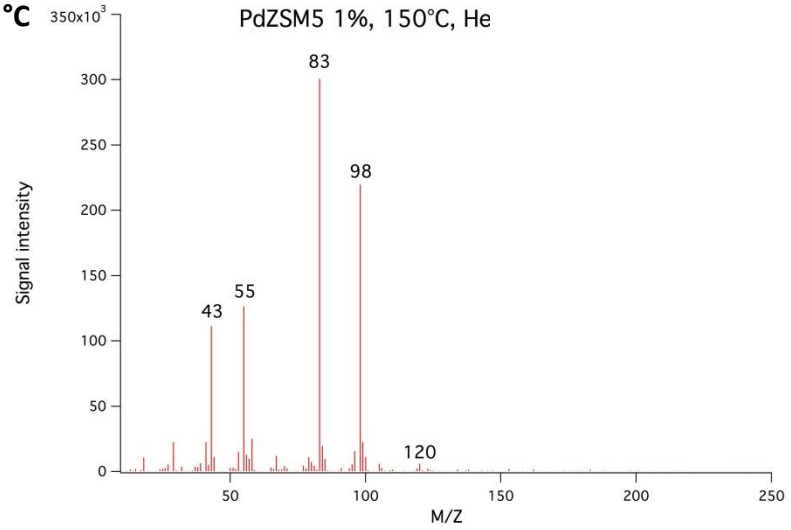

b) 250 °C

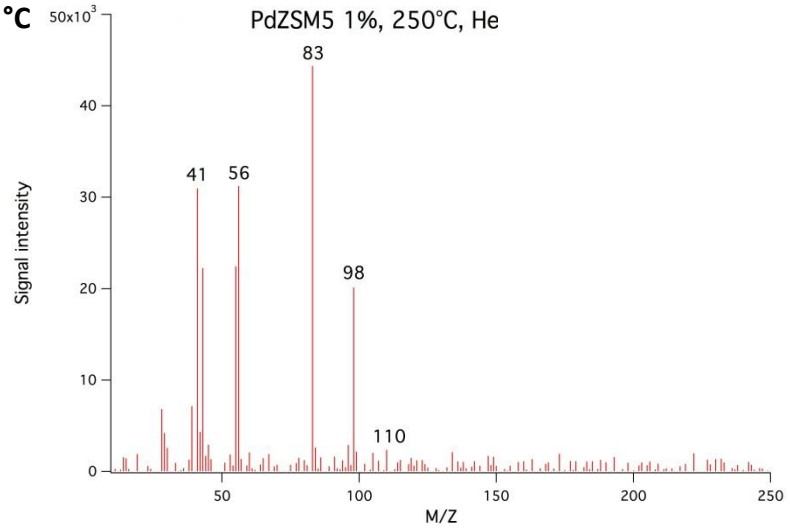

c) 350 °C

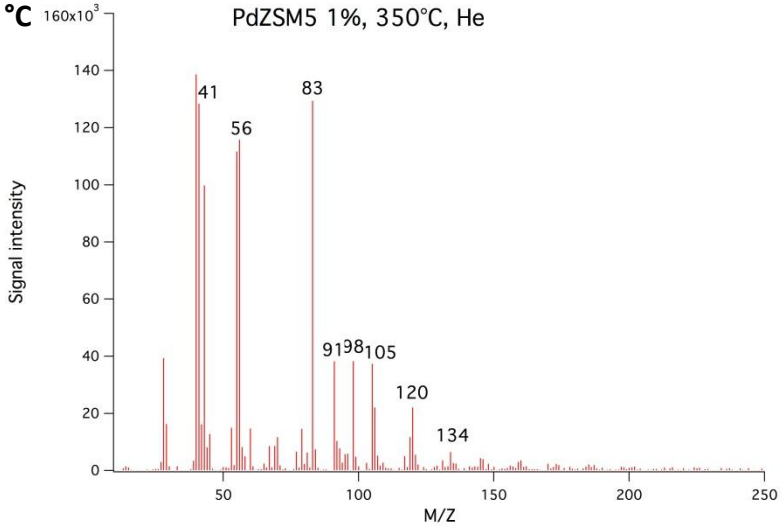

APPENDIX C.3 - PD (0.5 WT%) ZSM-5 (SAR 30), HYDROGEN ATMOSPHERE

a) 150 °C

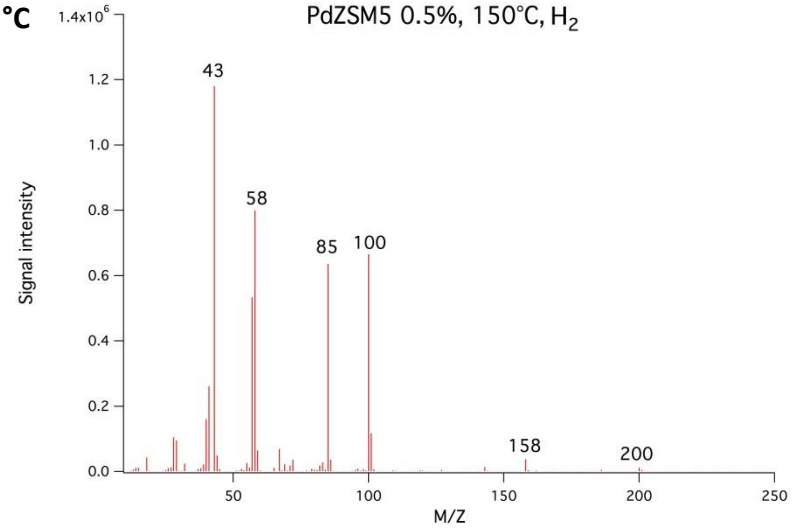

b) 250 °C

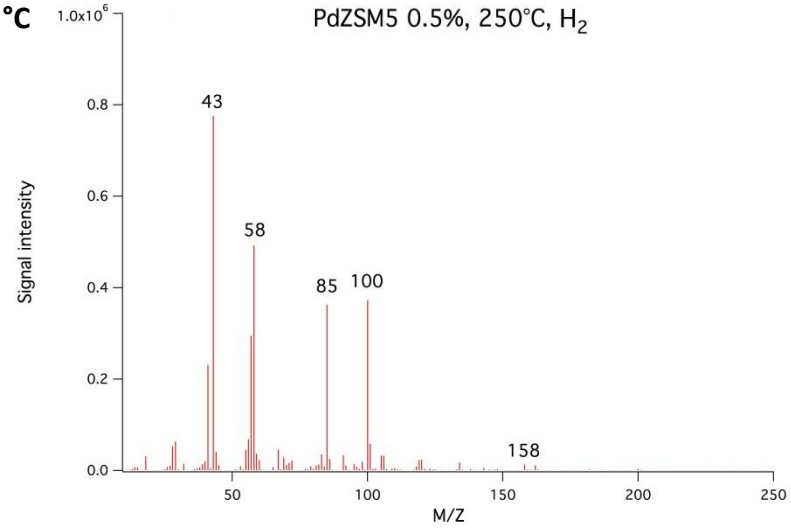

c) 350 °C

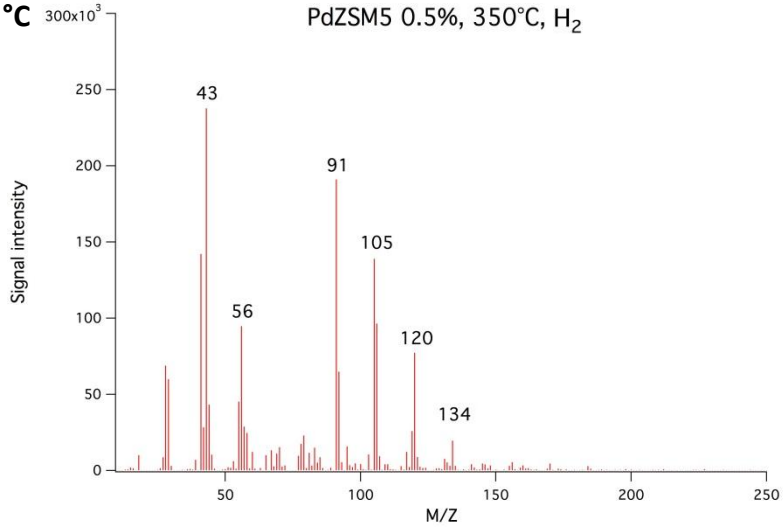

APPENDIX C.4 - PD (1 WT%) ZSM-5 (SAR 30), HYDROGEN ATMOSPHERE

a) 150 °C

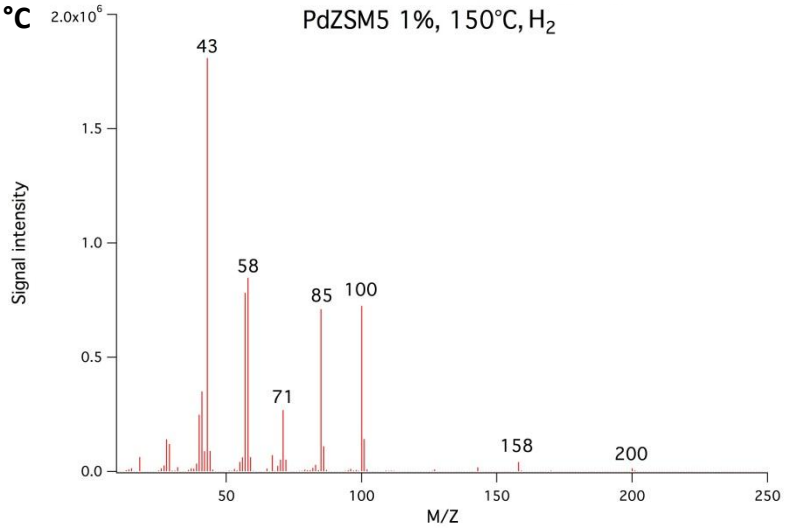

b) 250 °C

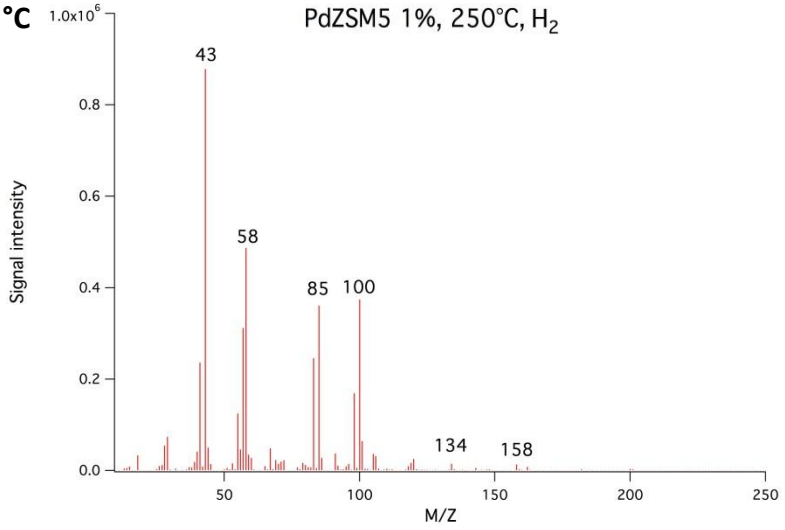

c) 350 °C

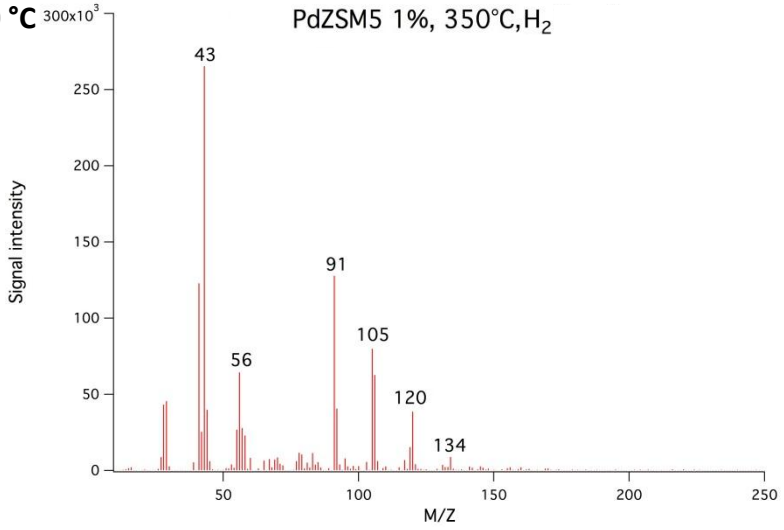

APPENDIX C.5 - CU (0.5 WT%) ZSM-5 (SAR 30), HELIUM ATMOSPHERE

a) 150 °C

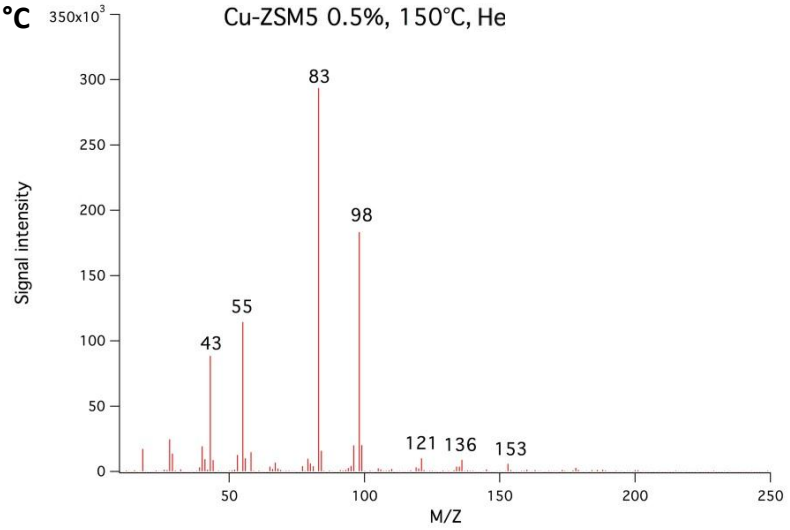

b) 200 °C

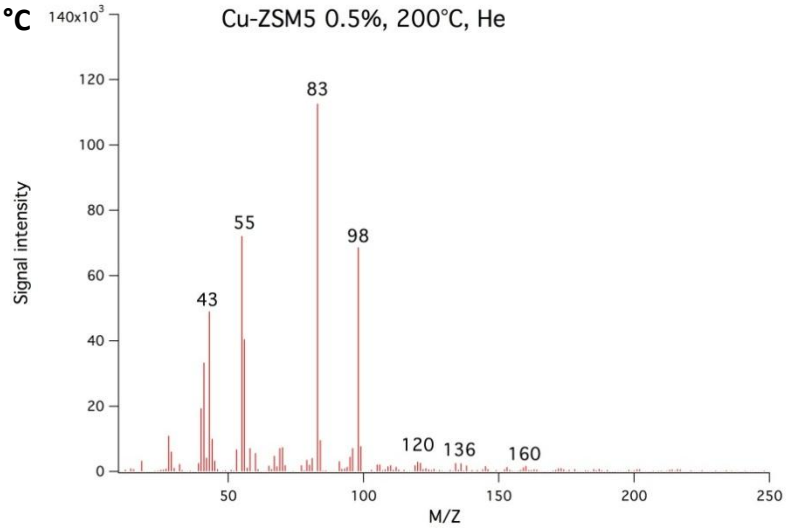

c) 250 °C

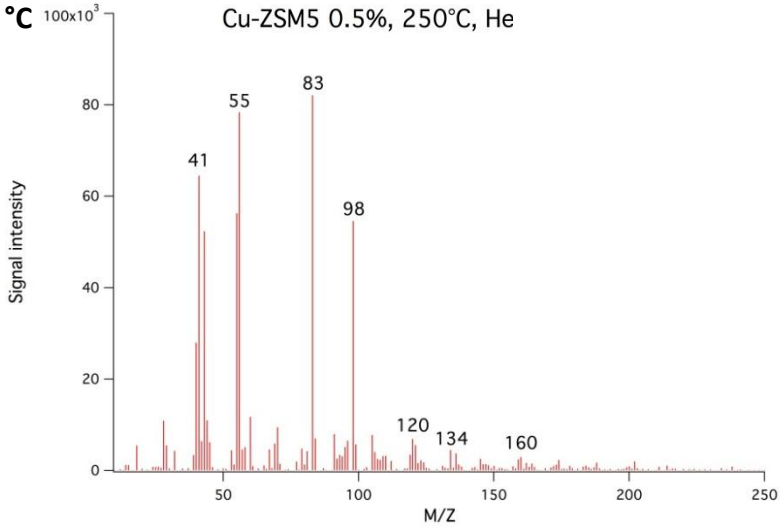

APPENDIX C.6 - CU (1 WT%) ZSM-5 (SAR 30), HELIUM ATMOSPHERE

a) 150 °C

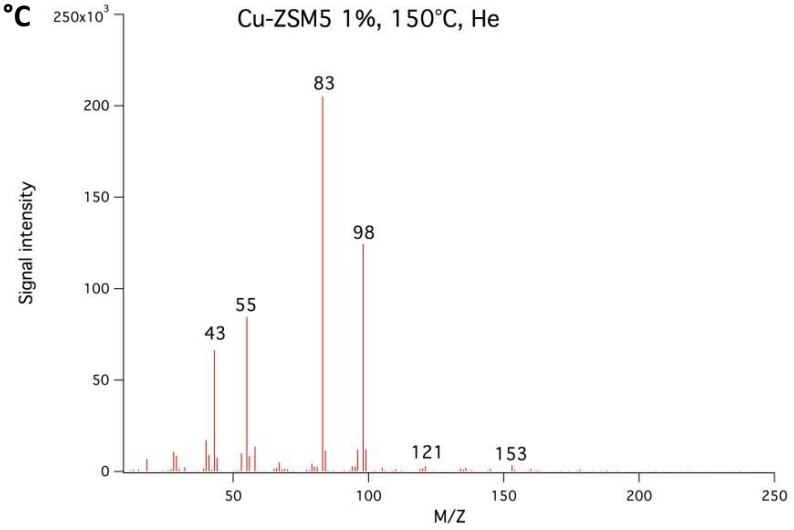

b) 200 °C

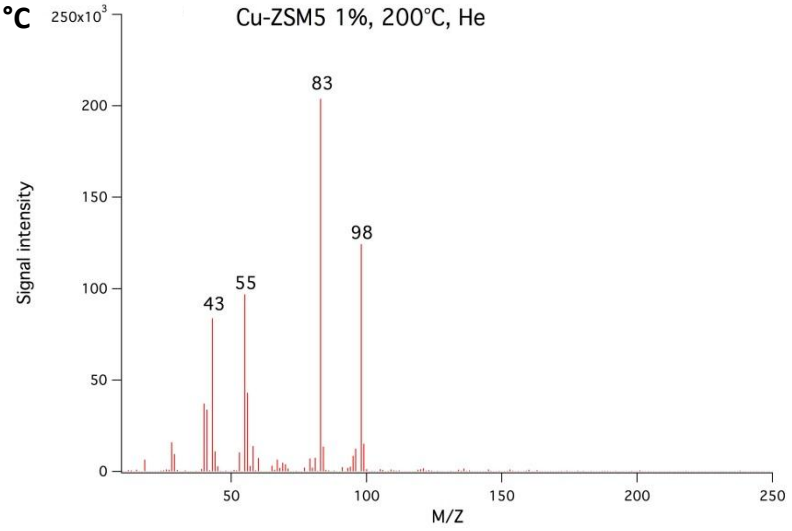

c) 250 °C

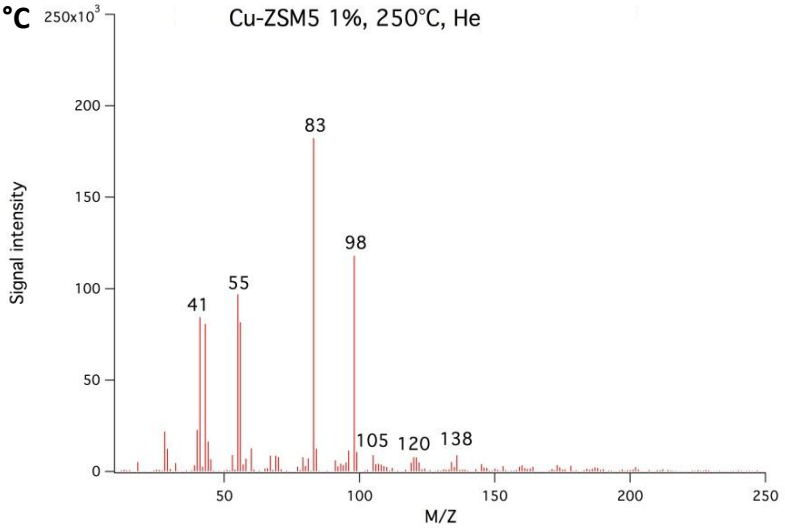

APPENDIX C.7 - CU (0.5 WT%) ZSM-5 (SAR 30), HYDROGEN ATMOSPHERE

a) 150 °C

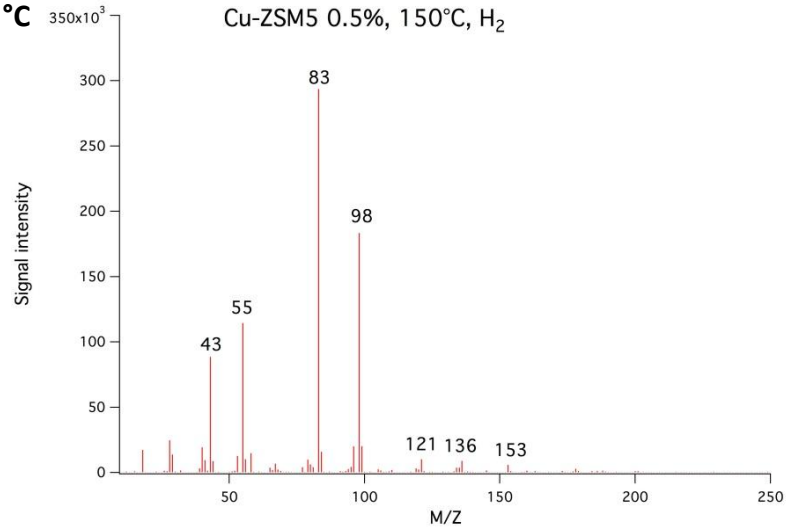

b) 200 °C

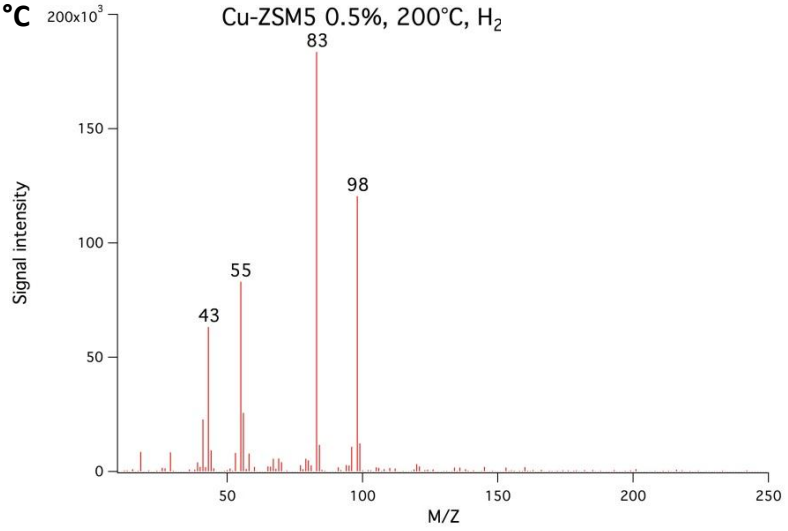

c) 250 °C

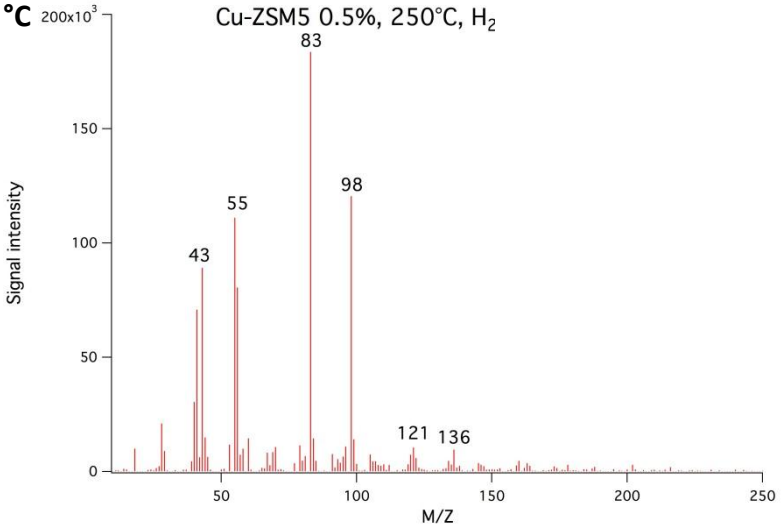

APPENDIX C.8 - CU (1 WT%) ZSM-5 (SAR 30), HYDROGEN ATMOSPHERE

a) 150 °C

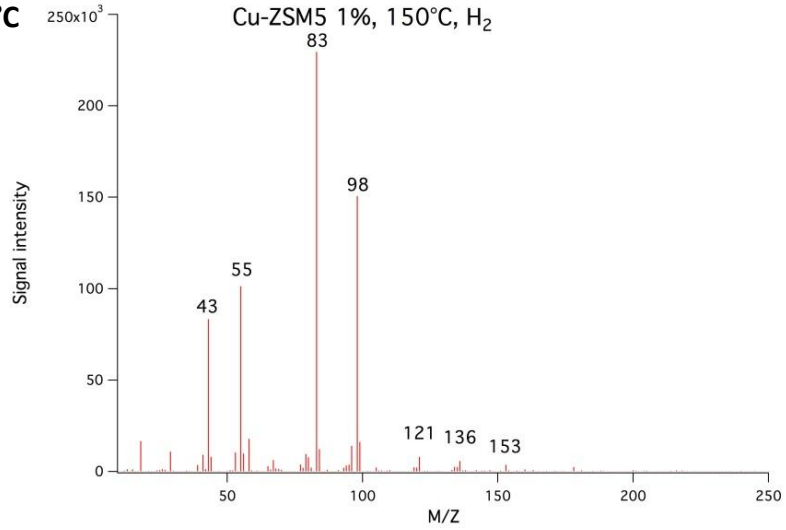

b) 200 °C

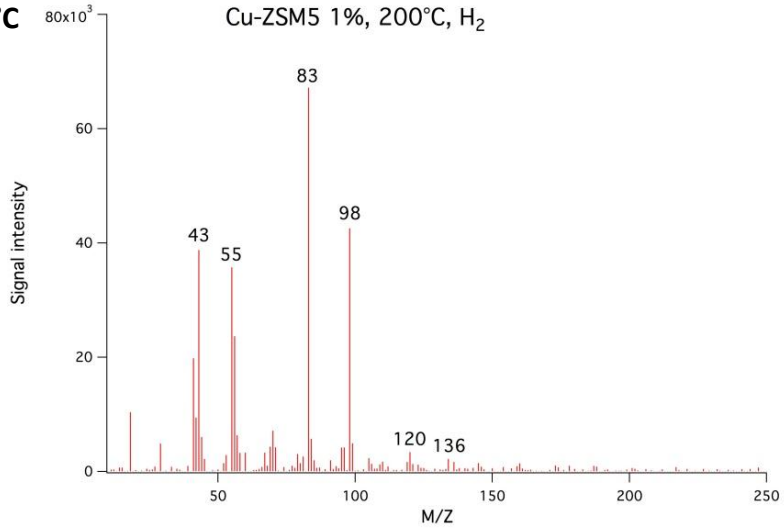

c) 250 °C

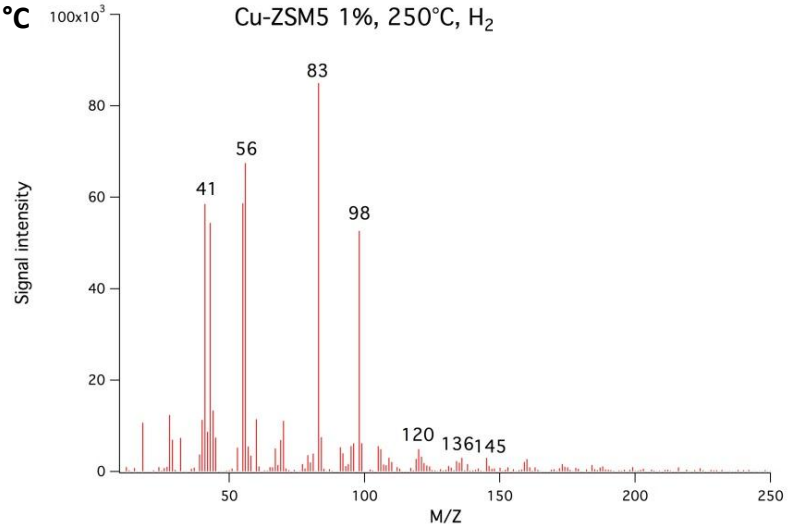

APPENDIX C.9 - PD (0.2 WT%) ZSM-5 (SAR 80), HELIUM ATMOSPHERE

a) 150 °C

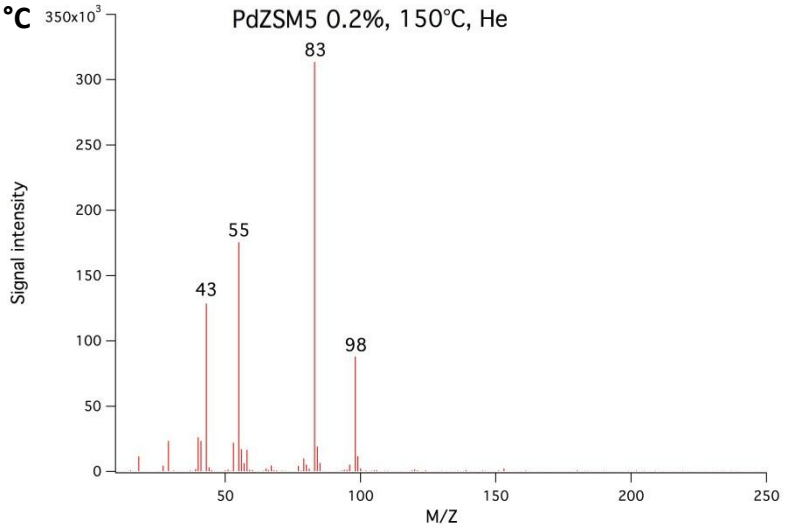

b) 250 °C

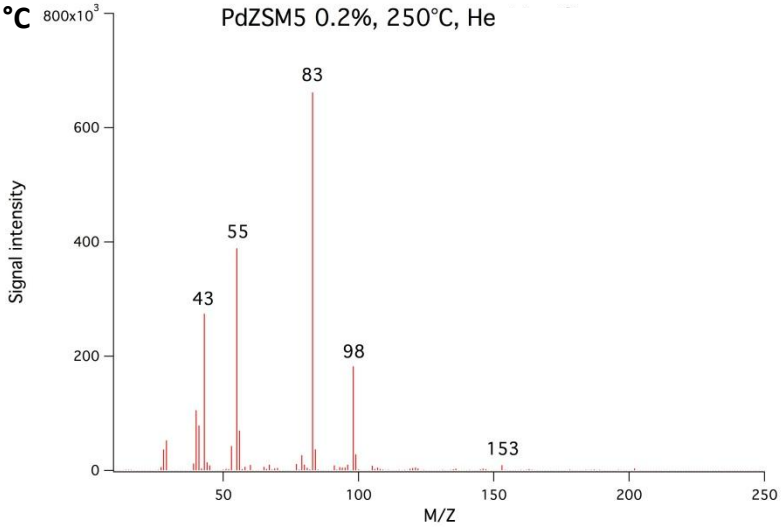

c) 350 °C

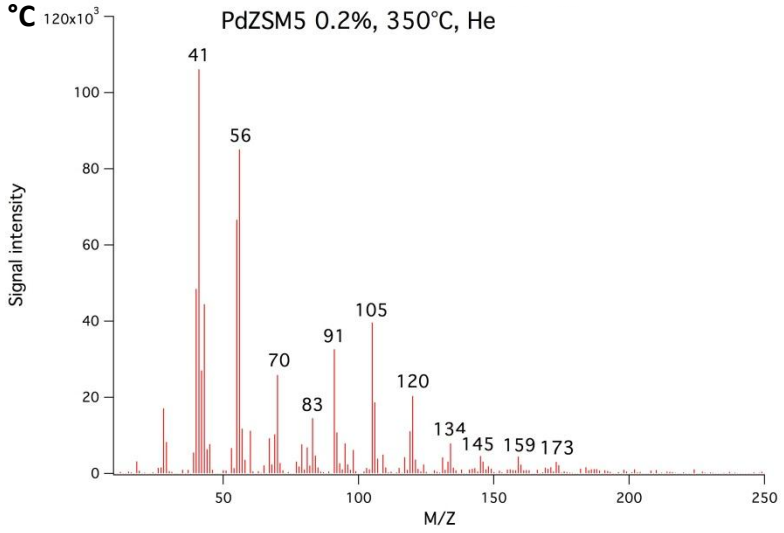

APPENDIX C.10 - PD (0.5 WT%) ZSM-5 (SAR 80), HELIUM ATMOSPHERE

a) 150 °C

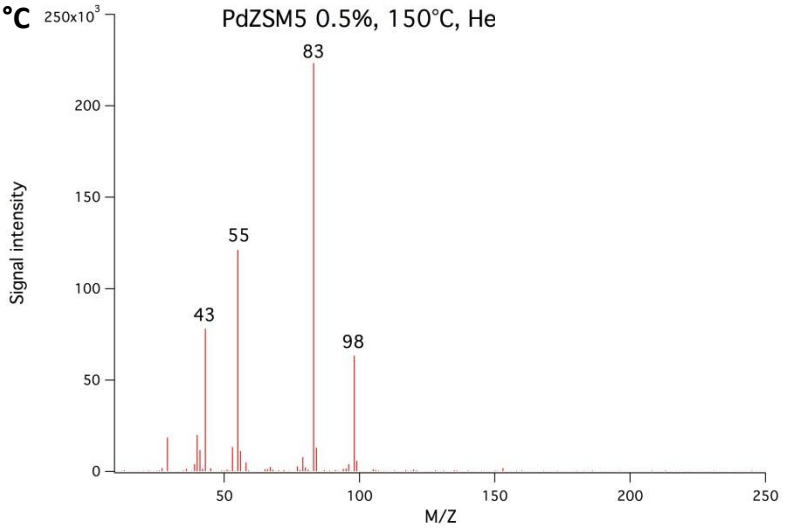

b) 250 °C

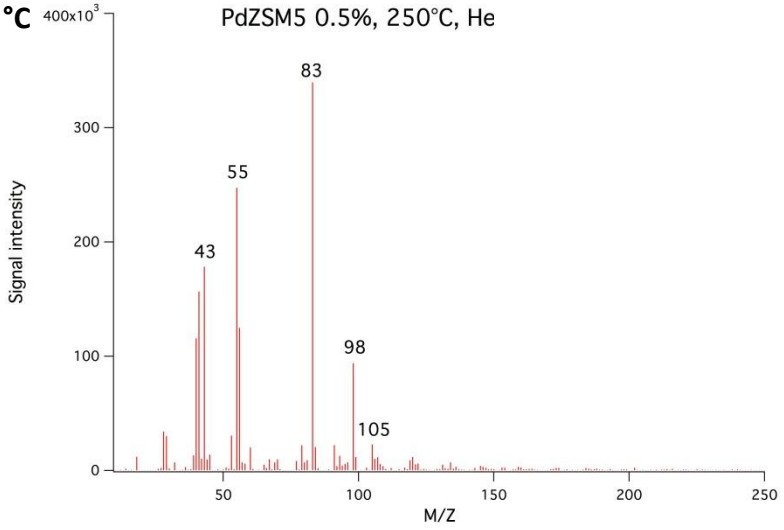

c) 350 °C

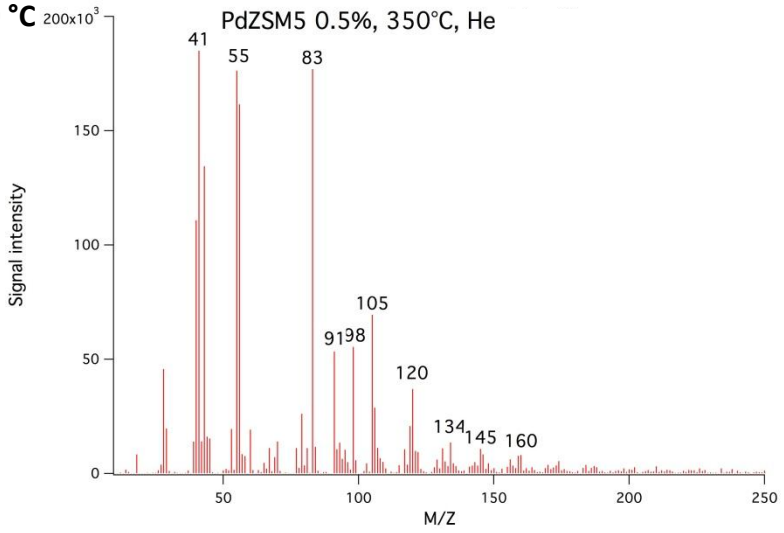

APPENDIX C.11 - PD (1 WT%) ZSM-5 (SAR 80), HELIUM ATMOSPHERE

a) 150 °C

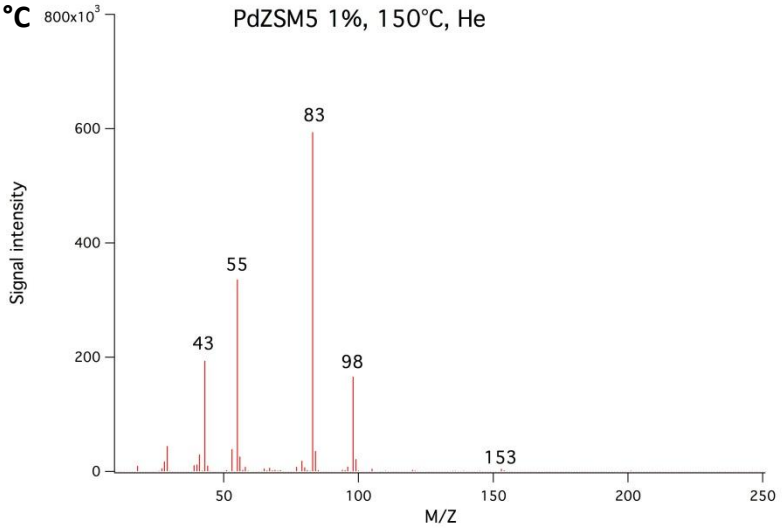

b) 250 °C

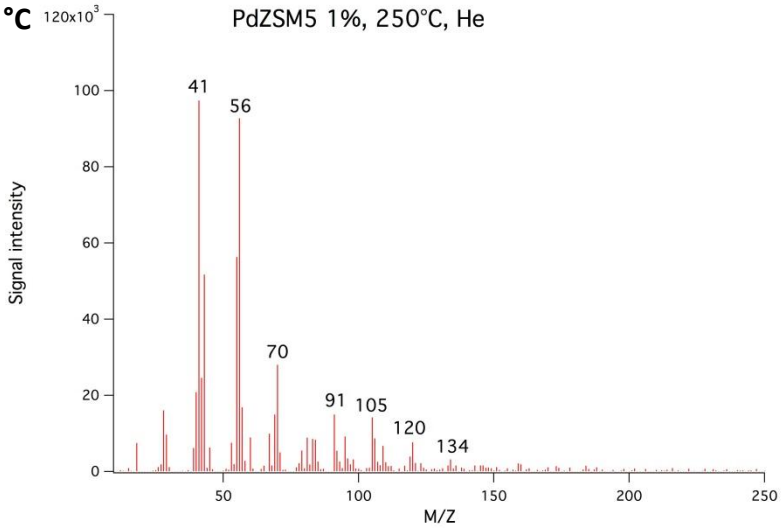

c) 350 °C

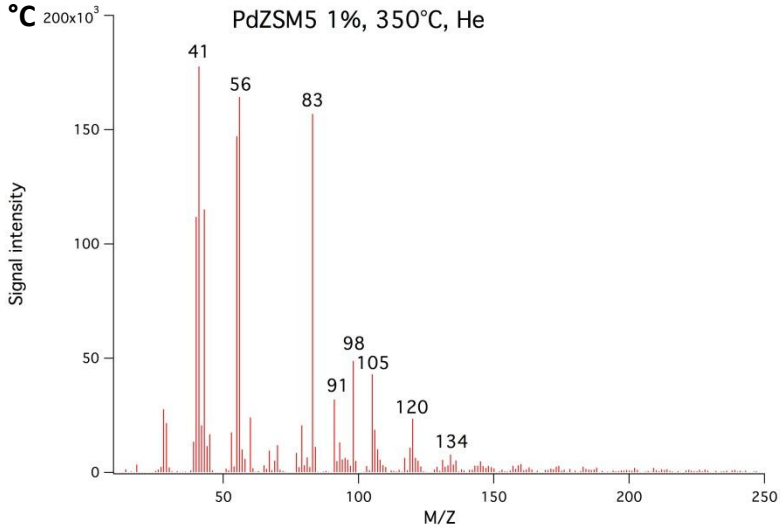

APPENDIX C.12 - PD (0.2 WT%) ZSM-5 (SAR 80), HYDROGEN ATMOSPHERE

a) 150 °C

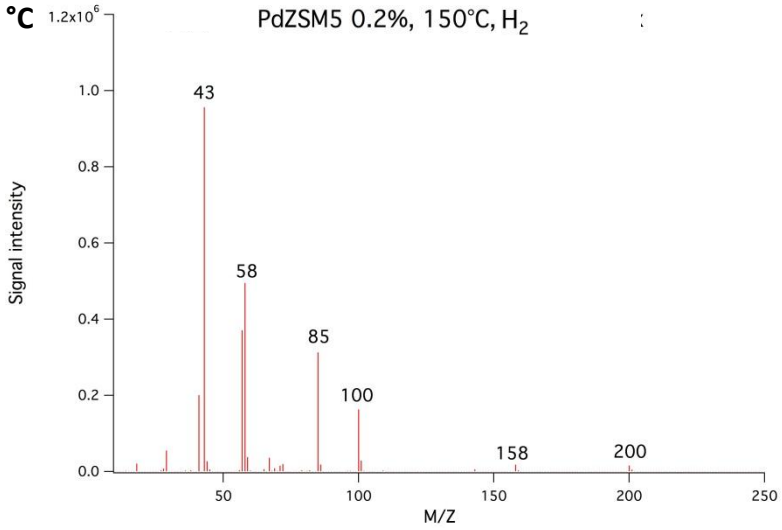

b) 250 °C

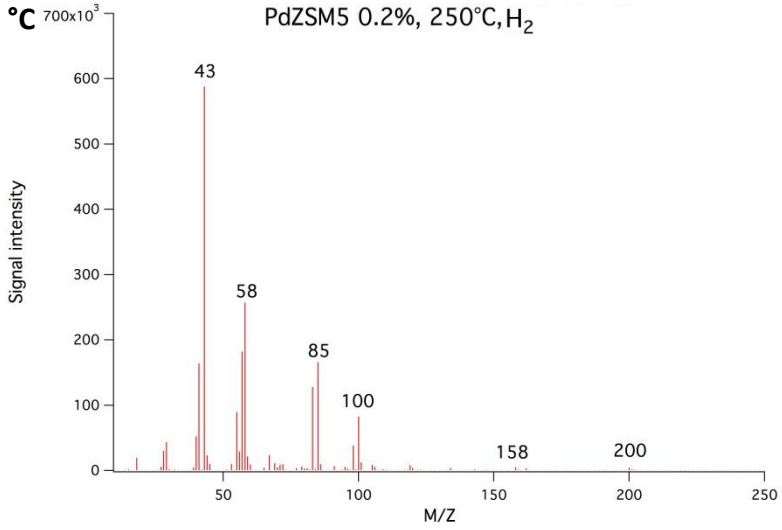

c) 350 °C

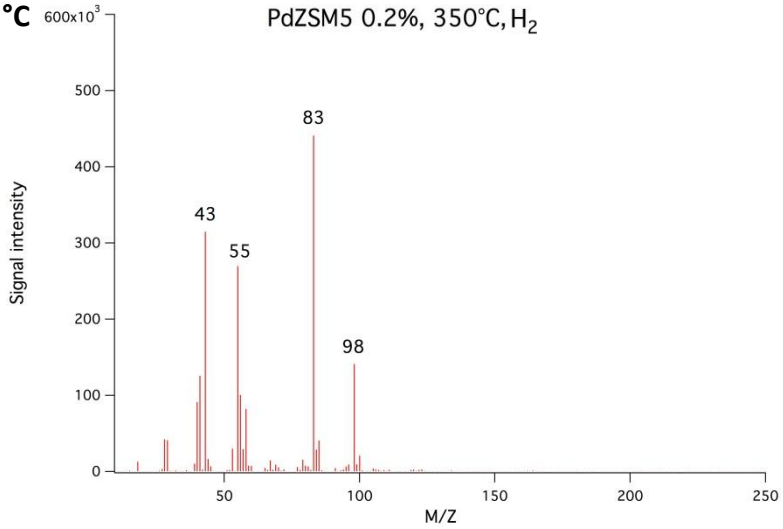

APPENDIX C.13 - PD (0.5 WT%) ZSM-5 (SAR 80), HYDROGEN ATMOSPHERE

a) 150 °C

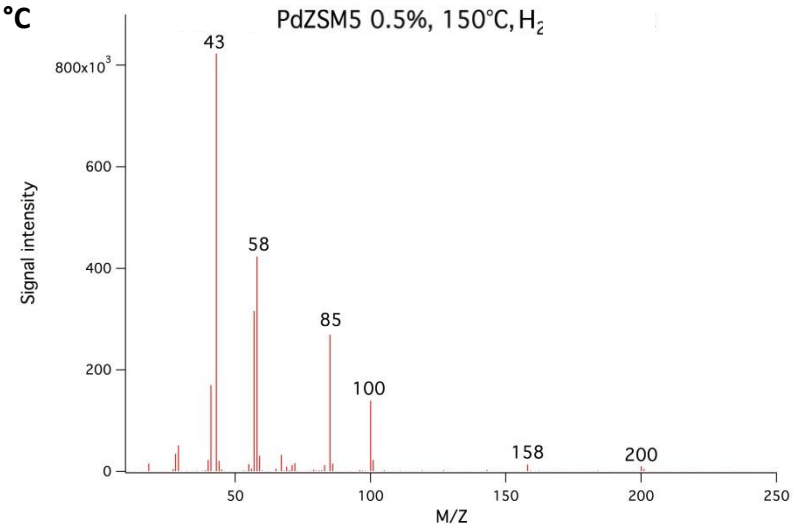

b) 250 °C

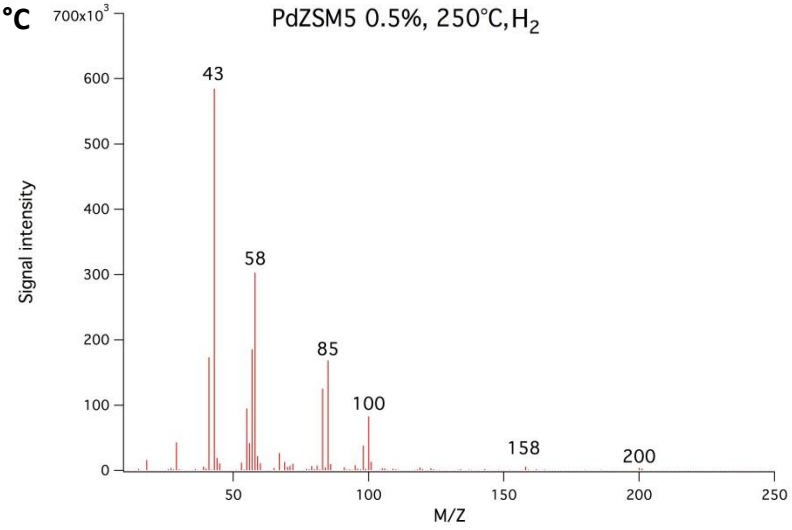

c) 350 °C

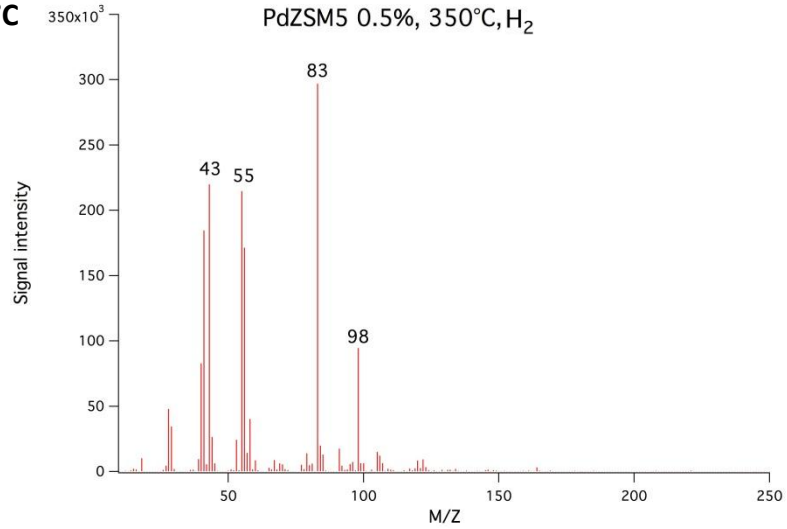

APPENDIX C.14 - PD (1 WT%) ZSM-5 (SAR 80), HYDROGEN ATMOSPHERE

a) 150 °C

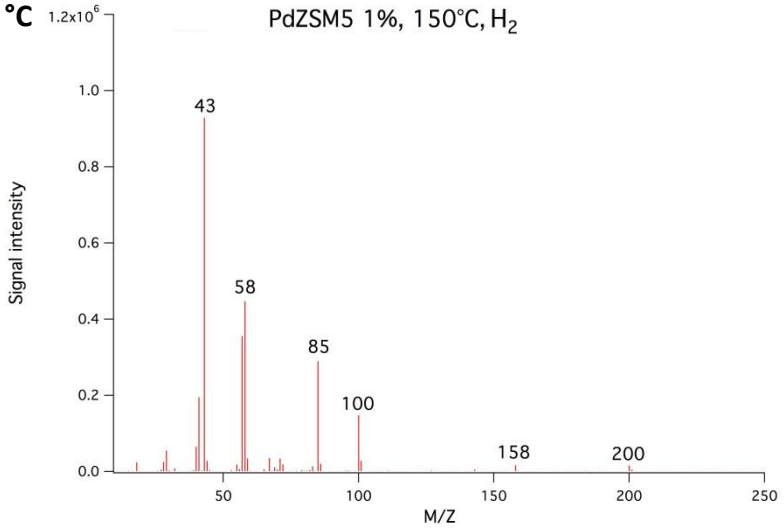

b) 250 °C

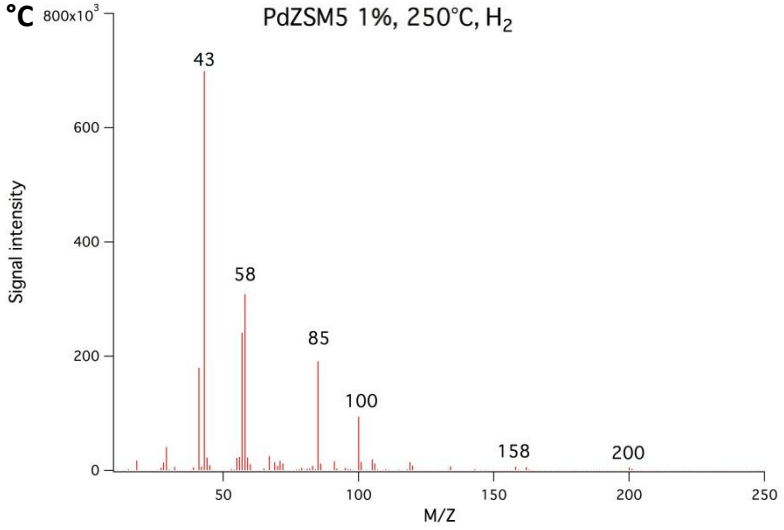

c) 350 °C

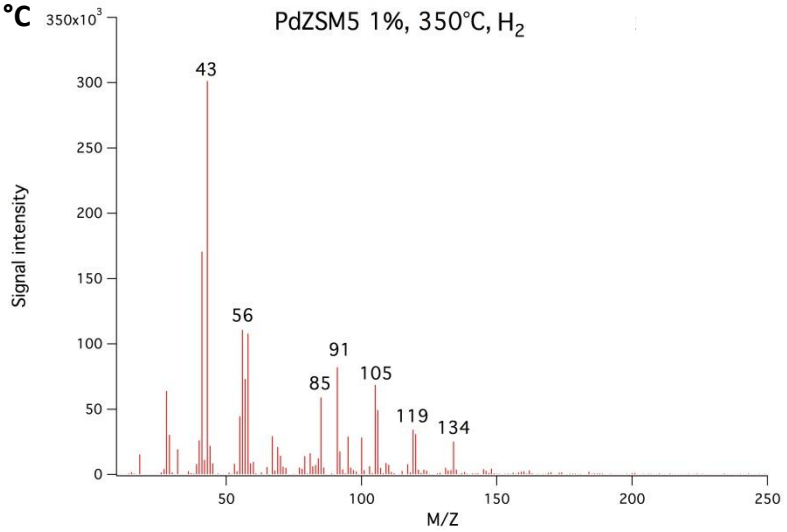

APPENDIX C.15 - PD (0.2 WT%) ZSM-5 (SAR 280), HELIUM ATMOSPHERE

a) 150 °C

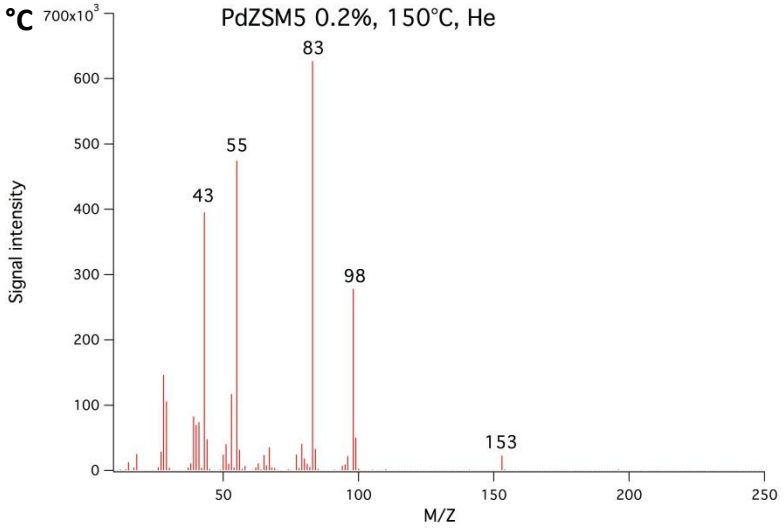

b) 250 °C

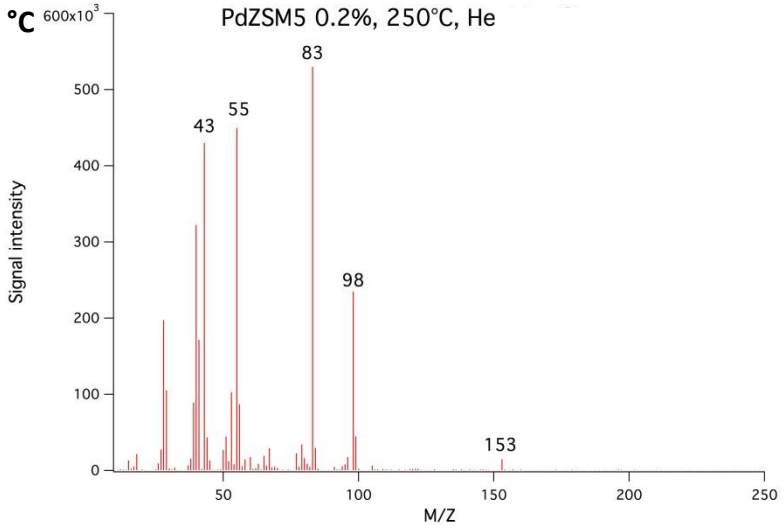

c) 350 °C

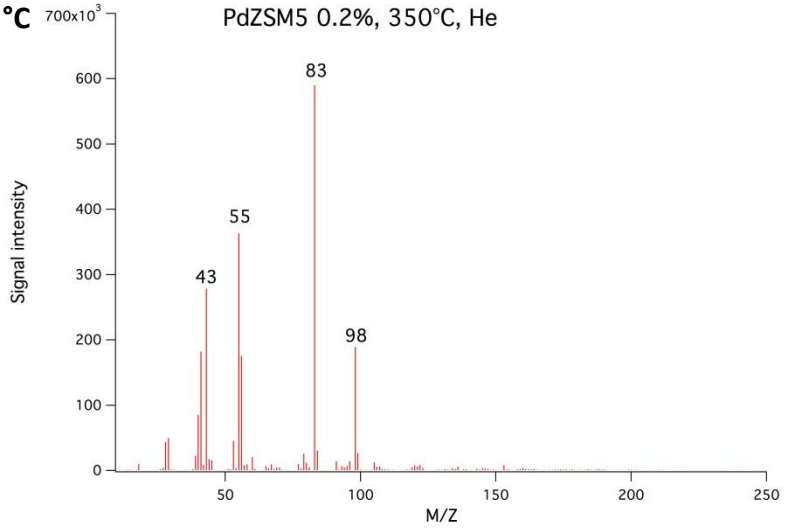

APPENDIX C.16 - PD (0.5 WT%) ZSM-5 (SAR 280), HELIUM ATMOSPHERE

a) 150 °C

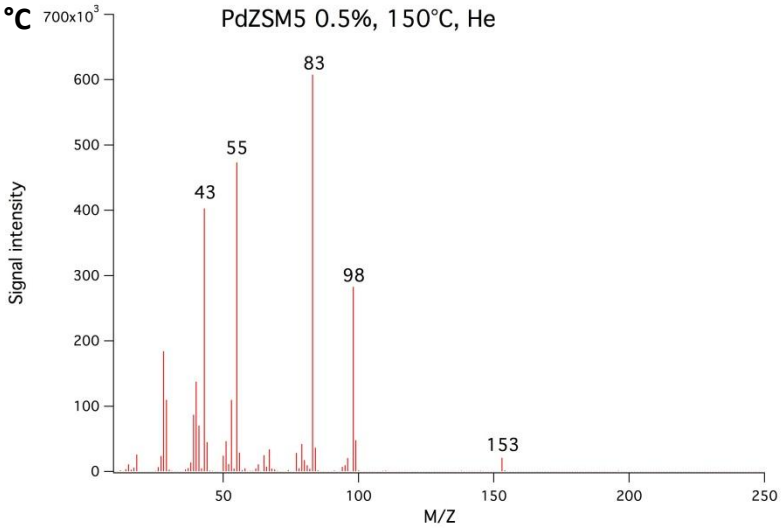

b) 250 °C

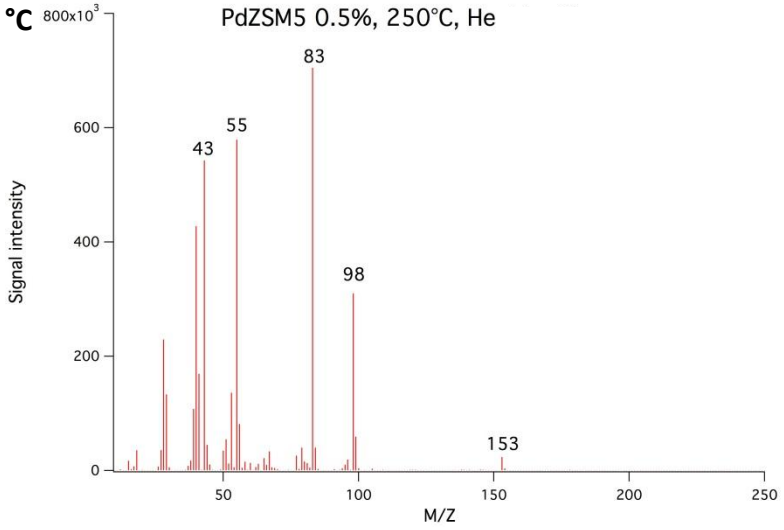

c) 350 °C

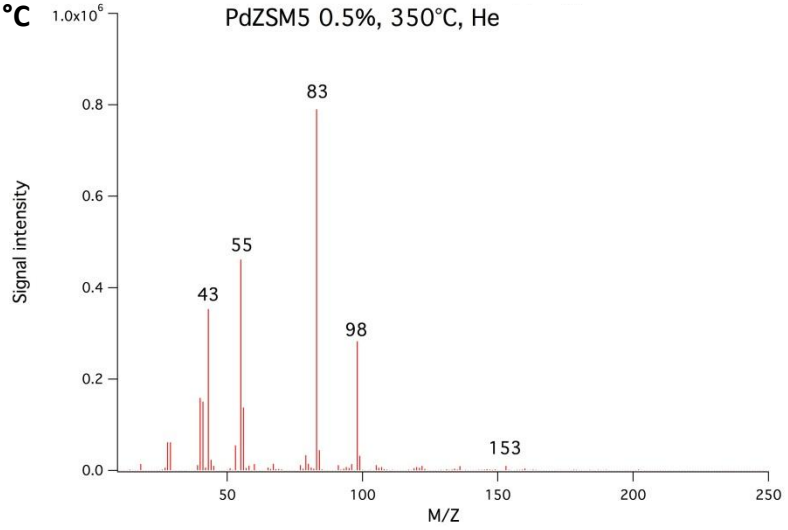

APPENDIX C.17 - PD (0.5 WT%) ZSM-5 (SAR 280), HELIUM ATMOSPHERE

a) 150 °C

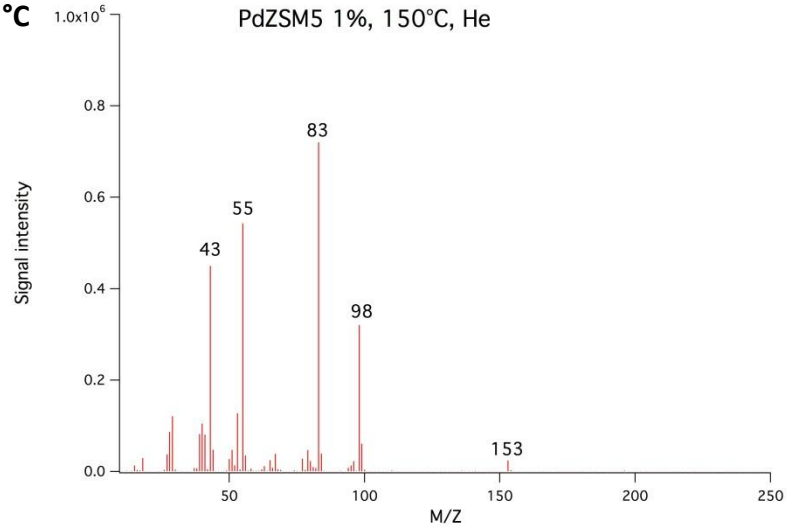

b) 250 °C

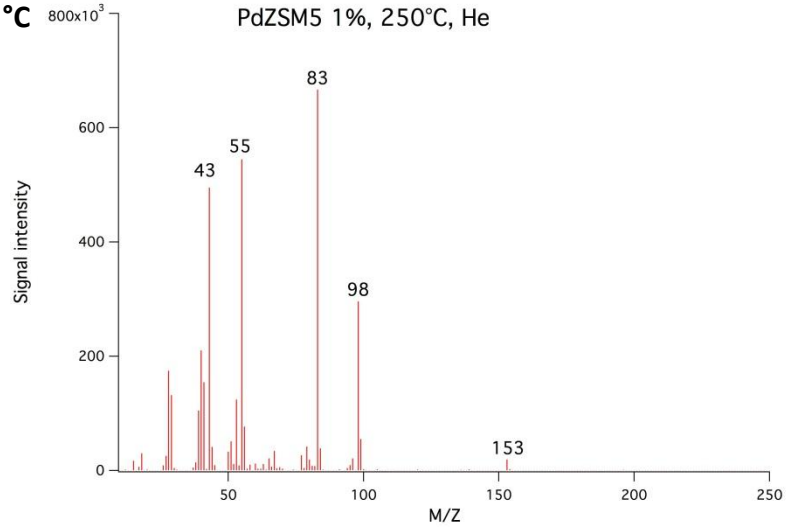

c) 350 °C

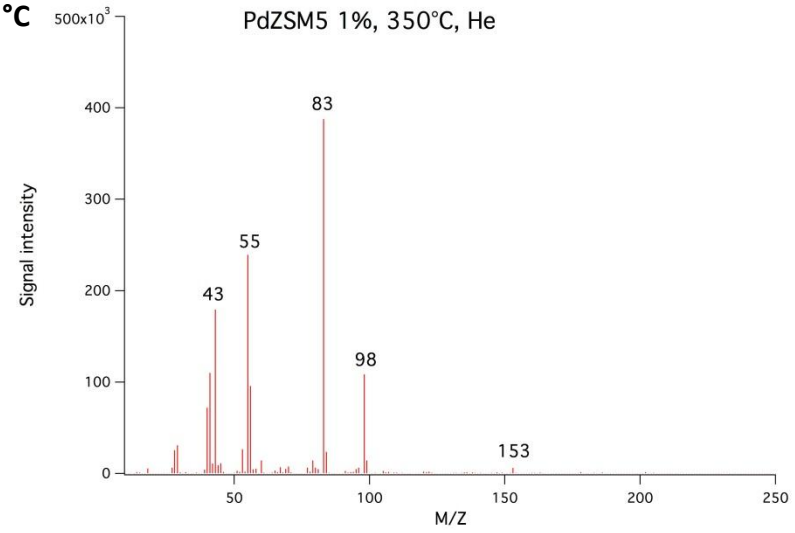

APPENDIX C.18 - PD (0.2 WT%) ZSM-5 (SAR 280), HYDROGEN ATMOSPHERE

a) 150 °C

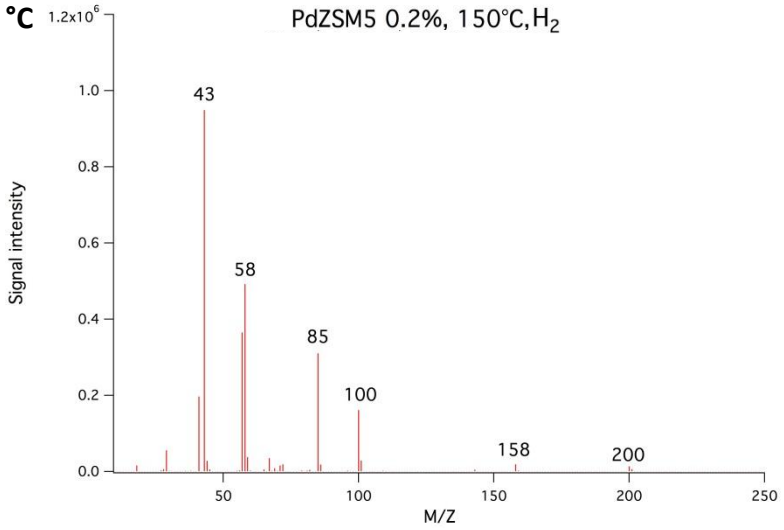

b) 250 °C

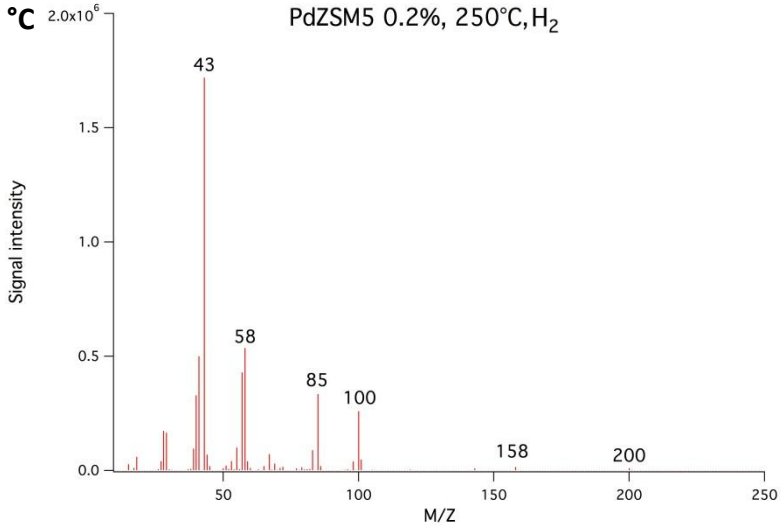

c) 350 °C

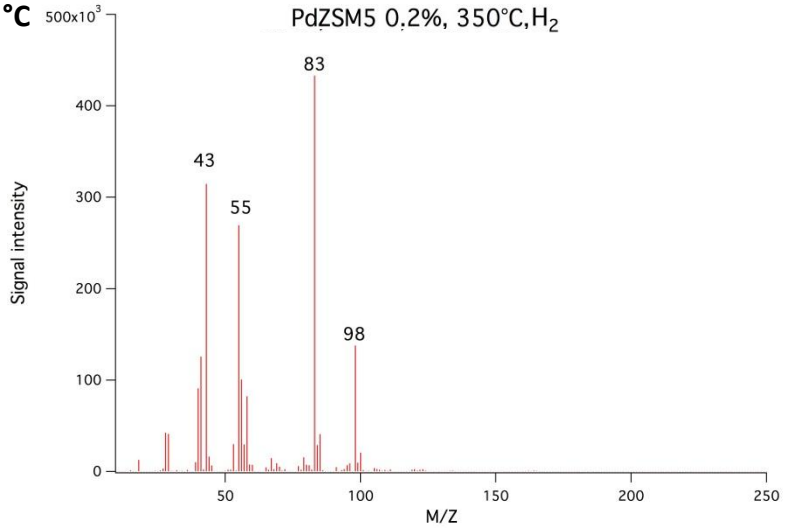

APPENDIX C.19 - PD (0.5 WT%) ZSM-5 (SAR 280), HYDROGEN ATMOSPHERE

a) 150 °C

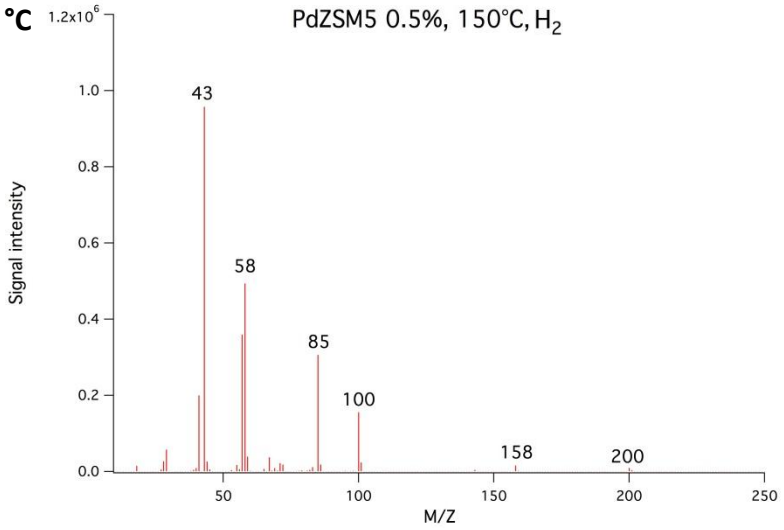

b) 250 °C

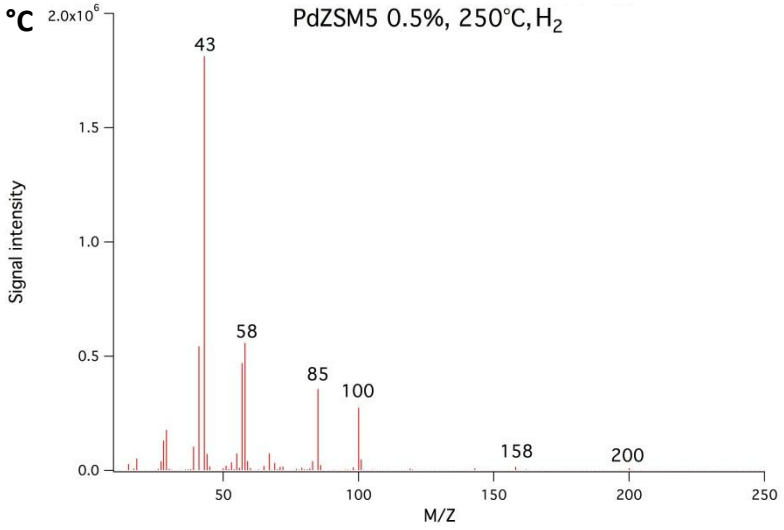

c) 350 °C

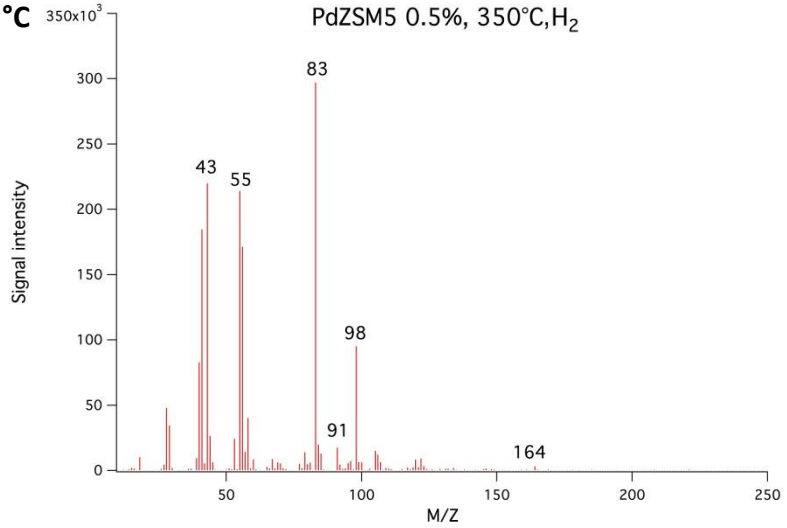

APPENDIX C.20 - PD (1 WT%) ZSM-5 (SAR 280), HYDROGEN ATMOSPHERE

a) 150 °C

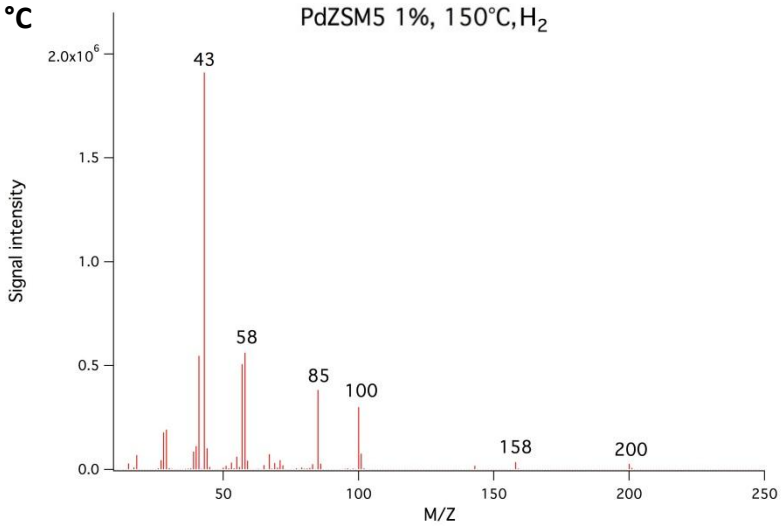

b) 250 °C

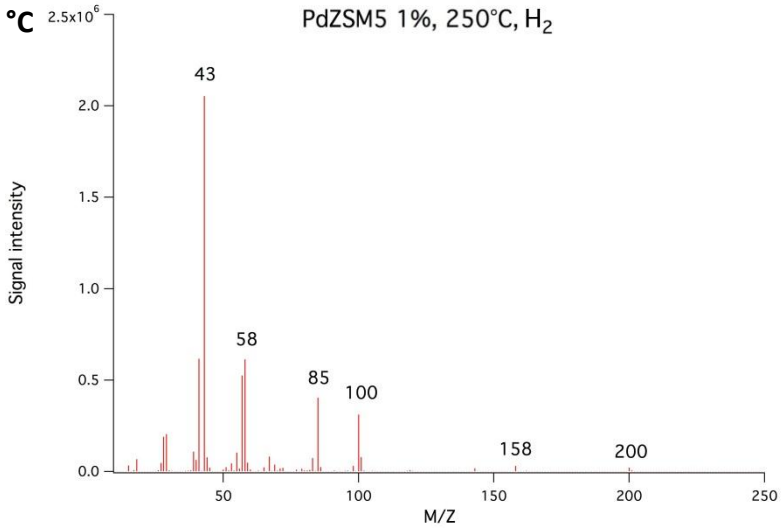

c) 350 °C